

https://dspace.org/

Impact of different materials on cracking of corrugated fibrecement sheets

Mtsweni, Ntombikayise Beauty

2014-07-07
http://hdl.handle.net10539/14890

Downloaded from a DSpace repository. https://dspace.org/

IMPACT OF DIFFERENT MATERIALS ON CRACKING OF CORRUGATED FIBRECEMENT SHEETS

Ntombikayise Beauty Mtsweni

A Thesis submitted to the Faculty of Science, University of the Witwatersrand, Johannesburg, in fulfillment of the requirements for the degree of Doctor of Philosophy.

Johannesburg, 2014

DECLARATION

I declare that this Thesis is my own, unaided work. It is being submitted for the degree of Doctor of Philosophy at the University of the Witwatersrand, Johannesburg. It has not been submitted before for any degree or examination at any other University.

_____

(Signature of candidate)

_____ day of _____ 20_____ in _____

ABSTRACT

The replacement of asbestos fibres with cellulose fibres in producing corrugated fibre reinforced cement sheets by the Hatschek process resulted in edge cracking for stacked sheets. This was due to the hydrophilic nature of cellulose, which increases its tendency for exchanging water with the surroundings. The drying process of corrugated sheets, in a stack, resulted in shrinkage hence edge cracking along the sheet. To reduce the magnitude of drying shrinkage and edge cracking potential, several mitigation strategies were proposed including the surface treatment of cellulose fibres, incorporation of wollastonite microfibres, addition of admixtures and superplasticizers, kaolin inclusion as partial replacement of cement and different exposure conditions. A fundamental understanding in mechanisms behind volume changes and how cracks form was crucial for optimization of the mitigation strategies.

This thesis initially used a review approach to understand the mechanisms involved in different types of shrinkage and the role of different mitigation techniques. The ultimate goal was to achieve lower drying shrinkage and cracking risks in corrugated sheets along with reducing its economic impact. As a result, surface treatment of cellulose fibres, based on transforming the hydrophilic nature of cellulose to hydrophobic state, was investigated. Furthermore, inclusion of wollastonite/ kaolin as partial replacement of cement, were evaluated. Also, the potential of adding admixtures/ superplasticizers was explored. Finally, investigation on development of edge cracks in stacked corrugated fibrecement sheets was conducted under different exposure conditions.

The results and findings of this research showed no significant improvement in permeability with cellulose surface treatment. Wollastonite microfibres promoted pore discontinuity hence significant reduction in permeability thus

lower drying shrinkage. However, the resultant sheets were brittle. By reducing water content with addition of superplasticizers, density was enhanced thus reducing volume change from drying and wetting. Kaolin acted as internal restraint for shrinkage, refining the microstructure at the interfacial transition zone thus increasing density and its pozzolanic reaction enhanced mechanical properties. The inclusion of kaolin in the fibrecement mix in conjunction with controlling exposure conditions managed to eliminate edge cracking.

Keywords: Drying shrinkage, permeability, edge cracking, corrugated fibrecement sheets, wollastonite microfibres, kaolin, superplasticizer, cellulose, exposure condition.

DEDICATION

This study was dedicated to:

My father, Charles

My mother, Harriet

My brother, Themba

My sisters, Thoko, Thandi, Zanele

My late aunt, Johanna (May her soul rest in peace)

And my beloved sons, Nhlakanipho and Thamsanqa

ACKNOWLEDGEMENTS

I would like to thank Almighty God for the wisdom, guidance and understanding provided throughout my doctoral studies. I wish to express my sincere gratitude to my supervisor, Prof E. Cukrowska, for her support, guidance and continuous encouragement.

I am indebted to Everite Building Products and management for supporting this project financially and the opportunity to run trials in the production machine. These trials were crucial for the success of this project, I am forever grateful. My deep gratitude goes to the technical staff, especially Mr. I.P. Hlongwa and Mr. B.L. Ndabana, for their assistance in the physically demanding laboratory work.

Finally, I would like to express my special thanks and appreciation to my father, mother, brother and sisters for their continuous support, prayers and motivation throughout the period of this research. In particular, my sons your support, understanding and patience is highly appreciated.

CONTENTS **PAGE**

DECLARATION ii
ABSTRACT iii
DEDICATION v
ACKNOWLEDGEMENTS vi
LIST OF FIGURES x
LIST OF TABLES xvi
LIST OF SYMBOLS xvii
NOMENCLATURE xix

CHAPTER ONE – INTRODUCTION

1.1 General Introduction 1
1.2 Objectives 2
1.3 Research strategy 3
1.4 Literature review 3
1.4.1 – Types of shrinkages in cement composites 3
1.4.2 – Heat of hydration 12
1.4.3 – Durability of cementitious composites 15
1.4.4 – Impact of carbonation to mechanical properties 21
1.4.5 - Mitigation techniques for shrinkage 22
1.5 Structure of the thesis 37
1.6 Original contributions 38
1.7 Concluding remarks 39

CHAPTER TWO – METHODOLOGY AND ANALYTICAL TECHNIQUES

2.1 Hatschek process 40
2.2 Test methods 43
2.2.1 – Determination of water absorption and apparent density
2.2.2 – Measurement of mechanical properties 45
2.2.3 – Test method for modulus of rupture 47
2.2.4 – Test method for soak-dry evaluation 49

2.2.5 – Determination of moisture movement 51
2.2.6 – Determine impact of accelerated carbonation 51
2.2.7 – Evaluation of heat-rain performance 53
2.2.8 – Test method for flocculant selection 55
2.3 Analytical Techniques 58
2.3.1 – X-ray Diffraction Spectroscopy 58
2.3.2 – Scanning Electron Microscopy 62
2.4 Raw materials evaluated for mitigation 66
2.4.1 – Surface modification silanes 66
2.4.2 – Wollastonite 67
2.4.3 – Silicone resin as admixture 68
2.4.4 - Kaolin 69
2.4.5 – Superplasticizer 72
CHAPTER THREE - SURFACE MODIFICATION OF CELLULOSE
3.1 Introduction 73
3.2 Experimental Procedure 77
3.2.1 – Materials 77
3.2.2 – Surface chemical treatment of cellulose 78
3.2.3 – Specimen preparation 78
3.3 Results and discussion 79
3.4 Conclusions 85
CHAPTER FOUR – IMPACT OF WOLLASTONITE INCLUSION
4.1 Introduction 87
4.2 Experimental Procedure 88
4.2.1 – Sample preparation 88
4.3 Results and discussion 89
4.3.1 – Density development 89
4.3.2 – Flexural strength 91
4.3.3 – Mineralogical composition 93
4.4 Conclusions 96

CHAPTER FIVE – EFFECT OF ADMIXTURE IN FIBRECEMENT

5.1 Introduction 98

5.2 Materials and method 100

5.2.1 – Materials 100

5.2.2 – Preparation of samples 101

5.3 Results and discussion 102

5.3.1 – Effect of admixture on water absorption 102

5.3.2 – Effect of admixture on flexural strength 107

5.4 Conclusions 109

CHAPTER SIX – IMPACT OF KAOLIN ON MECHANICAL PROPERTIES

6.1 Introduction 111

6.2 Materials and specimen preparation 115

6.2.1 – Materials 115

6.2.2 – Preparation of pilot plant specimens 116

6.2.3 – Production of corrugated sheets 117

6.3 Results and discussion 118

6.3.1 – Flocculant selection 118

6.3.2 – Pilot machine results 122

6.3.3 – Production results of corrugated sheets 133

6.3.4 – Validation of kaolin production results 149

6.3.5 – Effect of various curing conditions 152

6.4 Summary 178

CHAPTER SEVEN – SUMMARY, CONCLUSIONS AND RECOMMENDATIONS

7.1 Summary and conclusions 180

7.2 Recommendations for future research 186

APPENDICES 187

REFERENCES 198

BIBLIOGRAPHY 229

LIST OF FIGURES

Figure 1.1: Chemical and autogenous shrinkage of concrete 4

Figure 1.2: Autogenous and chemical shrinkage during different stages, as a function of degree of hydration 5

Figure 2.1: Schematic diagram of a vat component 40

Figure 2.2: Schematic diagram of Hatschek machine 41

Figure 2.3: Balance capable of weighing dry and wet specimens 44

Figure 2.4: Lloyd machine for measuring breaking load 46

Figure 2.5: Lloyd machine for testing bending strength 48

Figure 2.6: Instrument for measuring lengths 50

Figure 2.7: Accelerated carbonation chamber 52

Figure 2.8: Heat cycle, showing UV lights, simulating sunshine 54

Figure 2.9: Rain cycle, nozzles spraying water, simulating rainfall 54

Figure 2.10: Equipment for flocculant selection test 57

Figure 2.11: PAnalytical X'Pert Pro powder diffractometer 59

Figure 2.12: SEM instrument showing electron column 63

Figure 2.13: Schematic drawing of the SEM components 64

Figure 2.14: Chemical composition of wollastonite samples 67

Figure 2.15: Particle size distribution of wollastonite samples 68

Figure 2.16: Kaolin structure 70

Figure 2.17: Particle size distribution of kaolin 71

Figure 3.1: Process water content monitoring 80

Figure 3.2: Density measurement of green cellulose pretreated sheets 81

Figure 3.3: Density development of cellulose pretreated sheets 82

Figure 3.4: Wet-dry movement of cellulose pretreated sheets 83

Figure 3.5: Strength development of cellulose pretreated sheets 84

Figure 3.6: Mineralogical composition of cellulose pretreated sheets 85

Figure 4.1: Water content of wollastonite fibrecement composites measured during manufacturing process 89

Figure 4.2: Development of density for wollastonite fibrecement sheets over time 90
Figure 4.3: Movement curves of wollastonite fibrecement sheets 91
Figure 4.4: Development of strength for wollastonite composites 93
Figure 4.5: Mineralogical composition of wollastonite composites 94
Figure 4.6: Fracture energy of wollastonite fibrecement sheets 94
Figure 4.7: SEM micrograph of 6% wollastonite fibrecement sheets 95
Figure 4.8: SEM micrograph of control fibrecement composite 96
Figure 5.1: Flocculation of cement particles by admixtures 100
Figure 5.2: Effect of superplasticizer on water absorption of fibrecement sheets 103
Figure 5.3: Effect of superplasticizer on density of fibrecement sheets 104
Figure 5.4: Development of water absorption for composites with admixture 105
Figure 5.5: Movement of composites with superplasticizer 106
Figure 5.6: Effect of admixture on wet-dry movement over 28 days curing 106
Figure 5.7: Comparison of strength development for standard and superplasticizer added composites 108
Figure 5.8: Strength development for composites with admixture 109
Figure 6.1: Schematic diagram of kaolinite structure 112
Figure 6.2: Flocculant retention results 119
Figure 6.3: Selection of flocculant type and dosage for optimal filtration 119
Figure 6.4: The development of density in fibrecement composites with kaolin 124
Figure 6.5: Comparison of water absorption for fibrecement composites with different kaolin levels 124
Figure 6.6: Effect of various kaolin levels on wet-dry movement of composites 126

Figure 6.7: Strength development in kaolin-incorporated fibrecement composites 128
Figure 6.8: Identification of crystal structures in kaolin-incorporated fibrecement composites
129
Figure 6.9: Accelerated aging test for kaolin modified fibrecement composites 130
Figure 6.10: Density comparison for fibrecement composites before and after accelerated carbonation test 132
Figure 6.11: Comparison of strength for kaolin-inclusion fibrecement composites, before and after accelerated carbonation 133
Figure 6.12: Density development of kaolin-incorporated corrugated sheets
135
Figure 6.13: Water absorption of kaolin modified corrugated sheets 136
Figure 6.14: Wet-dry movement of kaolin modified corrugated sheets 137
Figure 6.15: Rate of moisture loss and movement of fibrecement sheets138
Figure 6.16: Movement of corrugated sheets at different ranges of moisture
139
Figure 6.17: Standard and kaolin modified corrugated sheets 140
Figure 6.18: Development of flexural strength in corrugated fibrecement sheet 141
Figure 6.19: SEM micrographs of standard corrugated sheets 142
Figure 6.20: SEM micrographs of 3% kaolin modified corrugated sheets 143
Figure 6.21: SEM micrographs of 5% kaolin modified corrugated sheets 145
Figure 6.22: Density trend in aging of sheets with kaolin inclusion 146
Figure 6.23: Strength evolution of fibrecement corrugated sheets for natural and accelerated exposure 147
Figure 6.24: Thaumasite formation on fibrecement corrugated sheets 148
Figure 6.25: Monitoring solids during production of 3% kaolin modified corrugated sheets 149

Figure 6.26: Monitoring mechanical properties of 3% kaolin modified fibrecement sheets 150
Figure 6.27: Comparison of the two production trials to determine repeatability 151
Figure 6.28: Development of density under various curing conditions 153
Figure 6.29: Water absorption of kaolin modified sheets under different curing conditions 153
Figure 6.30: Strength development of kaolin modified sheets cured under different conditions 154
Figure 6.31: Quantitative XRD of 3% kaolin-incorporated sheets under different conditions 155
Figure 6.32: Monitoring moisture loss from sheets, cured under different conditions 156
Figure 6.33: Monitoring movement of kaolin modified sheets, under different conditions 157
Figure 6.34: Edge cracking in internally stored kaolin modified sheets, prior to natural exposure 158
Figure 6.35: Edge cracking in externally cured sheets, without wrapping 159
Figure 6.36: Density development of 3% kaolin modified sheets under different curing conditions 160
Figure 6.37: Effect of various curing conditions on water absorption of kaolin modified sheets 160
Figure 6.38: Development of strength in kaolin-incorporated corrugated sheets under different curing conditions 161
Figure 6.39: Quantitative XRD of fibrecement corrugated sheets with kaolin inclusion under various curing 162
Figure 6.40: Evaluation of moisture loss with time in fibrecement corrugated sheets with 3% kaolin under various conditions 163
Figure 6.41: Movement determination in kaolin modified sheets 163

Figure 6.42: Edge cracking in corrugated fibrecement sheets with kaolin inclusion stored indoors, wrapped 164
Figure 6.43: Kaolin modified corrugated fibrecement sheets stored inside, unwrapped 165
Figure 6.44: Change in length, as a result of wet-dry cycling 166
Figure 6.45: SEM micrograph showing ettringite formation 167
Figure 6.46: Density development of wrapped and unwrapped sheets 168
Figure 6.47: Reduction of water absorption for kaolin modified sheets 169
Figure 6.48: Development of strength for wrapped /unwrapped sheets 170
Figure 6.49: Quantitative XRD for wrapped and unwrapped sheets 171
Figure 6.50: Evaluation of the rate of moisture loss in corrugated sheets, under different curing conditions 172
Figure 6.51: Moisture-movement curves of kaolin modified sheets under various curing 172
Figure 6.52: Corrugated kaolin modified sheets with upturns in the direction of highest incidence of solar radiation 173
Figure 6.53: Corrugated kaolin modified sheets with downturns orientated in the direction of severe solar radiation 174
Figure 6.54: Corrugated kaolin sheets with edge micro-cracks 175
Figure 6.55: Durability test for kaolin modified corrugated sheets 175
Figure 6.56: SEM micrograph for kaolin modified sheets stored indoors 176
Figure 6.57: SEM micrograph for kaolin modified sheets stored indoors 177
Figure 6.58: SEM micrograph showing ettringite crystal 177
Figure 6.59: SEM micrograph with CSH and $CaCO_3$ 178
Figure A1: Moisture movement curve for batch 35S714 cured outside 187
Figure A2: Wet-dry cycling for batch 35S714 under various curing 188
Figure A3: Movement curves for all fibrecement sheets produced between 2012 and 2013. 188
Figure A4: Effect of kaolin addition on cement setting 189
Figure A5: Minerals formed during the hydration process 189

Figure B1: Quantitative XRD spectra for fibrecement corrugated sheets, batches 37S701, 35S704 and 35S714 190
Figure B2: Quantitative XRD spectra for fibrecement corrugated sheets batch 29S705 cured under different conditions 191
Figure B3: Quantitative XRD spectra for the first production trials – STD, Trial 1 and Trial 2 192
Figure C1: SEM micrographs for batch 37S701 stored indoors for 14 d prior to external exposure 193
Figure C2: SEM micrographs for batch 35S704 stored indoors for 14 d prior to external exposure 194
Figure C3: SEM micrographs for batch 35S714 stored indoors unwrapped for 14 d prior to external exposure 195
Figure C4: SEM micrographs for batch 35S714 stored indoors wrapped for 14 d prior to exposure outside 196
Figure C5: SEM micrographs for batch 37S701 cured outside without wrapping 197

LIST OF TABLES

Table 1.1:	Heat of hydration of cement compounds	14
Table 2.1:	Heat-rain cycle	55
Table 2.2:	Physical properties of silanes	66
Table 2.3:	Physical properties of silicone resin	69
Table 2.4:	Chemical composition of kaolin	69
Table 2.5:	Physical properties of kaolin	71
Table 2.6:	Physical properties of superplasticizer	72
Table 3.1:	Physical properties of fibres	78
Table 3.2	Chemical composition of powder raw materials	78
Table 6.1:	Physical and chemical properties of kaolin and cement	115
Table 6.2:	Properties of polyacrylamide flocculants	116
Table 6.3:	Results of settling rates of solids, with different flocculants	121
Table 7.1:	Best mitigation technique	185

LIST OF SYMBOLS

ACI	:	Academic Conferences International
Al_2O_3	:	Alumina
APTS	:	Amino propyl tri-ethoxy silane
ASTM	:	American Society for Testing and Materials
C_2S	:	Dicalcium silicate
C_3A	:	Tricalcium aluminate
C_3S	:	Tricalcium silicate
$CaCO_3$	:	Calcium carbonate
CH, $Ca(OH)_2$	:	Calcium hydroxide
CO_2	:	Carbon dioxide
CSF	:	Condensed silica fume
CSH	:	Calcium silicate hydrates
EDS	:	Energy dispersive spectroscopy
ESEM	:	Environmental scanning electron microscopy
Fe_2O_3	:	Ferric oxide
H_2O	:	Water
ISO	:	International Organization for Standardization
MOR	:	Modulus of rupture
MPTS	:	Methacryloxy propyl tri-methoxy silane
PP	:	Polypropylene
PSD	:	Particle size distribution
PVA	:	Polyvinyl alcohol
RCPT	:	Rapid chloride permeability test
SEM	:	Scanning electron microscopy
SiO_2	:	Silica
SRA	:	Shrinkage reducing admixture
STD	:	Standard
TMP	:	Thermo mechanical pulp

URL	:	Uniform Resource Locator
UV	:	Ultra-violet
XRD	:	X-ray diffraction spectroscopy
XRF	:	X-ray fluorescence spectroscopy

NOMENCLATURE

με	:	Micro strain
μm	:	Micrometer
cm^2/g	:	Centimeter squared per gram
cSt	:	Centistokes
d	:	days
e.g.	:	Example
et al.	:	And others
g/cm^3	:	Grams per cubic centimeter
h	:	Hour
i.e.	:	That is
J/g	:	Joules per gram
kN/m	:	Kilo Newton per meter
kV	:	Kilovolts
min	:	Minute
ml	:	Milliliter
mm	:	Millimeter
mm/m	:	Millimeter per meter
nm	:	Nanometer
ppm	:	Parts per million
RH	:	Relative humidity
s/l	:	Seconds per liter
v/v	:	Volume per volume
viz.	:	Namely
w/w	:	Weight per weight
θ	:	Theta
dtex	:	Decitex
cN/dtex	:	centiNewton per decitex

CHAPTER 1 – INTRODUCTION

1.1 General Introduction

Fibrecement asbestos based products had been widely used in the world due to their versatility as corrugated and flat roofing materials. However, the health risks associated with its use led to its ban in construction industry in many countries. The successful replacement of asbestos fibres with cellulose fibres brought new challenges in the production of these products and its properties. Cellulose fibres are hydrophilic, i.e. have a higher tendency to absorb water, hence more susceptible to degrade due to water absorption. When fibrecement composites absorb moisture, potential problems that can occur include reduced dimensional stability, reduced freeze/thaw resistance leading to cracking and warping, white efflorescence salts affecting appearance and reduce durability.

One characteristic of building materials is movement, in response to applied loads and with changes in ambient moisture and temperature. Heat causes expansion and, cooling causes contraction. Materials do not necessarily expand uniformly with changes in temperature. Wood, and composites containing wood, moves more on wetting and drying than heating and cooling.

Fibrecement corrugated sheets are air cured products reinforced by alkali-resistant synthetic fibres combined with refined cellulose fibres, produced by the Hatschek process (Akers, 2006). The composite sheets are stored in stacks during the curing stage. During the curing process, cracks appear along the edges of the corrugated sheets. The cracks could results from the different sources in the production stages. It could be from the drying process, edges drying faster than the center of sheet thus creating internal stresses, hence cracking. The other source could be the mix formulation,

where there is a variation in particle size of the raw materials resulting in a porous structure. This will allow easier absorption and release of water to the surroundings. The water exchange between the fibrecement composite and its surroundings is related to expansion and shrinkage of the material. The movement within the composite could result in cracking. The third possibility is related to the curing process. By exposing the composites to natural environment while the water content is too high, the drying shrinkage would result in cracking. The orientation of the stack in the stockyard, the highest incidence of solar radiation, needs to be investigated. The intensity of heat increases the rate of water loss at the edges hence drying shrinkage. The cracks appear as either fine multi cracks or as a narrow defined single crack. The major concern is the size of the crack.

This study investigated all the causes related to cracking in stacked fibrecement corrugated sheets. Also, to established mitigation techniques based on certain chemical processes that take place within the cement-based material microstructure. Finally, it evaluated how these mitigation techniques impacted on curing, mechanical properties and durability of the fibrecement composites.

1.2 Objectives

The main objective of this project was to determine the causes of edge cracking in corrugated fibrecement sheets piled in a stack, as well as find mitigation techniques for reduction or elimination of these cracks. The new technique should not have a negative effect on the durability of the corrugated sheets. It should be possible that these new materials are readily available in the market and cost-effective.

1.3 Research strategy

In fibrecement composites, the properties depend on the fibre, the cement matrix and the fibre-matrix interface. To be able to achieve the goal in the previous section, the research was carried out by first studying each raw material chemical composition and later using the knowledge to design formulations that will give denser fibrecement products with least movement. The curing conditions and layout of the sheets under natural exposure was evaluated.

1.4 Literature review

1.4.1 Types of shrinkages in cement composites

Other causes of cracking are plastic shrinkage, autogenous shrinkage, drying and swelling, carbonation shrinkage, thermal deformation (expansion and contraction), load and creep (Holt, 2001; Holt 2005; Bentur 2003; Tazawa 1999). Some of these deformations may appear simultaneously or sequentially. Plastic shrinkage can appear before solidification while product still retains its plastic properties. It results from premature loss of water due to evaporation. It can be avoided by appropriate cure techniques under moist environment.

Autogenous shrinkage is caused by chemical and physical processes resulting from hydration. It can be defined as the macroscopic volume change that occurs after the initial setting as a result of the withdrawal of moisture from capillary pores to continue cement hydration reactions (Mihashi and Leite, 2004). The volume of reactants is greater than volume of products. Chemical shrinkage, which is the reduction in the volume of hydration products compared with that of the reacting constituents, can be considered as the main driving mechanism behind autogenous shrinkage (Tazawa, 1999). This reduction in volume does not change the apparent dimensions of the hardened material but rather increases its porosity. The

water used for hydration is consumed from the pores. The consumption of water increases the capillary pressure and consequently the apparent volume decreases. This volume reduction is called self-drying shrinkage and is due to generation of tensile stress in small capillaries. This type of shrinkage cannot be avoided as it results from hydration process but, can be reduced by the release of internal curing water using super absorbent polymers (Tazawa, 1999; Esping, 2007). Autogenous shrinkage can have nearly the same value as drying shrinkage for low water-cement ratio concrete under normal condition (20ºC and RH=50%) (Tazawa and Miyazawa, 1995a). However, autogenous shrinkage is considered as an external volume change (apparent volume change), while chemical shrinkage as an internal volume reduction (absolute volume change) as shown in Figure 1.1 (Holt, 2001; Mihashi and Leite, 2004; Tazawa, 1999; Esping, 2007).

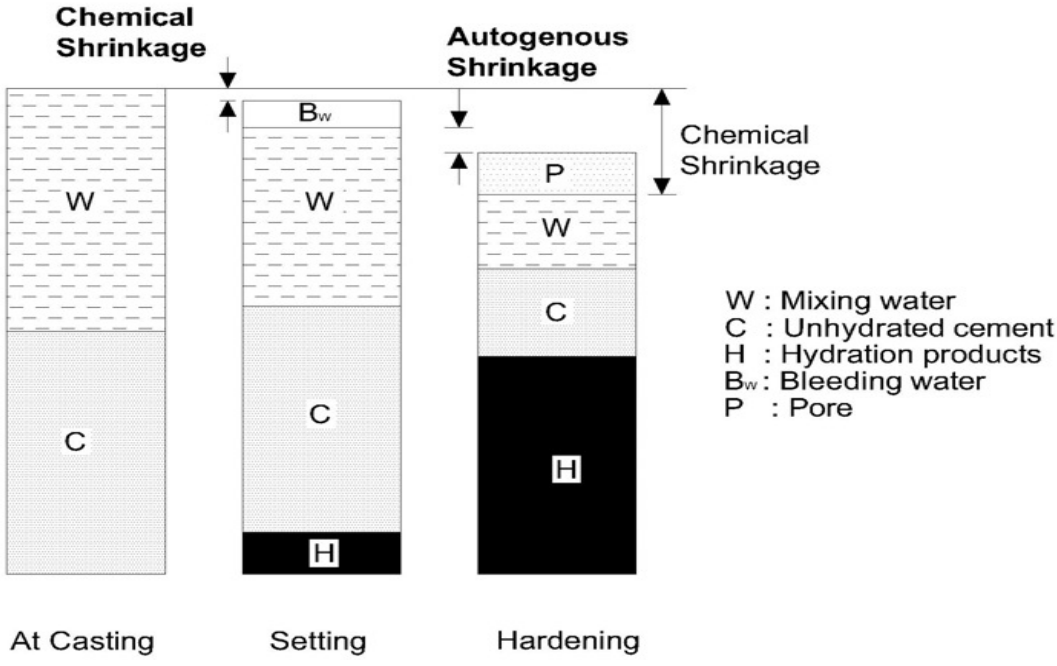


Figure 1.1: Chemical shrinkage and autogenous shrinkage of concrete [adapted after Mihashi and Leite (2004)]

During early-age, concrete undergoes three phases, viz. particulate suspension, skeleton formation and initial hardening (Fig. 1.2). At the initial phase, concrete is still plastic without a permanent structure, and autogenous shrinkage is equivalent to chemical shrinkage (part AB). Consequently, any applied stresses will cause movement of the body. A few hours after casting, the development of skeleton starts due to the formation of hydration products. During this stage, setting takes place and concrete can resist some of the chemical shrinkage. At this moment, the mineral percolation threshold, autogenous shrinkage starts to diverge from chemical shrinkage (part BC). Finally the hardening stage begins and the autogenous shrinkage becomes increasingly restrained due to the stiffening of the cement paste (part C) (Holt, 2001; Bentur, 2003; Tazawa, 1999; Esping, 2007).

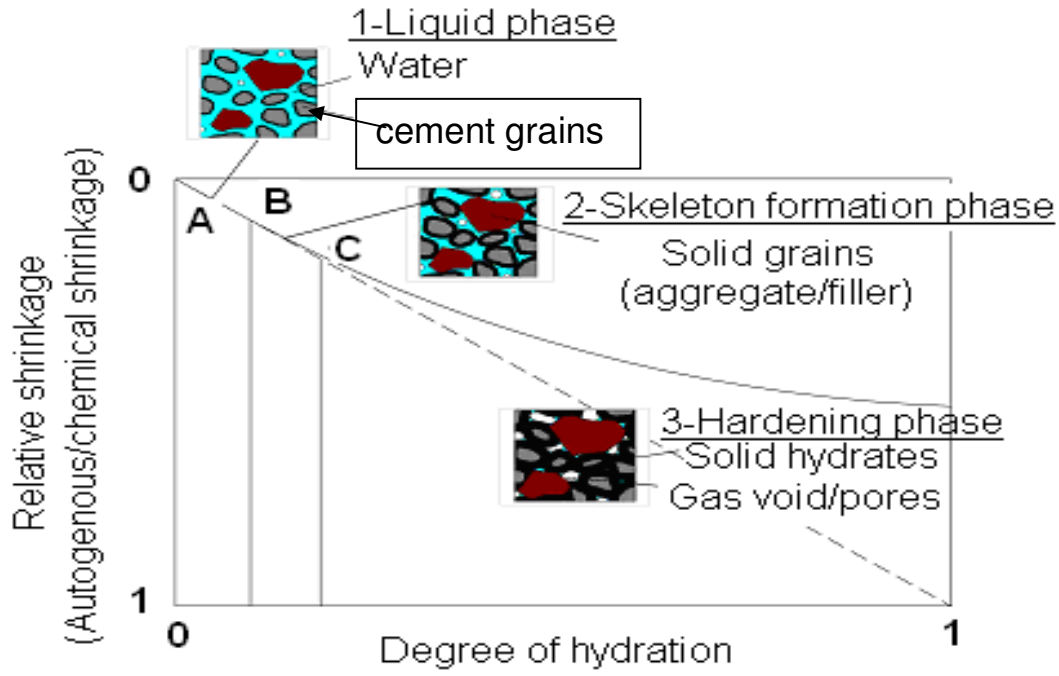


Figure 1.2: Autogenous and chemical shrinkage during different stages, as a function of degree of hydration [adapted after Holt (2001) and Esping (2007)]

A higher rate of hydration results in higher autogenous and drying shrinkage due to the decreased volume of hydration products relative to their constituents and the higher water consumption, which in turn reduces bleeding and increases the concrete temperature (Bentur, 2003; Holt, 2005; Tazawa, 1999; Esping, 2007; Topcu and Elgun, 2004). Water content has a major role during early-age shrinkage through controlling the amount of free water, and the development of the microstructure and pore system, which consequently affects the capillary tension and meniscus development.

After setting, concrete may undergo considerable irreversible drying shrinkage. Nevertheless, shrinkage cracking occurs more often at early age because the concrete has not developed enough strength to withstand the restraint-induced stress (Lin et al., 2012). Invisible and hairy cracks may propagate and expand in the long term due to drying shrinkage.

Drying shrinkage develops in cured materials due to moisture loss to surrounding environment, i.e. evaporation or absorption, at constant temperature and relative humidity (Holt, 2001; Holt, 2005). If the bleeding rate is higher than the evaporation rate, drying shrinkage will not occur since the excess water will be sufficient for further evaporation and act as a curing layer. When the reverse behavior occurs, the extra water required for evaporation will be extracted from the internal pores. Losing water from capillary pores at early-age will cause plastic shrinkage and subsequent internal stresses, leading to early-age surface cracks (Khan, 1995). The drying shrinkage and swelling arise from the surfaces which are in contact with dry or humid air. This process is not uniform throughout the material thus resulting in internal stresses. When external or internal restraint to this deformation exists, micro and macro cracking can result, affecting mechanical properties and durability.

The fundamental mechanism of drying shrinkage in concrete is partially described by Gauss-Laplace equation (Grasley, 2003 and D'Ambroisa, 2002). This equation can be used to calculate tensile stress in the pore fluid:

$$\sigma_{cap} = 2\gamma/r \qquad \text{Eqn 1.1}$$

Where σ_{cap} is tensile stress in the pore fluid, γ is surface tension of the pore solution and r is the radius of the largest water filled cylindrical pore (Lura et al., 2003). As concrete dries or is self-desiccated, curved menisci form in the pores, leading to a reduction in pore relative humidity, which in turn increases the internal capillary pressure. Thus, drawing the walls together and resulting in drying shrinkage (D'Ambroisa, 2002). Even at early age, the pore structure of the cement matrix is well defined, thus making the pore radius unchangeable. However, the other free variable, surface tension of pore solution, can be manipulated with chemicals called shrinkage reducing admixtures.

The drying shrinkage of concrete during curing is a source of residual stress and cracks. Drying shrinkage can be minimized and the concrete may remain in a relatively crack free condition for decades, insuring that the concrete structure survive its intended design life (Bentz et al., 2001). Various admixtures such as silica fume (Chen and Chung, 1996; Haque, 1996) and liquid chemicals (Balogh, 1996; Shah et al., 1998; Nmai et al., 1998) have been used to reduce the drying shrinkage. The low water cement ratio, addition of superplasticizer and incorporation of pozzolanic admixtures such as silica fume, creates a water starved, super dense microstructure within a few days (Bentz and Jensen, 2004). This rapid development of a very fine pore network within the cement paste creates an impermeable medium and effectively seals the concrete off from its environment. Since there is no water available externally for curing, the concrete consumes water from its own capillary pores. This self-desiccating action lead to microstructural stresses similar to the diffusion of pore water during drying.

The particle size distribution and quantity of cement, water-cement ratio and aggregates have an essential role in controlling bleeding, which in turn controls the mechanism of drying shrinkage on the macro-level. However, it

is believed that the drying shrinkage mechanism on the nano-level is a combination of four well-known mechanisms (Bentur, 2003), namely: surface free energy, capillary tension, movement of interlayer water and disjoining pressure. This combination was found to be highly affected by the relative humidity of concrete, which varies drastically during early ages. Drying shrinkage is an inherent property of all calcium silicate hydrate based materials. The pure hardened calcium silicate hydrate paste undergoes very high drying shrinkage, whereas the reinforced material shows significantly less shrinkage due to the restraint provided by aggregate or fibre reinforcement (Betterman et al., 1995). It can be avoided at an early age by curing the products under plastic wrapping.

Drying shrinkage is mainly attributed to environmental conditions. Thus, detrimental factors are those affecting the rate of evaporation, i.e. relative humidity, air velocity, air and concrete temperature (Esping, 2007). On the other hand, autogenous shrinkage is influenced by the type and properties of the binder, mixture proportions and admixtures that can refine the pore structure. Although early-age autogenous shrinkage is fully attributed to chemical shrinkage, its behavior may be different to chemical shrinkage with respect to factors affecting the setting time and formation of restraining structure (Esping, 2007).

A higher rate of hydration results in higher autogenous and drying shrinkage due to the decreased volume of hydration products relative to their constituents and the higher water consumption, which in turn reduces bleeding and increases the concrete temperature (Bentur, 2003; Holt, 2005; Tazawa, 1999; Esping, 2007; Topcu and Elgun, 2004). The work of Tazawa and Miyazawa (1995b) showed that the percentage decrease in the autogenous shrinkage nearly corresponds to the percentage of decrease in the surface tension. Laboratory results showed reduction in drying shrinkage of about 50 – 60% at 28 days and about 40 – 50% after 12 weeks (Nmai et al., 1998; Folliard and Berke, 1997; Shah et al., 1997). Studies by

D'Ambroisa (2002) showed about a 30% reduction in shrinkage at only 8 days at the addition of 1.5% shrinkage reducing admixture (SRA). Reduced shrinkage is a direct effect of the addition of an admixture. This reduction in early age drying shrinkage provides the concrete sufficient time to harden before extreme tensile stress is imposed on it. Since the drying shrinkage is delayed a substantial amount of time, then the cement matrix has more time to develop and build tensile strength. With this higher tensile strength, cracking due to drying shrinkage is unlikely. If cracking does occur at a later stage, the crack openings will be significantly small (Shah et al., 1997).

Although SRA reduce surface tension of the pore fluid, reducing shrinkage has potential negative side effects. These include a chance of strength loss early in the concrete's life, slight delay in set time and the potential to wash out over time. Folliard and Berke (1997) observed a reduction in flexural strength at the age of one day. He attributed such reductions on early cement hydrations. Research done by Nmai (1998) showed minimal effects on flexural strength with addition of an SRA. Weiss et al. (1998) found an increase in flexural strength with normal concrete when SRA was added.

As SRA reduces the surface force of attraction in pore water, the forces of attraction of the flocculated binder phase are also reduced, resulting in retardation of setting time (Brooks et al., 2000). This effect is more pronounced with larger dosages and more significant when combined with superplasticizer. The authors showed that the initial and final setting times could be retarded as much as 25% and 24%, respectively, with a dosage of 1.25% SRA.

Although there is no published data available on the likelihood of a SRA wash out, the possibility causes concern in terms of durability. SRA is a chemical that lowers the surface tension in the pore fluid but does not combine chemically with hydration products. It is thus potentially possible to wash out with migrating water.

Concrete drying shrinkage is a complex process that has several causes:

- When cement in concrete reacts with mixing water, calcium silicate hydrate (CSH) begins to form in water-filled spaces. The spaces are not completely filled with CSH, so the remnants of mixing water form a network of capillary voids in hardened cement paste. Although the voids are initially interconnected, they become discontinuous during curing if the water-cement ratio is less than 0.7. Other much smaller voids are present within CSH. Some of the space between these voids is filled with water adsorbed at the surface of the CSH. This adsorbed water and the water in the capillary pores play an important role in concrete shrinkage. The adsorbed water causes a disjoining pressure between the CSH surfaces (Mehta, 1994). When this water leaves the concrete as a result of drying, the disjoining pressure decreases and the cement paste shrinks.
- It has also been suggested that when capillary pores dry, the hydrostatic tension formed in the meniscus exerts a stress within the rigid skeleton of CSH, causing the cement paste to shrink (Mindess and Young, 1981). Since capillary water is held less tightly than adsorbed water, moisture is lost from capillary pores when drying begins. Thus, early shrinkage is attributed to surface tension in the water remaining in capillary pores.
- Surface tension develops in small pores within the cement paste. When these pores lose moisture, a meniscus forms at the air-water interface. Surface tension in this meniscus pulls the pore wall inward, and the concrete reacts to these internal forces by shrinking (Balogh, 1996). This shrinkage mechanism only occurs in pores within a fixed range of sizes. In pores larger than 50 nm, the tensile force in the water is too small to cause noticeable shrinkage. In pores smaller than 2.5 nm, a meniscus cannot form. The amount of cement paste shrinkage caused by surface tension depends primarily on water-cement ratio. It can also be affected by cement type and fineness and

any material that alters the pore size distribution in the hardened paste. After concrete hardens, the admixture remains in the pore system, where it continues to reduce the surface tension effects that contribute to drying shrinkage.

The carbonation shrinkage develops only in layers exposed to air with relative humidity limits of 30 – 70%. It is caused by the chemical reaction of hydration products with carbon dioxide gas from the air. Under the actions of drying and moistening the carbonation shrinkage is coupled with drying shrinkage and initiates very fine cracks.

The cement based composite product is exposed, when installed externally, to thermal influences caused by ambience temperature variations, sun radiance or artificially by industrial heating. The result of these influences is thermal deformation of the structure. Rapid thermal variation (heating or cooling) could cause self-stressing that may result in cracks. Thermal processes due to hydration affect the product at an early age and thermal exchanges with the environment cause a thermal gradient. This temperature difference causes not only uneven advancement of the hydration, but also self-stressing when the full strength has not yet developed. Thermal cracking is the origin of several phenomena that affect durability and shorten the lifespan of the material.

Durability of the fibrecement composite materials can be assessed by repeated cycles of wet-dry shrinkage properties and reaction to carbonation. Akers (2006) conducted studies by characterizing the various forms of cracking in fibrecement products and proposed a mechanism for this phenomenon. On exposure to natural weathering in a stack, these products undergo physical and chemical changes related to their life-span and cracking performance. There is an exchange of pore water between the composite and its surroundings. This mechanism is related to the product formulation, climate conditions, curing age of product or the combination of

these factors. The rate and magnitude of water loss within the product result in greater internal stresses. A study of migration of pore water within a product exposed to various environments has indicated that initial losses in pore water do not necessarily lead to greater internal stresses; more importantly are the rate at which the loss of water takes place and its range within the product (Akers and Partl, 1990). The density of the product dictates the absorption rate. When fibrecement composite materials are stored in a stack, the edges dry out while the covered portion in the stack is still wet. Moisture gradients will occur between the edge and the center of the material, resulting in differential shrinkage with ultimate failure in a form of cracking. Cracking is related to the density and mix composition of the product. Mix formulation can be adjusted to reduce the wet-dry movement of the products. This problem can be reduced or eliminated by coating the product and shrink wrapping with plastic foil to prevent edge drying. Hydration causes the matrix to harden, increasing strength with decreasing toughness. The interfacial bond weakens as a result of wet-dry movement, hence the strength of the material will decrease but the toughness could increase. The study by Akers (2006) concluded that migration of the pore water of fibrecement products has a significant influence on shrinkage, which will have an impact on product cracking.

1.4.2 Heat of hydration

During hydration, the water-cement suspension transforms to hardened cement paste; strength increases and a considerable amount of heat is discharged resulting in early age deformation (Glisic and Inaudi, 2006). The deformation due to hydration is caused by hydration heating and cooling; and by material transition to cured state. Different types of deformation can appear as a result of the hydration process and the external influences. Also, stresses may be generated. The strength of the material at this stage is still low thus the stresses can result in cracking. The duration of the early age

stage depends on the rate of hydration, material composition (mainly the water-cement ratio) and the curing conditions.

Generally, the early age is first few hours or days after casting concrete that are characterized by two main processes: setting (progressive loss of fluidity) and hardening (gaining strength). During these processes, the fluid multiphase structure of the fresh concrete transforms into a hardened structure due to the progress of hydration reactions, leading to the development of mechanical properties, heat liberation and deformations (Pane and Hansen, 2002). This heat liberation and water loss, due to either evaporation or consumption by hydration reactions, leads to internal or external deformations. Hence, proper curing after placement is crucial to maintain a satisfactory moisture content and adequate temperature in concrete during this early stage so that the desired properties can develop later (Huo and Wong, 2006).

The amount and kinetics of heat generated by cement hydration is an important parameter for predicting the temperature development and its distribution within the concrete. The hydration of cement is a highly exothermic chemical reaction (Neville, 1996). About one-half of the total heat of hydration is evolved between 1 and 3 days after mixing cement with water (Oluokun et al., 1990). At early age, the rate and total heat of hydration are mainly influenced by the type, total content and chemical composition of cement, the ambient temperature and the admixtures used (Khan, 1995). Cements with a high Dicalcium Silicate (C_2S) and/or Tetracalcium Aluminoferrite (C_4AF) content can usually be considered as low heat cements, while cements high in Tricalcium Silicate (C_3S) and Tricalcium Aluminate (C_3A) typically exhibit high heat liberation (RILEM, 1981). Table 1.1 shows the typical heat of hydration for each of the main cement phases (McCullough and Rasmussen, 1999).

Table 1.1: Heat of hydration of cement compounds

Compound	Heat of Hydration (J/g)
C_3S (Tricalcium Silicate)	500-520
C_2S (Dicalcium Silicate)	260
C_3A (Tricalcium Aluminate)	850-910
C_4AF (Tetracalcium Aluminoferrite)	420
C (Free Lime)	1165
MgO (Magnesium Oxide)	850

The use of mineral admixtures, such as blast furnace slag, fly ash and other supplementary cementing materials, in combination with ordinary Portland cement in a blended cement, have proven to be a cost-effective method for controlling the heat of hydration. The hydration process in blended cements involves the hydration reactions of the mineral additives (pozzolanic reactions) resulting in heat liberation, in addition to that of the Portland cement hydration (Pane and Hansen, 2005). The total amount of heat liberated will depend on the pozzolanic activity and proportion of the added mineral (Snelson et al., 2008). For example, adding silica fume can accelerate the hydration of cement resulting in a higher rate of heat of hydration, while on the other hand, addition of blast furnace slag usually exhibit an opposite trend (Alshamsi, 1997).

The ambient temperature has a significant impact on the rate of hydration and the heat liberated during early-ages. In hot weather, the hydration rate increases leading to more rapid generation of heat. Conversely, in a cold climate, the hydration rate slows down resulting in less heat liberated. Hence, chemical admixtures that affect the kinetics of hydration reactions are used as rate of heat liberation will change (Schindler, 2004). However, the total long-term heat generated usually remains almost unchanged (RILEM, 1981).

1.4.3 Durability of cementitious composites

Most research regarding durability of the fibrecement composites has been concerned with assessing their mechanical properties after exposure to wet-dry cycling. Though the degradation of toughness is fairly well established (Soroushian et al., 1994; El-Ashkar et al., 2002; Akers and Studinka, 1989; Mohr et al., 2005b), only limited research has been published that addresses the chemical and microstructural manifestations of chemical degradation. Previous mechanical testing (Mohr et al., 2005a) has shown that composite mechanical properties degradation does not occur linearly with increasing number of cycles. Major strength losses and toughness reduction occurred within the first five wet-dry cycles. Therefore, an assumption can be made that there may be more than one microstructural mechanism contributing to composite degradation.

Based on the data and scanning electron microscopy (SEM) micrographs collected by Mohr et al. (2005a), a three-part model for degradation during wet-dry cycling was proposed, consisting of (1) initial fibrecement or fibre interlayer debonding, (2) re-precipitation of secondary ettringite within the void space created by the first step, and (3) fibre embrittlement due to fibre cell wall mineralization. This model was intended for cast-in-place pulp fibrecement composites. The use of other manufacturing processes may minimize or prevent the first two degradation steps. The pressure induced during the Hatschek process may result in fibre being compressed and after curing, may not exhibit substantial dimensional changes upon wetting and drying. However, composite degradation may continue directly to the last step, calcium hydroxide re-precipitation within the cell fibre wall – hastening fibre mineralization. The composites also have the potential for lamina swelling and subsequent debonding of the lamina.

Prior to wet-dry cycling, pulp fibres are free to swell and shrink without any hindrance. Upon drying, diametrical fibre shrinkage may create a capillary expulsive pressure on the pore solution residing within the fibre lumen. The

pore solution will be expelled primarily through the fibre ends and pits along the fibre. During this drying, re-precipitation of hydration products can occur in the void space created by debonding. Hydration products such as ettringite occupying these voids, will restrain fibre swelling upon rewetting. During subsequent drying fibre shrinkage is also reduced thus minimizing the driving force for pore solution expulsion, hence retained within the fibre for longer period of time. There will then be deposition of hydration products, likely calcium hydroxide, within the fibre cell wall. This deposition or re-precipitation decreases fibre ductility leading to shorter fibre pull-out lengths in the composite. Fibre embrittlement due to mineralization appears to occur beyond ten wet-dry cycles as indicated by slight increases in composite strength (Mohr et al., 2005a). Bentur and Akers (1989) also found that pulp fibres became embrittled due to formation of hydration products within the fibre lumen. Examining sisal fibres in cement-based composites, the results confirmed the transport of cement hydration products, primarily calcium hydroxide, within the fibre lumen, as well as around the fibres due to wet-dry cycling (Toledo Filho et al., 2000; Savastano and Agopyan, 1999).

Mohr et al. (2006) investigated microstructural and chemical mechanisms responsible for pulp fibrecement composite degradation during wet-dry cycling through SEM, energy dispersive X-ray spectrometry (EDS) and mechanical testing. The research revealed appears that Kraft pulp fibres exhibit poor resistance to degradation due to their inferior dimensional stability, as compared to thermo mechanical pulp fibres. This is due to the high quantity of lignin, alkali sensitive, present in thermo mechanical pulp (TMP) fibres. Hence, composite containing these fibres exhibit improved resistance to degradation during wet-dry cycling. This improvement in durability is attributed to the presence of lignin in the cell wall restricting fibre dimensional changes during wetting and drying thus minimizing fibrecement debonding. Also, lignin acts as a physical barrier to pore solution ingress/egress and prevents re-precipitation of mineral phases within the

fibre cell wall, minimizing fibre mineralization. The presence of lignin in unbleached kraft fibres does decrease fibrecement bond strength and as a result, the tendency for fibre interlayer debonding is decreased as well (Mohr et al., 2005a). Regardless of debonding mechanism, the void created allows for the precipitation of ettringite upon subsequent wetting and drying. This secondary ettringite formed minimizes further debonding, indicated by relative stabilization in the values for first crack strength beyond two cycles and peak strength beyond five cycles (Mohr et al., 2005).

Other studies have shown that the re-precipitation of ettringite in micro cracks and voids of cement paste can occur under normal curing conditions (Batic et al., 2000). Upon rewetting after initial drying cycle, Ca^{2+} (primarily from calcium hydroxide and monosulfate) and SO_4^{2-} may react with $Al(OH)_4^-$ provided by monosulfate to form ettringite. The form of ettringite precipitation, needle-like or sheath-like, depends upon the fibrecement debonding mechanism. Sheath-like ettringite appears to form only in the case of fibre debonding (primarily unbleached Kraft fibre) and needle-like crystals are formed when fibre interlayer bonding was observed (primarily bleached Kraft fibres). The form of ettringite debonding creates a space of 10 – 15 µm while fibrecement debonding appears to create a void space width of only a few microns (Mohr et al., 2006). Therefore, a more constrained void space appears to favor sheath-like ettringite. No radical micro cracking was evident around the Kraft pulp fibres after 25 wet-dry cycles. Thus, ettringite re-precipitation does not appear to exert tensile stresses against the cement matrix which exceed the tensile strength of this region. However, ettringite formation most likely exerts some pressure on the fibre, eventually restricting fibre swelling. Fibre shrinkage upon subsequent drying is minimized or eliminated. Thus, capillary forces responsible for initial expelling the pore solution from the fibre lumen are minimized.

Durability of corrugated fibrecement sheets can deteriorate by water leaching. Compounds, such as portlandite, ettringite, gypsum and calcium

silicate hydrate (CSH), can be removed from the matrix by flow of water (Taylor, 1997). Fibrecement sheets are very thin (~4 – 10 mm) and acid rain, resulting from SO_x pollution, can result in more severe deterioration than leaching. Deterioration from sulfate attack has been widely reported in cement-based materials such as concrete and mortar (Gollop and Taylor, 2005; Zivica and Bajza, 2001). As deterioration starts at the surface, proceed inwardly to the material's core where it creates a deteriorated layer. Zivica and Bajza (2001) used the following equations to explain the acidic attack of cement-based materials:

$$H_2SO_4 + Ca(OH)_2 \rightarrow CaSO_4 \bullet 2H_2O \qquad \text{Eqn 1.2}$$

$$3CaSO_4 + 3CaO \bullet Al_2O_3 \bullet 6H_2O + 25H_2O \rightarrow 3CaO \bullet Al_2O_3 \bullet 3CaSO_4 \bullet (31\text{-}32)H_2O \qquad \text{Eqn 1.3}$$

Deterioration proceeds with carbonation of ettringite, which forms more gypsum (soluble products), calcium and aluminum hydroxide (insoluble products) and releases water (Manns and Wesche, 1969; John et al., 2005; Chen et al., 1994). Ageing affects the properties of fibrecement corrugated sheets, which are directly influenced by the environment to which they are exposed (Dias et al., 2008). Carbonation of the matrix was the main alteration of the sheets. Pore size distribution of the superficial layer and core, mineralogical composition and mechanical performance are indications of these effects. Consequently, it can be concluded that surface leaching can have significant mechanical impact in the thin sheets of fibrecement, potentially limiting its service life.

Berhane (1987, 1994) have reviewed the durability of mortar roofing sheets reinforced with sisal fibres and reported that the service life of roofing sheets made of Portland cement mortar reinforced sisal fibres is very short, deteriorated more in hot-humid climatic conditions. It was noticed that pozzolanic materials have a protective effect on sisal fibres in the cement

composites. Savastano and Agopyan (1992) have studied the transition zone of hardened cement paste having sisal fibres. The effects of water-cement ratio (from 0.30 – 0.46) and the age of the composite (up to 180 days) on this zone characteristics were analyzed. They observed that an increase in the water-cement ratio enhanced the thickness of the transition zone and the accumulation of portlandite crystals without any defined arrangement. The results also showed higher porosity of the matrix near the interface at the initial ages of hydration. The authors proposed a correlation between the interfacial characteristics and the bulk properties – during mixing of the composite, the porous vegetable fibres attract an enormous quantity of water. The fibre debonding from the matrix must be the result of its great shrinkage. The fibre decay was more evident with the increase of the age.

The long-term properties of sisal fibres reinforced-mortar composites were assessed by Toledo Filho (1997) throughout creep, shrinkage and durability tests. The influence of volume fraction, fibre lengths, cure types, mix proportions and replacement of Portland cement by slag and silica fume on the dimensional stability of mortar matrices was determined using drying shrinkage tests for a period of 320 days. The presence of fibres appears to create moisture paths deep into the mortar which enhance the route of moisture loss and aid the development of higher shrinkage strains. Sisal fibres reinforcement increased the shrinkage of the matrix by about 0 – 27%. The mixes with slag and silica fume presented an initial rate of shrinkage smaller than that observed for the mix made with Portland cement. After 320 days, the shrinkage of the silica fume-cement specimens approached that of the Portland cement specimens and still presented a tendency to increase the shrinkage. This behavior may be attributed to the lower permeability of slag-cement matrices, even more so, to silica fume-cement matrices than Portland cement matrices, resulting in a slow rate of moisture loss and hence shrinkage, with time.

The durability of fibre-reinforced mortars after 320 to 360 days, stored under water, exposed to cycles of wetting and drying as well as to outdoor weathering, was assessed by Toledo Filho (1997). Composites manufactured with short sisal fibres and Portland cement matrix showed a significant reduction in toughness after 6 months of ageing outdoors or submitted to cycles of wetting and drying. Some embrittlement was also observed in specimens aged in water. The embrittlement is mainly associated with lignin decomposition and mineralization of fibres due to migration of hydration products, especially calcium hydroxide, to the fibre lumen and spaces, and seems to happen at a higher rate for short fibres. Several treatments were studied by the author to enhance the durability performance of the composites:

- Modification to the matrix through the replacement of Portland cement by undensified silica fume and/or blast-slag;
- Carbonation of the cementitious matrix and
- Immersion of fibres in slurry of silica prior to being incorporated into the Portland cement matrix.

The results obtained indicated that the embrittlement of the composite can be avoided completely by immersing sisal fibres in silica fume slurry before addition to the mix. The early cure of the composites in a CO_2 rich environment and the replacement of Portland cement by undensified silica fume also are efficient approaches for reducing embrittlement of the composite. The use of slag had no effect on reducing the embrittlement of the composites.

Persson and Skarendahl (1980) studied sisal fibre concrete for roofing sheets and other purposes. The influence of matrix strength, fibre content and fibre arrangement on the flexural strength of the composite was investigated. They concluded that an increase in the matrix quality, keeping constant the volume fraction of fibres, increases the flexural strength of the composite. When

changing the volume fraction of continuous fibres, but keeping the quality of the matrix constant, an increase in the post cracking behavior was observed.

1.4.4 Impact of carbonation to mechanical properties of composites

Carbonation in cement based composites is a chemical neutralization process of hydration products (Lea, 1970). It starts at the surface, works inwards and can be accelerated by exposure to natural weathering. The carbonation products of calcium hydroxide are $CaCO_3$ and water and those of CSH are $CaCO_3$, SiO_2 and water. Calcium hydroxide is essentially in crystal form and CSH is amorphous. The steps of the reaction are first the dissolution of calcium hydroxide followed by reaction with dissolved carbon dioxide.

$$Ca(OH)_2 \rightarrow Ca^{2+} + 2OH^- \qquad \text{Eqn 1.4}$$

$$Ca^{2+} + 2OH^- + CO_2 \rightarrow CaCO_3 + H_2O \qquad \text{Eqn 1.5}$$

The mineralogical forms of calcium carbonate are vaterite, aragonite and calcite. Their precipitate follows Ostwald's rule of successive transformation in that order (Cole and Kroone, 1960). The transformation of calcium hydroxide into $CaCO_3$ causes an increase in volume, depending on the crystal form, i.e. 3% for aragonite, 12% for calcite and 19% for vaterite. Calcite is the stable form under normal temperature and pressure. The increase in volume decreases the porosity of the product. Only vaterite is fibrous and adds more microstructural strength than calcite and aragonite. Powers (1962) attributed carbonation shrinkage to the dissolution of calcium hydroxide crystals which are under compression due to the drying shrinkage resulting in formation of stress-free $CaCO_3$ in the pores. Swenson and Sereda (1968) suggested that carbonation promotes polymerization and dehydration of CSH, leading to shrinkage. Furthermore, it has been shown

that at relative humidity higher than 30%, the shrinkage due to simultaneous drying and carbonation is lower than that of the sum of drying shrinkage and subsequent carbonation shrinkage (Kamimura et al., 1965).

It has been shown that an increase in the carbon dioxide concentration does not always induce accelerated carbonation because the released water blocks capillary pores, decreasing carbon dioxide diffusion (Arliguie and Grandet, 1991). At low relative humidity, the pore water content allowing dissolution of calcium hydroxide is the limiting factor of carbonation rate. Carbonation leads to large modification of the microstructure, affects CSH and release water. The loss of water induces shrinkage similarly to drying shrinkage. Carbonation shrinkage can increase the carbonation rate because of the formation of superficial cracks.

1.4.5 Mitigation techniques for shrinkage in cementitious materials

Several methods have been advocated to minimize the cracking potential of concrete, including using coarser cement particles, expansive additives, shrinkage reducing admixtures and/or improving curing conditions (Bentz and Peltz, 2008; Van Breugel and De Vries, 1998; Tazawa, 1999; Nmai et al., 1998). These approaches primarily focus on reducing shrinkage strains in concrete, thereby reducing the level of residual stress that develops (Shah et al., 1998). Adding methyl cellulose, a cellulosic water soluble polymer, has been reported effective on enhancing the interfacial bond between carbon fibres and cementitious matrix (Chen et al., 1997; Fu and Chung, 1998). Results reported by Lin et al' (2012) showed that higher aspect ratio fibres yielded better early age crack resistance. On the other hand, microfibres were reported to act as a local restraint for shrinkage (Zhang and Li, 2001). Microfibres generally bridge micro-cracks, leading to a reduction in crack widths and delaying the occurrence of cracking (Lawler et al., 2003). Water soluble polymers when used in combination with 0.1 – 0.2% fibre content illustrated synergistic effect on reducing the total crack area and the average

crack width by increasing fibre matrix bond strength. Therefore, preventing early age shrinkage cracking by adding water soluble polymers, not only can reduce fibre requirements but keep mixture workable too. .

A case study was conducted by Fiorelli et al. (2012) to evaluate the influence of raw materials applied in the composite formulation on the occurrence of edge cracks in the fibrecement corrugated sheets produced by the Hatschek process (Fiorelli et al., 2012). Sheets of different formulations with PVA and PP fibres, as well as combination of the two fibres, with and without silica fume were evaluated after 24 months of natural exposure. Stacks of roof sheets were orientated with coverage wave facing North (highest incidence of solar radiation in southern hemisphere) and consequently with the waiting wave facing to the south. All stacks were wrapped with transparent plastic cover during the 24 months of analysis to avoid excessive loss of water by evaporation. The results showed higher incidence of edge cracks on the covering waves facing north after 9 months of natural exposure for all formulations evaluated. This implies that exposure to higher temperatures (average temperature >25ºC) maximizes the rate of water evaporation hence increases the shrinkage as a stress-induced edge crack. The increased loss of water in the edge of the sheet stack as compared with the central portion of the stack results in significant moisture gradients and tensile stress over the edge of the sheet. The results also indicated that PP formulations with silica fume in the matrix seemed to be effective to reduce the incidence of cracks in the north facing stacks for up to 6 months. However, the results were inconclusive for PVA formulation. This study showed the possibility of delaying the appearance of edge cracks in stacks while exposed to natural conditions.

A potential microfibre is wollastonite, which is widely used in other industrial applications such as ceramics, plastics, paints, etc. (Azarov et al., 1995). Previous studies have shown the potential for using natural wollastonite microfibres as a reinforcing material in cementitious materials (Low and

Beaudoin, 1992, Low and Beaudoin, 1993, Low and Beaudoin, 1994a). The addition of wollastonite in cement-silica fume matrices showed significant improvements in pre-peak and post-peak load, flexural toughness and ductility (Low and Beaudoin, 1993). Moreover, wollastonite microfibres imbedded in cementitious materials achieved high stability without surface or bulk deterioration with time (Low and Beaudoin, 1994b).

Studies were made on cement concrete and cement fly ash concrete mixes incorporating wollastonite as partial substitute of cementitious material and sand respectively (Mathur et al., 2007). Improvement in flexural strength of concrete by incorporation of wollastonite can be attributed to the modification in microstructure of transition zone in the vicinity of wollastonite. It impacted on pore distribution; water absorption reduction hence drying shrinkage was reduced. Wollastonite inclusion can affect rate and extent of hydration of cement in addition to calcium hydroxide formation and matrix permeability thus impeding water access to cement grains. This may result in limited hydration relative to mixes without wollastonite. The mechanical behavior of cement binders reinforced with wollastonite was confirmed in other studies (Norman, 1993; Low and Beaudoin, 1992).

Sanjuan and Toledo Filho (1998) have studied the influence of fibre reinforcement in controlling free and restrained shrinkage during the early age of mortar mixes; cracking due to restraint, the phenomenon of crack self-healing and the effectiveness of crack control at early age on the corrosion of steel bars in low modulus sisal fibre reinforced mortar composites. Limiting free plastic shrinkage strains of 2300 με and 1700 με were recorded at 300 min after casting for a 1:2:0.45 mortar (proportions by weight of cement, sand and water) with and without 0.2% sisal fibre 25 mm long. The sisal fibres acted as porous bridging elements across cracks and permitted the deposition of new hydration products and the subsequent infill/closure of the cracks.

Carbon fibre addition was found to be effective for decreasing drying shrinkage (Chen and Chung, 1996; Banthia, 1994; Ohama, 1989; Park and Lee, 1993; Chen and Chung, 1993). The effectiveness was further enhanced by surface treatment of the fibres. The significant effectiveness of silane treatments for drying shrinkage reduction showed consistency with its greater impact for improving the mechanical properties and decreasing air void content. The results showed that both carbon fibres and silica fume particles surfaces were bonded to silane molecules. Due to the hydrophilic nature of silane, the treated fibres and treated silica fume are expected to be uniformly distributed in the cement.

Addition of aggregates to concrete and mortar contribute to formation of a transition layer between them and mortar. With proper incorporation of fibres, the failure mode of cement composites can change from brittle to quasi-ductile (Li and Leung, 1992; Li and Wu, 1992, 1992a; Leung, 1996). The toughness of the material can also be significantly increased. Prevention of crack formation is highly desirable in the design of durable thin sheets, fibre-reinforced cement composites. It is interesting to note that irrespective of the type of composite, fibres improve its behavior but the level of improvement at each position is different for different composites. This too depends upon the type of fibres and their geometry. Generally, wollastonite microfibres are fine fibres with lengths less than 10 mm and diameter in range 25 – 40 µm. with their high surface areas (>200 cm^2/g), they provide a large number of fibres in a given section of composites and thus furnish more effective reinforcing mechanisms.

Sharma et al. (2013) found that both wollastonite microfibres and silica fume increase the water demand, initial and final setting time of cement pastes. At their equal ratios, the mix starts losing plasticity very early and sets earlier with respect to pure cement or cement plus wollastonite microfibre mix. Therefore possibility of shrinkage is more for this ration, for blends with the ratio 2:1 of wollastonite microfibres: silica fume, the initial and final setting

time increase and then drops. Increasing wollastonite microfibre content, compression and flexural strength decrease to a small extent due to replacement of cement. But with addition of silica fume these values become comparable to those of pure cement mixtures. It was found that with an increment in wollasonite microfibre content, there was an apparent increment in flexural strength whereas compression strength decreased significantly, when the mixes were compared with control mix at 56 days. It was also found that silica fume addition led to a decrement in flexural strength at lower wollastonite microfibre content. At higher wollastonite microfibre content, the flexural strength rose to more than 20%, with the ageing from 28 to 56 days. The flexural strength improvement in concrete is due to limited fibre action by wollastonite microfibres. Hence, pore size improvement is a major factor apart from fibre action, which improves flexural strength. The rate of flexural tensile strength and compression strength gain in concrete, was less than 60% and 30% respectively as compared to the same gain in mortar.

The cracking strain of brittle matrices, such as cement paste mortar and concrete, could be significantly increased by using closely spaced fibres (Romauldi and Batson, 1963). The experimental studies showed that the stress at which the brittle matrix will crack can be slightly increased by using high modulus fibres but, in general, the cracking strain of the matrix remains unaltered. Considerable modification in behavior of the material was observed once the matrix has been cracked. Although the strain at cracking does not increase due to fibre reinforcement, the tensile strain at rupture does, resulting in tough material with high resistance to impact loading (Bentur and Mindess, 1990). In a well-designed composite the fibres can serve two functions in the post-cracking zone:

- To increase the strength of the composite over that of the matrix by providing a means of transferring stresses and loads across the cracks and

- To increase the toughness of the composite by providing energy absorbing mechanisms related to the debonding and pull-out processes of the fibres bridging the cracks.

A shrinkage reducing admixture (SRA) can decrease the surface tension of the capillary pore solution resulting in a reduction of the capillary tension. It was found to reduce both autogenous and drying shrinkage strains (Bentur, 2003; D'Ambroisa, 2002; Holt, 2005; Esping, 2007; Lura et al., 2007; Bentz et al., 2001). About 60% reduction in the early-age unrestrained shrinkage due to an SRA dosage of 1 – 2% by mass of cement, was observed within the first week after casting concrete (D'Ambroisa, 2002). SRA has a more significant effect at low water-cement ratio. SRA was found to induce early expansion after the time of set, maintaining a higher relative humidity level in concrete, and facilitate water loss from smaller pores, which result in reducing the concrete shrinkage as discussed by Weiss et al. (2008).

Greater early-age shrinkage was observed with the addition of superplasticizer (SP) as a result of improving cement dispersion, which consequently increases the rate of hydration reactions (Holt, 2005; Esping, 2007). Also, it was highlighted that excessive SP dosage would delay the setting time and result in higher early-age drying shrinkage (Holt and Leivo, 2004). However, the general trend was an increase of the autogenous shrinkage rate before it diverges from chemical shrinkage, followed by a decrease thereafter. Conversely, air entraining admixtures were found by Kronlof et al. (1995) to cause a considerable decrease in early-age shrinkage.

It was reported by Xu and Chung (1999a-d) that surface treatment of an admixture improves the mechanical properties, decreases the air void content, improves workability and increases the specific heat of cement paste. Their latest research work (Xu and Chung, 2000) reported the surface treatment of an admixture as effective for enhancing the use of the admixture in reducing the drying shrinkage. The drying shrinkage was decreased by the

use of silane-treated silica fume in place of as-received silica fume. The drying shrinkage strain at 28 days decreased by 5% in the absence of fibres and silane-treated silica fume used in place of as-received silica fume. In presence of both silane-treated fibres and silane-treated silica fume, drying shrinkage strain decreased by 10% and further improved to 15% at 28 days. Compared to cement paste without fibres but with untreated silica fume, the drying shrinkage strain decreased by 25% in the presence of silane treated fibres. When both silane-treated fibres and silane-treated silica fume were added to cement paste, drying shrinkage strain decreased by 32%.

The type, fineness and percentage of cement replacement are the main parameters controlling the effect of pozzolanic materials on early-age shrinkage. Silica fume was found to increase the autogenous shrinkage significantly due to refining the pore structure of concrete (Tazawa, 1999, Wiegrink et al., 1996). Similar behavior was observed for ground blast furnace slag (Lee et al., 2006, Lim and Wee, 2000). A high level of cement replacement by metakaolin (MK) (10 – 15%) was found to reduce both autogenous and drying shrinkage at early age. This reduction may be a result of dilution effect of reducing the cement content (Brooks and Megat-Johari, 2001, Kinuthia et al., 2000). Conversely, Gleize et al. (2007) observed an increase in autogenous shrinkage due to MK addition, which was interpreted as a result of the heterogeneous nucleation of hydration products on the surface of MK particles. Fly ash was also found to reduce autogenous shrinkage of concrete (Lee et al., 2003, Termkhajornkit et al., 2005). In contrast, it was reported that very fine fly ash had a similar effect to that of silica fume (Tazawa, 1999).

Treatment of the matrix to reduce its alkalinity was studied by Gram (1983). The products studied included high alumina cement, replacement of ordinary Portland cement by silica fume, slag, fly ash and natural pozzolans. Replacing 45% of cement with silica fume eliminated the loss of toughness of the composite. A significant improvement was observed when using high

alumina cement and natural pozzolans. With fly ash and slag replacement, however, no marked improvement was observed.

Comparative study of cellulose and PVA fibres reinforced cement, made with different pozzolanic materials partially substituting cement were reported by Nita et al. (2004). Silica fume, being the most common pozzolan in fibrecement composites produced by Hatscheck process, reduces the cement matrix alkalinity. The hydration of silica fume reaction consumes calcium hydroxide released from the hydration of C_2S and C_3S; and diminishes the CaO/SiO_2 ratio of the CSH phase. The pozzolanic reaction increases the content of CSH in the hydrated matrix resulting in refinement of pores. The overall alkalinity reduction as well as permeability reduction aid to protect cellulose fibres from alkali degradation. Metakaolin is a pozzolanic material too. Metakaolin hydration removes calcium hydroxide in a similar way of silica fume, but additional phases to the CSH are formed known as hydrogarnet or hydrogrossular (Frias and Cabrera, 2002, 1996). The results indicated that both pozzolans were effective in calcium hydroxide reduction from the matrix, but the removal was not completed after 28 days of wet curing. Metakaolin samples showed high pore volume content but no significant difference in hygroscopic movement. Water diffusion was remarkably reduced by both pozzolans.

Ninov et al. (2010) studied the kinetics of the pozzolanic reaction of enriched kaolin from the “Senove” deposit in Bulgaria, in saturated solutions of calcium hydroxide. The composition and the structure of the reaction products of kaolinite with hydrated lime were investigated through the preparation and curing of mixtures of clay, lime and water at a definite ratio at various temperatures, ranging from 23 to 60ºC (Arizumi, 1968; Diamond et al., 1964). Based on X-ray diffraction analysis and thermal analysis of reacted mixture, the authors established the formation of the following new phases: a poorly crystallized gel of calcium hydrosilicate and some other crystalline hydrates

containing aluminium – C_2ASH_8 (gehlenite hydrate), C_4AH_{13} and $C_3AS_zH_{6-2z}$ (hydrogarnet).

According to Silva and Glasser (1993), at temperatures ranging from 20 to 55ºC and hydration time intervals of 3 days, C_2ASH_8 and C_4AH_{13} are being formed as primary crystalline phases, but they are thermodynamically unstable and are gradually transformed into hydrogarnet. On the contrary, Rojas and Cabrera (2002); Cabrera and Frias (2001) and Rojas (2006) reported that under identical experimental conditions C_2ASH_8 and C_4AH_{13} are formed as stable products of the pozzolanic reaction and there is no evidence for their conversion into hydrogarnet.

Donchev et al. (2010) studied the pozzolanic reaction in the system kaolinite-lime-water in suspension using saturated solutions of calcium hydroxide. The interaction between kaolin and the portlandite solution indicated that:

- At 100ºC, a structure of needle-like morphology, resembling whiskers was formed upon increasing the duration of lime treatment. Two well distinguished crystalline hydrate phases were formed – gehlenite hydrate and hydrogarnet. Both hydrates were located in the layer of the silicate gel, which in contact with the saturated lime solution formed a needle-like structure.
- After six hours of lime treatment, no other crystalline aggregates were observed, except for those of kaolinite and portlandite.
- After nine hours of treatment, some small crystallites with needle-fibre-like shape appeared in separate zones of the reaction mixture.
- After 24 hour treatment, there was abundant formation of this kind of products.
- At a temperature of 23ºC, the reaction products were identical in shape to those formed at 100ºC, but the process of hydration was slowed down. This was due to a decrease of the rate of the pozzolanic reaction or to a lower rate of crystallization of the secondary products formed (Rojas and Cabrera, 2002).

- Another artificial mineral was formed, which possessed an isometric (cubic) form, characteristic of the hydrogarnet. The transformation of the gehlenite into hydrogarnet is a process, which influences negatively the properties of clay materials stabilized with lime. It is so because the gehlenite enhances the mechanical properties, while the hydrogarnet diminishes the strength of such materials.
- In the process of curing, the amount of needle-fibre-like product diminished as a result of crystal chemical transformation of this product into hydrogarnet.
- The thermo gravimetric results indicated that no transformations were formed at 23ºC, except for dehydration/dehydroxylation of the residual clay minerals. At 100ºC, liberation of physisorbed water and probably dehydration of CSH were observed during the initial step (20 - 220ºC). The dehydration of hydrogarnet was registered as a separate mass loss in the temperature interval between 220 - 400ºC.

Metakaolin reaction rate is rapid, significantly increasing flexural strength, even at early ages, which can allow for earlier release of form work. Mixes with metakaolin at 8% of the total cementitious materials have produced concrete flexural strength increases of more than 20% for one day and 40% at 28 days (Justice and Kurtis, 2007). These authors evaluated the use of metakaolin with different surface area through measurements of workability, setting time, strength, elastic modulus, heat evolution and calcium hydroxide content. The results showed improved flexural and flexural strength of concrete and the rate of increase was faster with the use of finer metakaolin. The addition of metakaolin increased early age (i.e. 1 – 3 days) flexural strength by as much as 60%. The effect of metakaolin surface area was more evident at the lower water-to-cementitious materials ratios examined and generally at later ages (i.e. ≥ 7 days). However, although greater in the metakaolin-cement concretes than the ordinary concretes, particularly at

lowest water-cement ratios examined (0.40); elastic modulus measured at 28 days was not affected by the metakaolin surface area. The greater surface area metakaolin caused a greater and more rapid heat evolution, indicating higher reactivity and a greater rate of hydration product formation. Metakaolin decreased calcium hydroxide content compared to control concrete, with the consumption of calcium hydroxide extending beyond 14 days. Surface area measurements indicated a more refined pore structure relative to control by 28 days. These analyses illustrated the effect of metakaolin fineness on pozzolanic reactivity, associated calcium hydroxide consumption and pore structure refinement, leading to enhanced mechanical properties of metakaolin concretes.

In addition to increasing strength, the densification of the microstructure that results from the pozzolanic and hydraulic reactions of metakaolin also leads to greater impermeability. Very low 28 day rapid chloride permeability test (RCPT) results have been reported for concretes containing 8% metakaolin at water-cement ratios of 0.40 and 0.50, with the metakaolin concrete achieving remarkably lower RCPT values than other comparable mixes (Justice et al., 2005). In concretes containing metakaolin at 8 to 12% of the total cementitious materials, 50 – 60% decreases in chloride diffusion coefficient suggest that significant improvements in service life can be achieved through metakaolin utilization in chloride environments (Gruber et al., 2001). In addition, metakaolin has been shown to be highly effective in mitigating expansion due to alkali-silica reaction (ASR) and sulfate attack (Khatib and Wild, 1998; Ramlochan et al., 2000).

When pozzolanic materials are added with cement in a fibrecement based composite, the reaction between these materials and calcium hydroxide forms calcium silicate hydrates in the hydrated cement matrix (Taylor, 1997; Vedalakshmi et al., 2003) and refine the pore structure depending on the hydrated material that is actually formed. Addition of a finer material that results in higher strength is more durable.

Some mineral additions are finer than cement particles. They improve the particle packing of cement paste, in particular in the transition zone between aggregate and the cement paste, filling the pores thus reducing the permeability. The smaller particles allows filling up of the voids between the larger cement and aggregate grains, contributing to a less porous composite (Smith and Midha, 1997). There is also an effect of reduction of the size of the average pore which is significant for the mechanical strength of the cement matrix (Taylor, 1997).

Bezerra et al. (2006) evaluated the effect of different types of pozzolans and carbonate addition on the physical and mechanical properties of cementitious composites containing cellulose and synthetic fibres. The study concluded that the lowest permeable void volume was related to the formulations with metakaolin additions both at 28 days of age and after the accelerated aging test. They also established that the reduction in strain to failure and toughness after 50 soak and dry cycles was more abrupt to the formulations containing lower concentration by mass of the PVA fibres. The observed reduction of strain to failure and toughness values can be attributed to the densification of fibre-matrix transition zone and consequently to the improved bond of the fibres. Incorporation of silica fume into cement based composites resulted in enhanced strength performance for the composites after accelerated aging test. The toughness measurements of composites after exposure to soak and dry cycles also showed that silica fume prevents fibre degradation.

Organosilanes are widely used chemicals for the modification of surface properties (Plueddemann, 1990) and mostly performed in alcoholic solutions (Brochier-Salon et al., 2008). Silane treatment can be carried out by hydrolyzing silane into silanol, reacting with surface hydroxyl groups of cellulose, thus forming a covalent bond, which can restrain the swelling of fibres. The swelling of natural fibres in moisture conditions is due to water uptake by the hydrophilic hemicellulose. Water uptake can be reduced by

thermal/hydrothermal treatment but results in deterioration of fibre properties. However, temperatures of about 120ºC, the degree of polymerization starts to drop, causing increased fibre brittleness and reduced strength. Previous work done by Paquet (2010) focused on providing a better understanding of the reactions undergone by organosilanes in purely aqeous media.

Tonoli et al. (2009) evaluated the effect of surface modification of cellulose pulp fibres on the mechanical and microstructure of fibrecement composites. Surface modification was performed with methacryloxypropyl tri-methoxysilane (MPTS) and aminopropyl tri-ethoxysilane (APTS) in an effort to improve their durability in fibrecement composites. The choice of silane coupling agents is dependent on their mechanism of interaction that consists of the formation of a continuous hydrophobic siloxane network responsible for the formation of interfacial bonding (Abdelmouleh et al., 2002). Hence the objective is to protect the cellulose fibres from water uptake and improve the quality of the fibre-matrix interface.

The composites were prepared in the laboratory using eucalyptus bleached pulp. The results showed no significant differences on the physical properties between the composite with modified and unmodified fibres, after 28 days curing. Nevertheless, after 200 ageing cycles, composites with APTS-treated fibres resulted in lower water absorption and apparent porosity. Low surface energy fibres would suffered slow disjointing and increase the porosity while high surface energy would slowly promote intimate contact between fibres and cement materials. Xu and Chung (1999a) reported the lower porosity of composites reinforced with silane-treated (mixture of N-(β-amino ethyl)-ɣ-aminopropyltri-methoxysilane and ɣ-glycidoxypropyltri-methoxysilane) carbon fibres. The authors attributed this behavior to the hydrophilic character of the silane used, which improved the fibre-matrix bonding. It was also found that in the MPTS-modified fibre-reinforced composites, the fibres are not filled with hydration products due to the formation of MPTS sesquisiloxane macromolecules during hydrolysis (Mohr et al., 2007). These

macromolecules are adsorbed on the surface of the cell wall fibres and act as a barrier to the aqueous solution. It prevents re-precipitation of mineral phases within the fibre cell wall, minimizing fibre mineralization by interpenetration of cement hydration products. The surface modification of fibres showed significant influence on the microstructure of the composite. Accelerated ageing cycles decreased modulus of rapture (MOR) and toughness of composites indicating the degradation of the composites irrespective of treatment.

Yamane et al. (2006) attempted to clarify the hydrophilic and hydrophobic nature of cellulose based on its structural anisotropy. The authors proposed that the hydrophilic behavior of cellulose was due to the location of hydroxyl groups at the equatorial positions of the glucopyranose rings. Conversely, the axial direction of the glucopyranose ring is hydrophobic because atoms of C-H bonds are located on the axial positions of the ring. Since there is a large amount of hydroxyl groups along cellulose chains, strong hydrogen bond networks can be formed, which makes cellulose a relatively stable polymer with a high axial stiffness, thus a desirable component for reinforcement in a composite. According to the authors, this suggests that the hydrophobic property of cellulose may be created by structural controls such as reversing the planar orientation. Several approaches have been explored, such as physical treatments by corona (Belgacem et al., 1994) or plasma (Tu et al., 1994), and chemical grafting with molecules and macromolecules which display a good compatibility with the matrix and introduce surface hydrophobicity (Trejo-O'Reilly et al., 1998; Botaro and Gandini, 1998; Gandini et al., 2001; Rowell, 1980; Zadoreki and Flodin, 1985; Kokta et al., 1990a; Vadez et al., 1999).

The chemical modification by coupling agents susceptible to react with the fibres and the matrix constitutes a particularly astute way of controlling the quantity and nature of the groups present at their surface. Moreover, it creates covalent bridges between the fibres and the matrix which ensure the

best mechanical properties for the composite. Studies on the interaction between silane-based reagents and cellulose, and the effect of this treatment on the mechanical properties of the composites have been published (Kokta et al., 1990a; Vadez et al., 1999). These studies concentrated on the final result and did not focus on the actual interactions between cellulose and the silane used.

Research work was conducted to evaluate the effects of the supercritical carbonation in the curing stage, after pre-curing for three days, on extruded fibrecement reinforced with bleached eucalyptus pulp and residual sisal fibres (Santos et al., 2012). The effect of carbonation in the cement paste composition, porosity and permeability has been widely reported in literature (Peter et al., 2008; Fabbri et al., 2009). Accelerated carbonation curing has been identified as the technology which may have the potential for the mitigation strategy to reduce deterioration of cellulosic fibres and improve mechanical behavior of these composites (Almeida et al., 2010; Soroushian et al., 2012; Toledo Filho et al, 2003). The supercritical CO_2 has a high diffusion coefficient due to low viscosity; low surface tension and a density that is higher than gaseous CO_2 at atmospheric pressure and temperature conditions. The results indicated the escape of the pore water at 100ºC, different stages of dehydration of the CSH observed between 100 and 300ºC, thermal decomposition of cellulose fibres from 300 to 380ºC, dehydroxylation of calcium hydroxide at 450ºC and decarbonation of $CaCO_3$ at 700ºC.

The massive precipitation of $CaCO_3$ after supercritical carbonation in the early age leads to decreased water absorption and an increase in bulk density (Santos et al., 2012). This can be explained by carbonation products filling the pores thus leading to the pore refinement of the microstructure. It was also noted that non-carbonated composites had higher amount of capillary and gel pores before and after accelerated ageing. The low viscosity and high density of supercritical carbon dioxide allowed the massive

precipitation of $CaCO_3$ during the accelerated carbonation reducing the amount of capillaries and gel pores around fibres. The results showed an improvement in the fibre-matrix interface caused by supercritical carbonation in the curing stage, mainly after exposure to 200 soak and dry cycles. Thierry et al. (Thierry et al., 2005) has reported the reactions involved in the carbonation process and Kalbskopf (2002) noted that formation of calcium carbonate increased density, stiffness, bending or tensile strength and lowered dimensional instability of fibrecement composites. Carbonation reduced porosity and slowed down liquid transportation. It also reduced the alkalinity of pore water.

The curing method, duration and temperature have a significant effect on early-age shrinkage. Shrinkage was found to increase with increasing curing temperature during the first 10 hours after casting, and then it decreased with temperature increase. This may be attributed to an increase in moisture loss at high curing temperature, leading to an increase in the development of plastic shrinkage (Zhao, 1990). Furthermore, the longer the curing period, the lower was the shrinkage deformation (Tazawa, 1999).

1.5 Structure of the thesis

The thesis consists of seven chapters. Chapter 2 is the experimental methods and materials considered as possible mitigation techniques. A more detailed description of the experimental setups is given here, complemented with some analysis of the methods. Analysis techniques are also briefly discussed. The third chapter describes surface coating of cellulose fibres as mitigation technique before addition to cement matrix. The physical and mechanical properties of the fibrecement composites incorporated with surface coated cellulose are studied, as well as durability in accelerated weathering and ageing conditions. The impact of wollastonite inclusion in the formulation of fibrecement composites is studied in chapter 4. To be able to

determine shrinkage, wet-dry movement and accelerated ageing tests were conducted for air-cured products. Image analyses were done to evaluate the effect of wollastonite on the microstructure of the composite. The performance of fibrecement materials with silicone resin and superplasticizer admixtures as water repellents is presented in chapter 5. The physical properties were compared with those of the current mix formulation. Mechanical behavior of these materials was also evaluated. The durability of corrugated fibrecement sheets incorporated with kaolin is studied in chapter 6. To be able to determine durability, wet-dry cycle tests and accelerated ageing tests were conducted. Effects of curing conditions and carbonation under natural exposure were evaluated. Chapter 7 summarizes the conclusions of this study, and presents some recommendations for future research.

1.6 Original contributions

This research introduced a series of investigations related to the shrinkage and the role of different shrinkage mitigation techniques under laboratory and natural exposure conditions. It explored the influence of a wide range of outdoor conditions and the efficiency of available shrinkage mitigation strategies. Also, it proposed new strategies to production of corrugated fibrecement composites with lower shrinkage and less risk of cracking. Specific original contributions of this thesis include:

- Evaluating the performance and efficiency of different shrinkage mitigation techniques and their interaction with the surrounding environment. Also, investigating combination of these techniques for optimal shrinkage reduction.
- Identifying external curing conditions essential for shrinkage mitigation techniques to work adequately.

- Implementing the use of kaolin as a natural pozzolan in corrugated fibrecement composites as a replacement of cement, which has economic and environmental benefits. More specifically, (i) kaolin enhanced the flexural strength of composites; (ii) kaolin promoted pore discontinuity, leading to lower moisture movement hence reduction in drying shrinkage.

1.7 Concluding remarks

Based on the literature review, the mitigation technique suggested by Akers (2006) – shrink wrapping corrugated sheets in a stack with transparent plastic – has been implemented on site but as soon as the stacks are exposed to natural condition without the wrapping, edge cracks appear. This research looked at modification of the microstructure of fibrecement composites as a mitigation technique. Wollastonite has succeeded in having an effect in concrete microstructure hence a potential mitigating material in fibrecement composites. Most of the research work has been reported on pozzolans such as silica fume and metakaolin but no literature could be found on kaolin in air cured fibrecement composites. The idea behind investigating kaolin in its natural state, before calcination, was to determine its impact on the mechanical properties and microstructure of fibrecement composites as it is cost-effective than that of calcined kaolin (metakaolin). Since cellulose is hydrophilic and responsible for retaining the water in the fibrecement composite, surface treatment of these fibres is the solution to drying shrinkage as well as durability of these materials. The work documented was conducted with eucalyptus bleached pulp and showed promising results. There are new silanes that have been developed recently and this research evaluated their performance with unbleached softwood pulp, physical properties of modified cellulose fibrecement composites and durability of these composites.

CHAPTER 2 – METHODOLOGY AND ANALYTICAL TECHNIQUES

2.1 Hatschek process

The process for fibrecement composite manufacturing was originally developed by Ludwig Hatschek at the end of the 19th century based on the paper industry process. This is a continuous operation using slurry of cement, water, fibre and additives to form a flat sheet. The forming machine relies on winding very thin sheets (often one millimeter or less in thickness) around an accumulator roll until the target thickness is achieved. At this stage, the green sheet is cut, drops onto a conveyor belt that carries it on for further processing (i.e. pressing, embossing, corrugation, etc.) (Buchmayer, 1999).

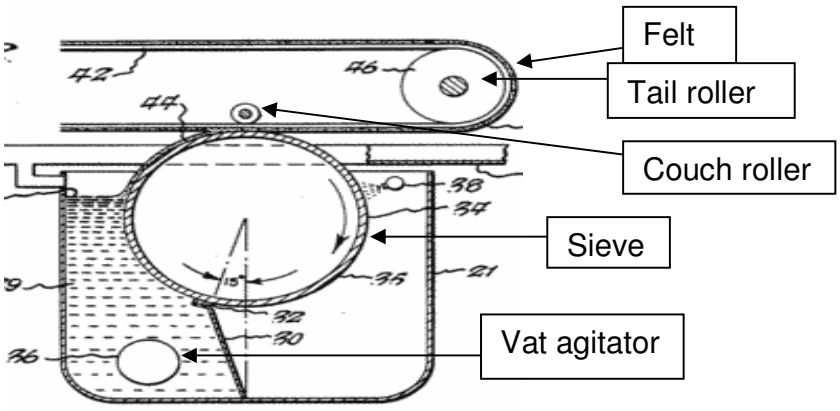


Figure 2.1: Schematic diagram of a vat component

The fundamental part of the Hatschek machine consists of a vat in which a cylindrical sieve rotates in contact with dilute water based slurry of fibres capable of forming a filtering film and mineral materials including Portland

cement (see Figure 2.1). The sieve cylinder is driven by a continuous felt wrapped around the top of the sieve by a couch roller. The felt is threaded around an anvil roller and a tail roller (Cooke). The anvil roller is pushed into contact with an accumulation roller, Figure 2.2.

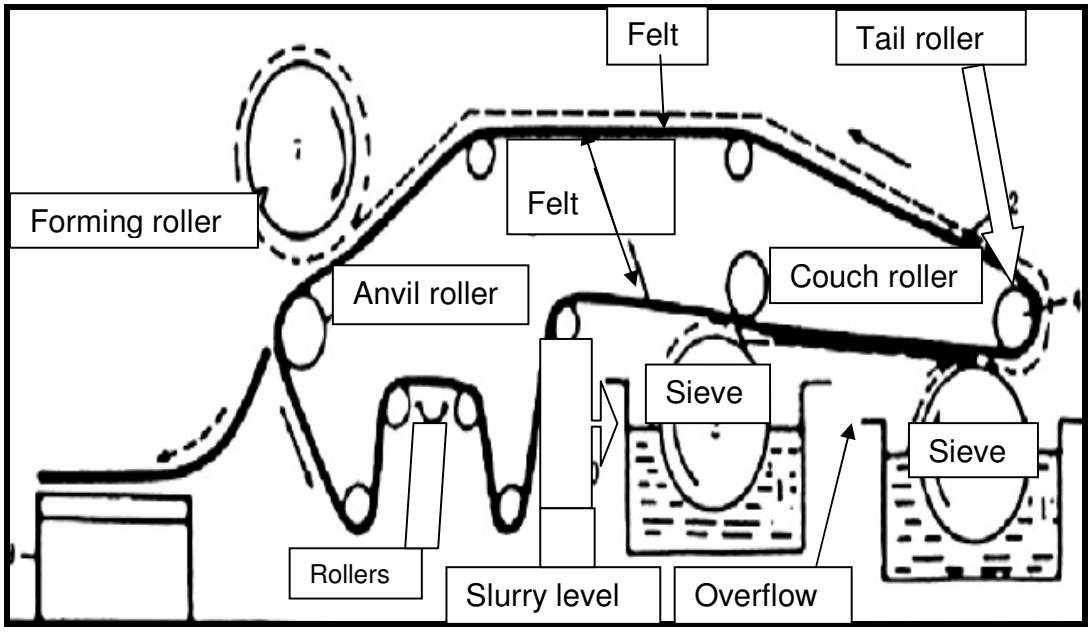


Figure 2.2: Schematic diagram of Hatschek Machine showing principal components

The sheets are formed on the machine as the clean cylindrical sieve is rotated in contact with slurry of fibres and non-fibrous materials. A filter layer of fibres forms on the surface of the sieve upon immersion into the slurry. The sieve brought into contact with the felt stretched tightly across the sieve. This removes much of the water from the film by forcing it back through the film. The film continues to build up on the sieve but now contains a lower proportion of fibres and greater amount of non-fibrous materials. The solid film floats on this layer of water and is transferred to the felt partly in response to the effect of removal of water and partly because the felt has a

greater affinity for the film than the sieve. The film carried on the felt, dewaters as it passes above the vacuum boxes, to an accumulator roll to which it was transferred by further removal of water at high pressure. The film was wrapped on the accumulator roll in a number of turns to form a sheet of the desired thickness, then removed from the roller and dropped on the conveyor belt as a flat sheet. The dewatering process under pressure was sufficient to bind the films together and formed a solid sheet.

For the pilot plant:

The pilot trials made were 20 kg batch sizes. The raw materials were all mixed in the stirrer and then transported to the mix box. There, the flocculant was added at 130 ppm to the mix followed by a thin layer of the mix transferred to the felt which finally formed multilayers on the production roller. The felt passed through a single vacuum box and the machine contained only a single vat. After a buildup of six turns on this roller the sheet was cut off the roller. The flat sheet was cut into 250 mm x 250 mm samples, placed onto steel plates, shrink-wrapped with transparent plastic and cured under laboratory conditions for 28 days. All the results of samples made in the pilot plant included mini machine as part of identification.

For production plant:

The sheets were transferred to the corrugator at the end of the machine, corrugated into a width of 920mm then stacked onto steel form plates and pushed into the steam chamber for 8 hours at 65ºC. At the end of this period, the sheets were taken off the steel plates, stacked in a pile of forty sheets and shrink wrapped in transparent plastic. The curing of the sheets took place in a closed area under cover, tested at intervals of 7 days.

The basic mechanism of film formation is by filtration. The sieve apertures are approximately 400 µm and the non-fibrous materials are significantly smaller than the apertures hence would pass through the sieve. On the other hand, the fibres bridge the wires of the sieve thus entrapping the non-fibrous

materials. Therefore, the entrapment process depends on the formation of a filter layer of fibres on the surface of the sieve. The efficiency of the formation of this layer depends on the refining process of the fibres, where fibres are fibrillated, and providing means of fibre entanglement with each other. The process results in the ability of fibres to form a network of fine fibres capable of trapping the larger non-fibrous particles. This forms an initial layer on the surface of the sieve that builds up forming the film.

2.2 Test methods

2.2.1 Determination of water absorption and apparent density

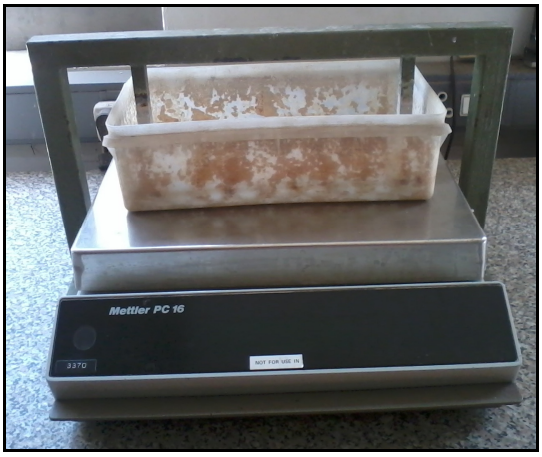
Water absorption is the measure of pore space in the material. It gives an indication of how dense the material is or the packing structure of the material. The higher the water absorption, the more porous and less dense the material will be. The volume of a saturated specimen is determined by weighing sample immersed in water. The tests were carried out as per ISO 9933 (1995) standard.

Apparatus:

- Oven, ventilated, capable of achieving a temperature of 100 ± 5ºC with full load of specimens.
- Balance, accurate to within ± 0.1% of the specimen mass, equipped to determine both the immersed mass and the non-immersed mass of the specimens, Figure 2.3.

Water bath filled with water to the ¾ mark

Sample placed on basket before immersion in water



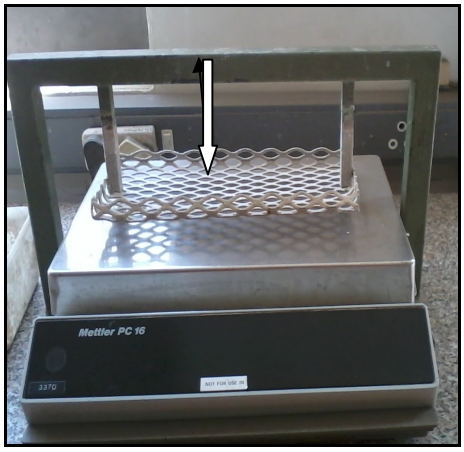


Figure 2.3: Balance capable of weighing dry and wet specimens

Test Procedure:

- Five specimens of 40 mm x 60 mm were prepared from the cured sheets.
- The specimens were immersed in water for at least 24 h to obtain complete saturation. After this period, the specimens were removed from the water bath and excess water wiped off with a cloth.
- The wet specimen was placed on the balance after zeroing it and the mass recorded, value to be used for water absorption calculation.
- The same specimen was placed in the basket and weighed in water. This is the volume for density measurement.
- The specimens were then dried in a ventilated oven at 100 ± 5ºC until constant mass was reached (24 h).
- After drying, the specimens were cooled in a desiccator and weighed, dry mass.

Calculations:

$$Water\ absorption\,(\%) = \frac{(A-B)x\ 100}{B} \qquad \text{Eqn 2.1}$$

$$Density\,(g/cm^3) = \frac{B}{C} \qquad \text{Eqn 2.2}$$

Where A is the mass of wet specimen measured in air, in grams;

B is the mass of oven dry specimen, in grams;

C is the mass of wet specimen in water, in cubic centimeters

2.2.2 Measurement of mechanical properties of corrugated sheets

Mechanical testing is a legal requirement for building materials. There are standards prescribed by South African National Standards (SABS ISO 9933, 1995) that must be adhered to.

The tests were carried out on corrugated sheets after immersion in water for 24 h to achieve saturation. The values of the force and deflection at breaking point were obtained directly from the instrument.

Apparatus

- Bending test machine, with a constant rate of deflection when applying the load and with an error of reproducibility ≤ 3% as shown in Fig. 2.4.
- The machine comprises of:

i. Two parallel supports in the same horizontal plane and longer than the sample width. The upper surface of the support is flat, 50 mm in width

and lined with a 10 mm thick strip of soft material. The distance between the supports is 1.1m.

ii. A flat loading beam of 230 mm width located parallel to and equidistant from the supports, attached to the mechanism by means of a flexible joint. The base surface of the beam is also lined with a 10mm thick soft material.

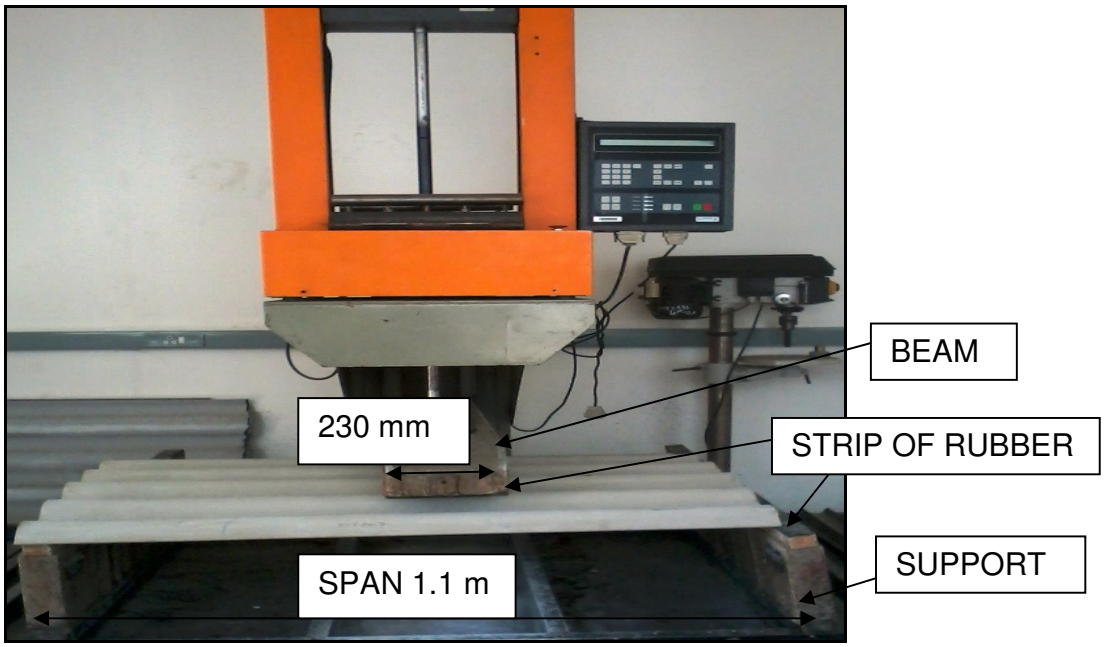


Figure 2.4: Lloyd machine for measuring breaking load of corrugated sheets

Test Procedure

The geometry of the transverse loading is a three-point bending test. Before testing, the sheets were immersed in water at an ambient temperature greater than 5ºC for 24 h. The sheets were then removed from the bath, left in a vertical position for 3 min to eliminate excess water. Then placed on the supports at right angles with the corrugation and loaded at midspan by the flat beam evenly distributing the load applied to its center. The load was then applied until the sheets broke into half.

Calculation

The breaking load is usually defined per unit width of the sheet (in this case 920mm).

$$Breaking\ load\ (kN/m) = \frac{Force\ at\ breaking\ point\ (kN)}{width\ of\ sheet\ (m)} \qquad \text{Eqn 2.3}$$

In bending loadings, it is the moment of inertia that determines when the sample/product breaks since the span between the supports is also relevant (Vidovic et al., 2010). In the transversal loading, the moment of force could be used as the criterion for the quality of corrugated sheets; the span between the supports is uniquely prescribed by the standard (Fig. 2.4).

2.2.3 Test method for determination of fibrecement modulus of rupture (MOR)

The pilot machine does not have a corrugator therefore the sheets produced in this plant were flat with no corrugations. Hence the bending strength was tested as the MOR. A specimen of 250 mm x 250 mm was cut from a sample sheet and subjected to a flexural bending load until failure occurred, the failure load and specimen thickness were recorded. The test was repeated on the specimen with the bending mode at right angles to the initial test. The average modulus of rupture for the material is calculated from both test results.

Apparatus

Lloyd test machine, capable of applying a load at a constant rate of deflection with an error of accuracy and an error of repeatability of 3% comprising:

- Two parallel horizontal supports, free to permit alignment with the specimen (Fig. 2.5)
- A loading beam
- A computer with a Nexygen Plus software

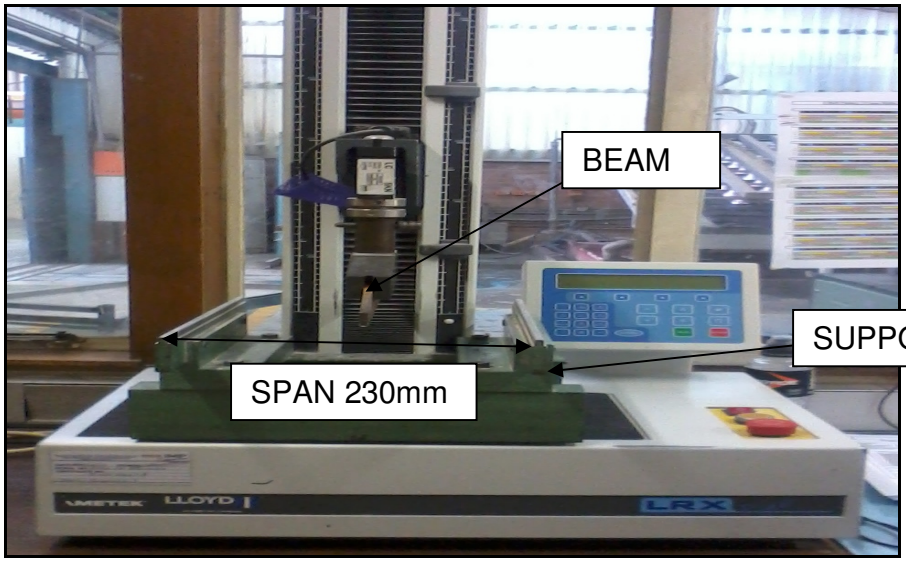


Figure 2.5: Lloyd machine for testing bending strength of flat fibrecement composites

Test Procedure

Samples were immersed in water for 24 h to attain full saturation. They were then removed from the water bath and the excess water wiped off with a cloth. The samples were then placed on the supports (span 230mm) of the Lloyd machine and the force applied until the composite sample broke. The force at the breaking point was recorded, thickness of the sample measured and the width of the sample recorded.

Calculations

The MOR, in mega Pascal's, for each breaking load direction is given by equation 2.4:

$$MOR = \frac{3FL}{2bt^2} \qquad \text{Eqn 2.4}$$

Where: F is the breaking load in Newtons;

L is the span between the center-lines of the support, in millimeters;

b is the width of the test specimen, in millimeters;

t is the thickness in millimeters

2.2.4 Test method for soak-dry evaluation of fibrecement sheets

Paired fibrecement specimens were cut, from the corrugated sheets, into smaller sizes of 250 mm x 250 mm. One of each specimen pair was subjected to a number of test cycles comprising a period of immersion in ambient temperature water and drying in an oven. A comparison of the bending strengths of the specimens exposed to soak-dry cycling test to the exposed specimens was conducted.

Apparatus

- Oven, ventilated, capable of maintaining a temperature of 100 ± 5ºC at a relative humidity of less than 20% with a full load of specimen.
- Water bath, with water at ambient temperature (>5ºC). The water in the water bath was saturated with soluble salts derived from the fibrecement sheets.
- Test equipment for measuring length (Fig. 2.6) and bending strength (Fig. 2.5).

Test Procedure

- The sheet specimens were divided into pairs to form two sets of 10 specimens each.
- One set of specimens was conditioned to the laboratory conditions. Following the conditioning period, the bending strength of these specimens was determined in accordance with section 2.2.3.
- The second set of 10 specimens was immersed in the water bath for 24 h to commence the soak-dry test cycle. The soak-dry test cycle consisted of:
    i. immersion in water at ambient temperature for 24 h,

ii. drying in a ventilated oven, as described in apparatus section above.

- At the end of each interval, the length of each specimen was measured and recorded. The instrument (Fig. 2.6) was switched on, zeroed with the steel plate in place. The steel plate was removed, substituted with the specimen and the value displayed by the instrument was recorded.
- The soak-dry test cycle was repeated until a constant change in length was obtained. At this point, the bending strength of all the specimens was evaluated.

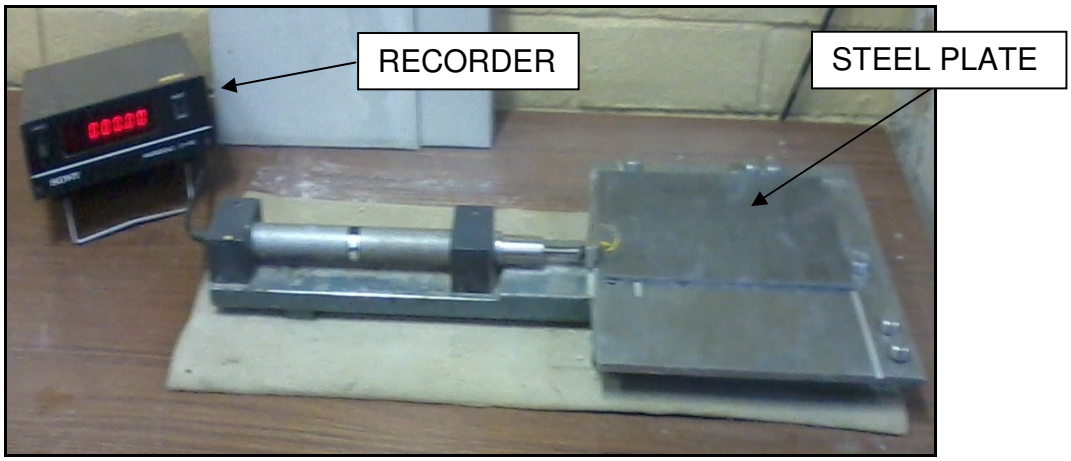


Figure 2.6: Instrument for measuring lengths of fibrecement sheets

Calculation

The linear expansion, L_E, expressed in mm/m, due to a change in the moisture is calculated from Equation 2.5:

$$L_E\ (mm/m) = \frac{(l_w - l_d)x\ 1000}{l_d} \qquad \text{Eqn 2.5}$$

Where l_w is the measured length of saturated specimen, in mm;

L_d is the measured length of oven-dry specimen, in mm.

2.2.5 Test method for determination of moisture movement characteristic of fibrecement sheets

Twenty samples were cut from fully cured sheets such that each specimen contained two full corrugations. The specimens were conditioned in air, at ambient temperature and relative humidity, in the laboratory for 6 days. Two of the samples were drilled and two steel pins glued on the corrugation, 20 mm from the edges, onto each sample with epoxy glue.

Apparatus

- A vernier caliper, maximum length 300mm
- Balance, accurate to within 0.1% of the specimen mass

Test Procedure

- Each specimen was weighed after conditioning and, internal and external lengths measured for each specimen with steel pins.
- The intervals for measurements were initially at ambient temperature, then after 4 days immersion in water followed by hourly measurements while drying in the oven at 80ºC for the first day. Then once on daily basis thereafter for 4 days.
- The recorded weights were used to calculate percentage moisture changes and the length measurements for movement calculations.

Calculation

The calculation is similar to the one above in Equation 2.5.

2.2.6 Test method to determine impact of accelerated carbonation to fibrecement composite sheets

Samples of 250 mm x 250 mm were prepared from the sheets.

Apparatus

- Oven, ventilated, capable of achieving a temperature of 100 ± 5ºC
- Carbonation chamber
- Water bath at ambient temperature, filled with water saturated with salts from the fibrecement sheet

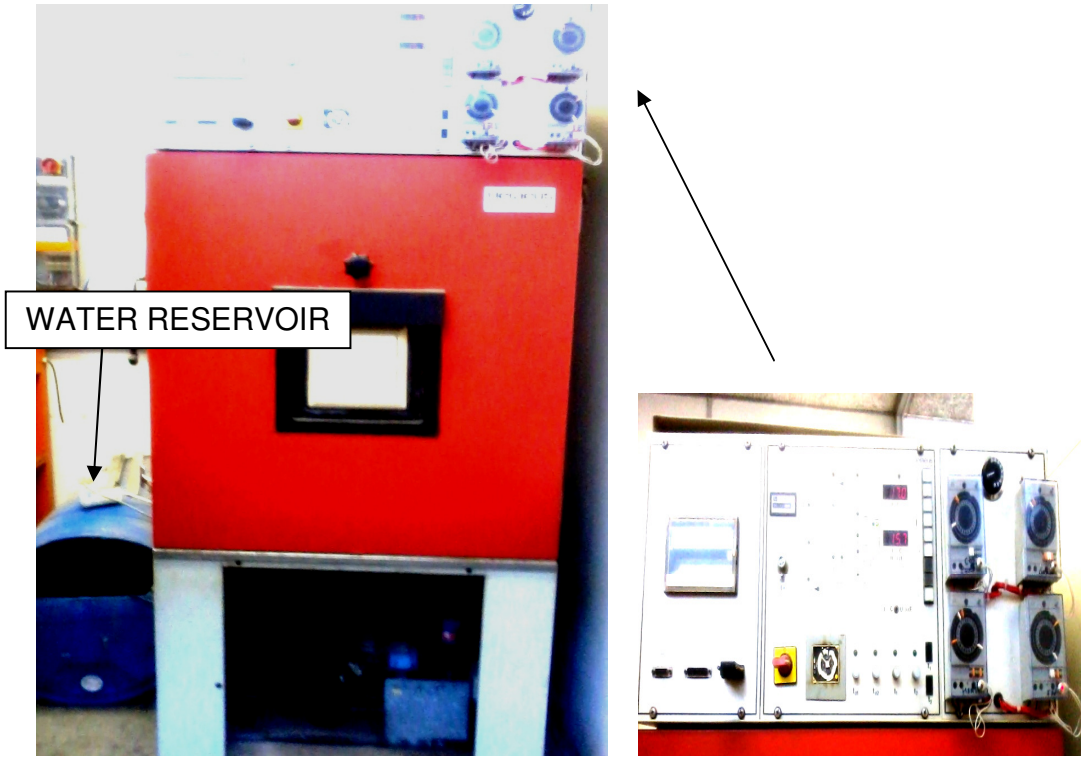


Figure 2.7: Accelerated carbonation chamber, with switches to change over from carbonation to ventilated oven to filling water bath with saturated water

Procedure

The exposure test and measurements were carried out as per following cycle:

- Dry samples in ventilated oven at 80ºC – length measurement
- Immersion in water at 20ºC for 8 hours – length measurement
- Dry samples in ventilated oven at 80ºC for 1 hour

- Exposure to CO_2 for 15 hours – length measurement
- Dry samples in ventilated oven at 80ºC for 8 hours – length measurement
- Immersion in water at 20ºC for 16 hours – length measurement
- Dry samples in ventilated oven at 80ºC for 1 hour
- Exposure to CO_2 for 15 hours – length measurement
- Then the cycle was repeated.

At the end of the test, mechanical properties were tested then comparison done to the specimens not exposed to these conditions.

2.2.7 Test method for the evaluation of heat-rain performance of fibrecement sheets

Sample sheets are fixed to a framing system to simulate a typical sheet installation system. One side of the test assembly was subjected to a number of test cycles comprising a water spray and radiant heating. A visual assessment of the sheet performance was done.

Apparatus

- Framing system, inclined at 25º ± 5º, placed in a space without draught but well ventilated.
- Water sprinkling system, capable of completely wetting the sheet faces (upper side), having a water flow rate of approximately 2.5 $l/m^2/min$ (Fig. 2.9)
- Ultra-violet (UV) lights at close proximity to one another, capable of heating and uniformly maintaining a blackbody surface temperature of 70 ± 5ºC on the surface at the crown of corrugations. (Fig. 2.8)



Figure 2.8 Heat cycle, using UV lights, simulating sunlight over a prolonged period



Figure 2.9 Rain cycles, simulating rainfall, evaluating permeability of sheets

Test Procedure

- The sheets were laid with simulated overlaps at the edges then fixed to the frame using screws.

- The corrugated sheets were subjected to 25 water spray and drying cycle as given in Table 2.1.

Table 2.1: Heat-rain cycle

Cycles	Duration
Water spray	2 h 50 min ± 5 min
Pause	5 min to 10 min
Radiant heat	2 h 50 min ± 5 min
Pause	5 min to 10 min
Total cycle	5 h 55 min ± 15 min

- After 25 cycles, visual inspections for cracking, delamination, water permeability and other defects were conducted.

2.2.8 Test method for flocculant selection

Flocculants are required in the manufacturing of asbestos free, PVA superplasticizer products. The slurry is positively charged and the polymers used are negatively charged, therefore the oppositely charged particles attract each other (Winter et al., 2012). Consequently a bridge is formed between the polymer and the particles. The correct selection of flocculants is crucial in the process due to its effect on mineral fines retention, dewatering, formation and, as a consequence, on the overall efficiency of the machine (Blanco et al., 2006). Therefore, optimisation of the flocculant process during fibrecement production is the key issue for the fibrecement industry.

The molecular weight and charge density of the polyacrylamide polymers used varied from one polymer to the other. Floc A had 10 – 12 million Daltons and 20 – 25 Mol% charge density, Floc B 10 – 15 million Daltons and 20 – 25 Mol%, Floc C 10 – 15 million Daltons and 25 – 30 Mol% charge density. Flocculants B and C were blended together in the ratio 40:60.

Apparatus

- 500 ml beakers
- Magnetic stirrers
- 1000 ml measuring cylinders
- Stop watch
- Hobart mixer
- 1000 ml container with sieve at the bottom, Fig. 2.10

Test Procedure

Flocculants are added to the process for solid retention in the vat and for settling solids in the cone tanks.

- A solution of 1% was made with floc A and also with the blended flocculants, stirred for 2 hours to achieve polymerization.
- Fibrecement slurry was prepared by mixing cement, cellulose fibres, PVA fibres and additive in water using the Hobart mixer.
- The slurry was divided into seven equal portions of 500 ml and flocculant was dozed into the slurry in the seven beakers varying from 90 ppm to 150 ppm respectively.
- Immediately after flocculant dosage, the slurry was mixed until a homogeneous mixture was obtained. It was then poured onto the container, with the 45 mesh sieve at the bottom in order to simulate the dewatering in the vat of the Hatschek machine, and timed for a minute while filtration took place.
- The filtrate was filtered through a filter paper in a Buchner funnel. The solids in the filter paper were dried in the oven at 80ºC for 24 hours and the retention calculated.

Calculation

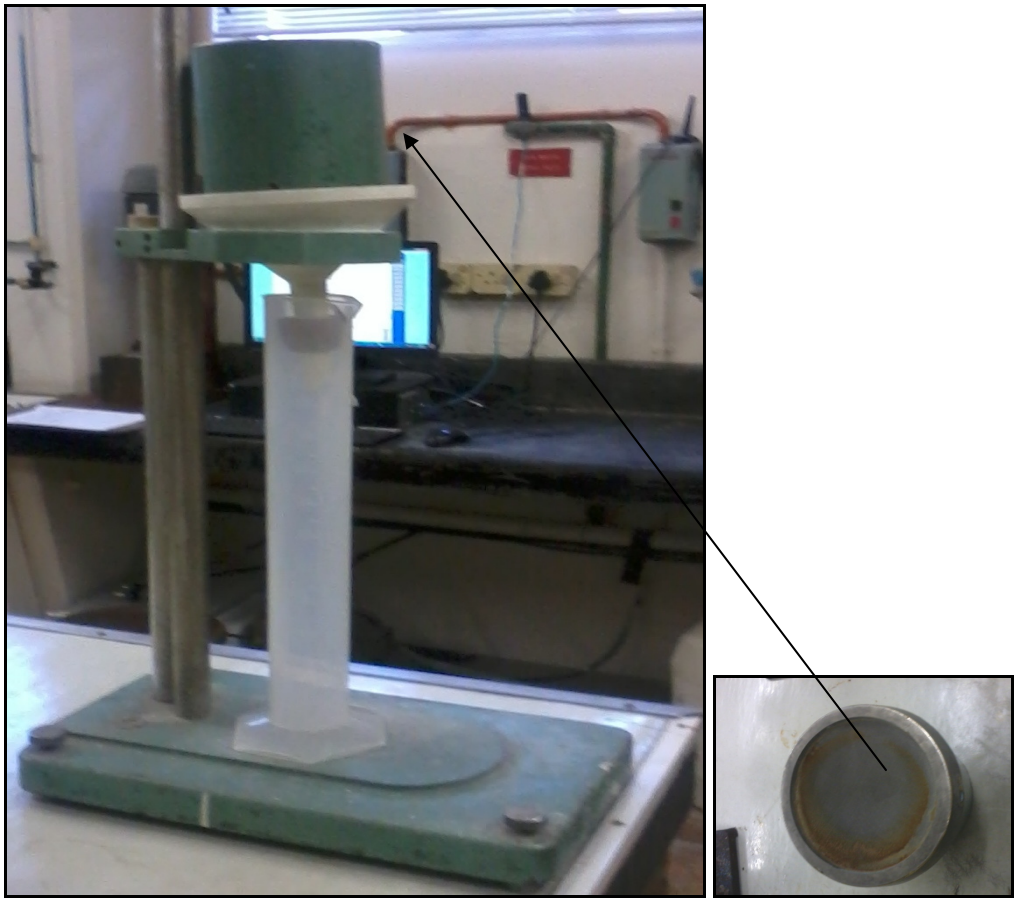
$$Retention\ (\%) = \frac{(C_{mix} \times V_{mix} - V_{filtrate} \times C_{filtrate}) \times 100}{C_{mix} \times V_{mix}} \qquad \text{Eqn 2.6}$$

Where C_{mix} is the mix consistency, in g/l;

V_{mix} is the mix volume used (i.e. 500 ml);

$V_{filtrate}$ is the filtration volume obtained after test, in l;

$C_{filtrate}$ is the solids in the filtrate, in g/l.



(a) (b)

Figure 2.10: (a) Equipment used for flocculant selection, simulating the loss of solids at the sieves, (b) bottom of the container with a 45 mesh sieve

2.3 Analytical techniques

2.3.1 X-ray Diffraction Spectroscopy (XRD)

Quantitative Phase Analysis is a powerful tool for determining the quantities of crystalline and amorphous components in multiphase mixtures. X-rays are generated when electrons accelerated by high voltage from the filament bombard a target. Almost all the energy from the electrons is transformed into heat, and a small amount of energy into X-rays. Characteristic X-rays are produced when an outer orbital electron falls into a vacancy in the K-shell created when high speed electrons eject an inner electron.

The Rietveld method was developed by Hugo M. Rietveld (1969) to refine neutron diffraction data. Later the method was adapted to X-ray diffraction data by Malmros and Thomas (1977) and by Young et al. (1977). Rietveld refinement was originally developed as a method of refining crystal structures using powder neutron diffraction data (Rietveld, 1969), and the application of the method to mineralogy was summarized by Post and Bish (1989). Refinement is done by minimizing the sum of the weighted, squared differences between observed and calculated intensities at every 2θ step in a digital powder diffraction pattern. Thus, refinement is done on a point-by-point basis rather than on a reflection basis. The technique of Rietveld refinement enables the amounts of different phases in anhydrous cementitious materials to be determined to a good degree of precision (Scrivener et al., 2004).

The positions and intensities of the X-rays diffracted by a crystalline solid can provide information such as crystal structure, composition of a solid, particle size, evidence of decomposition, preferred orientation and disorder. In order to obtain a satisfactory powder pattern, a crystalline powder must meet certain specifications. The most important factors requiring attention in sample preparation are grain size, sample thickness, preferred orientation, sample homogeneity and surface planarity (Young, 1993).

Quantitative analysis requires knowledge of the approximate crystal structure of all phases of interest in a mixture. The input data to a refinement include space group symmetry, atomic positions, site occupancies and unit cell parameters. The Rietveld method provides numerous advantages over conventional quantitative analysis methods. As the method uses a whole pattern-fitting algorithm, all lines for each phase are explicitly considered, and even severely overlapped lines are usually not a problem. It is also possible to refine structural parameters, including atom positions, site occupancies and unit cell parameters for each phase in a mixture. The method uses calculated standard data.

The instrument used for analysis of fibrecement composite samples was a PANalytical X'Pert Pro powder diffractometer with X'Celerator detector and variable divergence- and fixed receiving slits with Fe filtered Co-Kα radiation (Figure 2.11). The phases were identified using X'Pert High score plus software. The relative phase amounts were estimated using the Rietveld method.



Figure 2.11 : PANalytical X'Pert Pro powder diffractometer

The Rietveld method is a full profile (rather than a single peak), diffractogram fitting technique that generates calculated diffractograms and attempts to match these to experimentally derived ones. It operates by calculating a theoretical diffractogram for a given phase, then proceeds through a series of least squares iterations wherein a variety of experimental (e.g. background, two-theta displacement) and physical (e.g. unit-cell parameters, site occupancy factors) parameters are varied until a defined convergence value is obtained (Bish and Howard, 1988). The result is a calculated X-ray diffraction profile that best fits an experimental one, both in terms of intensity, peak position and peak shape.

The intensity of the k^{th} Bragg reflection, I_k, is given by the expression:

$$I_k = SM_k L_k [F_k]^2 \qquad \text{Eqn 2.7}$$

Where S is the scale factor, M_k is the reflection multiplicity, L_k is the Lorentz-Polarization factor and F_k is the structure factor.

$$F_k = \sum_{j=1}^{n} f_j exp(2pi h_k^t r_j - h_k^t B_j h_k) \qquad \text{Eqn 2.8}$$

Where fj is the scattering factor atom j, h_k is a matrix representing the atomic co-ordinates, B_j is a matrix representing the anisotropic displacement parameters, and t represents the transpose of the matrix.

The spectrum depends on:

- Phases: crystal structure, microstructure, quantity, cell volume, texture, stress, chemistry, etc.

- Instrument geometry characteristics: beam intensity, Lorentz-Polarization, background, resolution, radiation, etc.
- Sample: position, shape, dimensions, orientation.

High performance X-ray equipment with efficient X-ray detectors enables short time data acquisition in the range of about 5 minutes. The precision and accuracy of the calculation is directly linked to the quality of the generated diffractogram and the control file (Walenta and Fullmann, 2004). This file contains all the information regarding the crystalline structures of the phases contained in the material to be analysed, as well as the crystallographic parameters that needs to be refined. The quantitative analysis can only take account of phases that are contained in the control file. Precise knowledge of the phase content of the respective material is therefore the prerequisite for application of the Rietveld method. The reliability and accuracy of the control file and thus of the quantification must always be established by quantifying model mixtures with known contents and by comparing with the results of other quantification techniques. A further criterion for the analysis precision is the sample preparation. In order to obtain a reproducible result, the sample material should be ground to a specific particle size for analysis by X-ray. However, if the grinding period is too long, the crystalline structures can be destroyed. X-ray can then no longer identify particularly the gypsum contained in Portland cement. In order to ensure that a precise Rietveld analysis is obtained, it is therefore necessary not only to adapt the control file of the Rietveld software to the respective diffractometer and the measuring conditions, but also to optimize the sample preparation.

The strengths of the method are:

- Suitable for homogeneous and heterogeneous samples,
- Works with powdered materials,
- Relatively fast,

- Cost-effective,
- Effective at distinguishing between phases.

Limitations include:

- Requires atomic structure of phase to be known,
- Sometimes difficult to extract modal data for samples containing two or more minerals of the same group.

2.3.2 Scanning Electron Microscopy (SEM)

The scanning electron microscope (SEM), Figure 2.12, uses a focused beam of high energy electrons to generate a variety of signals at the surface of solid specimens. The signal that derive from electron sample interactions reveal information about the sample including external morphology (texture), chemical composition, crystalline structure and orientation of materials making up the sample. In most applications, data are collected over a selected area of the surface of the sample, and a two-dimensional image is generated that displays spatial variations in these properties. The SEM is also capable of performing analyses of selected point locations on the sample; this approach is especially useful in qualitatively or semi-quantitatively determining chemical compositions, using energy dispersive X-ray spectroscopy (EDS), crystalline structure and crystal orientations (Goldstein, 2003).

Fundamental Principles of Scanning Electron Microscopy (SEM)

Accelerated electrons in a SEM carry significant amounts of kinetic energy, and this energy is dissipated as a variety of signals produced by electron-sample interactions when the incident electrons are decelerated in the solid sample (Reimer, 1998). These signals include secondary electrons (that produce SEM images), backscattered electrons (BSE), diffracted backscattered electrons (EBSD) that are used to determine crystal structures



Figure 2.12: SEM instrument showing the electron column, sample chamber, EDS detector, electronics consoles and visual display monitors.

and orientations of minerals, photons (characteristic X-rays that are used for elemental analysis and continuum X-rays), visible light and heat. Secondary electrons are most valuable for showing morphology and topography on samples; whereas backscattered electrons illustrate contrasts in composition in multiphase samples (i.e. for rapid phase discrimination). The secondary electron image is used mainly to image fracture surfaces and give high resolution image. The backscattered electron image is used typically to image a polished section and its brightness depends on the atomic number of the specimen. The backscattered image is basically an atomic number map of the specimen surface. X-ray generation is produced by inelastic collisions of the incident electrons with electrons in discreet orbitals (shells) of atoms in the sample. As the excited electrons return to lower energy states, they yield X-rays that are of a fixed wavelength (i.e. related to the difference in energy levels of electrons in different shells for a given element). Thus, characteristic X-rays are produced for each element in a mineral that is

"excited" by the electron beam. SEM analysis is considered to be non-destructive, as X-rays generated by electron interactions do not lead to volume loss of the sample thus making it possible to analyse the same material repeatedly.

Essential components of the SEM include the following:

- Electron source (gun)
- Electron lenses
- Sample stage
- Detectors for all signals
- Display / Data output devices

- Infrastructure requirements – power supply, vacuum system, cooling system, vibration-free floor, room free of ambient magnetic and electric fields.

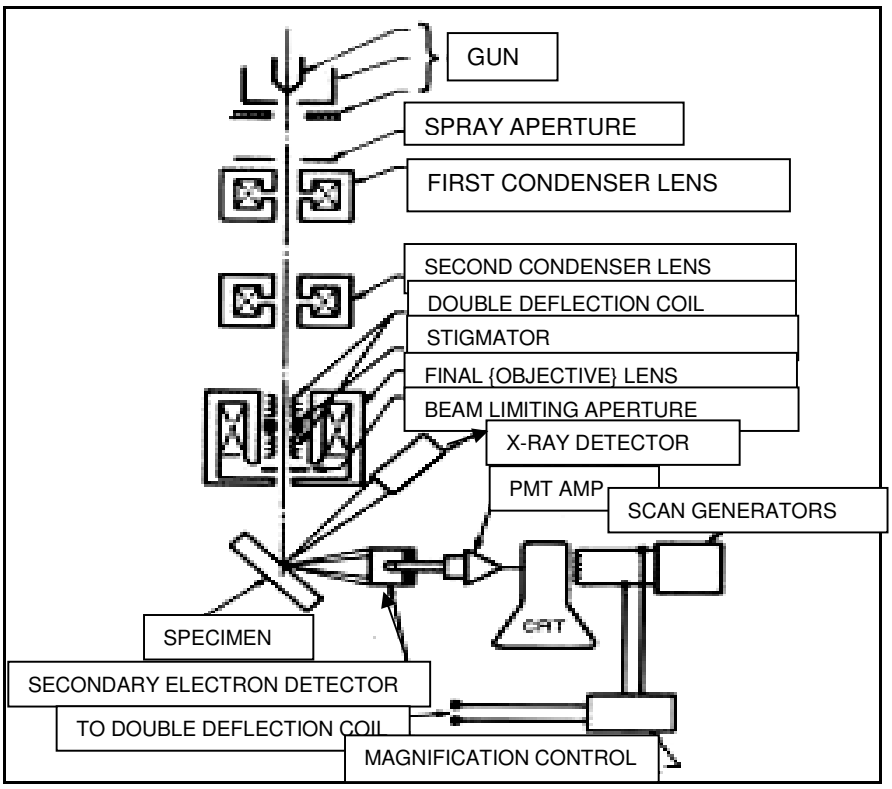


Figure 2.13: Schematic drawing of the SEM components [adapted after Swapp (2013)]

A normal SEM operates at a high vacuum. The basic principle is that a beam of electrons is generated by a suitable source, typically a tungsten filament or a field emission gun (Clarke, 2002). The electron beam is accelerated through a high voltage (e.g. 20kV) and pass through a system of apertures and electromagnetic lenses to produce a thin beam of electrons. Then, the beam scans the surface of the specimen by means of scan coils. Electrons are emitted from the specimen by the action of the scanning beam and collected by a suitably positioned detector. The electron detector controls the brightness of the spot on the screen. When there are fewer electrons, the spot on the screen gets darker. The magnification of the image is the ratio of the size of the screen to the size of the area scanned on the specimen.

Fundamental Principles of Energy-dispersive X-ray Spectroscopy (EDS)

EDS is complementary to SEM. It enables determination of the composition of the features in the SEM image. The principle of EDS is that the electron beam generates X-rays within the specimen (Egerton, 2005). Many of these X-rays have energies characteristic of the elements that emitted them.

There are three principal components to a basic EDS system:

- The X-ray detector,
- The pulse processor and
- Computer

The pulse processor measures the voltage pulses corresponding to the X-ray energies. The X-ray detector is positioned to intercept X-rays emitted from the specimen. On entering the detector, an X-ray generates a small current, which is then converted into a voltage pulse. The size of the voltage pulse is proportional to the energy of the X-ray. A computer measures the voltage pulses over a period of time and plots them as a histogram. The histogram shows a spectrum of the X-ray energies that were measured; by examining the spectrum, the elements present can be determined.

2.4 Raw materials evaluated for mitigation

2.4.1 Surface modification silanes

Two types of materials were tested:

- A bifunctional organosilane possessing a reactive organic epoxide and hydrolysable inorganic methoxysilyl groups (1).
- An organofunctional silane featuring a methacrylate organ reactive group and trimethoxy hydrolysable groups on silicon (2).

The properties of these materials are tabulated in table 2.2 below:

Table 2.2: Physical Properties of Silanes

Properties	Silane 1	Silane 2
Appearance	Colourless	Clear, white to light straw
Density at 25ºC	1.07	1.04
Refractive index at 25ºC	1.429	1.43
Flash point(ºC)	122	138
Boiling point(ºC)	90	190
Viscosity at 20ºC (cSt)	3.5	2.5

The silane (2) is used as a coupling agent to improve adhesion of free radical cured resins, such as polyester, to inorganic surfaces, including fibreglass, clay, quartz, and other siliceous materials. The improved adhesion increases dry and wet flexural flexural strength of the composite. Wet strength improvements of approximately 100% are possible. Silane can also be used as a resin additive in mineral reinforced polyester resin. When used as an additive, this silane can provide improvements in composite properties similar to those obtained from a composite fabricated with a silane-treated mineral reinforcement. Its features are methacrylate organo reactive group, trimethoxy hydrolyzable groups on silicon and high purity. The benefits are

coupling agent to improve adhesion of organic resins to inorganic surfaces, increased composite tensile and flexural strength—both dry and wet, improved chemical bonding, increased transparency of polyester and fibreglass composites. The bifunctional organosilane possesses a reactive organic epoxide and hydrolysable inorganic methoxysilyl groups. The dual nature of its reactivity allows the silane to bind chemically to both inorganic materials and organic polymers, thus functioning as a crosslinking agent and/or surface modifier.

2.4.2 Wollastonite

Wollastonite is a naturally occurring, non-metallic calcium metasilicate material of high elastic modulus. The wollastonite is used to reduce the wet-to-dry dimensional changes in both autoclaved and nonautoclaved products including sheets. The chemical composition of the materials used in this project was characterized by XRF techniques and results are shown in Figure 2.14 below.

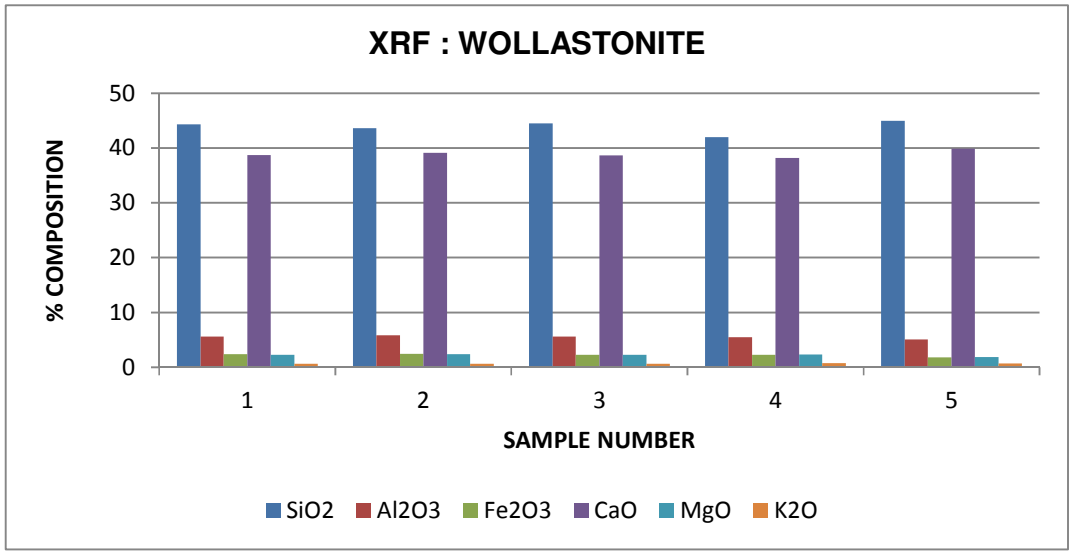


Figure 2.14: Chemical composition of five wollastonite samples received during testing

The particle size of wollastonite is the key in its effectiveness at modification of the microstructure of fibrecement composites. Therefore, it is of importance to monitor the PSD of the incoming material as shown in Figure 2.15.

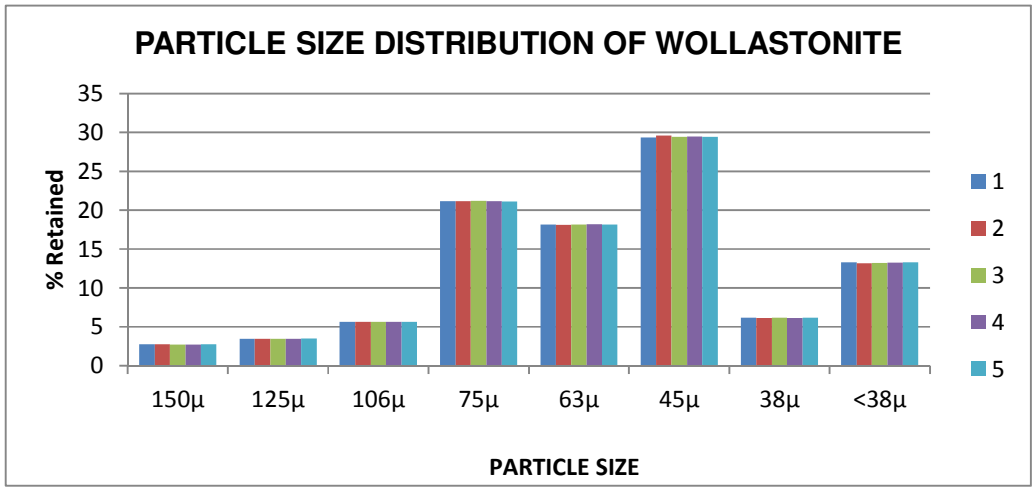


Figure 2.15: Particle size distribution of five samples of wollastonite

2.4.3 Silicone-resin as admixture

It is a water repellent admixture that is a solvent-free, alkyl-functionalized, low viscosity silicone resin. It disperses easily upon proper mixing of the product into cement-based formulation. Addition of this material provides hydrophobicity and decreases dramatically the water ingress of cementitious materials. Alkoxysilyl chemical group in the resin can chemically react with cement hydrate during cement cure. Alcohol is released upon reaction of the resin. This product can be used in many application areas where the protection of the substrate from liquid water ingress is required. When used as an additive to cementitious matrix, silicone-based resin results in reduction in capillary absorption of water. Also, it reduces ingress and transfer of water-soluble salts through the matrix and related aesthetic problems such as efflorescence.

Table 2.3: Physical properties of silicone resin

Physical Properties	Specification
Colour	Clear liquid, transparent to light yellow
Active content (%)	>95
Viscosity (cSt)	100 - 300
Density (g/cm^3)	0.99

2.4.4 Kaolin

The material that will be used for this project is a refined and milled crystalline prototypical phyllosilicate. The free moisture of the product is less than 5%. It is mined in the Eastern Cape Province, South Africa, and its chemical composition is tabulated in Table 2.4.

Table 2.4: Chemical composition of kaolin, supplied by Micronized Group

Elements	Composition (%)
SiO_2	67.5
Al_2O_3	24.1
K	5.38
TiO_2	0.89
MgO	0.43
Na	0.38
FeO	0.28
L.O.I	5.93

Kaolin is a plastic raw material, particularly consisting of the clay mineral kaolinite. The chemical formula is $Al_2O_3 \cdot 2SiO_2 \cdot 2H_2O$. The group of kaolinites include di-octahedral minerals (1:1) with two layers, one silica [SiO_4]

tetrahedral layer and one aluminium [$Al_2(OH)_4$] octahedral layer, see Figure 2.16. The layers are bonded together by sharing oxygen anion between Al and Si. Together these two layers are called platelets. The platelets are held together strongly via hydrogen bonding between the OH of the octahedral layer and the O of the tetrahedral layer. Due to this strong attraction, these platelets do not expand when hydrated and kaolinite only has an external surface area. Also, kaolinite has very little isomorphic substitution of Al for Si in the tetrahedral layer. Accordingly, it has a low cation exchange capacity. Kaolin with its stratified structure, allows adsorption of water to the surface layer only.

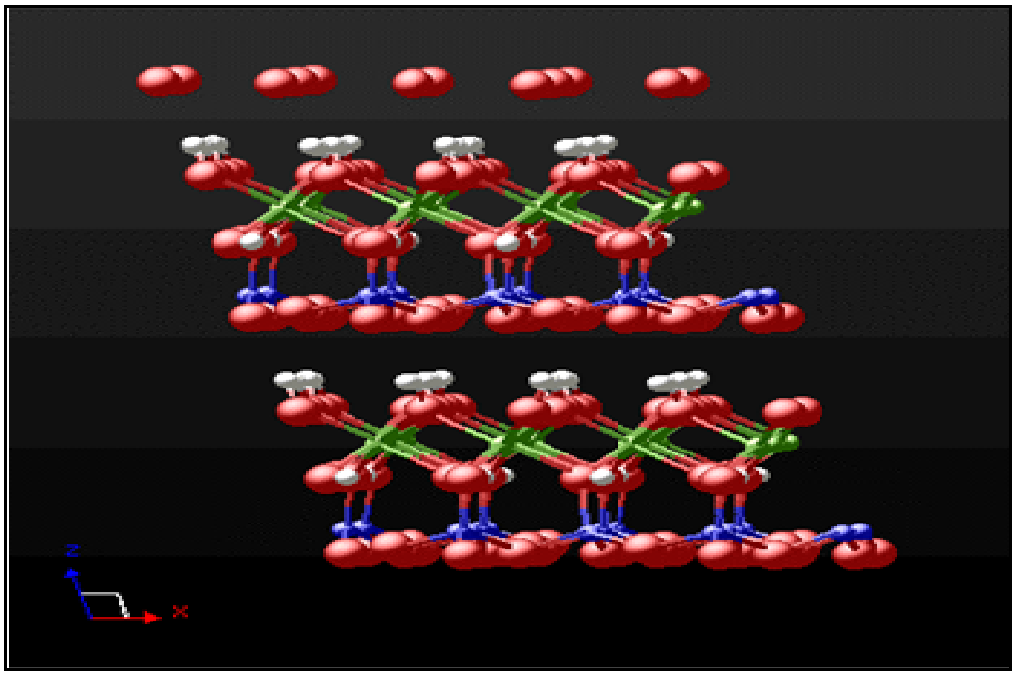


Figure 2.16: Kaolin structure showing the octahedral and tetrahedral sheets. (The white colour represents hydrogen atoms, red colour for oxygen atoms, green colour for aluminium atoms and blue for silicon atoms).

The product has been milled such that 99% of the particles passing 45 µm and 50% passing 9 µm. The particle size distribution curve is illustrated in Figure 2.17 and its physical properties in table 2.5 below:

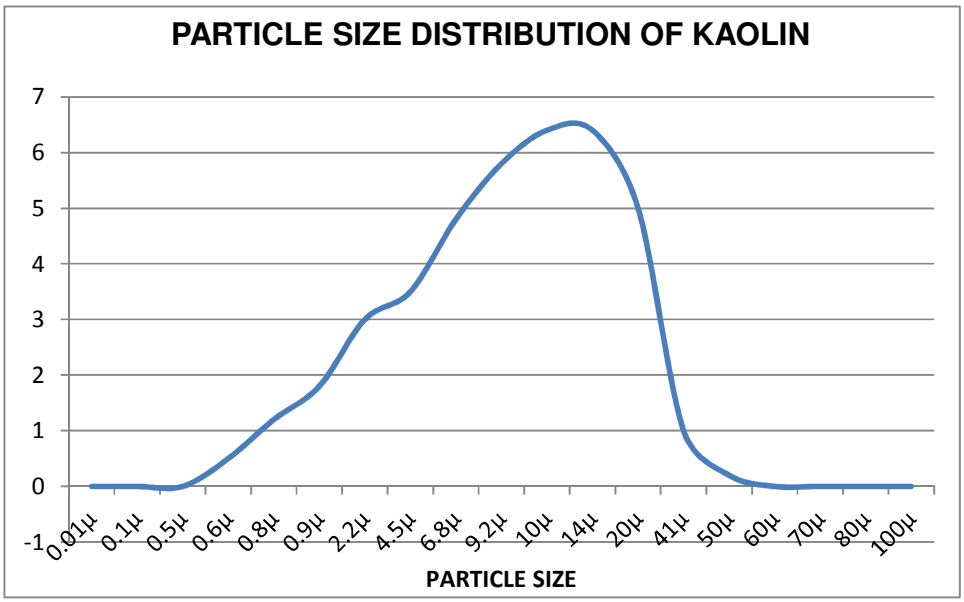


Figure 2.17: Particle size distribution of kaolin

Table 2.5 Physical properties of kaolin, supplied by Micronized Group

Properties	Results
Particle sizing	99% passing 45µm 50% passing 9µm
Oil absorption	28% (Linseed oil)
Hardness	2 – 3 Mohs
Colour	Off-white
Reflectance	79 – 83 (opacity reflectometer)
Melting point	>1000ºC
Bulk density	620 – 660 g/l
Free moisture	< 5%

2.4.5 Superplasticizer

The material used is a chloride free water reducing admixture based on a blend of selected lignosulphonate and hydrolysed carbohydrate materials. It disperses the fine particles in the concrete mix, enabling water content of the concrete to perform more effectively and improving the consistency of the concrete. This produces high levels of workability for the same water content, allowing benefits such as water reduction and improved strengths. Water reduces significantly thus improving flexural strengths at all ages and enhances durability through the production of low permeability concrete.

It is used to improve the effectiveness of the water content of the concrete mix. At higher dosages it provides a cost effective means of reducing concrete permeability and thereby reducing water penetration. Its physical properties are listed in table 2.6.

Table 2.6: Physical properties of superplasticizer

Physical properties	Specification
Appearance	Brown liquid
Specific gravity @ 20ºC	1.2
Air entrainment	< 2%
Alkali content	< 4.0g Na_2O equivalent/l of admixture
Chloride content	Nil to BS5075

CHAPTER 3 – SURFACE MODIFICATION OF CELLULOSE FIBRES

3.1 Introduction

Cellulose fibres are the most utilized reinforcing agents in the preparation of composite materials because of their availability in variety of forms and recyclability. The main reason for incorporating the cellulose fibres into the cement matrix is to improve the toughness, tensile strength and the cracking deformation characteristics of the resultant composite. One of the drawbacks associated with cellulose fibres in cement application is their dimensional instability in the presence of changing relative humidity atmospheres. This occurs as a result of the water sensitivity of cellulose fibres and, the effects of carbonation, high alkali and generation of incompatible stresses (Fan et al., 1999; Fan et al., 2004). Exposure under weathering induce cellulose water uptake and release; resulting in volume changes of the porous cement matrix and hydrophilic cellulose fibres cell wall. As a consequence, there is a loss of adhesion at the fibre/cement interface and an increase of micro- and macro-cracks, which contributes to strength decay and loss of durability of the fibrecement composites (John et al., 1998; Jones, 1989). It is therefore necessary to modify the surface properties of cellulosic fibres to minimize these problems.

Coupling agents are substances that are used in small quantities to treat a surface so that bonding occurs between it and the other surface. The chemical modification of cellulose fibres by coupling agents creates covalent bridges between the fibres and the matrix which ensures best mechanical properties for the composite. Two studies on the interaction between silane-based reagents and cellulose, and the incidence of this treatment on the mechanical properties of the ensuing composites have been published (Kokta et al., 1990b; Valdez-Gonzalez et al., 1999). Surface modification

reduces the number of reactive hydroxyl groups responsible for bond formation between cellulose fibres and the cementitious matrix. The objective is to protect the cellulose fibres from water uptake and to improve the quality of fibre-matrix interface.

The existence of stepwise reactions (hydrolysis of the silane, condensation onto substrate) and concurrent reactions (self-condensation of the silane) brought the need for an optimization step of the grafting protocol (Bel-Hassen et al., 2008). The reactions of alkylsilane can be described by the following sequence (Bae et al., 2009):

- Alkylsilane initially hydrolyze in acid or basic conditions to form silicic acid and then the formed silicic acid condensates with another alkylsilane or with itself to form a cross-linked polysiloxane network; thus a gel is formed.
- The hydroxyl groups of polysiloxane can react with the hydroxyl group over the surface of a fibre therefore the gel actually can be covalently attached to the fibre support.

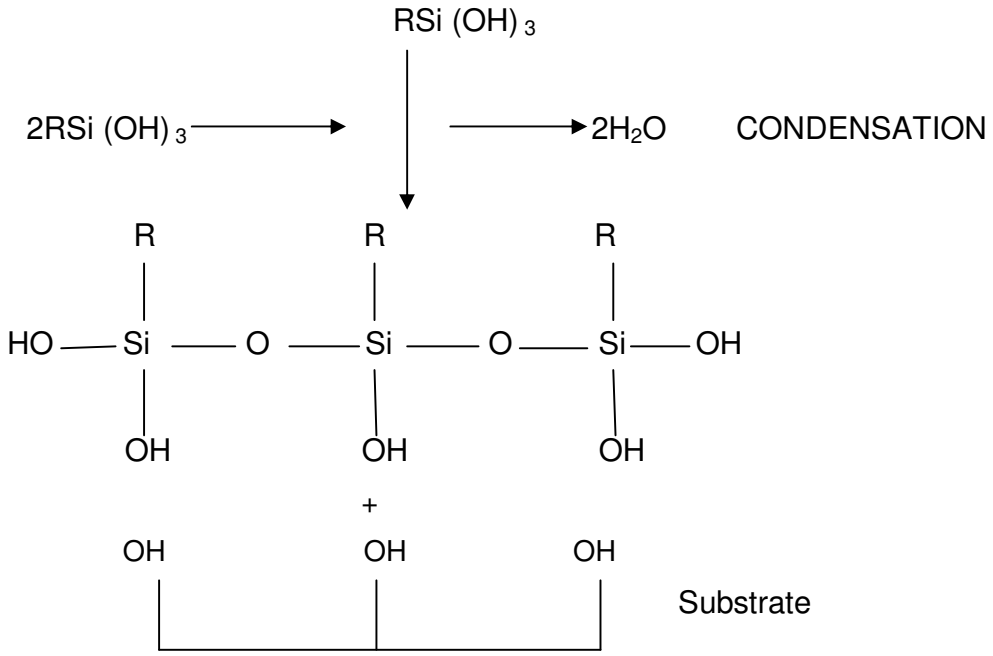
Reaction of the organosilanes involves four steps:

1) Initially – hydrolysis of the 3 labile X-groups attached to silicon occurs

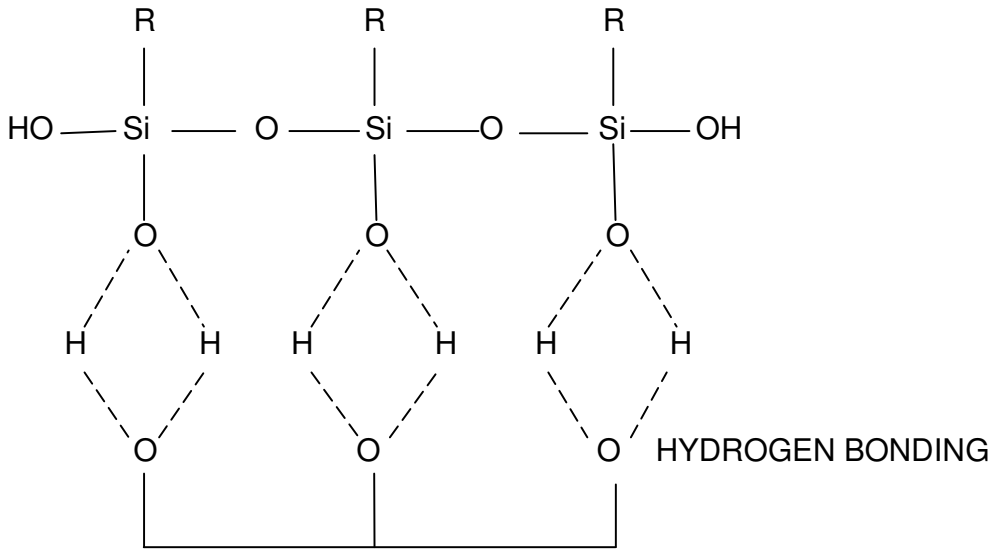
$RSi(OCH_3)_3 + 3H_2O \rightarrow RSi(OH)_3 + 3\,CH_3OH$ HYDROLYSIS

Where R is a non-hydrolysable organic radical and Si is silicon atom.

2) Condensation to oligomers follows:

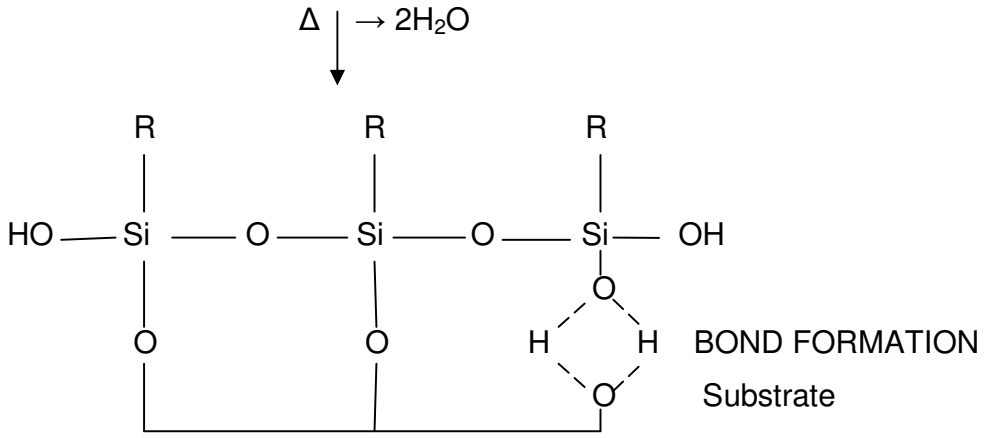


3) The oligomers then hydrogen bond with OH groups of the substrate:



Finally, during drying or curing, a covalent linkage is formed with the substrate accompanied by loss of water. At the interface, there is usually one

bond from the silicon of the organosilane to the substrate surface. The two remaining silanol groups are present either bonded to other coupling agent silicon atoms or in free form.



The number of reactive sites on a surface area and the type of silane deposition sought, i.e. monolayer, multilayer or bulk, are all factors which can be used in calculating the amount of silane required to silylate a surface. The number of hydrolysable groups on the silane is an important parameter in controlling bond characteristics. The silanes with one hydrolysable group yield the most hydrophobic interfaces but have the least long term hydrolytic stability.

Chemical surface treatment on cellulose fibres reduce hydrophilic character and improve adhesion on the matrix, exploit reactive hydroxyl functions of the fibre surface, reduce hydroxyl groups resulting in reduction of water absorption and improvement in mechanical properties of composites. The silane bridges the fibre surface, the silica fume and the cement matrix yielding denser and stronger composites.

3.2 Experimental Procedure

3.2.1 Materials

Two types of organosilanes used in this study were methacryloxypropyl tri-methoxysilane (Z6030) and 3-Glycidyloxypropyl methoxysilane (DYNASYLAN) supplied by Dow Corning and Evonik Industries respectively. The Portland cement intergrounded with 10% calcium carbonate, was supplied by Afrisam in South Africa. The synthetic fibre used for reinforcement in fibrecement composites was polyvinyl alcohol (PVA) fibre. PVA, Mewlon fibre, used was supplied by Unitika in Japan. Densified silica fume was supplied by Silicon Smelters in South Africa. It is a by-product of the fabrication of ferrosilicon alloys and a very reactive pozzolan with constant chemical composition. It consists of very fine particles, 100 times finer than those of cement, almost exclusively amorphous SiO_2. The content of is SiO_2 usually above 85%.

The cellulose, unbleached softwood pulp, with kappa number of 28±4 and fibre length ≥3 mm was obtained from Sappi, South Africa. Cellulose was mixed in the pulper with water then refined to 110 Canadian Standard Freeness. Refining defined as the mechanical treatment of pulp carried out in the presence of water, usually by passing the suspension of pulp fibres through a relatively narrow gap between the revolving rotor and a stationary stator, both carrying bars aligned across the line of flow of the stock. At this freeness, adequate fibrillation has been obtained in the refiner for the pulp to achieve optimum solids retention in the fibrecement composite. The properties of fibres and powder materials are tabulated in Table 3.1 and Table 3.2 respectively.

Table 3.1: Physical properties of fibres

Fibre Type	Length (mm)	Kappa number	Count (dtex)	Tenacity (cN/dtex)	Elongation @break (%)	Young's Modulus (cN/dtex)
PVA	6	-	2.11	13.6	7.1	314
Cellulose	3.63	28.4	-	-	-	-

Table 3.2: Chemical composition of powder materials

Raw materials (%)	CaO	SiO_2	Al_2O_3	Fe_2O_3	MgO	SO_3	L.O.I
Cement	65.54	21.17	4.69	2.70	1.71	2.73	4.1
$CaCO_3$	47.66	6.6	0.72	6.6	3.07	-	39.13
Silica fume	-	86.6	-	-	0.9	-	3.7

3.2.2 Surface chemical treatment of cellulose fibres

The refined fibre was mixed with Z6030 at very high shear without any additional solvent for 2 h under continuous stirring. The silane/cellulose ratio was 6% w/w. The second mixture with DYNASYLAN was prepared as with Z6030 above. The concentration of DYNASYLAN for the third mixture was 0.1% of 80/20 v/v ethanol/distilled water. The silane was prehydrolyzed for 2 h under stirring in the ethanol/distilled water mixture, at room temperature. Then, refined cellulose was added to the reactive prehydrolyzed silane and the resulting suspension was kept under stirring for 2 hours. At the end of the reaction, the pulp was used in the production of fibrecement composites.

3.2.3 Cellulose fibrecement specimen preparation

The fibrecement composites were prepared in the pilot plant using the Hatschek process as described in detail in section 2.1 above. The PVA fibres were mixed at a very high speed to disperse the fibres in water for 5 min, followed by addition of refined cellulose, untreated and treated, under

continuous stirring for another 2 min. Silica fume was added at high speed for 1 min then the stirrer speed was reduced as cement and calcium carbonate were added. The slurry was maintained under continuous stirring for an additional period of 2.5 minutes. The slurry was diluted, then transferred to the mix box in the Hatschek machine, resulting in a concentration of approximately 7% solids. The sheet obtained from the Hatschek process was cut into 250 mm x 250 mm x 6 mm specimens for physical properties test. The specimens were placed in between steel plates (300 mm x 300 mm) and shrink-wrapped with transparent plastic. The tests were carried out at 7 days intervals, up to 28 days.

The fibrecement specimens manufactured for the studies described in this chapter have been categorized as follows:

STD - normally cured specimens containing 2% synthetic fibres, 3% cellulose, silica fume and cement.

Z6030 – naturally cured specimens with same mix formulation as STD but with cellulose modified with Z6030 only.

DYNASYLAN – naturally cured specimens with same mix formulation as STD but with cellulose modified with DYNA only

DYNASYLAN + ETHANOL – naturally cured specimens with same mix formulation as STD but with cellulose modified with 0.1% DYNASYLAN prehydrolyzed in ethanol/distilled water.

3.3 Results and Discussion

The effect of fibre treatment on fibrecement composites was evaluated by measuring the moisture content of the green composite sheet. The quantity of water retained after the vacuum process and application of pressure by the forming roller, was measured using the electronic moisture analyzer.

Figure 3.1 shows the average results of water content of the fibrecement based composites monitored during production. The results indicate a

reduction in water content with composites containing treated cellulose fibres. Prehydrolyzation of silane with ethanol before surface modification of cellulose did not show a significant improvement in water content compared to the other two surface modifications.

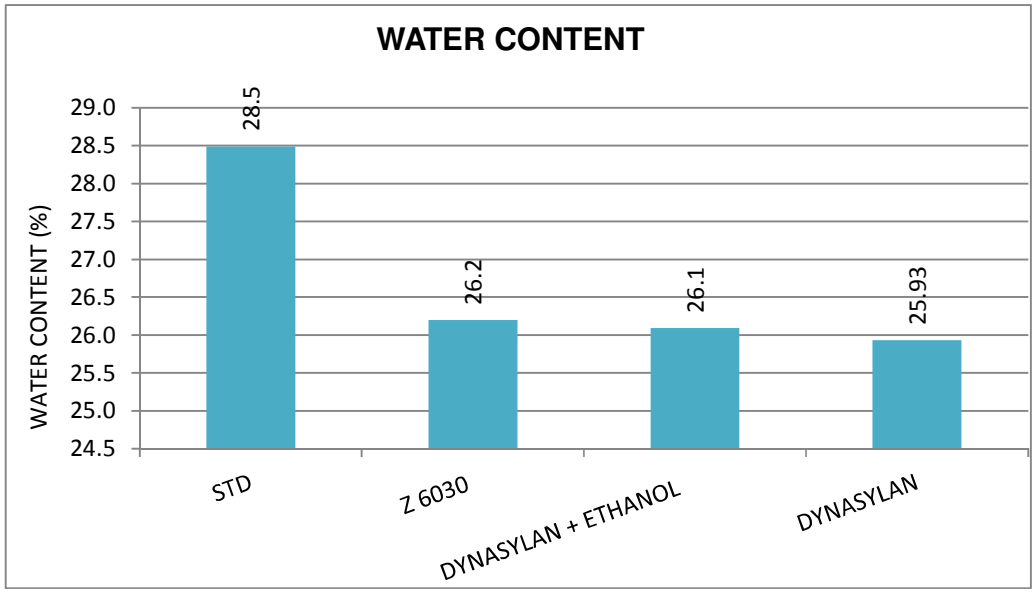


Figure 3.1: Process water content monitoring

The DYNASYLAN + ETHANOL reinforced specimens resulted in improved density compared to the standard specimens but, slightly lower than the other treated cellulose specimens (Fig. 3.2).

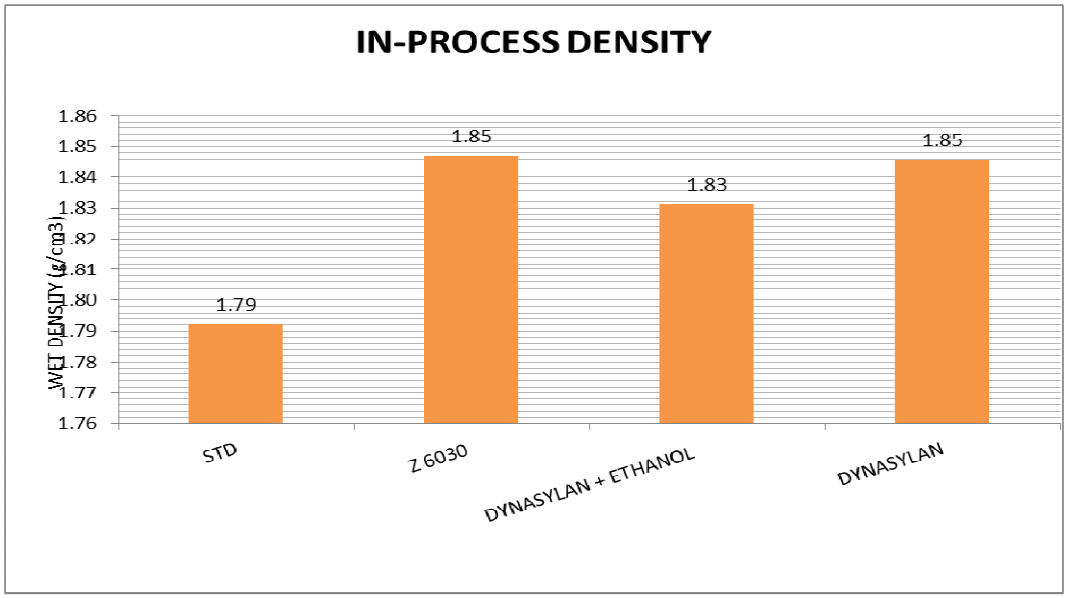


Figure 3.2: Density measurement of green cellulose pretreated sheets during the manufacturing process

Density and porosity are related. The increase in density with cellulose treated fibrecement composites is attributed to the improvement in porosity hence the reduction in water absorption. Although the process density of DYNASYLAN + ETHANOL specimens was lower than that of Z6030 and DYNASYLAN specimens, the density development of these specimens over 28 days showed a significant improvement, see Figure 3.3. The formation of chemical bonds at which silane serve as bridges between the surface of fibre and the cement matrix yield a stronger and denser matrix (Xu and Chung, 1999a). Therefore, drying shrinkage is decreased by silane treatment of fibres.

There was reduction in water absorption with the surface treated composites as a consequence of the treated fibres lower hydrophilic character. It is expected that these composites would display high mechanical properties due to the lower water/cement ratio (Neville, 1996). This interfacial layer made the specimens less porous thus the restriction in ingress/egress of moisture from the surroundings. By reducing the water absorption of silane

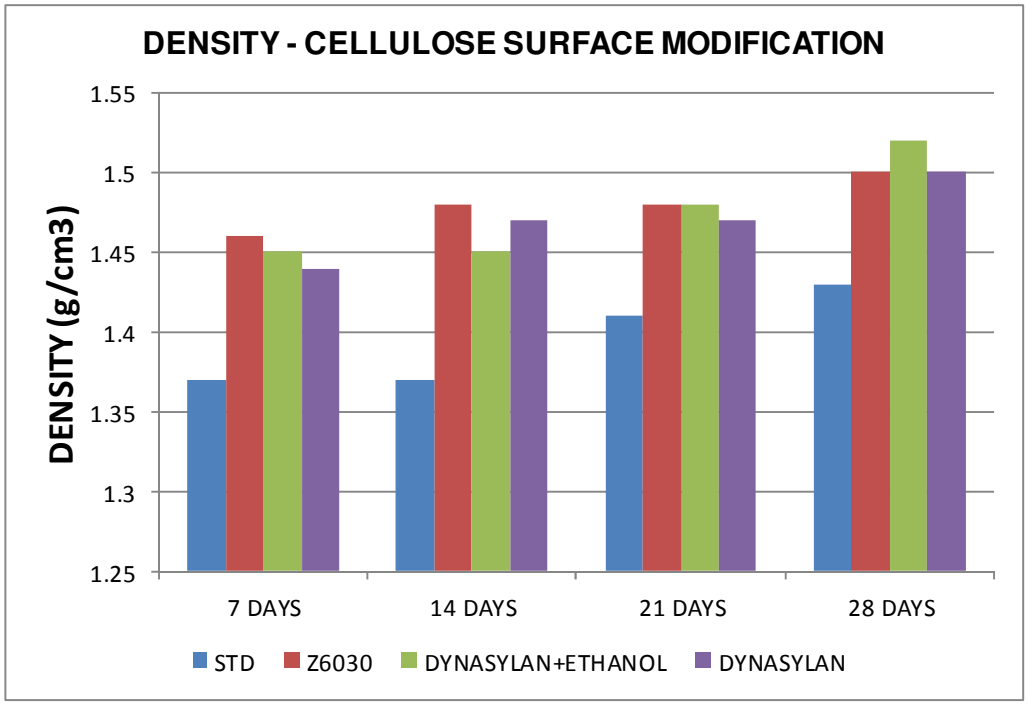


Figure 3.3: Density development of cellulose pretreated sheets over time

treated specimens, the wet-dry movement decreased over 28 days. Silane treatment reduced wet-dry movement of composites; this effect was more pronounced with DYNASYLAN treatment as shown in Figure 3.4. This indicated that the treated wood fibres stabilized the dimension changes in the wood fibrecement composites.

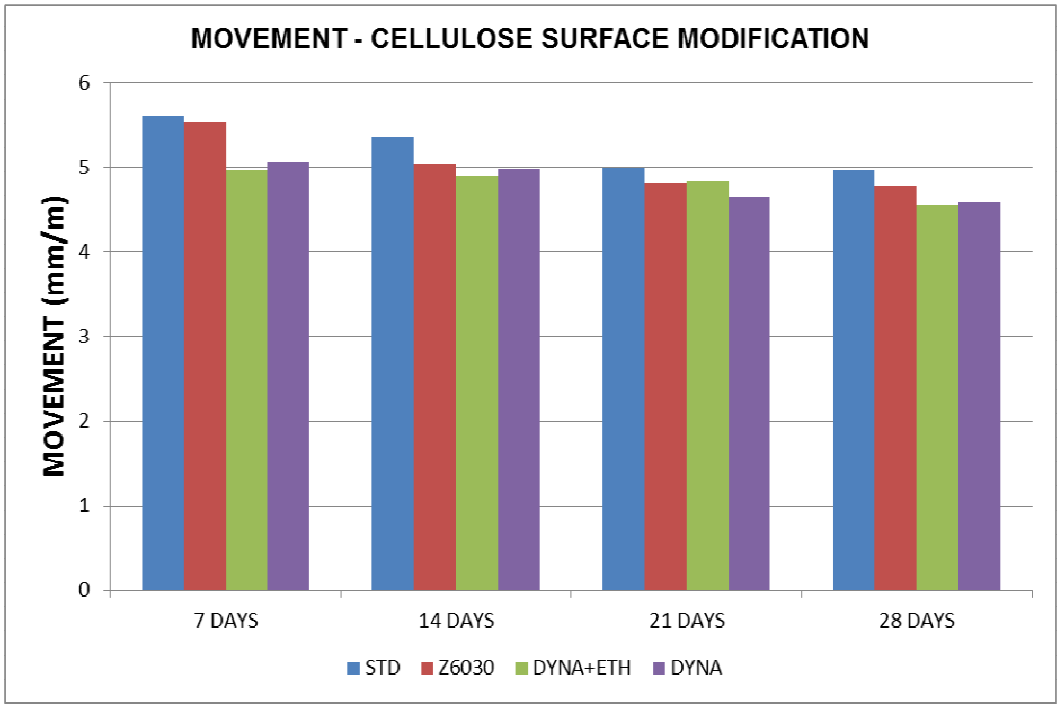


Figure 3.4: Wet-dry movement of cellulose pretreated sheets during curing

Figure 3.5 presents the evolution of the composite strength over 28 days for the investigated fibrecement specimens. After 28 days of cure, composites reinforced with Z6030-modified fibres presented higher MOR values than those associated with composites made of unmodified and DYNASYLAN-modified fibres. The strong adhesion of fibres with the matrix increased the modulus of rupture of the composites at 28 days. These observations could be supported by the hypothesis that hydrogen bonds and / or hydroxide bridges play a major role in the bonding hence in the mechanical performance of the composite (Coutts and Ridikas, 1982).

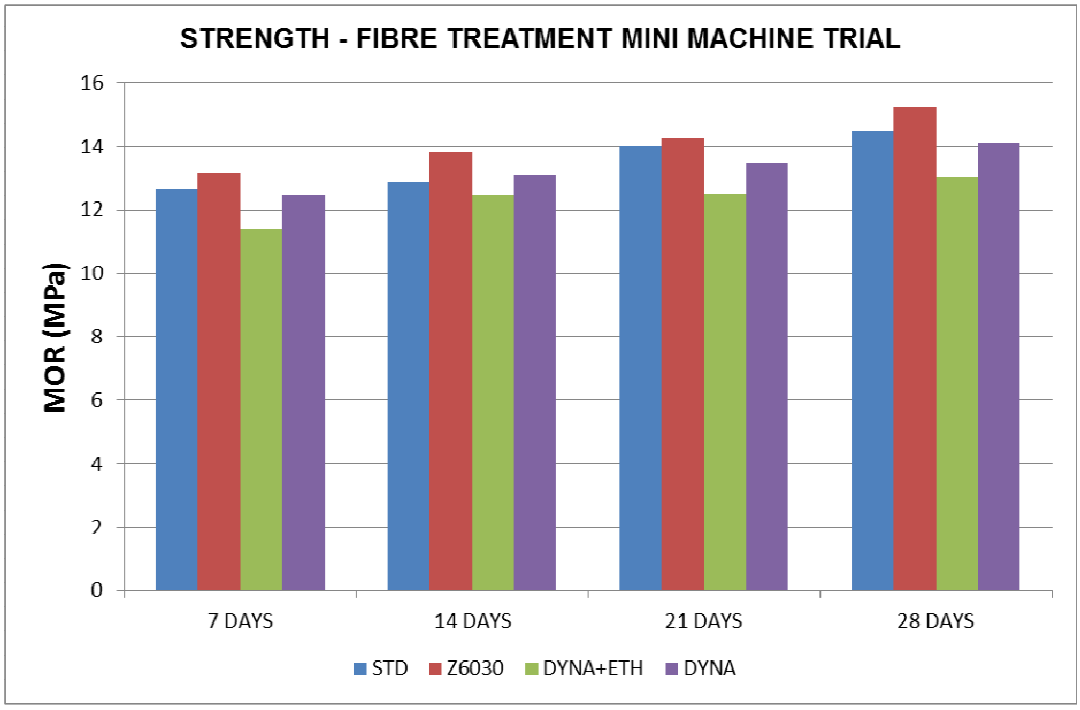


Figure 3.5: Strength development of cellulose pretreated sheets over 28 days

The results in Figure 3.6 show the mineralogical composition of fibrecement composites investigated at 28 days. C_3S and C_2S are essential to the build-up of strength in Portland cement. C_3S hydrates and hardens rapidly and, responsible for initial set and early strength (2 – 3 h to 14 days). C_2S hydrates and hardens slowly and, displays the better long-term strength development performances (beyond 7 days). The silicate phases (C_3S and C_2S) produce calcium silicate hydrates (CSH) and portlandite (CH) as reaction products, while the interstitial phases (aluminate and ferrite) form a variety of products (hydrogarnet, ettringite and a monosulfoaluminate phase) depending on the amount of gypsum present in the system. C_2S produces less CH. CSH give strength to the composite due to covalent / ionic bonding and van der Waals bonding within the complex structure. CH does not contribute much to strength. Gypsum is added to the clinker to regulate the reactivity of the aluminate phases. $CaCO_3$ formation by CO_2 reacting with CH. This is attributed to the carbonation process that occurs over time when

composite is exposed to the environment. Therefore, the quantities of the phases shown in Fig. 3.6 give an indication on how far the hydration process has progressed.

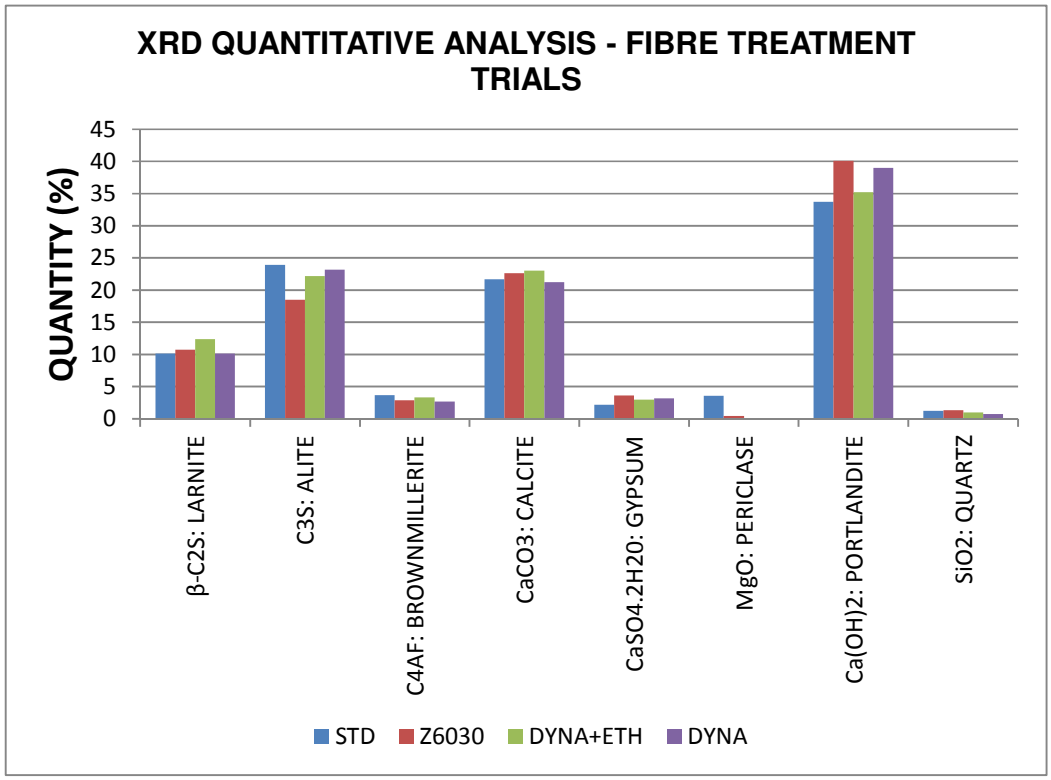


Figure 3.6 Mineralogical composition of cellulose pretreated sheets, 28 days

3.4 Conclusions

- Surface modification of fibres with silanes resulted in denser structures of fibrecement based composites.
- Pre-hydrolyzation of silanes in alcohol did not show any improvement in wet-dry movement of fibrecement based composites in relation to the specimens that were treated with silane only.
- The composites with fibre treated cellulose showed resistance to moisture absorption compared to composites with untreated fibre,

consequently a reduction in wet-dry movement hence a reduction in drying shrinkage can be expected.

Although small improvements in composite, mechanical performance has been observed from the use of pretreated fibres, the costs of such operations are currently prohibitive.

CHAPTER 4: THE IMPACT OF WOLLASTONITE INCLUSION IN FIBRECEMENT COMPOSITES

4.1 Introduction

Natural wollastonite, a calcium metasilicate material of high elastic modulus with the chemical formula β-$CaO.SiO_2$, is an economical reinforcing material used in certain cement products. It has been reported that the addition of a small percentage of wollastonite microfibres can reduce shrinkage in cement-based composites (Johnson and Melling, 1983). The wollastonite fibres are relatively inert; the cement fibre bonding is physical and mechanical rather than chemical in nature. Wollastonite fibres are not expected to have a significant effect on the heat of hydration liberated during the hydration process (Low and Beaudoin, 1992). Adding very fine inert particles displaced some of the water from the voids between cement particles, making it available; hence allowing more hydration reactions to take place (Schmidt, 1992). Simultaneously, adding these inert materials as a partial replacement for cement induced a dilution effect, leading to a lower hydration rate. Hence, the availability of space for hydration products to form is the main restriction on hydration development (Lea, 1988).

The microstructure of the cement-fibre interface zone therefore has an important influence on its mechanical properties. Previous studies have shown the potential for using natural wollastonite microfibres as a reinforcing material in cementitious materials (Low and Beaudoin, 1992, 1993, 1994a). The addition of wollastonite in cement-silica fume matrices showed significant improvements in flexural toughness and ductility (Low and Beaudoin, 1993). Moreover, wollastonite microfibres embedded in cementitious materials achieved high stability without deterioration with time (Low and Beaudoin, 1994b). However, there appears to be little or no

information with regards to the early-age properties, shrinkage and cracking behavior of fibre-reinforced composites with natural wollastonite microfibres. The inclusion of wollastonite in mixes results in higher residual strength and show increased durability (Lawler et al., 2005). Increase in durability can be associated with decrease in permeability due to formation of discontinuous pores. Also, the sequence of interactions within the matrix leads to unique pore size distribution. The wollastonite microfibres improve inherent tensile properties; provide reinforcement and mix properties are also improved so as to resist any adverse chemical and physical attack.

4.2 Experimental Procedure

4.2.1 Sample preparation

The fibrecement composites were prepared in the pilot plant using the Hatschek process as described in details in section 2.1 above. The control samples were made by mixing Mewlon PVA fibres, fibre properties in table 3.1, at a very high speed to disperse the fibres in water for 5 min, followed by addition of refined cellulose, 110 Canadian Standard Freeness, under continuous stirring for another 2 min. Silica fume was added at high speed for 1 min then the stirrer speed was reduced as cement and calcium carbonate were added. For trial samples - wollastonite was added as a replacement of cement at different percentages ranging from 2 to 10%. The slurry was maintained under continuous stirring for an additional period of 2.5 minutes. The slurry was diluted then transferred to the mix box in the Hatschek machine, resulting in a concentration of approximately 7% solids. The sheet obtained from the Hatschek process was cut into 250 mm x 250 mm x 6 mm specimens for physical properties test. The specimens were placed in between steel plates (300 mm x 300 mm) and shrink-wrapped with transparent plastic. The tests were carried out at 7 days intervals, up to 28 days.

The samples under investigation were labeled as follows:

Control samples – STD

Composites with 2% wollastonite replacing cement – WOLL2%

Composites with 4% wollastonite replacing cement – WOLL4%

Composites with 6% wollastonite replacing cement – WOLL6%

Composites with 10% wollastonite replacing cement – WOLL10%

4.3 Results and discussion

4.3.1 Density development

The process was controlled in such a way that the water content of samples had to range between 26 and 28% to ensure enough free water for cement hydration. The results in Figure 4.1 displayed a decrease trend in water content of composites as wollastonite microfibres increased as replacement of cement. As water content decreased, density of the matrix increased. This can be attributed to the refinement of pore structure and reduction in interstitial voids, see Fig. 4.2. It indicates that the transition zone due to the addition of wollastonite microfibres tends to become denser than the cement matrix itself.

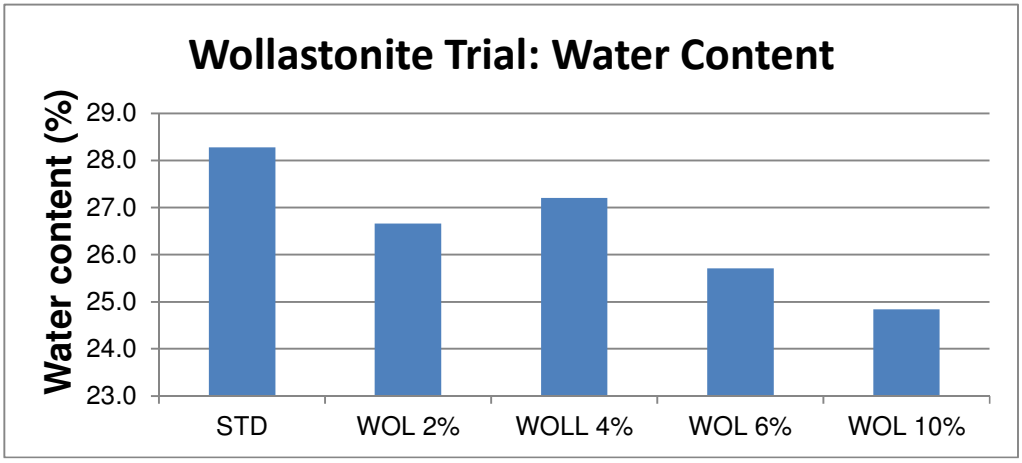


Figure 4.1: Water content of wollastonite fibrecement composites measured during the manufacturing process

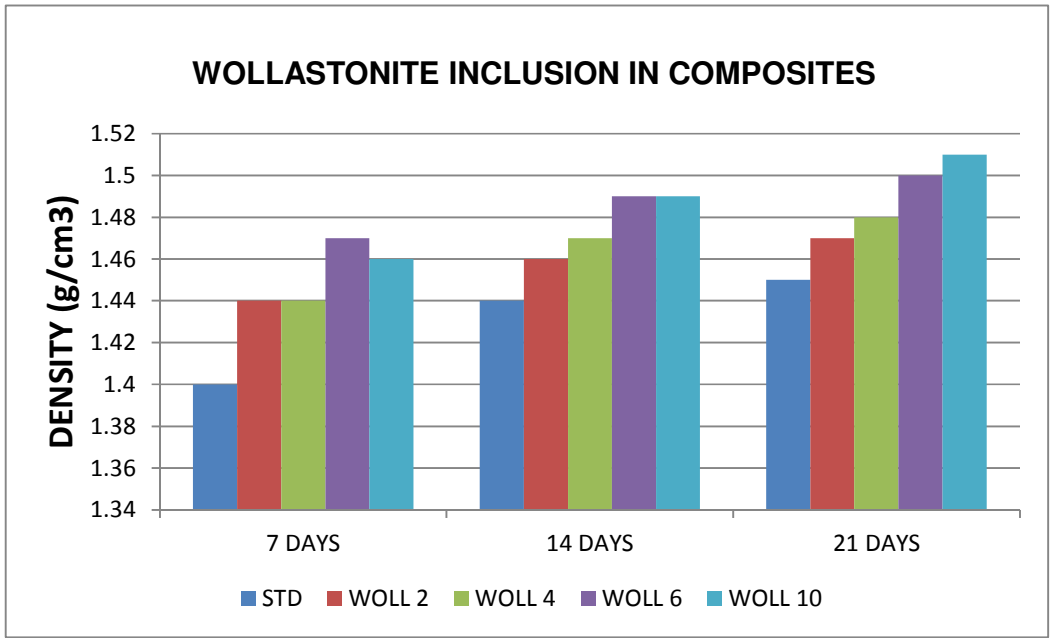


Figure 4.2 Development of density for wollastonite fibrecement sheets

Wollastonite microfibres promote pore discontinuity in cement system resulting in reduced water absorption (Mathur et al., 2007). Although the density increment was significant with wollastonite inclusion relative to the control samples, the change in water absorption was minimal. As the content of the wollastonite microfibres increased in the mix formulation, the wet-dry movement decreased with reduction in matrix permeability. The general trend of the movement results indicates a progressive reduction in movement with increasing content of wollastonite microfibres, as shown in Figure 4.3.

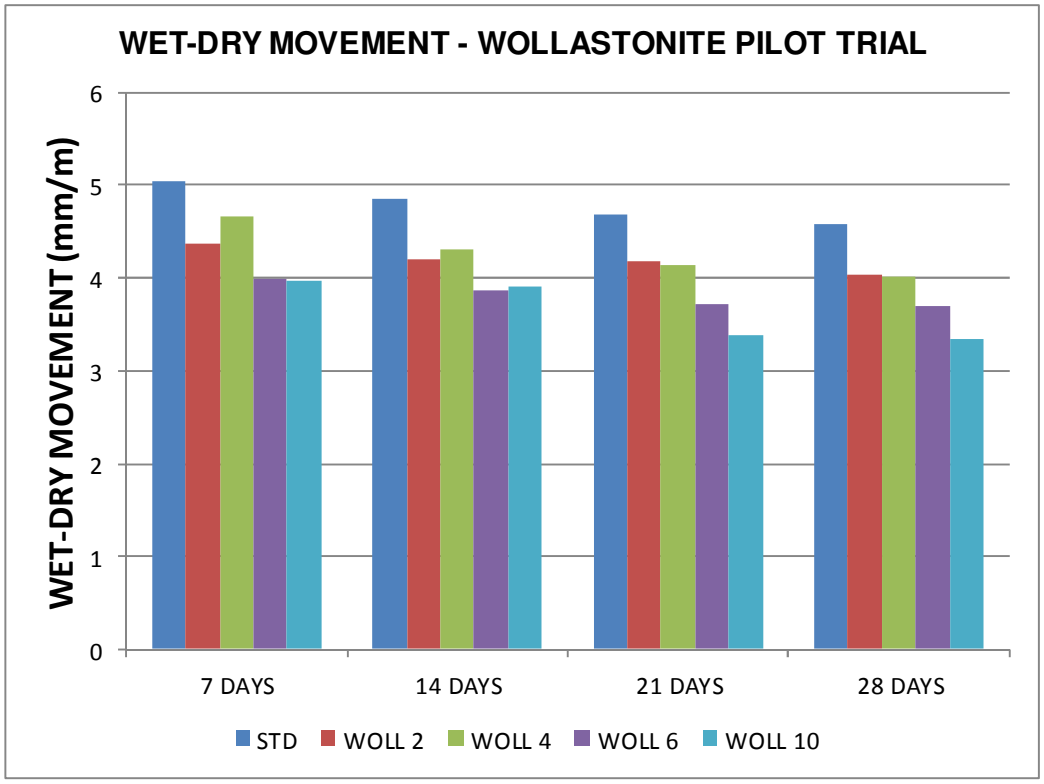


Figure 4.3 Movement curves of wollastonite composites over 28 days curing

Microfibres locally restrain shrinkage stresses in the cementitious matrix (Mangat and Azari, 1984). As the matrix around shrinks, shear stresses develop along microfibres, leading to flexural stresses in the microfibres and tensile stresses in the cementitious matrix (Zhang and Li, 2001).

4.3.2 Flexural strength

The formulations incorporating wollastonite microfibres exhibited flexural strength comparable or higher than that of the control formulation as shown in Figure 4.4. This improvement in flexural strength was more significant at higher wollastonite microfibre content. This is attributed to the delay in bond strength development as a result of dilution effect (Schmidt, 1992). The longer the hydration period, the higher was the matrix strength and consequent improvement of the microfibre/matrix bond, leading to higher

flexural strength (Chan and Li, 1997). This can be attributed to the improvement of the microfibre-matrix-bond with age, the modification in microstructure of transition zone in the vicinity of wollastonite and refinement of pore structure by pozzolanic reaction of wollastonite microfibres in addition to its fibre action.

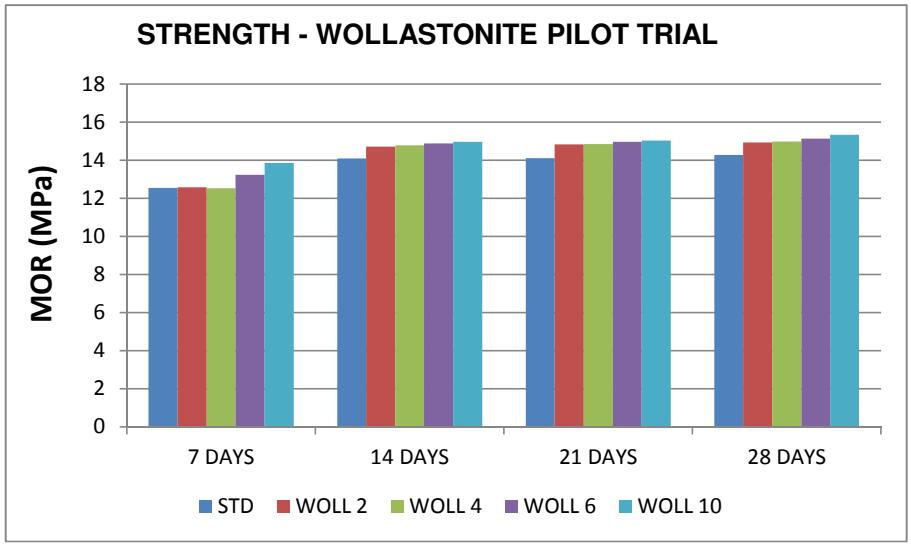


Figure 4.4 Development of strength for wollastonite composites over 28 days

During the early age, the degree of hydration is low and consequently the microfibre/matrix bond strength is low (Chan and Li, 1997). The longer hydration period results in higher matrix strength thus improving the microfibre/matrix bond. Adding very short microfibres can enhance the flexural strength due to its packing effect (Lange et al., 1997). Since the pore structure is significantly modified by wollastonite inclusion, flexural strength increases. Although the flexural strength increased with incorporation of wollastonite, extension or deflection decreased resulting in brittle materials. Brittleness has a negative effect on installation as the sheets crack when nailed to the roof structure. The efficiency of microfibres in restraining

shrinkage depends on several parameters, including the elastic modulus of the microfibres and matrix, the microfibre content and its aspect ratio (Mangat and Azari, 1984). Hence, the shrinkage restraining efficiency of microfibres at early age is higher due to the low elastic modulus of the cementitious matrix.

4.3.3 Mineralogical composition

The XRD results were plotted in Figure 4.5 below. The results show a reduction in hydration products, i.e. portlandite, with increasing wollastonite microfibres content. Increasing the wollastonite microfibres content, reduced the active sites (dilution effect) and improved the packing density, thus limiting the available space for hydration products to form and leading to a lower hydration rate. Adding very fine inert particles displaced some of the water from the voids between cement particles, making it available for hydration process (Schmidt, 1992). Wollastonite inclusion can affect the rate and extent of hydration of cement in addition to CH formation and matrix permeability. CH reduction in the matrix due to its deposition at interfaces can reduce permeability and access to cement grains by water. This may result in limited hydration relative to formulations without wollastonite (Cheng-Yi and Feldman, 1985; Mikhail and Youssef, 1974).

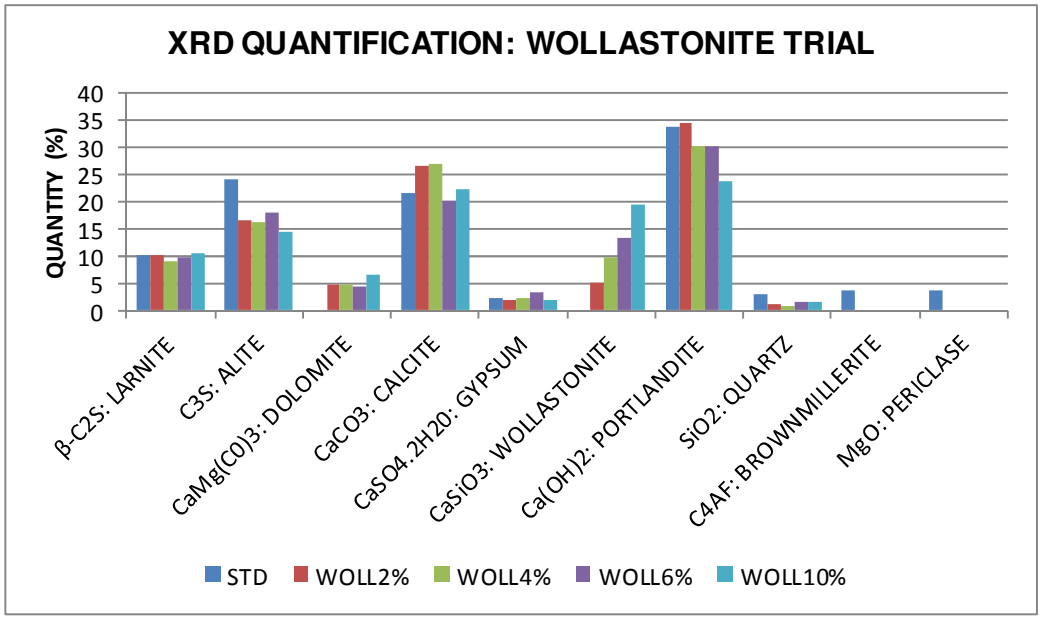


Figure 4.5 Mineralogical composition of wollastonite fibrecement composites at 14 days curing

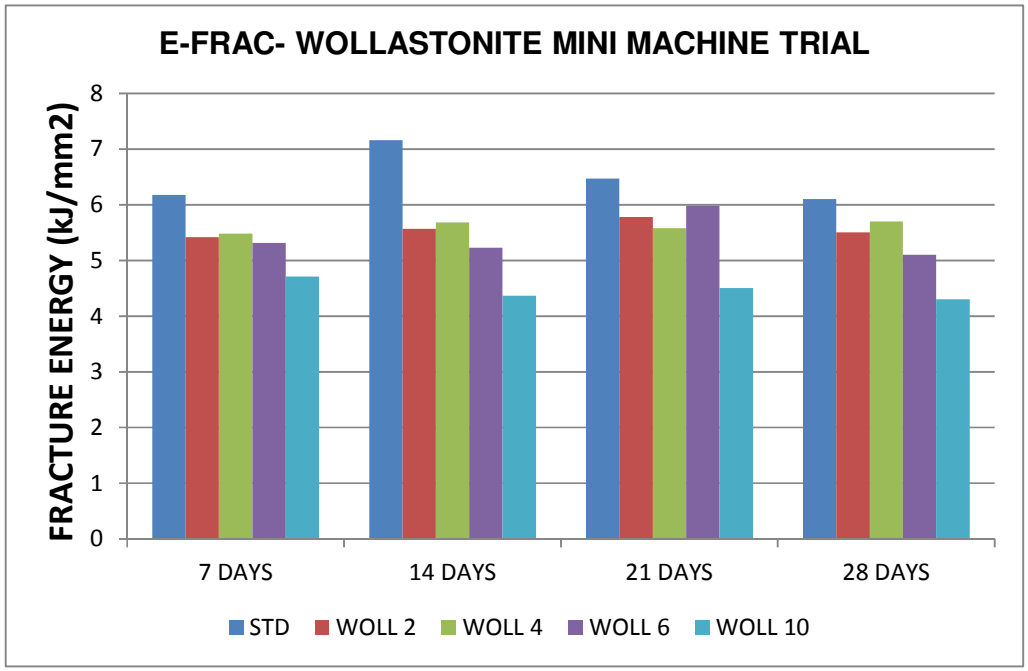


Figure 4.6 Fracture energy of fibrecement composites with different content of wollastonite

The addition of wollastonite microfibres as partial replacement of cement resulted in a decrease in fracture energy as seen in Fig. 4.6. The reduction was more evident in composites with the highest wollastonite inclusion. Previous studies (Ransinchung and Kumar, 2010; Low and Beaudoin, 1994) showed that wollastonite microfibres have the ability to react with cement and develop a strong chemical bond. This strong chemical adhesion will increase the bond strength, leading to fibre rupture rather than pull-out (Rathod and Patodi, 2010). A strong chemical bond promotes fibre rupture: the fracture energy is reduced while the strength of the composite increases; hence the material becomes strong and brittle.

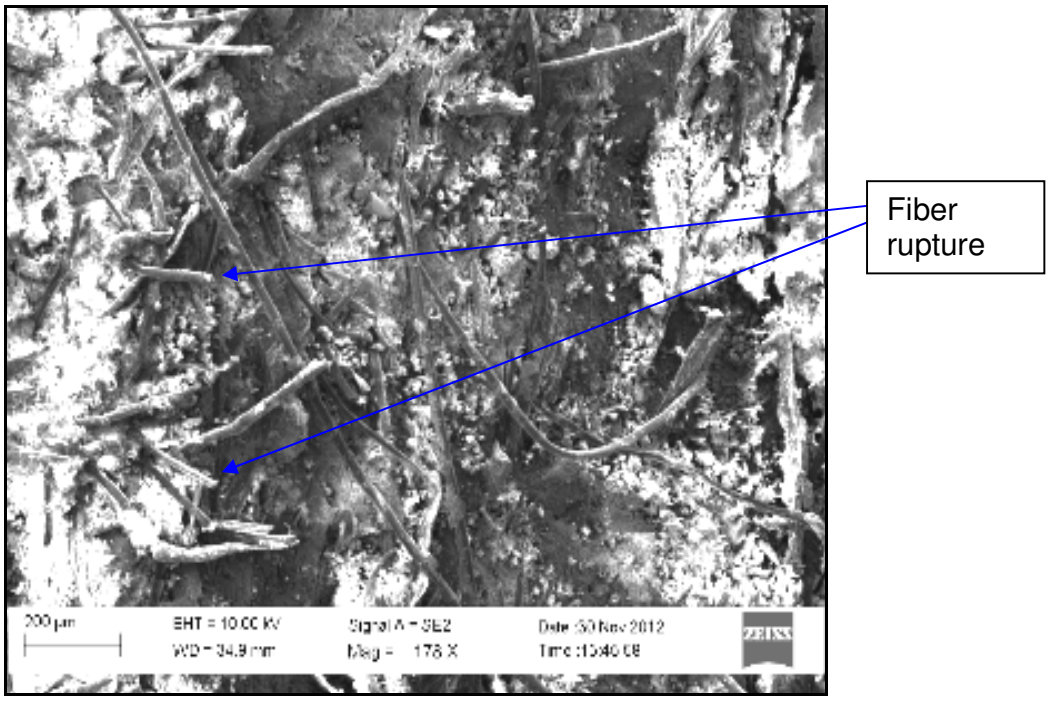


Figure 4.7 SEM micrograph of fibrecement composite incorporated with 6% wollastonite

The above SEM micrograph showed a composite matrix with some cellulose fibres that have ruptured as a result of hydration products formed at surface of the fibre (mineralization). There was no fibre pull-out observed with these

composites. Several voids were observed in the matrix of the control sample as shown in Figure 4.8. These voids are a result of the pulling out of fibres. These fibres present smoother pull-out surface, resulting in poor anchorage in the cementitious matrix.

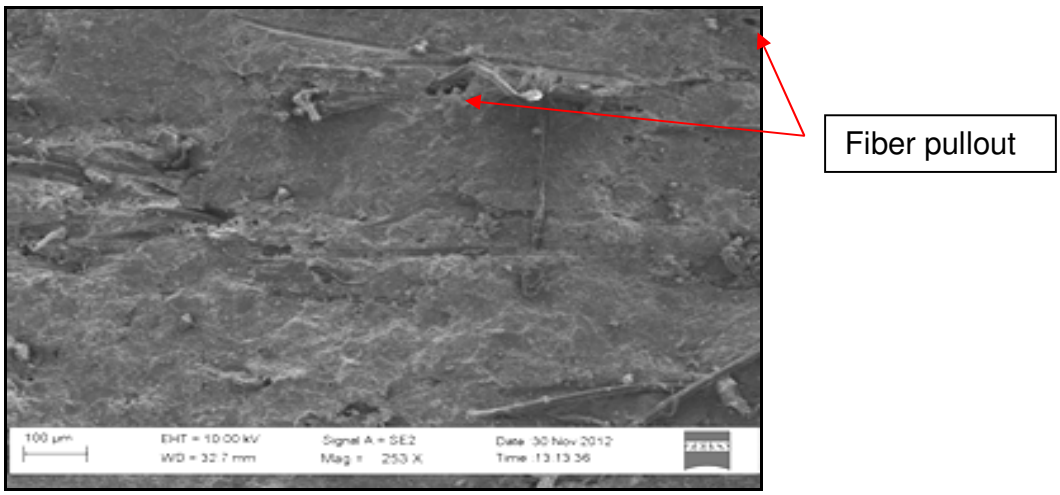


Figure 4.8 SEM micrograph of the control sample without wollastonite

4.4 Conclusions

The main conclusions that can be drawn from this study are the following:

- Influence of wollastonite microfibre addition on fibrecement composite mixtures flexural strength is highly influenced by its dilution effects.
- Addition of wollastonite microfibres appears to promote pore discontinuity leading to higher density and lower water absorption hence reduction in drying shrinkage.
- Although wollastonite inclusion resulted in reduction in wet-dry movement, the deflection was also reduced resulting in brittle materials. Brittleness will lead to cracking during installation.
- Wollastonite inclusion can affect the rate and extent of hydration of cement resulting in permeability reduction.

- Incorporation of wollastonite reduced fracture energy of fibrecement composites and resulted in strong but brittle materials.

CHAPTER 5: EFFECT OF ADMIXTURE IN FIBRECEMENT COMPOSITES

5.1 Introduction

An admixture, according to the ASTM C-125-97a standards, is a material other than water, aggregates or hydraulic cement that is used as an ingredient of concrete or mortar, and added to the batch immediately before or during mixing. Silicone resins are hydrophobic admixtures used in cement mortars and fibre-reinforced cement composites to reduce water absorption. The material is a water repellent admixture, solvent-free, ethoxy-functionalized, low viscosity silicone resin. The ethoxysilyl chemical group in the resin can chemically react with cement hydrate during cement cure and ethanol released upon reaction of the resin. The silicone becomes an integral component of the composite as it cures and therefore forms a water barrier throughout the entire sheet. Previous work carried out described the extent to which silicone resin used as admixture in fibrecement matrix can decrease significantly the ability for water absorption by capillary action (Lecomte, 2012). The experiment was conducted on a mix of cement, silica and cellulose. Results showed that water uptake tends to plateau at higher admixture content, with levels above 0.3-0.5% admixture having limited benefit. Addition of admixture led to a strong reduction in efflorescence even at the lowest level. At 0.25% admixture almost no crystal formation was visually observed on the surface of the boards. There was a 10% drop in flexural strength with modified formulation. No significant difference in setting times was observed with 0.25% admixture.

Superplasticizers are admixtures that can enormously increase the workability of normal Portland cement concrete or reduce its water content. They are adsorbed on the cement particles and act as dispersants by electrostatic and / or steric repulsion effects as demonstrated by Uchikawa et

al. (1997). The type, chemical composition and the molecular structure of the admixture influence the rheology (Yamada et al., 2000). Also, the chemical composition of the cement, especially the amount of C_3A and the availability of sulphate during early hydration affects the performance of superplasticizers (Flatt and Houst, 2001; Mollah et al., 2000). The work done by Maholtra (1978) indicated that the 28-day flexural strengths of superplasticized concrete were equal to or greater than the corresponding strengths of the reference mix.

Mechanism of water reduction by superplasticizer is achieved by deflocculating the cement particles, thereby releasing the water trapped between the cement agglomerates and making it available for mixing (Neville, 2005). Without incorporation of these admixtures, the positively and negatively charged cement particles will be attracted to each other, leading to flocculation. Flocculation of these cement particles will trap part of the mixing water, resulting in less water available for workability and cement hydration. With inclusion of these admixtures, flocculation of cement particles is prevented or minimized. These chemical admixtures are adsorbed by cement particles and are negatively charged, causing repulsion between the cement particles. With the deflocculation of the cement particles, the trapped water will be released and made available for workability and cement hydration. Also, more surface areas of the cement particles will be exposed for the hydration process. The concept is illustrated in Figure 5.1 below.

Effectiveness of a given dosage of superplasticizer depends on the water/cement ratio. Effectiveness increases with decreasing water/cement ratio. In the fresh state of concrete, utilization of superplasticizer will normally reduce the tendency to bleeding due to the reduction in water/cement ratio or water content of concrete. However, if the water/cement ratio is maintained, there is tendency that superplasticizer will prolong the time of set of concrete as more water is available to lubricate the mix. In the case of hardened concrete, Yamakawa et al. (1990) highlighted that the use of superplasticizer

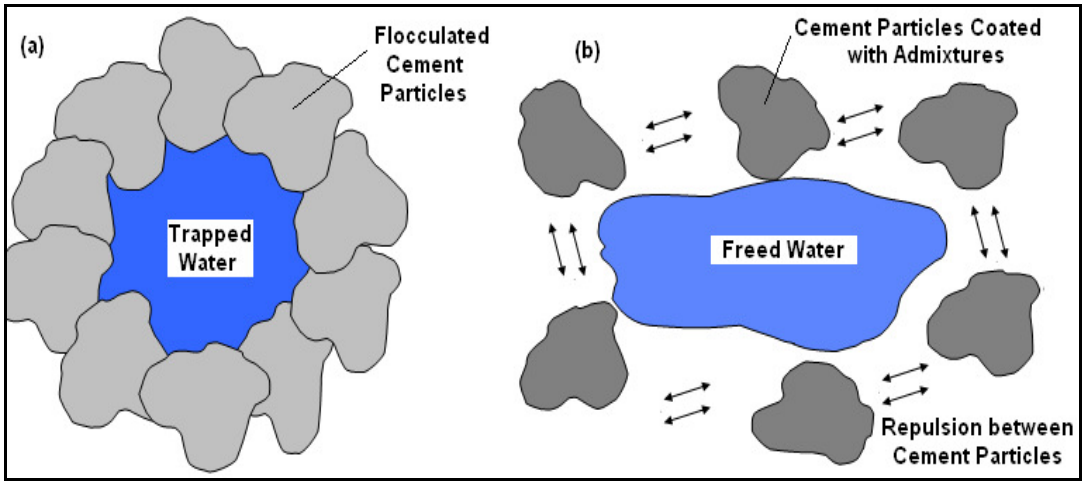


Figure 5.1 (a) Flocculation of cement particles resulting in trapped water. (b) Deflocculation of cement particles upon adsorption of water reducing admixtures (Law, 2004)

will increase flexural strength by enhancing the effectiveness of compaction to produce denser concrete. Risk of drying shrinkage will be reduced by retaining the concrete in liquid state for longer period of time. In addition, rate of carbonation become slower when water/cement ratio is decreased with the presence of superplasticizer.

5.2 Materials and method

5.2.1 Materials

The Portland cement intergrounded with 10% calcium carbonate, was supplied by Afrisam. The synthetic fibre used for reinforcement in fibrecement composites was polyvinyl alcohol (PVA) fibre. Densified silica fume was supplied by Silicon Smelters. It is a by-product of the fabrication of ferrosilicon alloys and a very reactive pozzolan with constant chemical composition. It consists of very fine particles, 100 times finer than those of

cement, almost exclusively amorphous SiO_2. The content of SiO_2 is usually above 85%.

The cellulose, unbleached softwood pulp, with kappa number of 28±4 and fibre length ≥3 mm, with an average of 3.47 mm, was obtained from Sappi. Cellulose was mixed in the pulper with water then refined to 110 Canadian Standard Freeness. Refining defined as the mechanical treatment of pulp carried out in the presence of water, usually by passing the suspension of pulp fibres through a relatively narrow gap between the revolving rotor and a stationary stator, both carrying bars aligned across the line of flow of the stock. At this freeness, adequate fibrillation has been obtained in the refiner for the pulp to achieve optimum solids retention in the fibrecement composite.

The silicone resin admixture was supplied by Dow Corning and superplasticizer supplied by Chryso. The properties of these materials were described in detail in Chapter 2.

5.2.2 Preparation of samples

The fibrecement composites were prepared in the pilot plant using the Hatschek process as described in details in section 2.1 above. The PVA fibres were mixed at a very high speed to disperse the fibres in water for 5 min, followed by addition of refined cellulose, 110 Canadian Standard Freeness, under continuous stirring for another 2 min. Silica fume was added at high speed for 1 min then the stirrer speed was reduced as cement and calcium carbonate were added. To investigate the effects of superplasticizer, three additional mixes were prepared using dosage of 10%, 15% and 20%. For the silicone resin admixture, the test specimens were prepared with a dosage of 0.3%. The third test specimens contained 3% kaolin and 0.3% silicone resin admixture. The slurry was maintained under continuous stirring for an additional period of 2.5 minutes. The slurry was diluted then transferred to the mix box in the Hatschek machine, resulting in a

concentration of approximately 7% solids. The sheet obtained from the Hatschek process was cut into 250 mm x 250 mm x 6 mm specimens for physical properties test. The specimens were placed in between steel plates (300 mm x 300 mm) and shrink-wrapped with transparent plastic. The tests were carried out at 7 days intervals, up to 28 days.

At each test interval, the samples were immersed in water for 24 hours. After this period, the samples were removed from water, dabbed with a cloth to remove excess water then tested for flexural strength.

The samples under investigation were labeled as follows:

- STD for fibrecement composites with standard formulation as control,
- SR for standard mix formulation incorporated with silicone resin admixture,
- SR+KAO for control mix formulation with silicone resin plus 3% kaolin,
- SP for control mix formulation with 10% superplasticizer,
- SPA for control mix formulation with 15% superplasticizer and,
- SPB for control mix formulation with 20% superplasticizer.

5.3 Results and discussion

5.3.1 Effect of admixture on water absorption of composites

Water absorption test was used to assess the pore space in the material that could impact the movement of water resulting in drying shrinkage. The water absorption results for composites with superplasticizer and silicone resin are summarized in Figures 5.2 and 5.4 respectively. The data recorded indicate the relation between dosages of superplasticizer and water absorption over a 28day curing period. With increment in curing age from 7 to 14 days, water absorption decreased by 5.3%, 8.6%, 4.8% and 5.6% for STD, SP, SPA and SPB samples respectively. The trend showed a decrease in water absorption as curing progressed; the reduction was more evident at the lowest dosage

of superplasticizer. Addition of superplasticizer and incorporation of pozzolanic admixtures such as silica fume creates a super dense microstructure within a few days or less (Bentz and Jensen, 2004). This rapid development of a very fine pore network within the cement paste creates an impermeable medium and effectively seals it from its environment. Unable to obtain the externally available curing water, the composite consumes water from its own capillary pores.

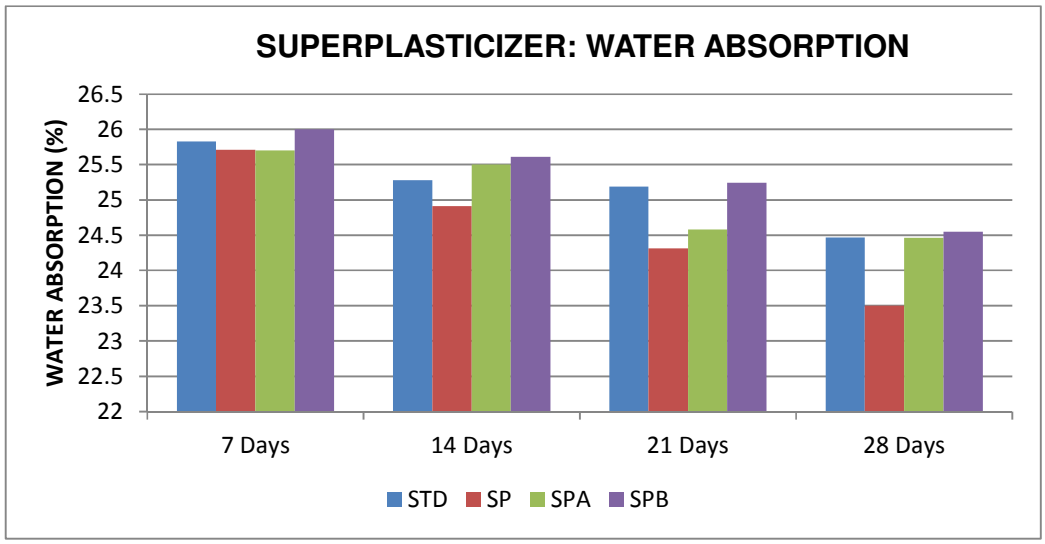


Figure 5.2: Effect of superplasticizer on water absorption of the fibrecement composites over a 28 days curing period

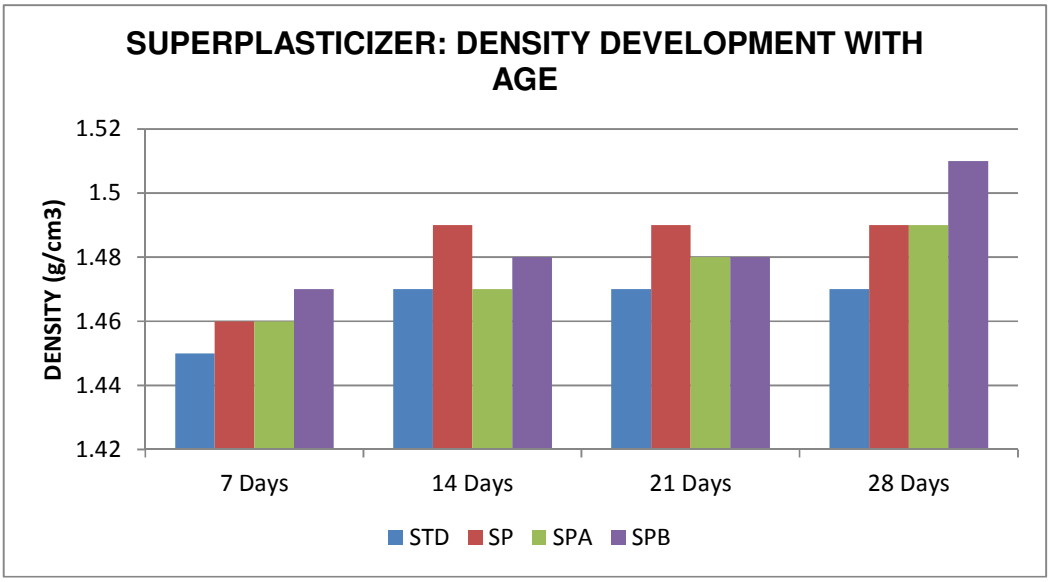


Figure 5.3 Effect of superplasticizer on the density as the fibrecement composites age

The inclusion of silicone resin admixture in composites resulted in significant reduction in water absorption than with the superplasticizers. Addition of kaolin to the mix formulation that contained the silicon resin admixture enhanced the water absorption further as the composites aged. Inclusion of silicon resin to the standard mix formulation reduced the water absorption by 10.4% and by also incorporating the pozzolanic material, kaolin, and further reduction was observed (17.9%). There was no significant reduction in water absorption noted as the composites aged.

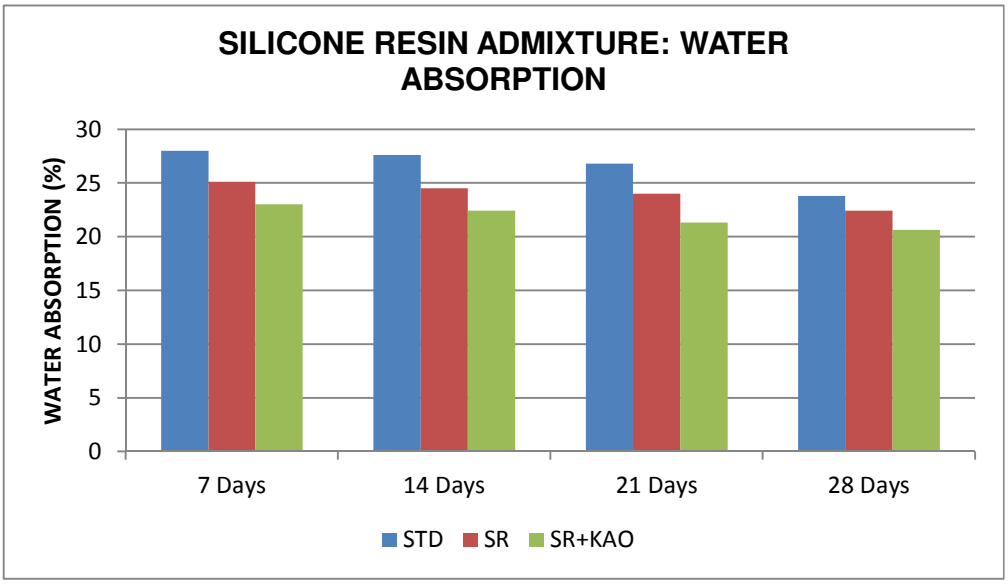


Figure 5.4 Development of water absorption for composites with admixture

Although the inclusion of silicone resin admixture resulted in significant reduction in water absorption, the wet-dry movement showed minimal change. The superplasticizer formulations resulted in significant reduction in wet-dry movement over the 28 day curing period as can be seen in Figures 5.5 and 5.6 below. The reduction in wet-dry movement in composites is an indication of a reduction in shrinkage. Since the drying shrinkage is delayed for a substantial amount of time, if not indefinitely, then the cement matrix has more time to develop and build tensile strength. With this higher tensile strength, cracking due to drying shrinkage is less likely.

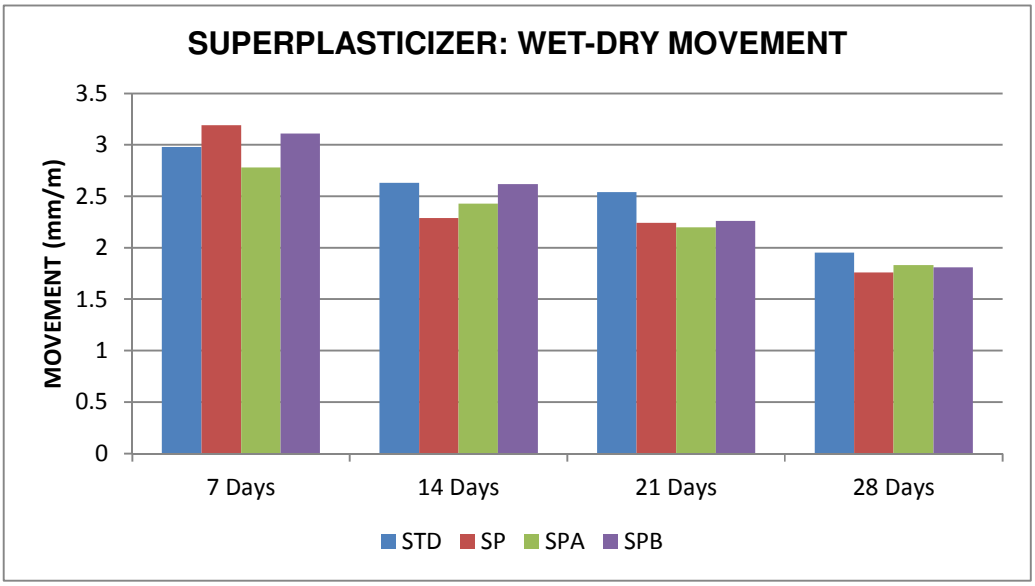


Figure 5.5 Movement of composite with superplasticizer after exposure to wet immersion for 24 h followed by 24 h drying during a testing interval

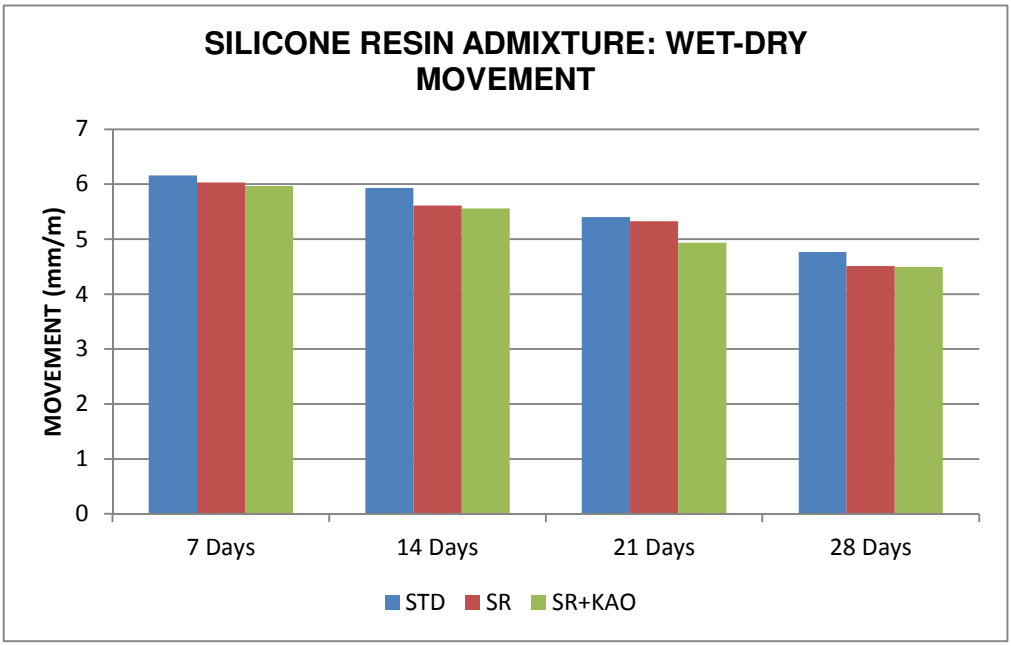


Figure 5.6 Effect of admixture on wet-dry movement of composites over a 28 day curing process

5.3.2 Effect of Admixture on flexural strength

The values of flexural strength for the different dosages of superplasticizer are shown as a graph in Figure 5.7 below. From the graph, incorporation of plasticizer did not increase strength at lower and higher dosage at 7 days curing. At early age, i.e. 7 days, a reduction of 12.8% and 11.4% was observed in flexural strength for incorporation of 10% and 20% superplasticizer, respectively. As the superplasticizer dosage increased, the lower the early-age flexural strength was achieved. This can be attributed to the retardation effect induced by superplasticizers, in agreement with previous work (He et al., 2006). The retardation effect can be attributed to a reduction in the ability of salts (e.g. alkali sulphates) to dissolve and ionize in the pore solution due to the lower polarity induced by superplasticizer addition (Rajabipour et al., 2008). The delay is due to an adsorption of the admixture on the surface of cement particles; forming a semi-permeable layer onto the cement grains, which acted as a diffusion barrier to delay the cement hydration. This indicates that the retardation of hydration process induced by superplasticizer is the dominant factor. On the other hand, composites with 15% superplasticizer inclusion resulted in an increment of 5.2% flexural strength. As the composites aged with time, an enhancement of 6%, 29.8%, 10.8% and 13.3% flexural strength for STD, SP, SPA and SPB respectively were noted. The admixture will affect the rate of cement reaction at early ages, and consequently affect the distribution of hydration products and later strength.

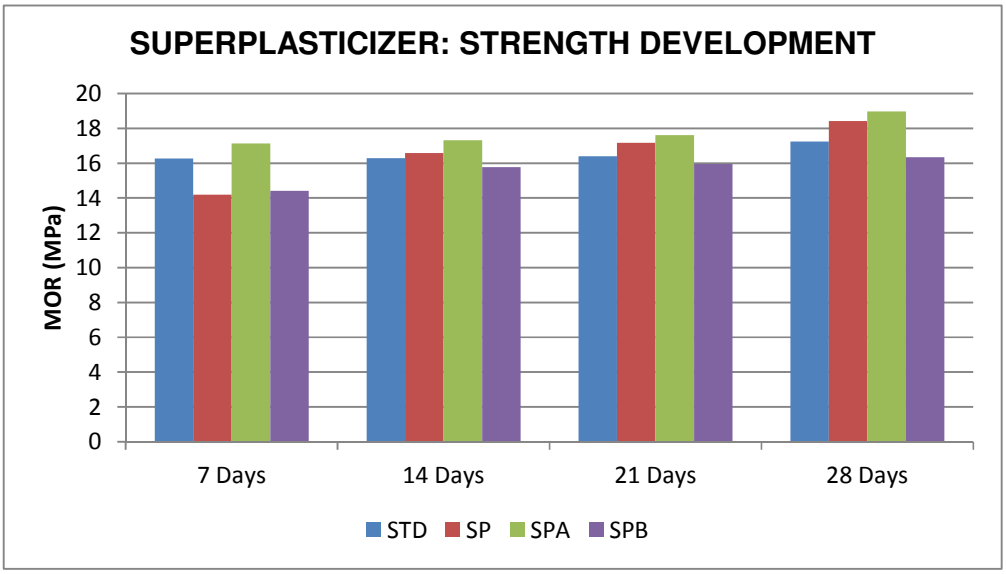


Figure 5.7 Comparison of strength development for standard mix formulation with superplasticizer incorporated mixes during the ageing process

Since addition of superplasticizer will provide more water for slurry mixing, not only the hydration process will not be disturbed, but it is accelerated by the additional water from deflocculation of cement particles. Though increment in dosage of admixture enhanced the strength, there is still an optimum limit for the usage of admixture. When dosages were above or below this limit, increase in dosage resulted in flexural strength reduction. Optimum dosage of superplasticizer is found based on the highest ultimate strength that they present at age 28 days (Nmai, 1998). Therefore, the optimum dosage of superplasticizer was found to be 15% as determined at 28 days curing, see Fig. 5.7.

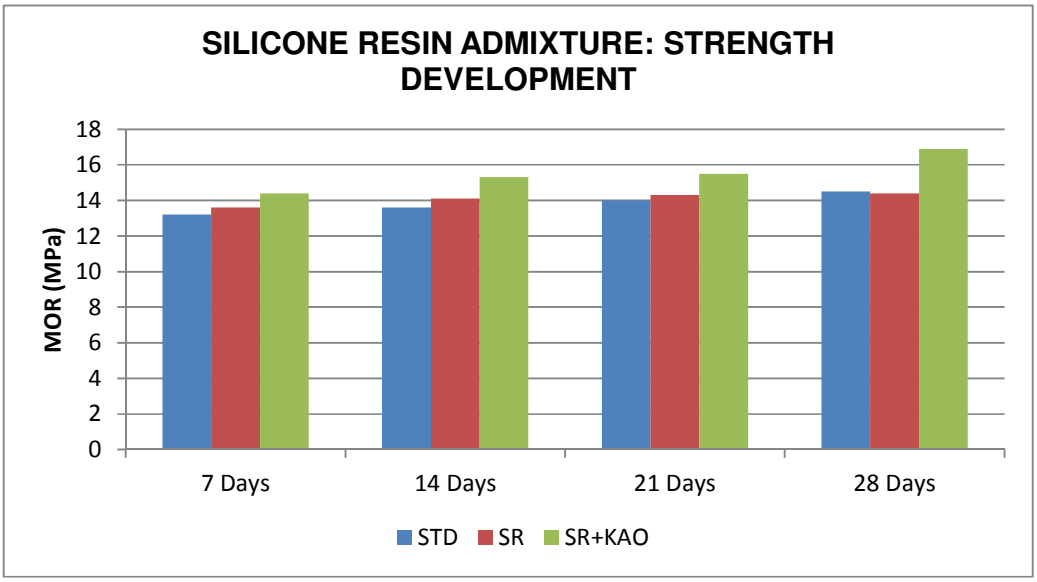


Figure 5.8 Strength development for composites with admixtures with age

Although addition of admixture did not have a huge impact on strength; development of composites during the curing process, addition of a pozzolanic material, kaolin, showed a significant enhancement in strength. Addition of silicone resin improved early age strength by 3% whereas incorporation of kaolin further improved the strength by 9%, relative to standard mix formulation. As the composites aged, the silicone resin inclusion did not improve the flexural strength but, additional kaolin indicated a 17% increase in flexural strength.

5.4 Conclusions

- Addition of admixtures to fibrecement composite mix formulation resulted in super dense microstructure within a few days.
- The admixtures were involved in the formation of a semi-permeable layer onto the cement grains, which acted as a diffusion barrier to delay the cement hydration. This layer also inhibited the transportation

of water in and out of the composite thus resulting in lower water absorption.

- Incorporation of admixtures enhanced the strength development of fibrecement composites over time. The higher dosage of superplasticizer resulted in lower achieved early age flexural strength. Addition of silicon resin to composites showed no improvement in flexural strength. On the other hand, addition of kaolin to the same mix resulted in significant increases in flexural strength.
- The flexural strength results indicated the importance of determining the optimum dosage level of superplasticizers. Dosages with lower or higher values than the optimum value will reduce the flexural strength.
- By reducing the amount of water with inclusion of superplasticizers, the density increased; yielding lower permeability hence reduced volume change from drying and wetting thus reducing drying shrinkage.

The admixtures are considerably more expensive therefore not economical for use in daily production process.

CHAPTER 6: IMPACT OF KAOLIN ON MECHANICAL PROPERTIES AND DURABILITY OF FIBRECEMENT COMPOSITES

6.1 Introduction

Kaolinite is a mineral belonging to the group of aluminosilicates, 1:1 layer mineral and a product of advanced weathering processes. The layers are bonded together by sharing oxygen anion between Al and Si. These layers are called platelets (Bailey, 1980; Duda et al., 1990; Bernard and Rost, 1992; Bish, 1993; Klein and Hurlbut, 1993; Slivka, 2002). One layer of the mineral consists of an alumina octahedral sheet and a silica tetrahedral sheet that share a common plane of oxygen atoms. The repeating layers of the mineral are hydrogen bonded together; see Figure 6.1 (Bear, 1965). The tetrahedral sheet is formed by the association of a tetrahedral arrangement in a plane. The four tips of the tetrahedral are occupied by oxygen ions and their center by a silicon ion which shares its four cations with the four oxygen ions of the tips. On the other hand, the six tips of the octahedral plane are occupied by oxygen ions of hydroxyl groups and their center by an alumina octahedral sheet (Gruner, 1932; Brindley and Robinson, 1946). Due to this strong attraction these platelets are non-expanding when hydrated. Hence, kaolinite is unable to absorb water into the interlayer position. As a consequence of its high molecular stability, isomorphic substitution of Al for Si in the tetrahedral layer is limited or non-existent (Mitchell, 1993). Accordingly, it has a low cation exchange capacity. Its chemical formula is $Al_2O_3.2SiO_2.2H_2O$ with the following composition 39.5% Al_2O_3; 46.5% SiO_2; 14% H_2O.

Frost (1998) discussed outer and inner hydroxyl groups of the alumina hydroxyl sheet. The outer groups are situated along the unshared plane of the alumina hydroxyl sheet, while the inner groups are located along the plane that is shared with and borders on the silica oxide sheet. The

movement of the inner hydroxyl plane is restricted as a result of chemical bonding between the silica and alumina sheets. As a consequence of its well-packed structure, kaolinite particles are not easily broken down and the layers are not easily separated. Hence, most sorption activity occurs along the edges and surfaces of the structure. The specific surface area is low because the external surface is increased by the surface area between the sheets, called interlayer area.

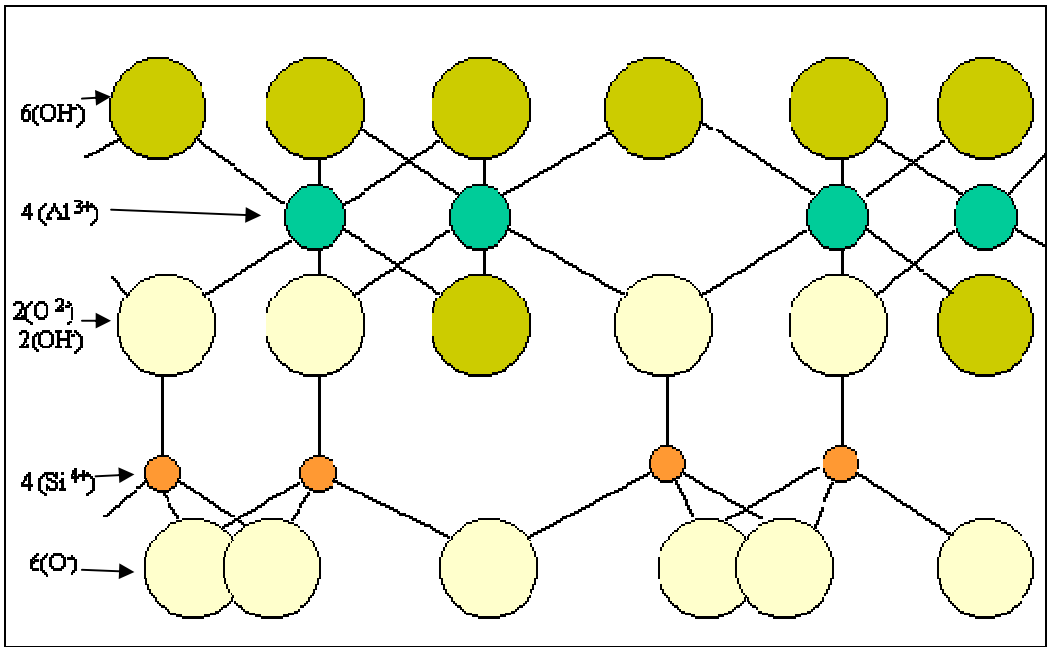


Figure 6.1 Schematic diagram of kaolinite structure

A pozzolan is defined in ACI 116R as a siliceous or siliceous and aluminous material, which in itself possesses little or no cementitious value but will, in finely divided form and in the presence of moisture, chemically react with calcium hydroxide at ordinary temperatures to form compounds possessing cementitious properties. A natural pozzolan is defined as either a raw or calcined natural material that has pozzolanic properties. The limits of pozzolans as per ASTM C618 are:

- $SiO_2 + Al_2O_3 + Fe_2O_3 = 70\%$;
- $MgO, CaO, Na_2O = 0\%$;
- $SO_3 = 3\%$.

The chemical composition of kaolin was compared with ASTM C618 for its suitability as a pozzolan. The content of silica, ferric oxide and aluminum oxide satisfies the standard for class “N” pozzolans, which is a high quality pozzolan category. Sulphur trioxide was absent, which is a positive characteristic. The other parameters that determine the behavior of any pozzolan include fineness, strength activity index, water requirement, soundness and uniformity requirements. Strength activity index is defined as the ratio of flexural strength of mortars incorporating pozzolans to the flexural strength of control mortars at age of 7 days and 28 days. The shape, fineness, particle size distribution, density and composition of natural pozzolan particles influence the properties of freshly mixed unhardened concrete and the strength development of hardened concrete. Natural pozzolans absorb water from the mixture and hold this water in the system allowing for improved finishing.

Sabir et al. (2001) observed that portlandite (CH) reacts with added pozzolan (S) resulting in additional calcium silicate hydrates (CSH). The pozzolan reacts with calcium hydroxide (CH) that is liberated by the hydration of C_3S and C_2S of Portland cement expressed as below (Cohen, 1990).

Cement hydration: $2\ C_3S + 6\ H_2O \longrightarrow CSH + 3\ CH$ Eqn 6.1

$2\ C_2S + 4\ H_2O \longrightarrow CSH + CH$ Eqn 6.2

Pozzolanic reaction: $3\ CH + 2\ S \longrightarrow CSH$ Eqn 6.3

Most natural pozzolans contain substantial amounts of constituents other than silica, such as alumina and iron oxide, which will react with calcium

hydroxide and alkalies (sodium and potassium) to form complex compounds. Generally, amorphous silica reacts with calcium hydroxide and alkalies more rapidly than does silica in the crystalline form (quartz). The larger particles (lower the surface area / unit volume) result in less rapid rate of reaction. Therefore, the chemical composition of a pozzolan does not clearly determine its ability to combine with calcium hydroxide and alkalies.

The pozzolanic reaction progresses like an acid-base reaction of lime and alkalies with oxides (SiO_2 + Al_2O_3 + Fe_2O_3) of the pozzolan. Firstly, there is a gradual decrease in the amount of free calcium hydroxide with time, and secondly, during this reaction there is an increase in the formation of CSH and calcium aluminosilicates that are similar to the products of hydration of Portland cement. According to Lea (1970), the partial replacement of Portland cement by pozzolan of high SiO_2 / (Al_2O_3 + Fe_2O_3) ratio has been found to increase the resistance of concrete to sulphate and seawater attack. This is attributable to the removal of free hydroxide formed in the hydration of Portland cements. Research done by Mehta (1987) highlighted the importance of pore refinement, resulting from pozzolanic reaction, for enhancing chemical durability and mechanical strength. The beneficial influence of pozzolans in cement matrix is due to a combination of physical and pozzolanic effects (Goldman and Bentur, 1989). The first is a filler effect leading to reduction in porosity of the transition zone in the fresh concrete and providing the infrastructure needed for a strong transition zone. This potential is materialized by the formation of bonds between the densely packed particles in the transition zone through the pozzolanic reaction.

6.2 Materials and specimen preparation methods

6.2.1 Materials

The physical and chemical properties of kaolin and cement are presented in Table 6.1 below.

Table 6.1: Physical and chemical properties of kaolin and cement

PROPERTIES	CEMENT	KAOLIN
SiO_2 (%)	22.08	67.5
Al_2O_3 (%)	4.4	24.1
K_2O (%)	0.46	5.38
TiO_2 (%)	0.37	0.89
MgO (%)	1.44	0.43
Na_2O (%)	0.10	0.38
Fe_2O_3 (%)	2.47	0.28
L.O.I (%)	≤ 5	5.93
Surface area (m2/g)	1.99	5 - 20
Color	Grey	Off-white

The flocculant used for pilot trials was Mag10 supplied by Improchem whereas for plant production flocculants 5275 and 5618 were supplied by Buckman. The properties of all the flocculants are found in Table 6.2. The flocculants were all anionic, polyacrylamide polymers, Buckman flocculants with same molecular weight but different charge density whereas Mag10 had both lower molecular weight and charge density.

Table 6.2: Properties of polyacrylamide flocculants

PROPERTIES	MAG 10	FLOC 5275	FLOC 5618	FLOC 5616
Appearance	White powder	White powder	White powder	White powder
Molecular weight (Daltons)	10–12 million	10 – 15 M	10 - 15 M	10 – 15 M
Charge density (mol %)	1 - 5	20 - 25	25 - 30	15 - 20

The other materials used were refined cellulose fibres, PVA fibres, silica fume and calcium carbonate.

6.2.2 Preparation of pilot plant specimens

The fibrecement composites were prepared in the pilot plant using the Hatschek process as described in details in section 2.1 above. The slurry was prepared with silica fume, cellulose and PVA fibres, calcium carbonate and cement for the control specimens. The trial mixes contained kaolin at 1%, 2%, 3% and 5% as a replacement for cement. The slurry was maintained under continuous stirring for an additional 2.5 minutes after all the powders had been added. It was diluted with process water then transferred to the mix box in the Hatschek machine, resulting in a concentration of approximately 7% solids. The Mag 10 flocculant was dozed into the mix box for optimum retention at the rate 3 s/l. The sheet obtained from the Hatschek process was cut into 250 mm x 250 mm x 6 mm specimens for physical properties test. The specimens were placed in between steel plates (300 mm x 300 mm) and shrink-wrapped with transparent plastic. The tests were carried out at 7 days intervals, up to 28 days.

6.2.3 Production of corrugated sheets

The production of corrugated sheets for this project was conducted in the plant using the Hatschek process. The process involved pre-treatment of cellulose fibres, by refining, to achieve optimum fibrillation. The treated fibres then act as filters to facilitate transfer of smallest of the cement particles from the slurry to the film, thus avoiding accumulation of inactive cement in the mixer or agitator. The flocculants 5275 and 5618 were blended in a vessel at a ratio of 60:40.

The treated fibres along with predetermined quantities of cement, fillers and synthetic fibres were charged into a mixing vessel to form slurry. The blend of flocculants was added into the mix box at a rate of 3 s/l to achieve optimum retention. The slurry was then fed into the vats where layers were deposited on rotating sieve cylinders. The thin layers were transferred to a moving felt which finally deposited them on a rotating drum / roller. The transference of layers on the rotating drum continued until the required thickness of sheet was achieved. The sheet was automatically cut and fell on the conveyor belt which transported it to the machine atmospheric corrugators, where the flat sheet was corrugated then placed onto the steel form plates. For trial purposes, 3% and 5% was used as a replacement of cement.

As the sheets are produced, they are cut into 920 mm widths hence the edge trimmings and damaged green sheets were automatically fed to waste pulper. This waste was re-pulped and returned back to the mixer. The flocculant dosage changed when wet waste was added to the fresh mix.

The corrugated sheets on steel form plates are loaded on a trolley and transferred to a steam chamber at 40 - 50ºC for 8 h. After pre-curing in the steam chamber the sheets were taken off the form plates, stacked in 40s on a wooden pallet. Thereafter, the sheets were shrink-wrapped with transparent plastic and kept under cover for 14 days to retain moisture required for the hydration process. At the end of this period, the sheets were unwrapped and physical tests conducted.

6.3 Results and discussion

6.3.1 Flocculant selection

Flocculants play an important role in the Hatschek process not only for retention of cementitious and filler particles on the laminar sheet formed by cellulose and synthetic fibres on the rotating sieve but, also retaining sufficient water to increase laminar bonding to facilitate the corrugation without causing cracks. The two major functions of flocculants in the Hatschek process are solids retention in the vat and settling of solids in the cone tanks to obtain clean circulating process water (Winter et al., 2012). The authors found that by introducing wet waste to fresh mix, the charge density of the mix changed hence for optimal efficiency coagulants had to be added to the circulating process water. Flocculants react with water to form insoluble hydroxides which, upon precipitating; link together to form long chains, physically trapping small particles into larger flocks.

Knowledge of flocculant characteristics is essential for the optimization of flocculation process (Glover et al., 2001; Ray and Hogg, 1987; Yu et al., 2006). The results of the retention and filtration tests for the different flocculants are illustrated in Figures 6.2 and 6.3 respectively. The tests were conducted on fibrecement composite slurries incorporated with 3% kaolin as replacement of cement, then diluted to 7% consistency. Different dosages were added to determine the optimum level for highest filtration and solids retention. The Mag10 and blend of 5275:5618 flocculants resulted in superior performance for solids retention whereas, the blend 5275:5616 showed poor retention performance, Fig 6.2. All the flocculants are in the same molecular weight range hence the performance of these flocculants can be attributed to their charge density. It was demonstrated by Nasser and James (2006) that the flock size and the settling rate show a strong dependence on flocculant charge type. Also, that the difference in the compression sensitivity of the

flocculated slurries might be attributed to flocculant structure related adsorption.

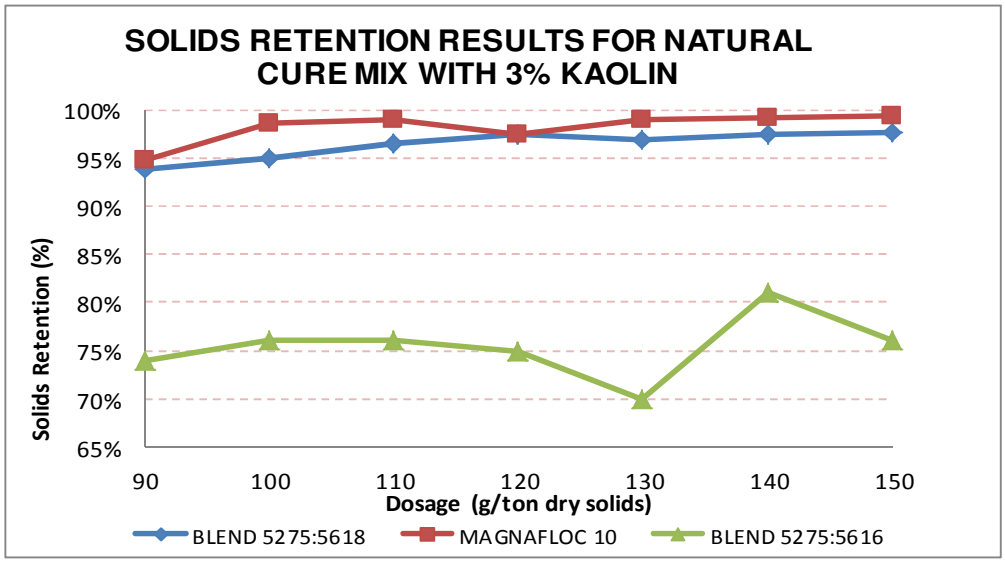


Figure 6.2 Flocculant retention results for fibrecement composite incorporated with 3% kaolin. For optimal performance, solids retention must be higher than 95%.

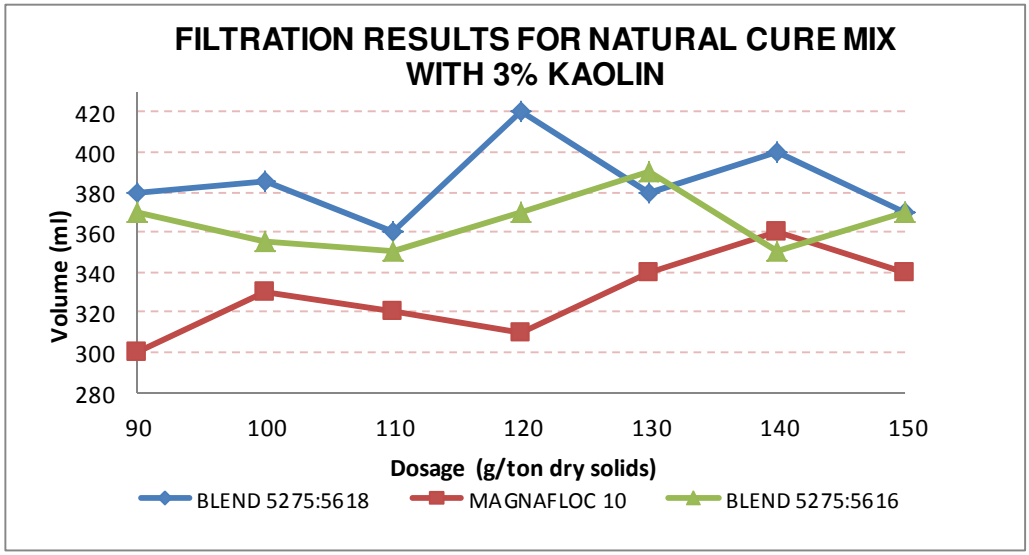


Figure 6.3 Selection of flocculant type and dosage for optimal filtration in the vats. Better filtration achieved with volume greater than 350 ml.

Figure 6.3 showed that the blend 5275:5618 gave the best filtration results followed by the blend 5275:5616 and lastly Mag 10. The electrostatic repulsion between kaolin particles and the anionic molecular chain allowed flocculation to occur mainly via bridging mechanism. These flocculant bridges prevented the particles from moving apart through random motion, but when such motion moved them together other active groups on the flocculant bridged the bond to the solids, holding them in the closer position. Therefore, the flocculant molecule interacted with particles at long distance arising from the electrostatic repulsion (Zhu et al., 2009). These repulsive forces allowed the flocculant molecule to be extended and produce loops and tails, leading to the formation of open structures flocks. Higher molecular weight flocculants had a stronger affinity for adsorption on the particle surfaces due to having more active groups. In order to produce corrugated fibrecement sheet with superior mechanical properties, the flocculant(s) used in the system must give optimal performance in both solids retention and filtration. Therefore, the blend 5275:5618 was the most effective in retaining solids in the sheet and filtration in the vats. Although this blend of flocculants resulted in superior results for both retention and filtration across the dosage range, the optimal performance was noted at 120 ppm. The more effective the flocculation process, the thicker the lamina formation thus increasing the efficiency of raw materials utilization and decreasing the production time.

Besides the solids retention and filtration in the vats, the flocculation process must be able to return the solids that pass through the sieve cylinder during formation of lamina. The solids must be returned back to the mixer at a faster rate to avoid reduction in reactivity with time. A settling test was conducted on a 1 liter slurry dozed with flocculant to determine the rate of settling and the maximum bed height obtained. The results of the settling test are tabulated in Table 6.3 below.

Table 6.3 Results for settling rates of solids, with different flocculants

Flocculants	Dosage (mg/l)	Bed height (mm)	Settling rate (ml/s)
Control	0	150	17.2
5275	3	110	47.3
5616	3	125	45.8
5618	3	100	55.7
Mag 10	3	130	37.9
60:40 5275:5618	3	100	60.1
60:40 5275:5616	3	120	48.3

The results in the table above indicate that the best settling rate at the lowest bed height was achieved with the blended flocculants 5275:5618 at the ratio of 60:40. Flocculant properties such as molecular weight, charge density and charge types affect flocculating and destabilizing actions (Zhou and Franks, 2006; Glover et al., 2001). The high molecular weight flocculants induced the production of fine particulates clumped into big flocks. The flocks floated to the top of liquid then settled at the bottom of the liquid. It would be expected that these flocculants would result in higher settling rates but the bed heights will be higher too. There was another parameter that had an impact on settling rate, the charge density. When flocculant anionicity increased, more compact or denser flocks were obtained because more bonding groups interacted with cement particles. Hydrogen bonds were formed between the amide groups of polyacrylamide polymer and surface hydroxyl groups. Linkage by polymer chains gave stronger bonds between particles than van der Waals forces. Mag 10 flocculant had medium molecular weight and lower charge density. Therefore, the flocks that were produced during the flocculation process were less as few amide groups interacted with cement particles.

The formation of flocks involves four stages:

- Diffusion of macromolecules towards the solid/liquid interface;
- Macromolecule adsorption onto particles and conformation forming loops, tails and trains;
- Formation of bridges and
- Flocks formation, growth and settling.

These mechanisms are related to properties of polymers such as charge, hydrophobicity, structure and molecular weight. Therefore, flocculation processes depend on several physical, chemical and operational parameters such as type, molecular weight and concentration of the polymer, agitation, pH and temperature. High shear rates resulted in broken polymer tails and loops and flocculant fragmentation. Thus rearrangement of polymer on the surfaces of the particles after breakage occurred; flattening the polymer chains onto the particle surface thus reduced their ability to form polymer bridges between particles.

6.3.2 Pilot machine results

Six formulation mixes were prepared in the pilot plant. The standard was the control mix which comprised of cement, cellulose and PVA fibres, calcium carbonate and a percentage of silica fume. Magnafloc 10 was used as the flocculant during production of these samples and dosage was only done in the mix box. The trial mixes were as follows:

- Kao 1 – standard formulation with 1% cement replaced by kaolin.
- Kao 2 – standard formulation with 2% cement replaced by kaolin.
- Kao 3 – standard formulation incorporated 3% kaolin as replacement for cement.
- Kao 5 – standard formulation with 5% inclusion of kaolin as cement replacement.
- Kao 5/ no CSF – standard mix formulation excluding CSF with 5% of cement replaced by kaolin.

Impact of kaolin as cement replacement on density and water absorption of fibrecement composites

The density and water absorption results are presented in Figures 6.4 and 6.5 respectively. Figure 6.4 shows development of density with age. It is observed from 14 days of curing that the density of the control samples did not develop further with age. The early age results, i.e. 7 days, showed an increase in density with increasing amount of kaolin in the formulation. This can be attributed to the filler effect of the smaller kaolin particles. The size of the kaolin particles is less than that of cement particles and thus able to fill the gap spaces formed between cement particles. Therefore kaolin increases the packing structure of the matrix resulting in higher densities. As the composites aged with time, beyond 7 days, density development was due to changes in the microstructure as a result of hydration and pozzolanic reactions. The standard formulation resulted in 2.1% increase in density over 28 days curing whereas kao 1, kao 2, kao 3, kao 5 and kao 5/ no CSF densities increased by 5.59%, 4.14%, 1.35%, 1.32% and 3.42% respectively. Although replacement of cement with 5% kaolin resulted in the highest density values throughout the curing period, the significant increase in density was attained with 1% substitution of cement. At 28 days curing, the three mixes incorporated with 1%, 2% kaolin and 5% kaolin with no CSF developed to the same density levels. Therefore, inclusion of 1% kaolin as replacement of cement would be the best option for density development at later stages of curing but, for consistently high values over the curing period the 5% kaolin mixes would be preferred.

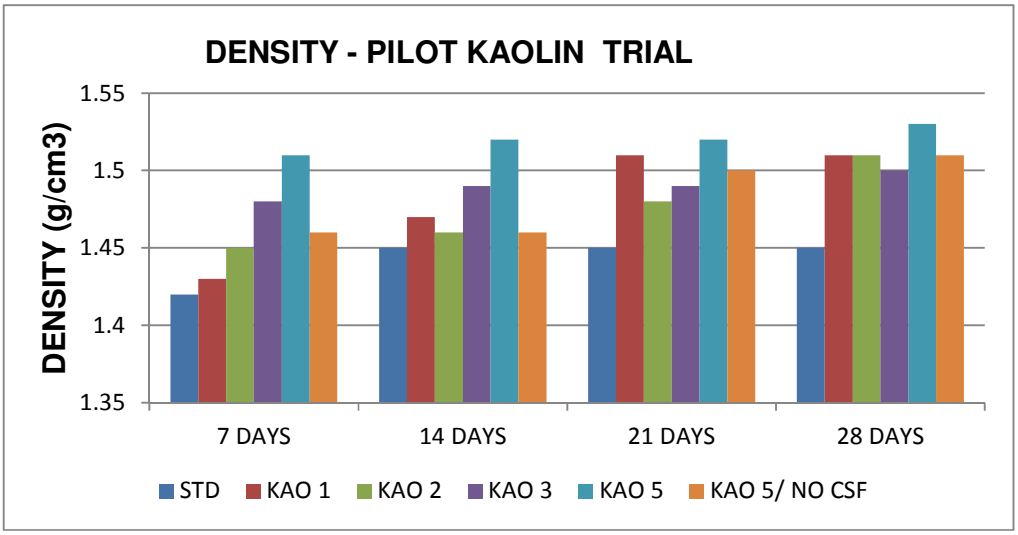


Figure 6.4: The development of density in fibrecement composite mixes with different kaolin replacement levels.

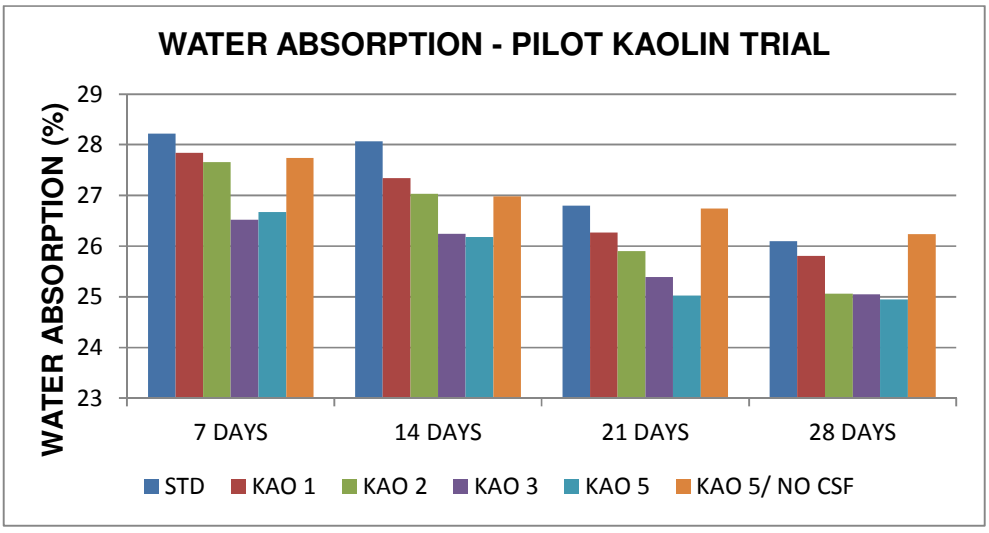


Figure 6.5: Comparison of water absorption for fibrecement composites with different kaolin replacement levels.

Water absorption results are shown in Fig 6.5 above. Water absorption is the measure of pore space in the material and gives an indication of the packing structure of the material. The reduction in water absorption over the curing

period was observed in all the formulation mixes. The control mix had a reduction of 7.5%, kao 1 had 7.3%, kao 2, kao 3, kao 5 and kao 5/no CSF had 9.4%, 5.5%, 6.4% and 5.4% respectively. The highest reduction in water absorption with time was obtained by replacing cement with 2% kaolin. At early stages of curing, 7 days, the least water absorption was observed in formulation with 3% kaolin inclusion. Water absorption is related to permeability of material. Permeability depends on the packing of the material. Supplementary cementing materials having size less than that of cement can improve the permeability of the matrix (Wild et al., 1996). Kaolin mix formulations showed lower water absorption than control mix with the exception of the mix without silica fume. Kaolin improved the microstructure of the matrix hence resulting in less permeable fibrecement composites. At 28 days curing, kao 2, kao 3 and kao 5 mixes had the same water absorption. Also, replacing 5% cement with kaolin in the absence of silica fume did not improve water absorption in comparison to the control mix. For minimal water absorption throughout the curing period, the best formulations were those with 3% and 5% kaolin inclusion as replacement of cement.

Effect of kaolin inclusion on wet-dry movement of composites

Fibrecement reinforced composites expand when immerse in water and contract on drying. This movement in composites result in cracking when not properly controlled. The objective was to reduce the wet-dry movement to its minimal level to eliminate probability of cracking. The results of the composites produced in the pilot plant are illustrated in Figure 6.6.

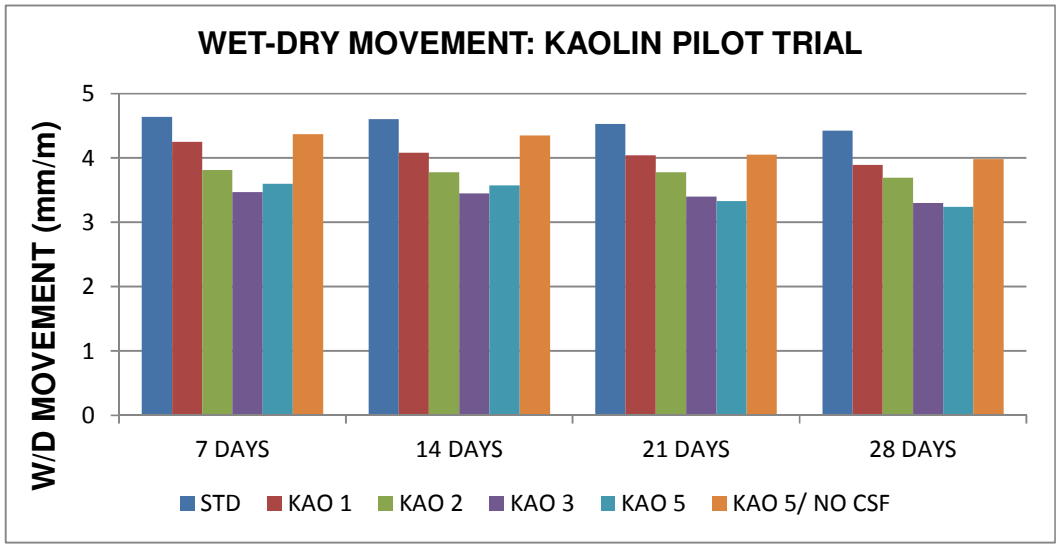


Figure 6.6: Effect of various kaolin levels on the wet-dry movement of fibrecement reinforced composites

The results indicated a reduction in movement with inclusion of kaolin in the mix formulation. At early age curing, 7 days, kao 1 resulted in 8.4% reduction in movement compared to the standard mix whereas kao 2, kao 3, kao 5 and kao 5/ no CSF had reductions of 17.89%, 25.21%, 22.41% and 5.82% respectively. The kaolin mix formulations with 2%, 3% and 5% replacement of cement showed markedly lower movement reductions than the control formulation. As curing progressed from 7 to 28 days, the movement of the composites was reduced by 4.7% for standard, 8.5% for kao 1, 3.2% for kao 2, 4.9% for kao 3, 10% for kao 5 and 8.9% for kao 5/no CSF. The reduction is attributed to refinement of pores in the matrix. The secondary CSH helps refine pore structure (McCormick, 2007). Kaolin reacted with calcium hydroxide from the clinker hydration, via pozzolanic reaction, to form calcium silicate hydrates. These products are less chemically reactive and densified the interfacial transition zone. Less permeable fibrecement composite was produced with a decrease in the volume pores (Sabir et al., 2001; Antonovich and Goberis, 2003). Therefore, the resistance to the transportation of water and diffusion of ions is enhanced. Although the best performance at 28 days,

in relation to movement, was achieved through inclusion of 5%, 1% and 3% kaolin in the mix formulation, only 3% and 5% formulations met the specification of less than 3.5 mm as required by the South African National Standards (SANS) for building. There is less micro cracking due to denser, reduced interfacial transition zone and refined pore structure.

Strength development in fibrecement composites incorporated with various levels of kaolin

Figure 6.7 show the variation of flexural strength with age for fibrecement mixes having different kaolin contents. The tests were conducted on flat sheet samples produced in the pilot plant. At 7 days curing, the kaolin mix formulations exhibited higher strengths than the standard mix, with 5% having a more pronounced effect. The strength increase, in comparison with standard mix, was 25% for kao 1, 12% for kao 2, 17% for kao 3, 33% for kao 5 and 14% for kao 5/no CSF. The strength enhancement is due to a combination of the filler effect and accelerated cement hydration. This is particularly significant in the interfacial zone regions where more efficient packing at the cement-paste aggregate particle interface is produced. Thereby, resulting in a denser, more homogeneous, transition zone microstructure; and pore refinement effected by fineness of kaolin. Kaolin rapidly removes $Ca(OH)_2$ from the system and accelerates cement hydration.

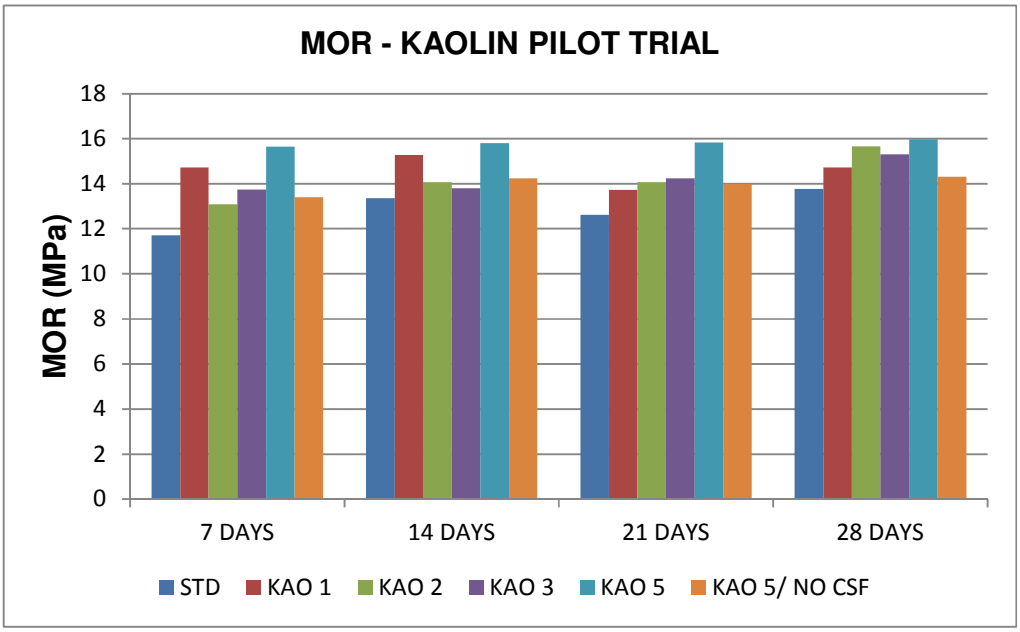


Figure 6.7: Strength development in kaolin-incorporated fibrecement composites with age

The 2% and 3% addition of kaolin, as cement replacement in fibrecement composites, are the optimum percentage enhancing the strength at 28 days by 20% and 11% respectively when compared with the control mix specimen. The higher strength in the above formulations is due to sufficient amount of kaolin available to react with $Ca(OH)_2$ which accelerate hydration of cement forming CSH gel. This is in agreement with previous findings by Poon et al. (2006) that the secondary CSH resulting from pozzolanic reaction enhanced early strength with no detrimental effect to the long-term strength.

Mineralogical composition of fibrecement composites with various levels of kaolin inclusion

The X-ray diffraction is one of the basic tools in the assessment of the formation of the crystal compounds in the cured fibrecement composites. The minerals found in the kaolin and standard mixes are displayed in Figure 6.8. The composites were tested after 28 days of air curing.

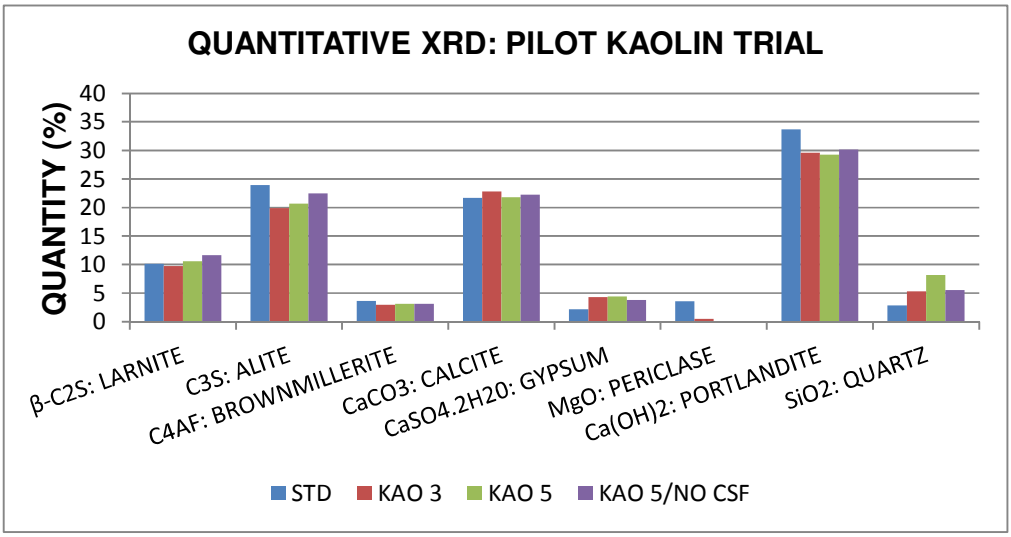


Figure 6.8: Identification of crystal structures in kaolin-incorporated fibrecement composites

The results showed a significantly increasing formation of portlandite. This growth of portlandite resulted from further hydration of unhydrated cement clinkers, C_3S and C_2S. Figure 6.8 still shows high quantities of unhydrated C_3S, responsible for early strength. Continuous formation of CSH is indicated by the decreasing intensities of unhydrated clinkers. It also means that the curing or hardening process is continuous at this age. With kaolin formulations, the intensities of portlandite patterns are smaller than those of control samples. Kaolin consumption of portlandite to create additional secondary CSH resulted in stronger composites. These results confirm that addition of kaolin decrease the quantity of portlandite through pozzolanic reaction.

Addition of kaolin facilitated the emergence of CSH phases. The kaolin formulation with the highest portlandite is kao 5/ no CSF followed by kao 3 then kao 5. This implied that the kaolin formulation with the least amount of portlandite produced secondary CSH thus enhancing the strength. These

results validated the strength results at 28 days curing. Therefore, maximum improvement in strength can be achieved for a replacement of 5% kaolin.

Durability of composites with various levels of kaolin as replacement of cement

The corrugated fibrecement sheets are primarily used in exterior applications where superior performance with continued environmental exposure is essential. All samples tested remained in the curing environment for 28 days prior to testing thereafter a set of five samples per formulation was subjected to four accelerated aging cycles before mechanical testing. The mechanical properties of fibrecement composites related to expansion and shrinkage are aimed at providing a fundamental understanding of these materials in order to describe their behavior when exposed to natural weathering conditions. The length was measured to monitor swelling and shrinkage behavior of composites during aging cycles. The percent length change over the exposure period for each composite when subjected to aging cycling is shown in Figure 6.9.

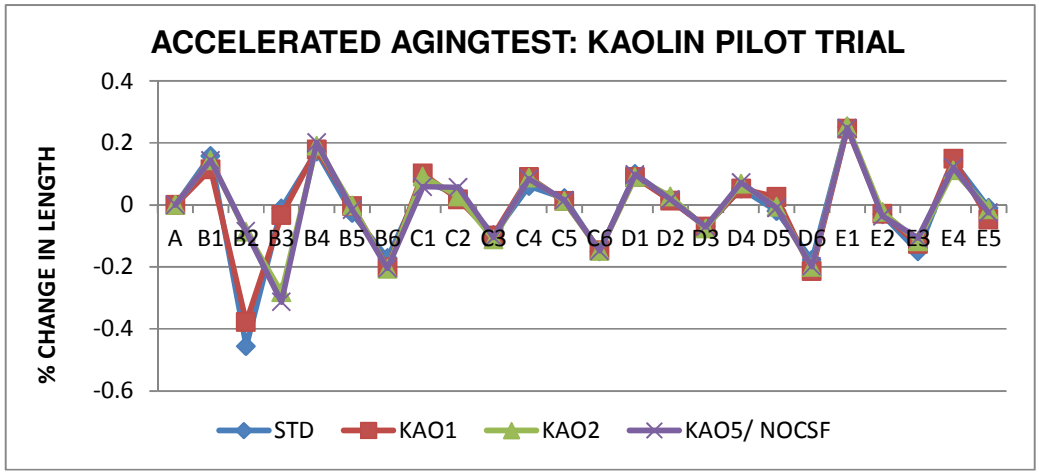


Figure 6.9: Accelerated aging test for kaolin-incorporated fibrecement composites. A- initial measurement, B, C, D, E represent 1st, 2nd, 3rd and 4th cycles respectively while the numbers 1, 2, 3, 4, 5 and 6 are wet, carbonation, dry, wet, carbonation, dry exposure respectively.

The results indicate that the kaolin composites experiences slightly less initial swelling compared to the control sample. This is due to the refinement of pores in kaolin formulation resulting in enhanced permeability. Cement based composites exposed to natural weathering absorb water and release it to their environment via a complex pore structure. As a result, the composites swell with increasing moisture content and shrink upon its loss. The extent and rate of water exchange depend on the type of application of product, the shape of product, the temperature and relative humidity of the surrounding environment, the wind velocity, the pore structure of the material, orientation of structure, type of fibre in the product and the age of the material (Akers and Partl, 1990). The exchange of water in the pores results in dimensional changes, expansion or shrinkage, within the product. Swelling / shrinking occurs primarily diametrically, with little dimensional change in the longitudinal direction. The authors also concluded that the density of product dictates the absorption.

The results in Fig. 6.9 indicated a higher degree of carbonation in the beginning and the rate slowed down with time. A lower degree of carbonation is observed in kaolin samples. This is attributed to the carbonation reaction where CO_2 reacts with calcium hydroxide forming calcium carbonate. The formation of calcium carbonate increases composite density, stiffness, bending strength and lowers dimensional instability (Kalbskopf et al., 2002). It reduces porosity thus slowing down liquid and vapor transportation. The subsequent low carbonation levels may result from the low water permeability and diffusion rates in high density matrices.

Comparison of the composite densities before and after exposure to accelerated aging is presented in Fig. 6.10. The control samples resulted in significantly high densities after accelerated aging test compared to the kaolin composites. This excessive increment can be associated with the formation of calcium carbonate from the carbonation process. Calcium carbonate reduces porosity thus changing the microstructure of the

composite. On the other hand, kaolin decreased the calcium hydroxide concentration by consuming it through a pozzolanic reaction. Filling the spaces between cement grains with secondary CSH will reduce formation of $CaCO_3$. Therefore, kaolin would be competing with carbon dioxide for available calcium hydroxide.

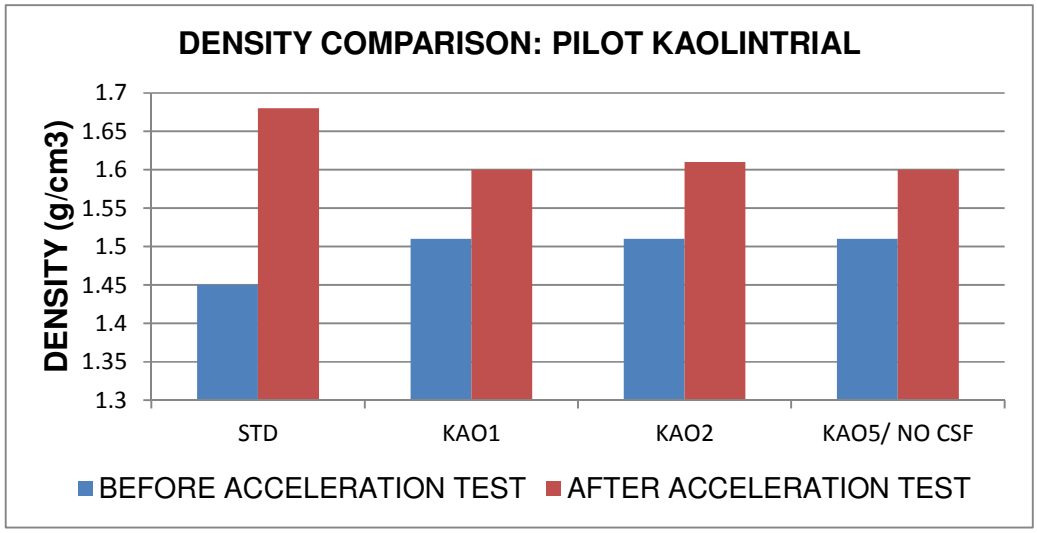


Figure 6.10: Density comparison for fibrecement composites, with various levels of kaolin inclusion, before and after exposure to accelerated aging cycles

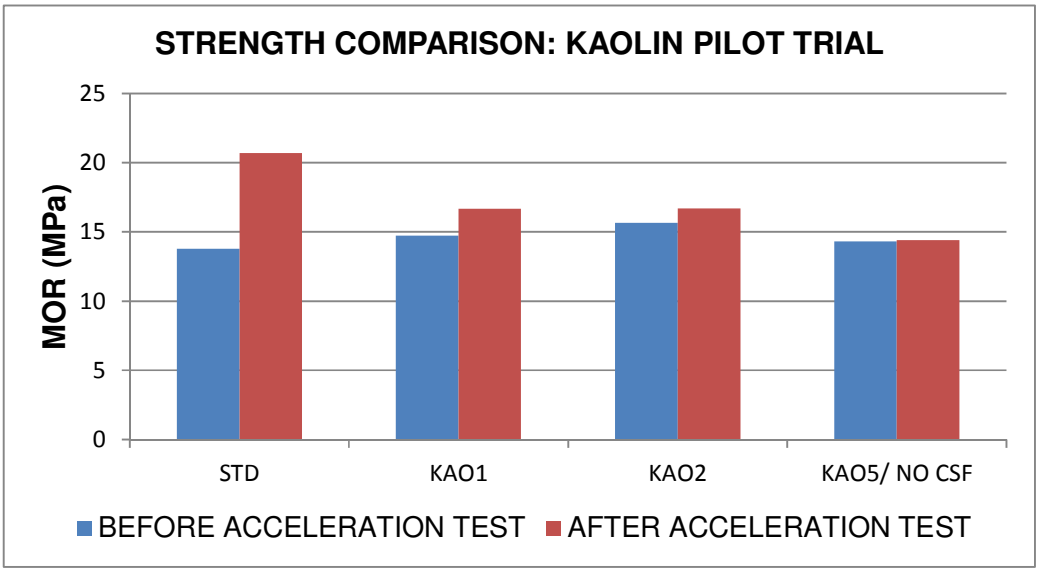


Figure 6.11: Comparison of strength with for kaolin-inclusion fibrecement composites, before and after accelerated aging

Fig. 6.11 indicated increased modulus of rupture (MOR) after accelerated aging test as a consequence of densification of the matrix and continued hydration of cement phase of the composite. This effect was more evident in the control samples. The kaolin formulations showed markedly small strength increases between exposed and unexposed composites before and after accelerated aging exposure. Reduction and refinement in pore size is beneficial to durability.

6.3.3 Production results of corrugated sheets

Based on the pilot test results, formulations with 3% and 5% inclusion of kaolin as replacement of cement were used in production of corrugated sheets, 3.6 m x 920 mm x 6 mm. The flocculants used for this trial production were the blend 5275:5618 in the ratio 60:40. Since these flocculants are in a powder form, the blending as per above ratio was done while dry then prepared in a tank to a concentration of 1.25%. All the sheets were shrink-wrapped with plastic after the curing chamber and kept indoors for 14 days

prior to testing. The plastic wrap was taken off thereafter but sheets remained indoors until 28 days.

Effect of kaolin inclusion as partial replacement of cement on the physical properties of fibrecement air-cured corrugated sheets

The average densities of five corrugated sheets per mix formulation were evaluated at 14 and 28 days and the results obtained are illustrated in Fig. 6.12. The results indicated marginal increase in density with inclusion of kaolin, i.e. 0.84% and 0.56% for 3% and 5% mix formulations respectively, at 14 days than the standard formulation. As curing progressed to 28 days, the improvement in density for standard, 3% and 5% kaolin sheets was 2.3%, 4.6% and 6.9% respectively. The density development of corrugated sheets for all mix formulations was higher than the development observed with the pilot samples. This could be related to production efficiency. The platelet-shaped particles of kaolin contributed to enhancement in retention of solids in the Hatschek process. These solids optimized micro packing and reactivity in the matrix. Also, the sheets were cured in the steam chamber for 8 h prior to shrink wrapping with plastic. Steam accelerated the hydration process thus calcium hydroxide was generated earlier for the pozzolanic reaction. The additional CSH produced by this reaction increased the density of the matrix thus refinement of pores of the microstructure.

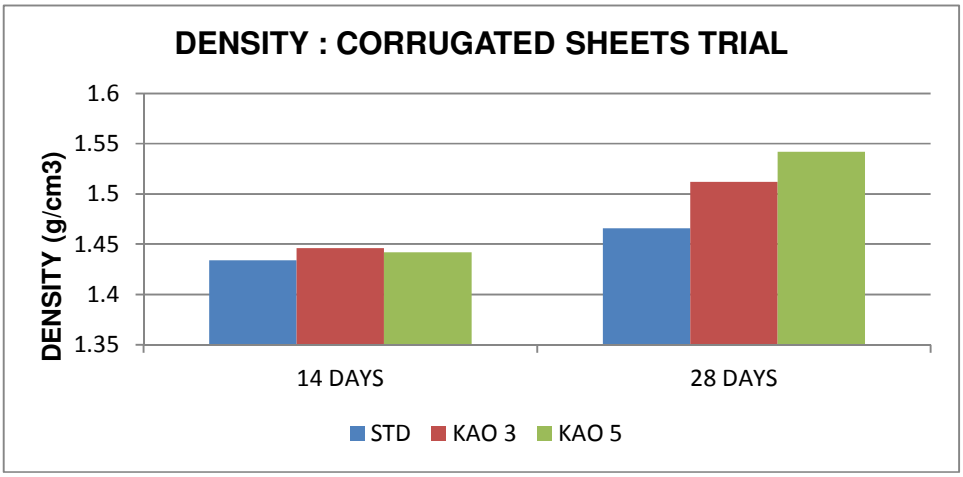


Figure 6.12: Density development of kaolin-incorporated corrugated fibrecement sheets, over 28 days curing

The subsequent modification of the microstructure resulted in less permeable sheets with a decrease in the volume pores. The reduction in permeability greatly improved resistance to transportation of water as can be seen in Fig. 6.13. The water absorption of the corrugated sheets followed the same trend as the density. At 14 days curing, the difference in water absorption was minute to none between the standard and kaolin formulations. A significant reduction was observed in water absorption in kaolin sheets. The decrease was 4.5%, 14.8% and 23.1% for standard, 3% and 5% kaolin incorporated sheets, respectively. These results confirm that permeability depends on density. The mix formulation that resulted in high density sheets had low water absorption.

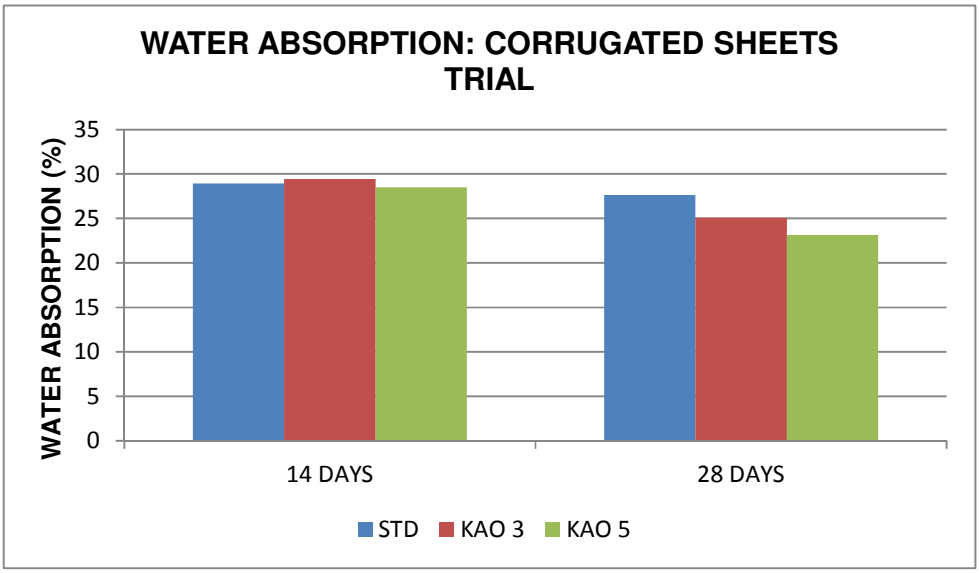


Figure 6.13: Water absorption of corrugated sheets as curing progressed and the impact of kaolin inclusion as replacement of cement.

The finer particles of kaolin improved the particle packing of cement paste, in particular the interfacial transition zone, filled the voids between large cement particles thus reducing permeability. The more dense structure reduced the ingress and egress of moisture in the sheets thereby reducing or preventing drying shrinkage. The results of moisture movement in corrugated sheets are presented in Fig. 6.14. The sheets with 3% and 5% kaolin as replacement of cement resulted in the movement reduction of 17.2% and 10.5% respectively. The reduction in movement on kaolin modified sheets at 28 days was less than the standard sheets (15.5% for STD, 12.4% for kao 3 and 15% for kao 5). The optimum results were achieved with 3% kaolin mix formulation.

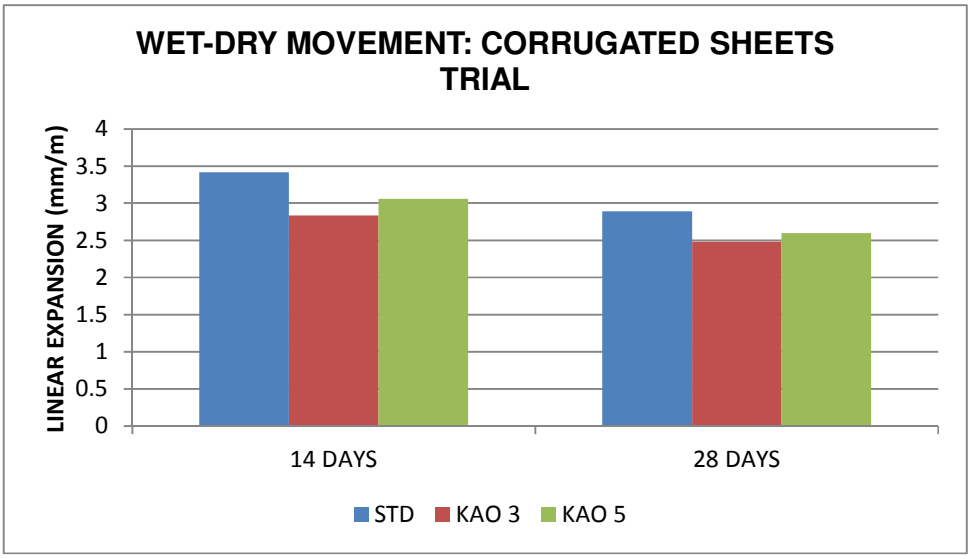


Figure 6.14: Wet-dry movement of corrugated sheets and the effect of incorporating kaolin as cement replacement over time.

The relationship between moisture and movement was studied in detail and the results are shown in Fig. 6.15 below. The moisture-movement tests were conducted on sheets after 21 days of curing. The moisture content of the sheets, after removal of the plastic wrap, was between 25% and 28% as shown in Fig. 6.15. Fig. 6.15 (a) indicated that the rate of moisture loss was slower in kaolin modified sheets than the standard sheets. The refined matrix permitted slow release of water to the surrounding. Both graphs (Figs. 6.15 and 6.16) showed that the sheets with 3% kaolin exhibited the least total movement followed by the 5% kaolin inclusion then the standard. The kaolin modified sheets showed less movement than the standard sheets due to the refinement of the microstructure thus reducing permeability. Since porosity was reduced then water within the kaolin modified sheets would be available for further hydration process.

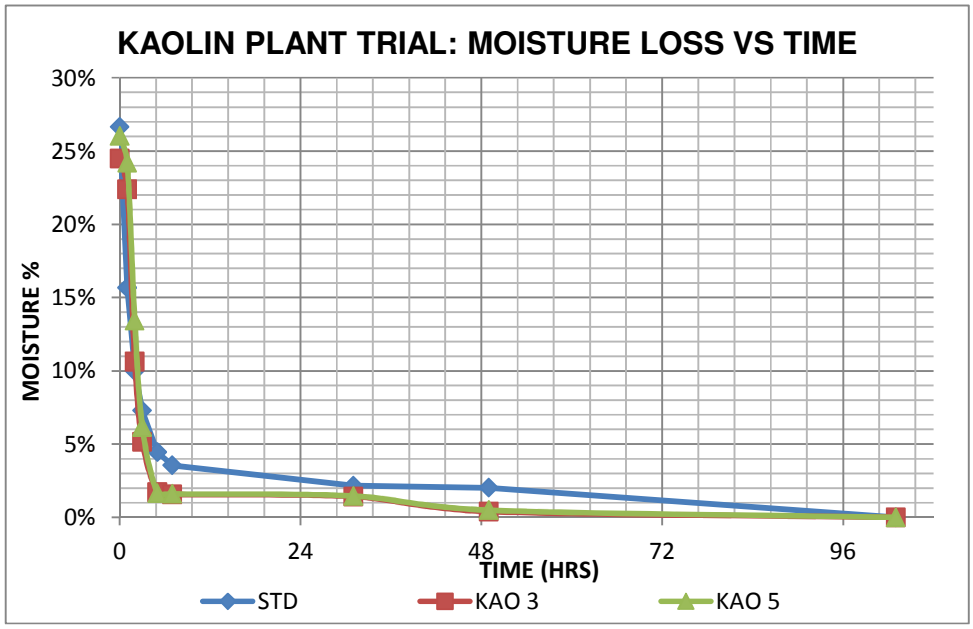


Figure 6.15 (a): Rate of moisture loss for corrugated sheets incorporated with kaolin at various contents.

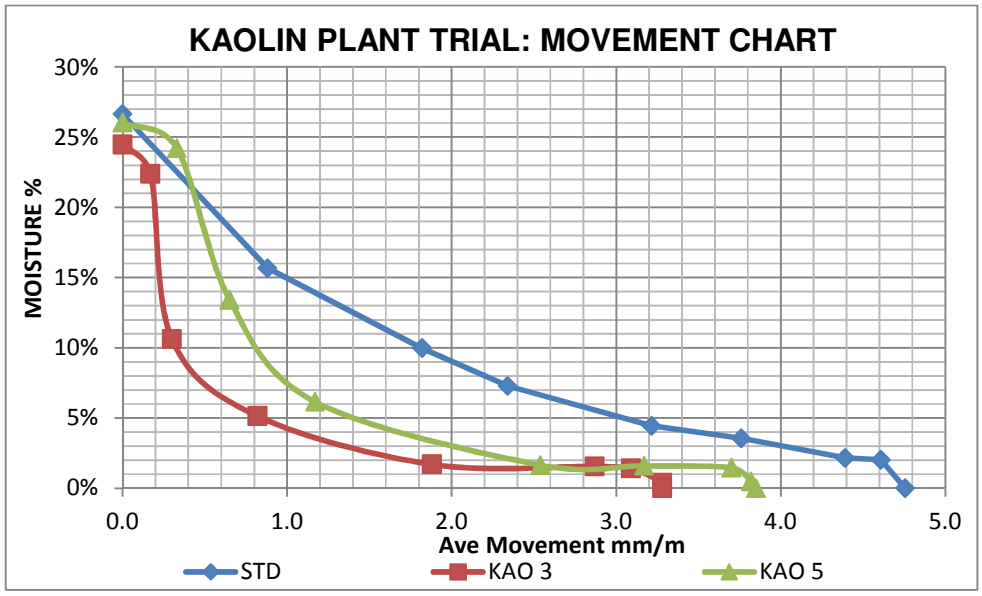


Figure 6.15 (b): Moisture movement in corrugated sheets incorporated with various levels of kaolin as partial replacement of cement

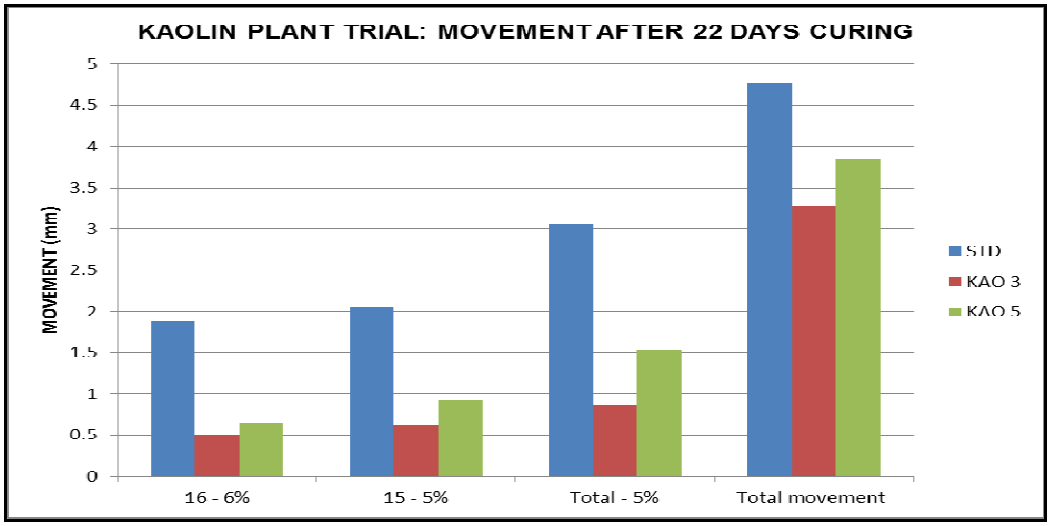


Figure 6.16: Movement of corrugated sheets at different ranges of moisture and the effect of various levels of kaolin to movement

The results in Fig. 6.16 demonstrated that the least movement for all mix formulations was attained when the sheets were dried from 16% to 6% moisture. The 3% inclusion of kaolin in the formulation reduced the total movement of sheets by 31% whereas that of 5% kaolin inclusion was only 19% than standard sheets. This implied that when sheets are unwrapped and immediately exposed outside then these sheets will move as shown by total movement. The main factor that contributed to drying shrinkage was not the high moisture content but the rate at which the water evaporated from the sheets. It is therefore important to control the curing process, as will be seen later in section 6.3.5.

At 14 days curing, efflorescence was observed on the surfaces of the standard corrugated sheets. This was due to the migration of calcium hydroxide to the surface then reacted with CO_2 in the atmosphere to form a whitish haze, see Figure 6.17 below. Addition of kaolin to the formulation prevented efflorescence in two ways:

- The calcium hydroxide combines chemically with kaolin and renders the lime unavailable to be leached to the surface by migrating moisture.
- The denser matrix reduces the ingress and egress of moisture in the composite mix. When moisture is prohibited from penetrating then the probability for efflorescence is eliminated.

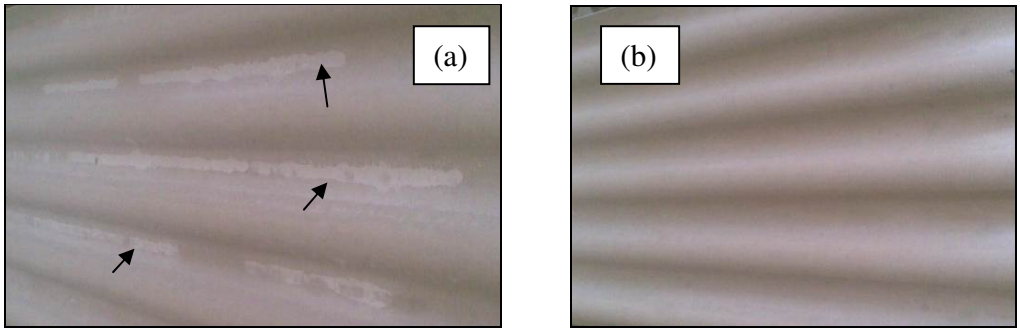


Figure 6.17: (a) Standard and (b) kaolin modified corrugated sheets

Effect of kaolin, as partial replacement of cement, on mechanical properties of fibrecement air cured corrugated sheets

The flexural strength development is a function of the chemical interaction between the pozzolan and the cement during hydration (Philleo, 1986). Cements and pozzolans contribute to strength not only because of their chemical composition but also because of their physical character in terms of particle packing.

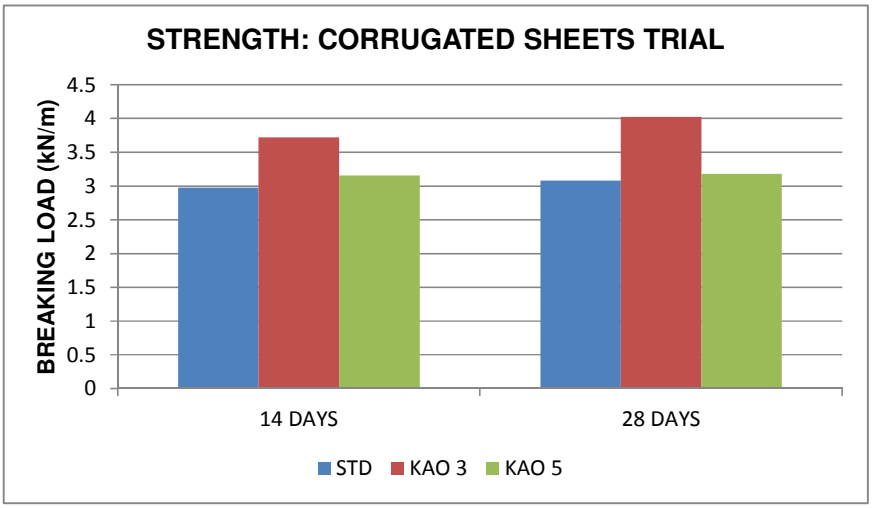


Figure 6.18: Development of strength in corrugated sheets with different kaolin replacement levels over time.

A significant increase in strength, at both 14 and 28 days curing, was observed for sheets with 3% kaolin inclusion as cement replacement compared to the 5% kaolin and standard sheets, Fig. 6.18. The flexural strength of sheets incorporated with 3% kaolin increased by 25% at 14 days curing and by 30% at 28 days as compared to control sheets. On the other hand, the flexural strength of sheets with 5% kaolin inclusion showed markedly low increase of 6% and 3% at 14 days and 28 days curing respectively. The increase in strength was due to the physical effect of fine grains of kaolin that allowed dense packing within the cement and reduced the pores in the transition zone between the paste and aggregates. The weaker zone was then strengthened due to the higher bond development between these two phases thus improvement in microstructure. Also, when the fine kaolin particles were dissipated in the cement paste, they generated a number of nucleation sites for precipitation of hydration products. This resulted in a homogeneous paste due to the reaction of amorphous silica of the pozzolanic material and $Ca(OH)_2$ generated during the cement hydration

reactions (Sabir et al., 2001; Rojas and Cabrera, 2002; Antonovich and Goberis, 2003).

Scanning Electron Microscopy (SEM)

Analysis of microstructure of corrugated sheets exposed to natural weathering for 4 months was conducted and the micrographs are presented in Figs. 6.19 – 6.21.

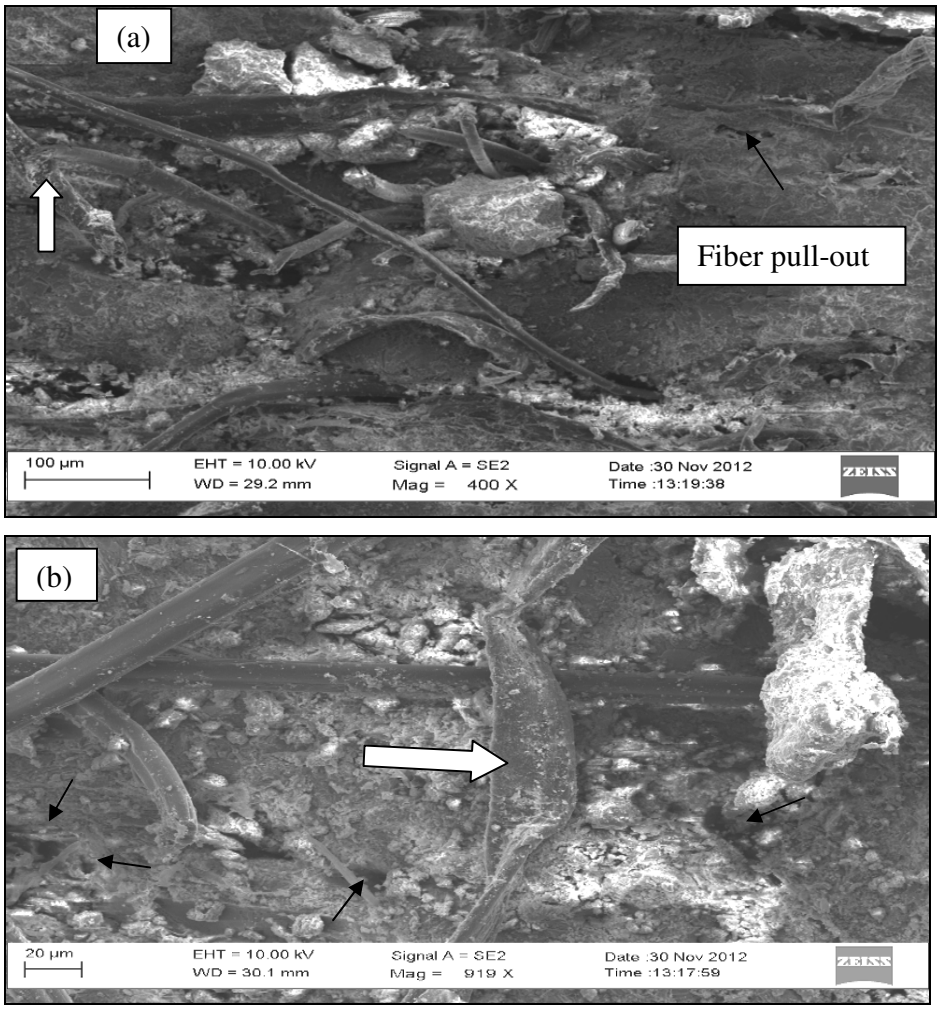


Figure 6.19: (a) and (b) SEM micrographs of corrugated sheets with standard formulation 4 months curing under natural weathering exposure

The above micrograph of standard formulation for corrugated sheets showed the presence of coarser particles in the matrix thus resulting in porosity. The matrix is not densely packed thus resulting in lower density and higher water absorption. Fracture surfaces of the standard sheets indicated that fibre pull-out remained the predominant mode of failure, as shown by the black arrows in Fig. 6.19. Void spaces were created as a result of cellulose fibres debonding from the matrix. The formation of hydration products within the fibre cell walls was identified with the white arrow in the micrographs. This deposition of hydration products, likely calcium hydroxide, within the lumen cavity would probably lead to the mineralization and subsequent embrittlement of fibre.

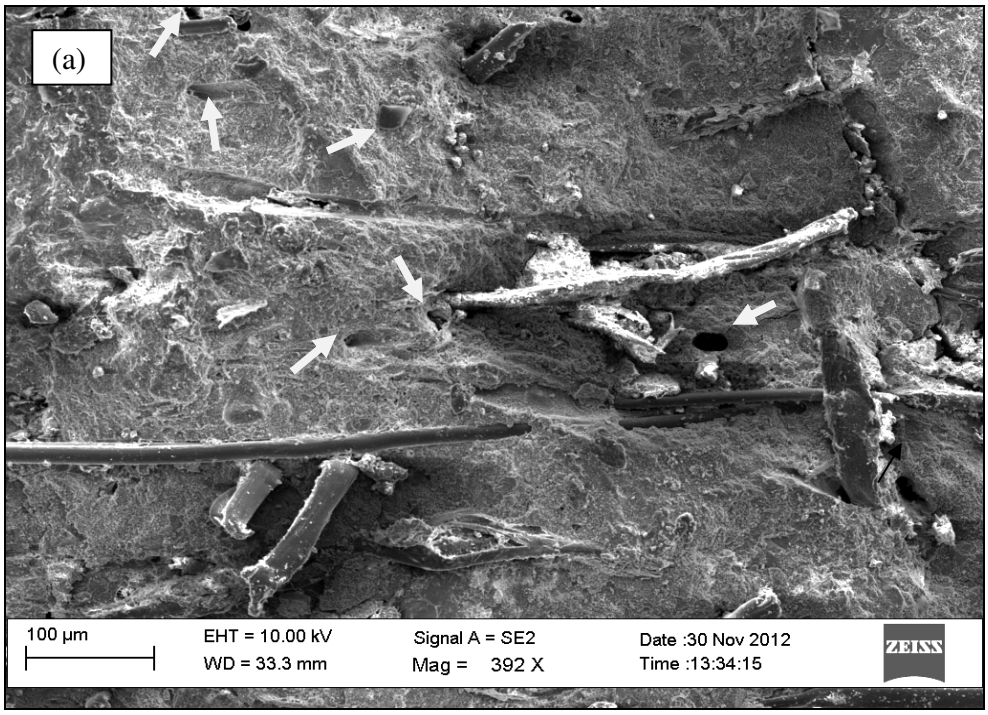


Figure 6.20 (a): SEM micrograph of fibrecement corrugated sheets with 3% kaolin as replacement of cement after 4 months.

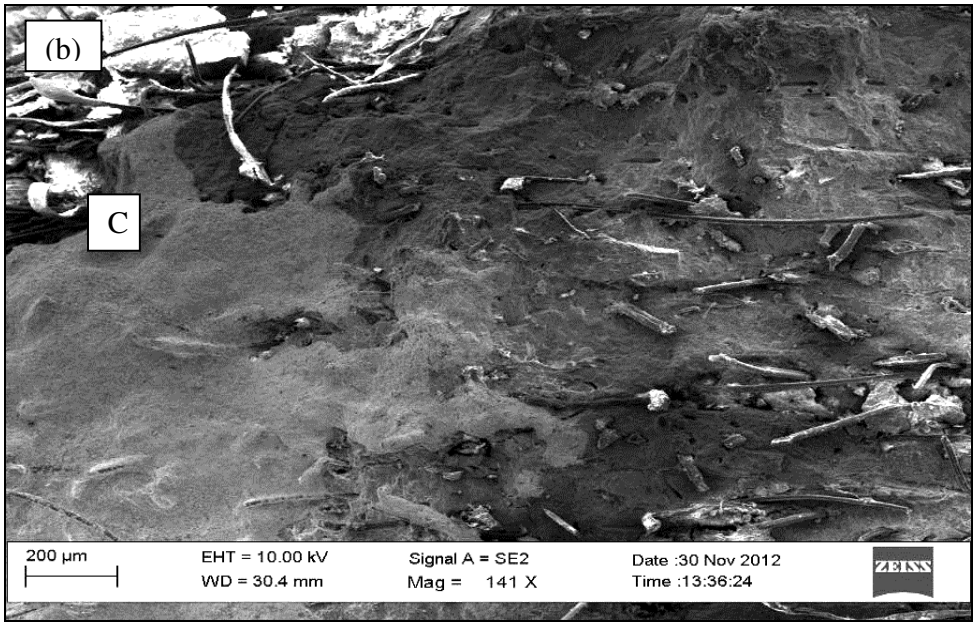


Figure 6.20 (b): SEM micrographs of corrugated sheets with 3% kaolin as replacement of cement taken after 4 months of natural weathering exposure.

The failure mechanism for these sheets was identified as fibre pull-out as shown in Fig. 6.20. The micrographs illustrated improvement in particle packing of cement paste as the pores were filled by the fine kaolin particles (filler effect). There was little deposition of hydration products, $Ca(OH)_2$, on the surface or lumen of cellulose fibres. This can be attributed to the consumption of calcium hydroxide by kaolin through the pozzolanic reaction generating secondary CSH. Fig. 6.20 (b) showed a homogeneous layer due to the reaction between amorphous silica of kaolin and calcium hydroxide, see area labeled C.

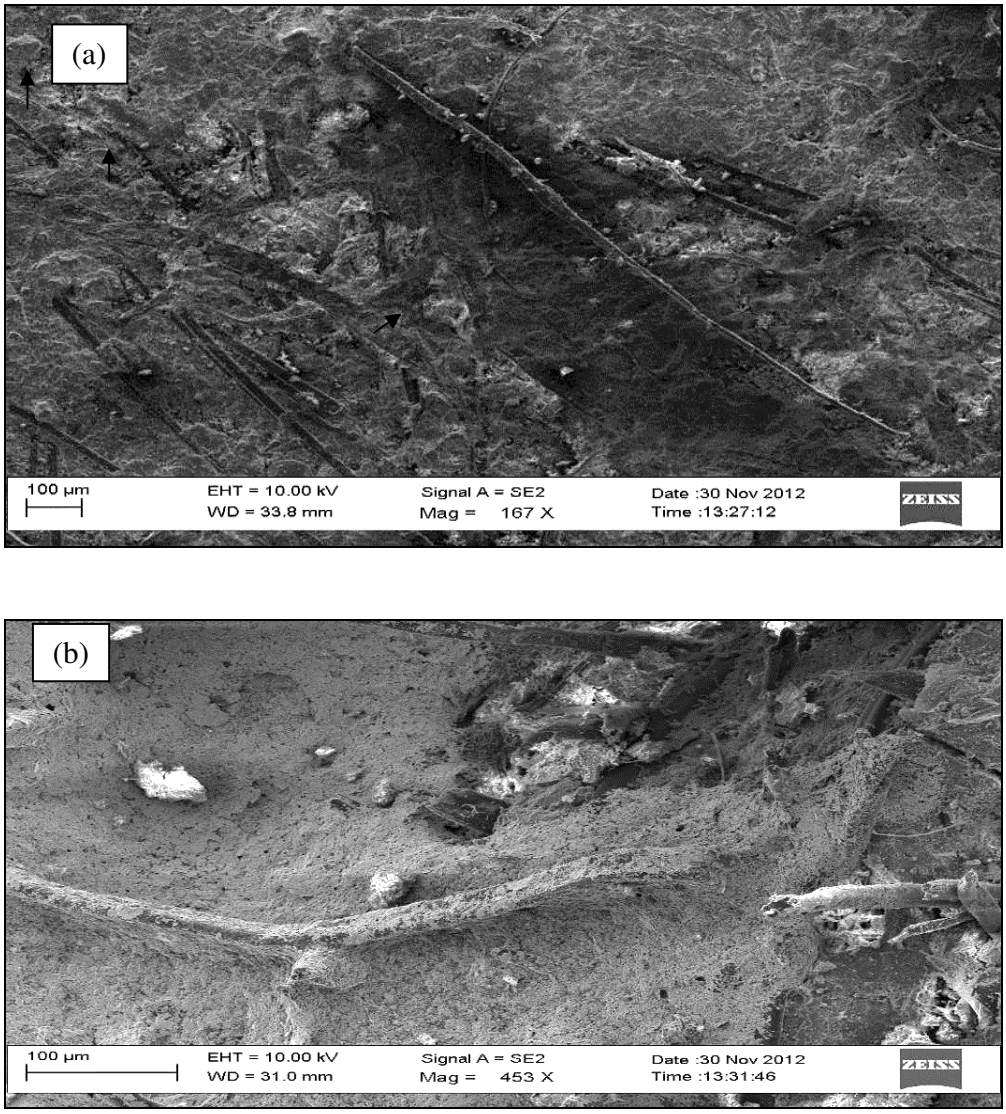


Figure 6.21: Micrographs of corrugated sheets with 5% kaolin inclusion as cement substitute after 4 months natural weathering exposure.

There was no evidence of precipitation of hydration products on the lumen of cellulose fibres. The presence of void spaces in the matrix indicated debonding of cellulose fibres from the matrix. Increasing the kaolin content resulted in more filling up of the voids in the cement paste and consumption of additional calcium hydroxide. This effect resulted in a less porous/ permeable matrix as can be seen in Fig. 6.21 (b).

Durability of fibrecement reinforced corrugated sheets

The corrugated sheets produced were subjected to accelerated aging test, accelerated weathering test (wet/dry cycles) and exposed to natural weathering. The density results in Fig. 6.22 showed that with age the sheets attained the same density, irrespective of formulation. The difference would be in the chemical composition of the matrices. In the standard formulation the voids in the matrix were filled by $CaCO_3$ resulting from the carbonation process. Carbon dioxide reacts with calcium hydroxide generated by the hydration reaction process to produce calcium carbonate. Calcium carbonate then occupied the voids in the cement matrix thus refining the pores. The resultant matrix was densely packed hence the increment in density of the standard corrugated sheets. This is in agreement with previous studies conducted by Kalbskopf et al. (2002) that carbonation densifies the cementitious matrices and reduces their dimensional instability. On the other hand, kaolin-modified matrices were occupied by the fine kaolin particles that allowed dense packing thus changing the microstructure of the sheets. The pore refinement resulted in permeability reduction in the composites.

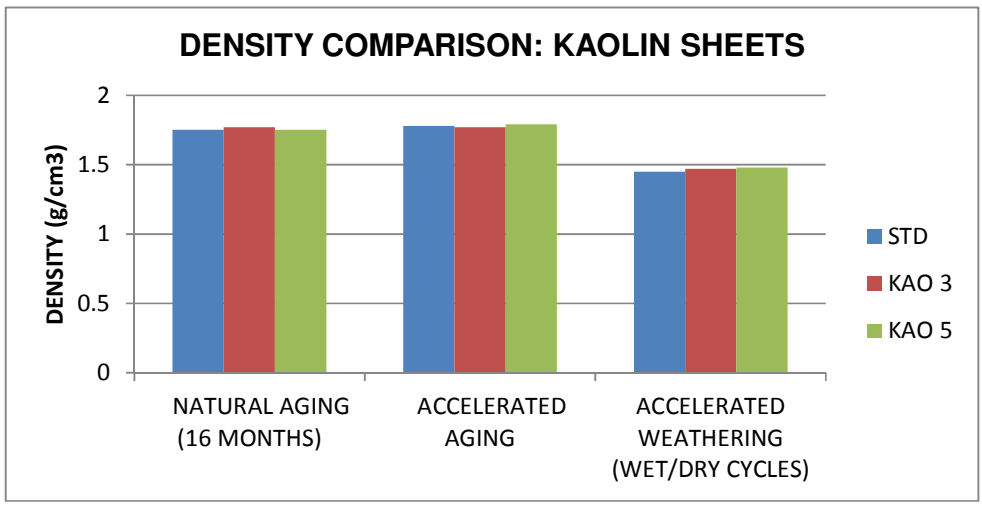


Figure 6.22: Density comparison between natural exposure and accelerated test results

There was strength increase after aging tests as a consequence of densification of fibre matrix transition zone and continued hydration of cement phases caused by the soak and dry cycles, Fig. 6.23.

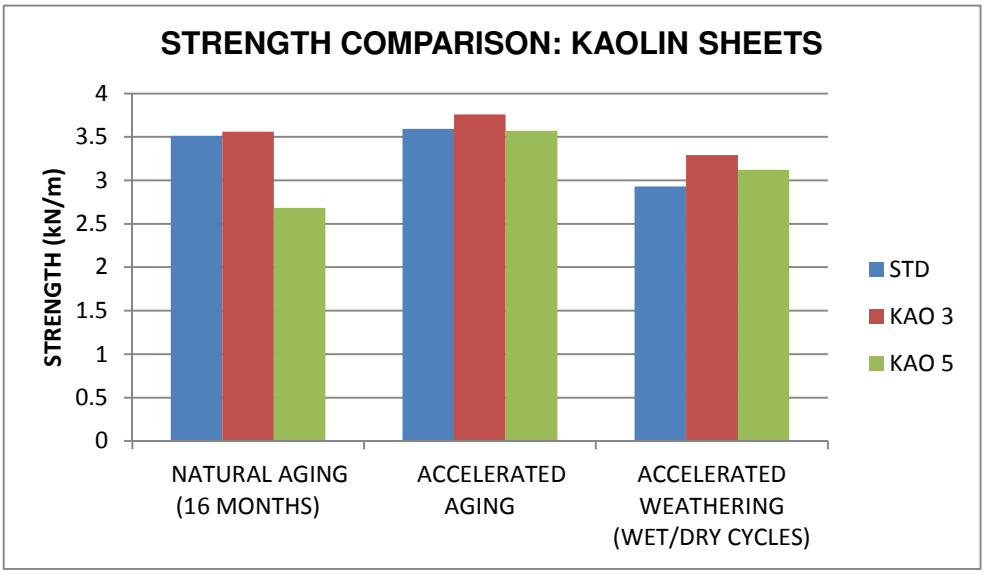


Figure 6.23: Strength comparison between natural exposure and accelerated test results

The kaolin sheets showed slight improvement in strength than the standard due to the secondary CSH generated by the pozzolanic reaction, above the refinement of the pores. The natural exposure results of kaolin sheets with 5% inclusion exhibited lower strength as a result of thaumasite formation on these sheets, Fig. 6.24.

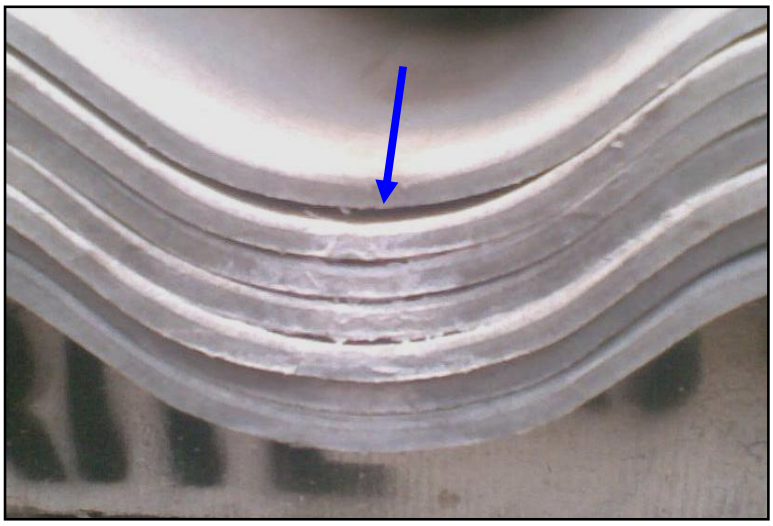


Figure 6.24: Thaumasite formation on corrugated fibrecement sheets with 5% kaolin inclusion as replacement of cement.

Four months after natural exposure the sheets incorporated with 5% kaolin showed deposition of white material on the edges of the sheets. A sample from the edges was evaluated using XRD analysis and the material was found to be thaumasite. Thaumasite has the chemical formulation $CaSiO_3 \cdot CaCO_3 \cdot CaSO_4 \cdot 15H_2O$. As this material formed, the cement composite converted to a friable material described as 'mush'. In these sheets thaumasite formation could have been formed due to the presence of either high amounts of gypsum in cement (Gaze, 1997) or the interaction between the limestone blended cement and sulphate enriched solutions. With adequate supply of sulphate and carbonate, thaumasite will continue to form until the calcium silicate hydrate is completely destroyed (Hooton and Thomas, 2002). Bellmann (2004) found that monosulfate can react with CSH to form thaumasite since monosulfate is metastable in the presence of calcite. Therefore, strength reduction in the 5% kaolin corrugated sheets was due to the consumption of CSH to form thaumasite.

6.3.4 Validation of kaolin production results

After evaluation of the results of the first production trial, the formulation mix with 3% kaolin showed superior performance in mechanical and physical properties, durability and resistance to cracking. The next objective was to then determine the repeatability of these results. The trial run for production of corrugated sheets with this formulation was conducted for a week to check process efficiency and stability with inclusion of such material. The sheets produced were tested at 14 days curing.

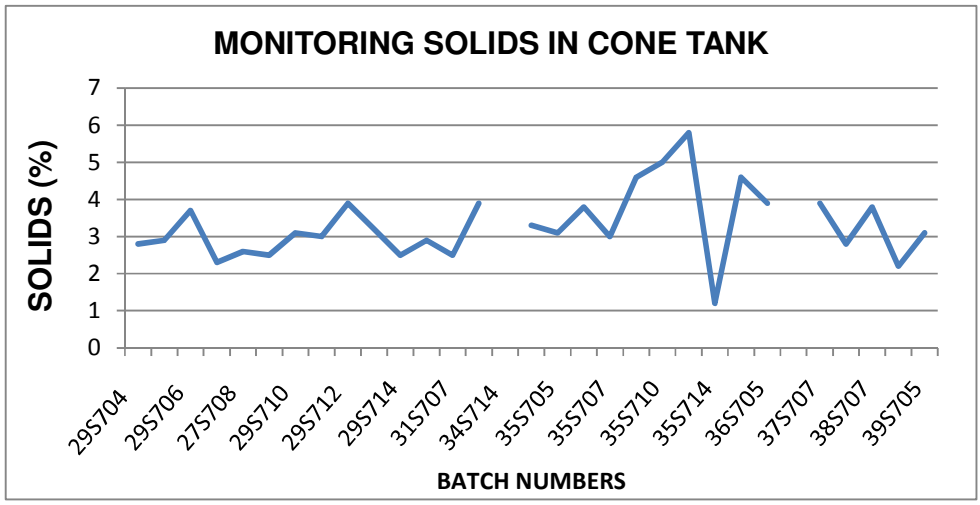


Figure 6.25: Monitoring solids during production of 3% kaolin modified corrugated fibrecement sheets.

The results in Fig. 6.25 indicated that the majority of the solids were retained in the sheet. The spike in the graph appeared when flocculants were over dosed. Bigger flocks are then produced resulting in a porous matrix. Therefore, the process water circulating in the system contained little solids in suspension. The corrugated sheets aged 14 days were tested for physical and mechanical properties and results are presented in Fig. 6.26.

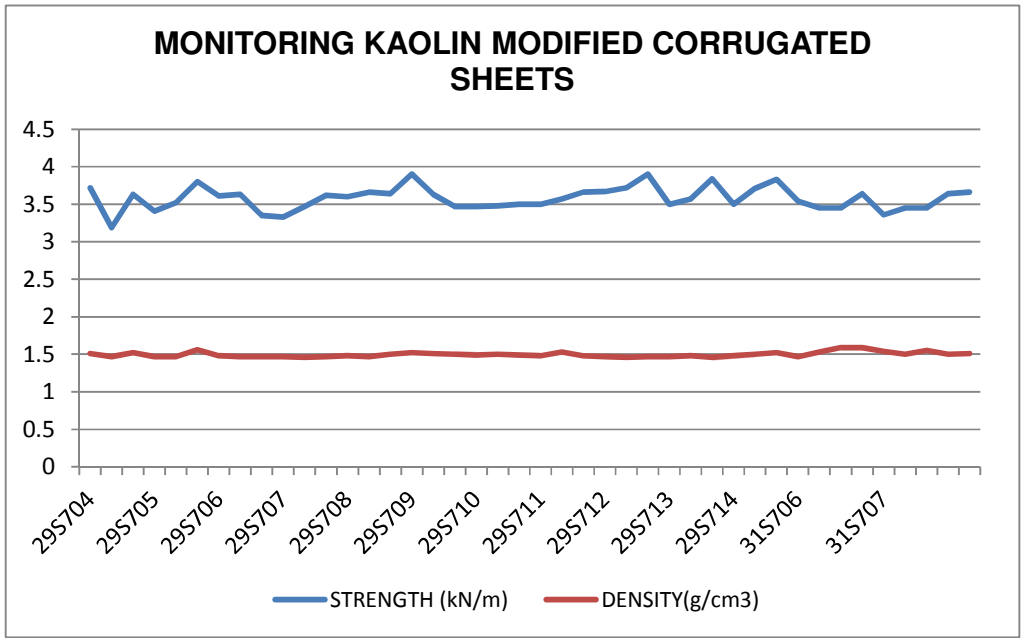


Figure 6.26: Monitoring mechanical properties of 3% kaolin modified corrugated fibrecement sheets, tested at 14 days curing.

The density of the sheets produced was high and the process showed stability. The effect of refinement of the microstructure was also observed in the strength results. The fluctuations in strength results were very minute and this implied that the flocculants used for filtration, retention and settling in the Hatschek process were performing at their optimum level. The results indicated that the process was efficient and stable. Also, the pozzolanic reaction occurred resulting in denser and stronger sheets.

The results of the previous trial at 14 days curing were compared to the average of these results to determine reproducibility in the properties of sheets.

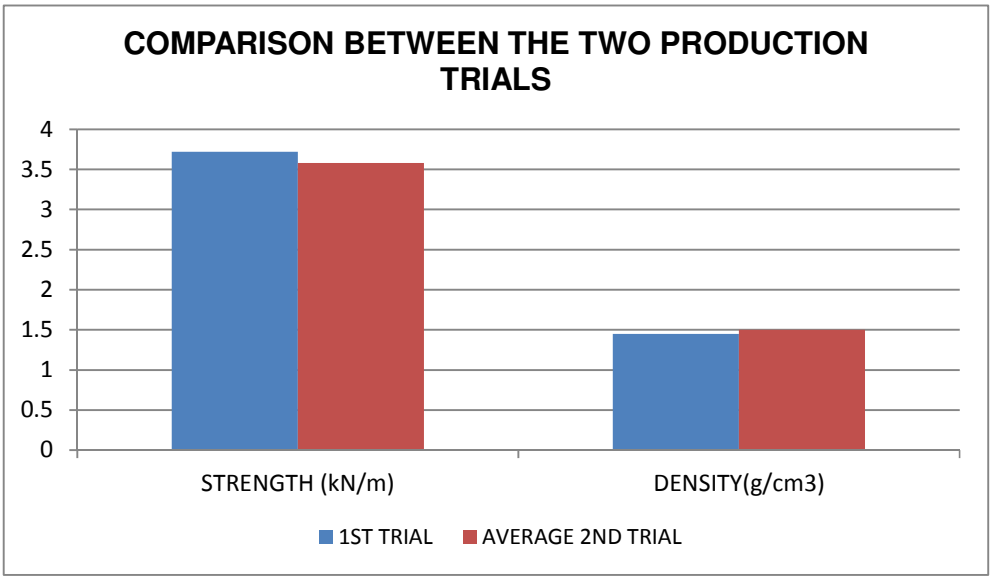


Figure 6.27: Comparison of the two trials to determine repeatability of results

The results did not show a significant difference in the properties of the corrugated sheets produced in both trials. It can therefore be concluded that addition of 3% kaolin, as replacement of cement, in the mix formulation resulted in kaolin fine particles filling up the voids between the large cement particles thus resulting in the refinement of the microstructure. The density of the sheets increased significantly and the water absorption decreased. Also, the finer particles of kaolin had high surface area that improved reactivity thus enhancing the strength of the sheets. The pozzolanic reaction of kaolin resulted in secondary CSH which contributed to the improvement of strength. The refined matrix resulted in permeability reduction hence moisture absorption and evaporation was minimized. By controlling the rate of moisture loss in corrugated sheets, drying shrinkage was eliminated. Therefore cracking was eliminated by refinement of the microstructure and controlling the rate of moisture evaporation from the corrugated sheets.

6.3.5 Effects of various curing conditions on the mechanical properties and cracking of corrugated fibrecement sheets

The corrugated sheets are currently shrink-wrapped with transparent plastic and stored inside a warehouse for 14 days prior to testing. After testing they are dried until the moisture content reaches 10% maximum thereafter stacked outside. This process is time consuming and environmentally unfriendly. As the microstructure of the sheets has been modified, the objective was to stack the sheets directly outside without the drying process.

The kaolin modified sheets were taken from the steam chamber and cured as follows:

- One stack of corrugated sheets was placed outside immediately after steam curing,
- The second stack was stored inside without wrapping,
- The third stack was stored wrapped, kept inside for 3 days then stacked outside without the plastic,
- The fourth stack was kept indoors with wrapping for 7 days then stacked outside,
- The last stack was kept indoors for a day with plastic wrapping thereafter cured outside.

The density results of these sheets under different curing conditions are plotted in Fig. 6.28. The least development in density was observed in the sheets that were kept indoors for 7 days prior to external exposure. The results showed a significant increment in density at 28 days for the sheets that cured outside for a longer period. This was as a consequence of CO_2 penetrating the sheets followed by transformation of $Ca(OH)_2$ generating $CaCO_3$. Its formation results in the refinement of the fibre-matrix transition zone thus increasing density. This was in agreement with the findings of Kalbskopf et al. (2002). Although the densities were high for the outdoor samples, the water absorption values were similar irrespective of curing conditions, Fig. 6.29.

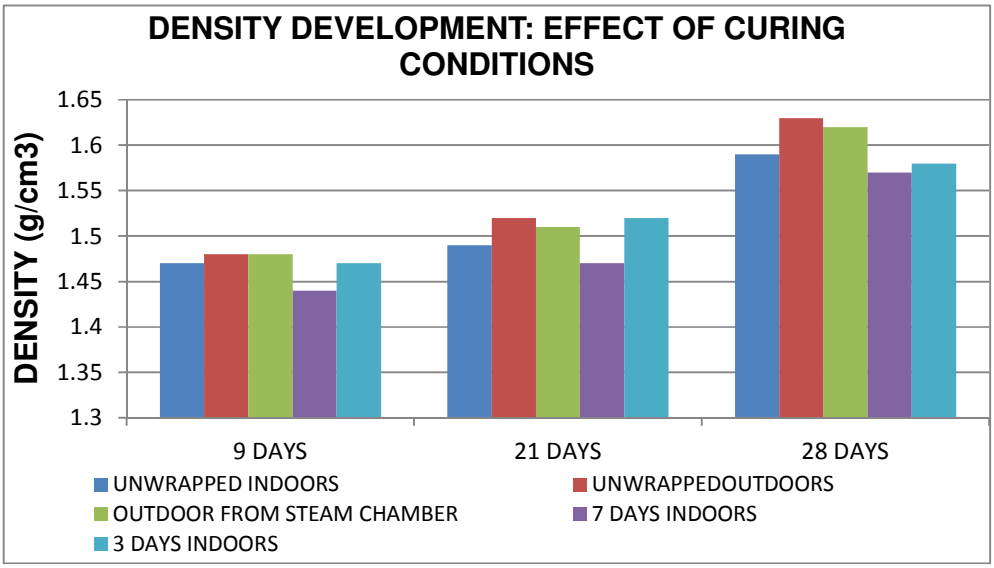


Figure 6.28: Development of density of 3% kaolin modified sheets over time, under various curing conditions

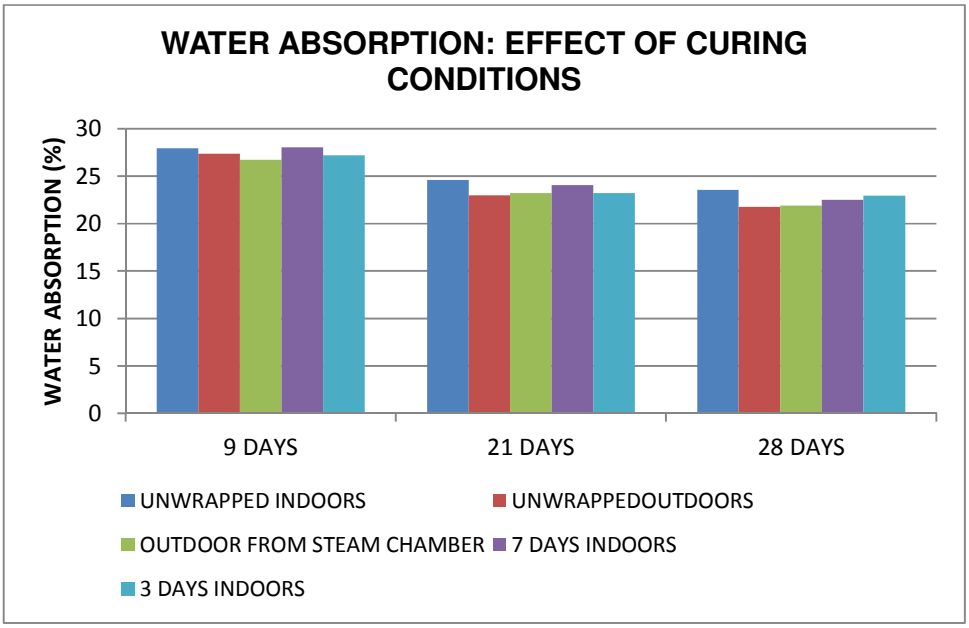


Figure 6.29: Water absorption of sheets with 3% kaolin, as replacement of cement, under different curing conditions for 28 days.

The strength results of these corrugated sheets are presented in Fig. 6.30.

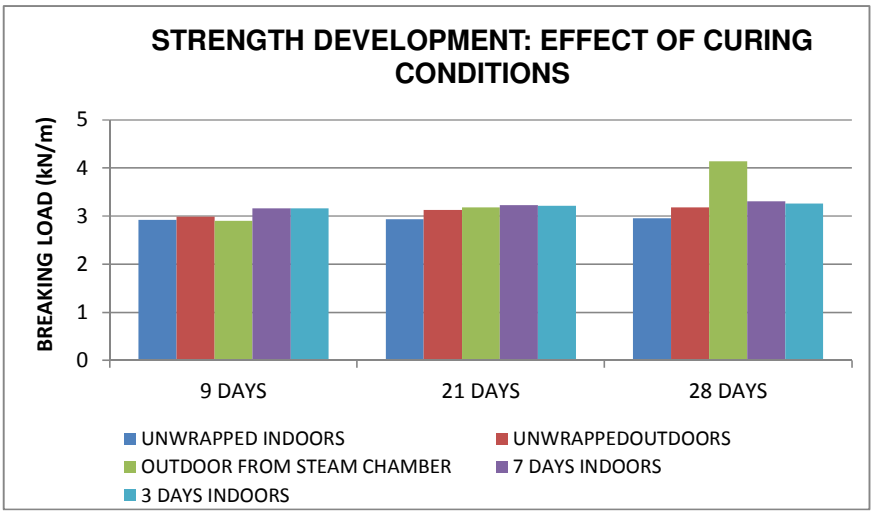


Figure 6.30: Strength development, over time, of kaolin modified sheets cured under different conditions.

There was little development in strength of the sheets during the curing period with the exception at 28 days, where optimum strength was attained by the sheets which were cured outside after the steam chamber. The calcite, formed during the carbonation process, refined the weaker interfacial transition zone improving adhesion between cement and the aggregates.

The calcite formation was confirmed by the XRD results in Figure 6.31. The results indicated the presence of ettringite in all the samples. Ettringite is formed as a result of the reaction of calcium aluminate with calcium sulphate in cement after addition of water. The presence of ettringite depends on the ratio of calcium sulphate to tri-calcium aluminate. When this ratio is low, ettringite forms during early hydration and then converts to the calcium aluminate monosulphate. When the ratio is high, the reaction does not proceed to the conversion phase.

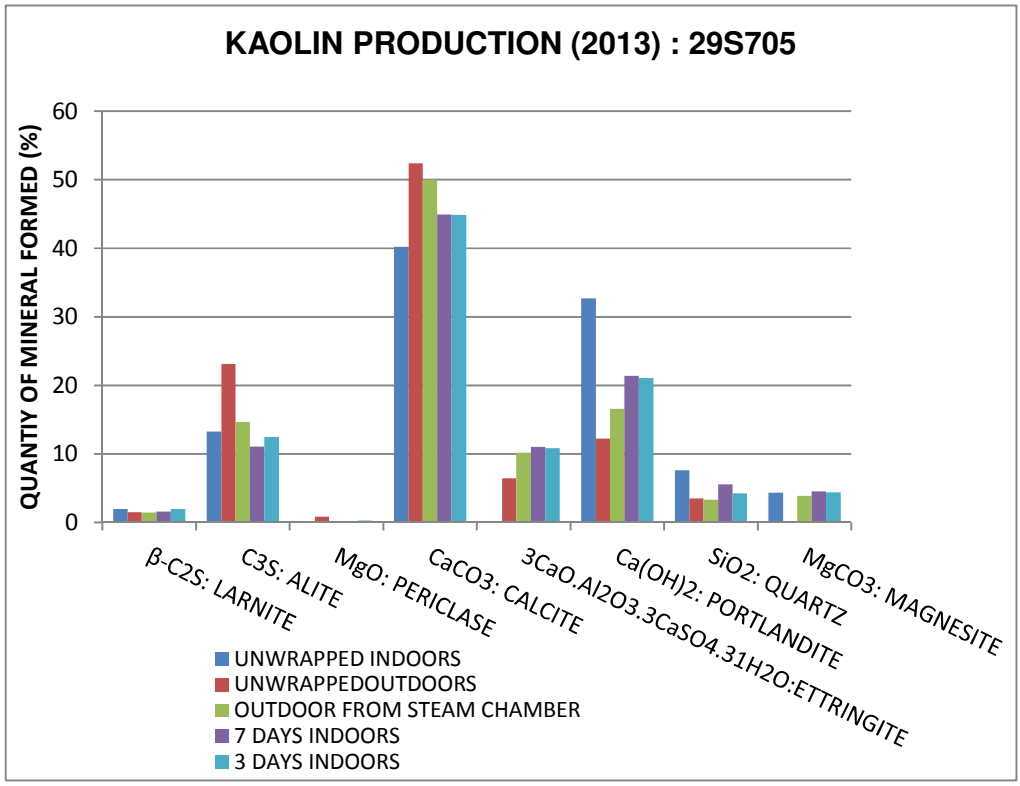


Figure 6.31: Quantitative XRD of fibrecement sheets, 3% kaolin, cured at various conditions.

The sheets that were exposed outside are shown to have the highest calcite as a result of the carbonation process. There was still a high quantity of unreacted clinker, C_3S, more in the samples that were exposed outside. This was due to the sheets losing moisture at a faster rate hence slowing down the hydration process. Also, these sheets had the least amount of portlandite as it was consumed by CO_2.

At the end of the curing period, i.e. 28 days, the movement of the sheets and the rate of moisture loss were evaluated. The results in Fig. 6.32 indicated that the sheets that were stored outside, taken directly from the steam chamber, exhibited the least rate of moisture loss. This was due to the refinement of the matrix resulting in reduced porosity. The sheets that were

initially cured indoors under plastic wrapping showed the fastest rate of moisture loss.

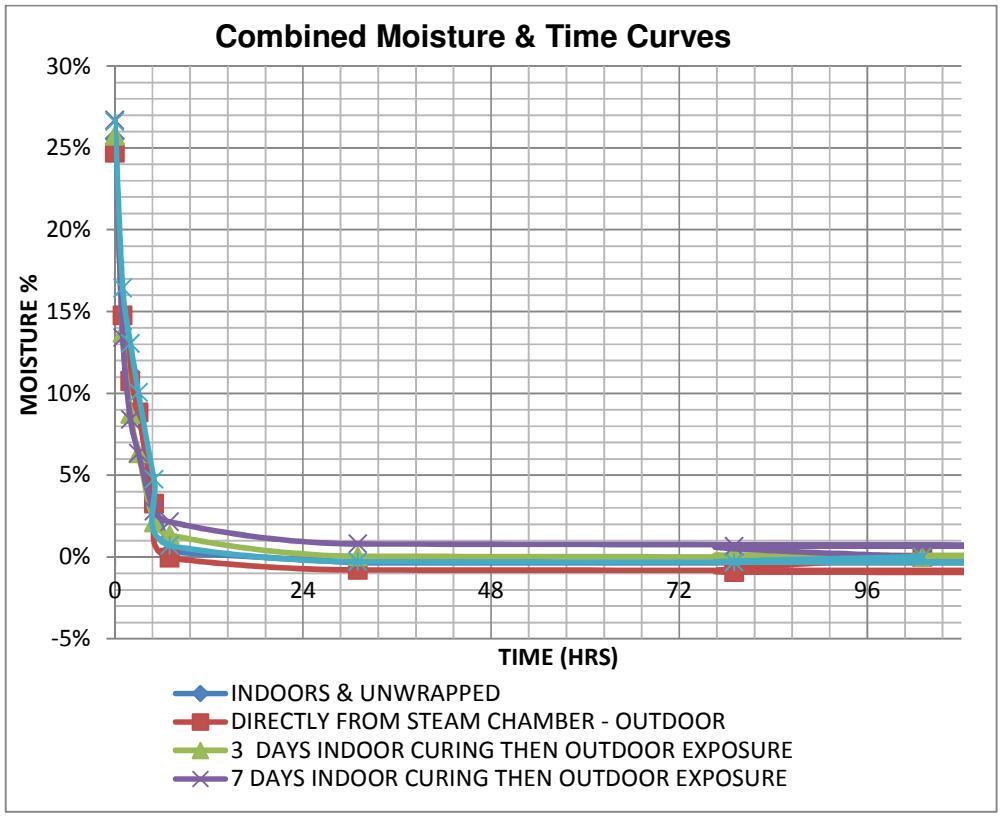


Figure 6.32: Monitoring moisture loss from the sheets, cured under different conditions, with time.

Although the rate of moisture loss was slower in most of these sheets, the results in Fig. 6.33 illustrated that the movement was high in all the sheets, irrespective of curing condition. With this amount of movement, the sheets will crack. All the results; density, water absorption, strength; indicated that the pozzolanic reaction did not occur. This observation was verified by the XRD results that showed high quantities of portlandite, with the exception of the outside samples were the portlandite was consumed by carbon dioxide. On investigation, it was found that the flocculant was changed during

production. The blend was not used, only a high molecular weight flocculant was used. These flocculants induce the production of bigger flocks as a consequence the water content inside the flocks increase. Therefore, the air content will be higher after curing thus reducing density. Also, as a result of the big flocks the sheet formation in the sieve was poorer hence the reduction in strength. As a result of these findings, the trial was repeated with the blended flocculants.

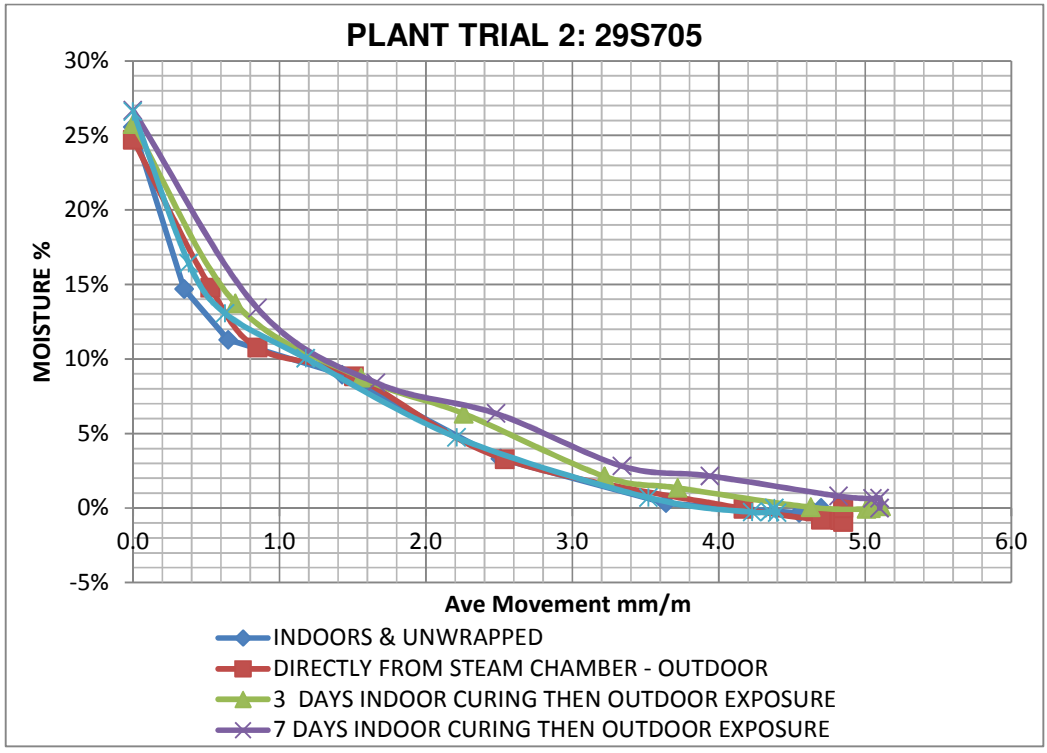


Figure 6.33: Monitoring movement of kaolin modified sheets, under different curing conditions, against moisture loss.

The following figures, Fig. 6.34 and 6.35 are the sheets from this batch that were inspected after 30 days. The pictures indicated formation of small edge cracks from the sheets that were initially cured indoors with wrapping and,

wider cracks were observed in the sheets that were cured outside without wrapping.



Figure 6.34: Corrugated sheets stored internally, with plastic wrapping, then cured outside without wrapping. Edge cracks appeared after 30 days curing period.



Figure 6.35: Kaolin modified corrugated sheets cured outside, without plastic wrapping, showed wide edge cracks after 30 days curing.

Second trial conducted with blended flocculants

The production of corrugated sheets with 3% kaolin as replacement of cement was conducted in the Hatschek machine using flocculants blended in the ratio 60:40 as described in the preparation section. The sheets were divided into three stacks; one was shrink-wrapped with plastic and kept indoors, the second was kept indoors without wrapping and the last one was stacked outside immediately after production without wrapping. The results in Fig. 6.36 showed that the wrapped sheets achieved the optimum development in density over the curing period. This was due to the moisture retained within the sheets by the plastic wrapping thus accelerating the hydration process. The least performance in density development over the curing period was observed with the sheets that were kept indoors without

the wrapping. The sheets kept outdoors obtained better development due to the carbonation process that resulted in refinement of matrix pores.

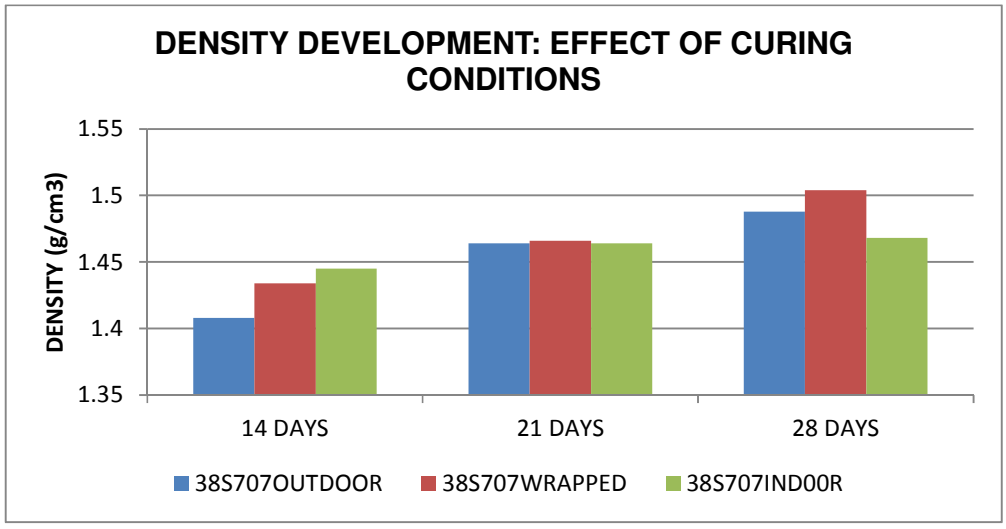


Figure 6.36: Density development of corrugated sheets incorporated with 3% kaolin as cement substitute under different curing conditions.

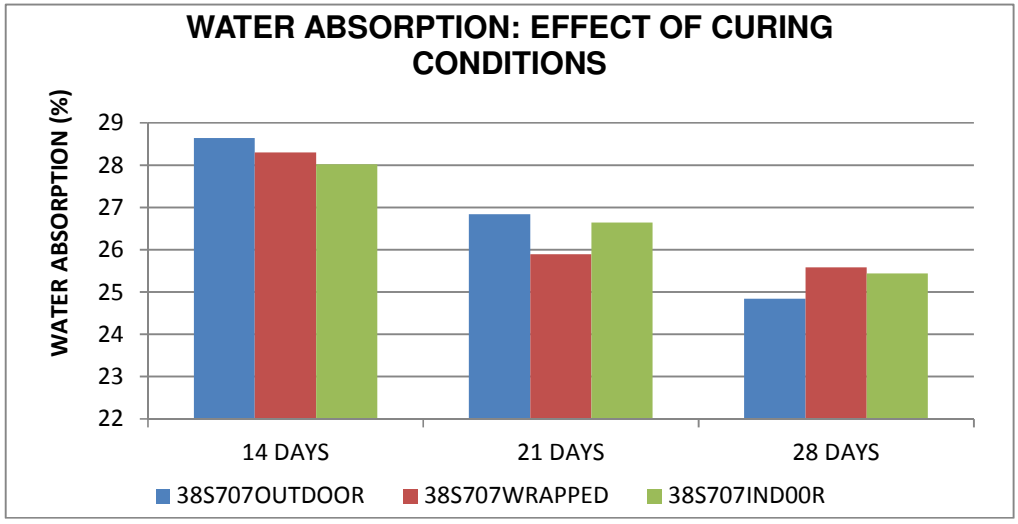


Figure 6.37: Effect of various curing conditions on water absorption of corrugated sheets with 3% kaolin inclusion as cement substitute.

As a consequence of improvement in particle packing of the cement matrix, porosity and permeability were reduced as seen in Figure 6.37. Hence, water diffusion was reduced as shown by the water absorption values. The total reduction in water absorption attained over 28 days by the sheets stored outdoors, wrapped indoors and indoors without wrapping was 13.3%, 9.5% and 9.2% respectively. These results showed the impact of carbonation on water absorption.

The strength results in Fig. 6.38 indicated that the sheets wrapped indoors attained the highest strength in 28 days. This can be attributed to the accelerated hydration process that generated CSH thus increasing strength and the pozzolanic reaction that consumed the calcium hydroxide resulting in secondary CSH. On contrary, the unwrapped sheets showed lower strength as a result of a slower hydration process. The sheets were not wrapped in plastic hence evaporation occurred with time resulting in less moisture available for the hydration process.

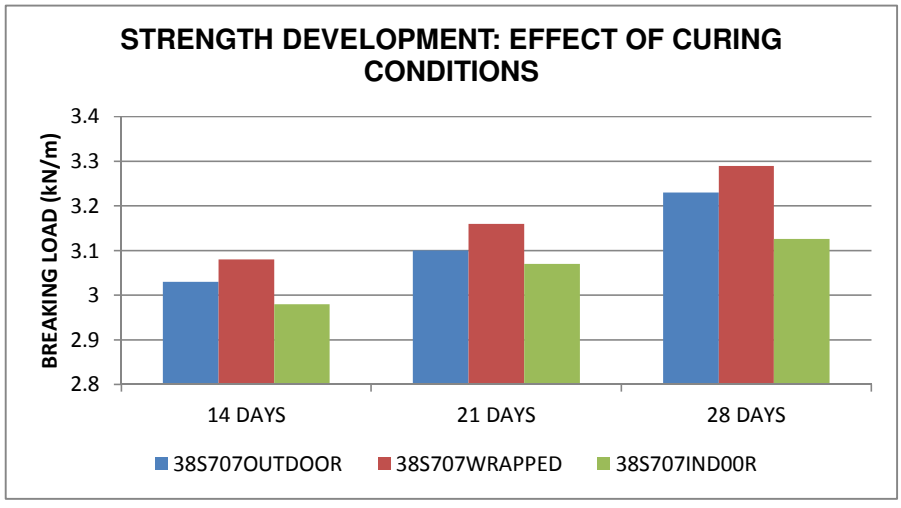


Figure 6.38 Development of strength of kaolin modified sheets over time under different curing conditions.

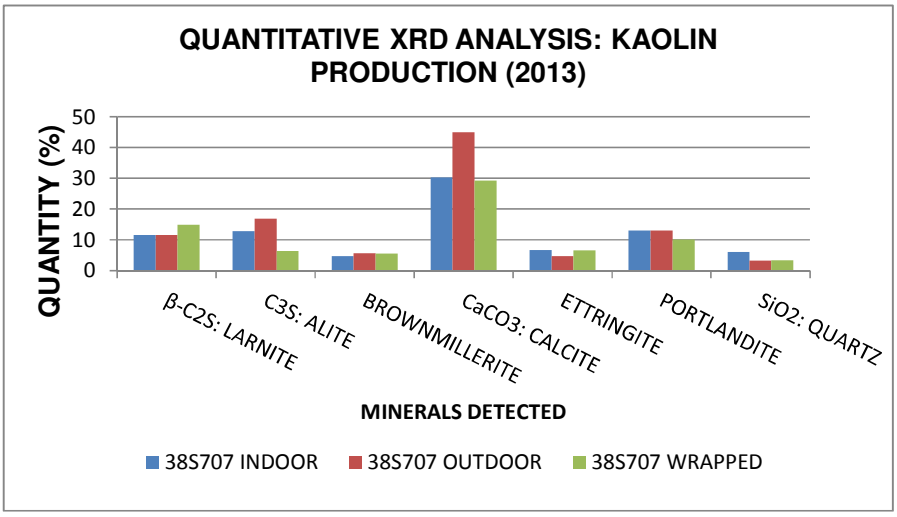


Figure 6.39: Quantitative XRD analysis of corrugated sheets with 3% kaolin as cement substitute identified at 28 days curing.

The presence of unreacted clinker and ettringite was observed in Fig. 6.39. This implies that the hydration process can still continue with availability of moisture. For the sheets stacked outdoors, there was reduction in portlandite due to the carbonation process that generated calcite, shown in high quantities in the figure above. The reduction in portlandite, more in wrapped sheets, in the indoor sheets indicated that the pozzolanic reaction occurred resulting in more CSH hence the higher strengths.

The moisture movement in all the sheets was measured at 22 days curing. The results showed rapid moisture loss in the sheets that were wrapped indoors, Fig. 6.40. This was due to wrapping of sheets during curing and as the plastic was removed evaporation took place resulting in the rapid loss in moisture. On the other hand, the sheets that were cured without the wrapping were already air dry and the moisture in the sheets had reached equilibrium with the moisture in the environment.

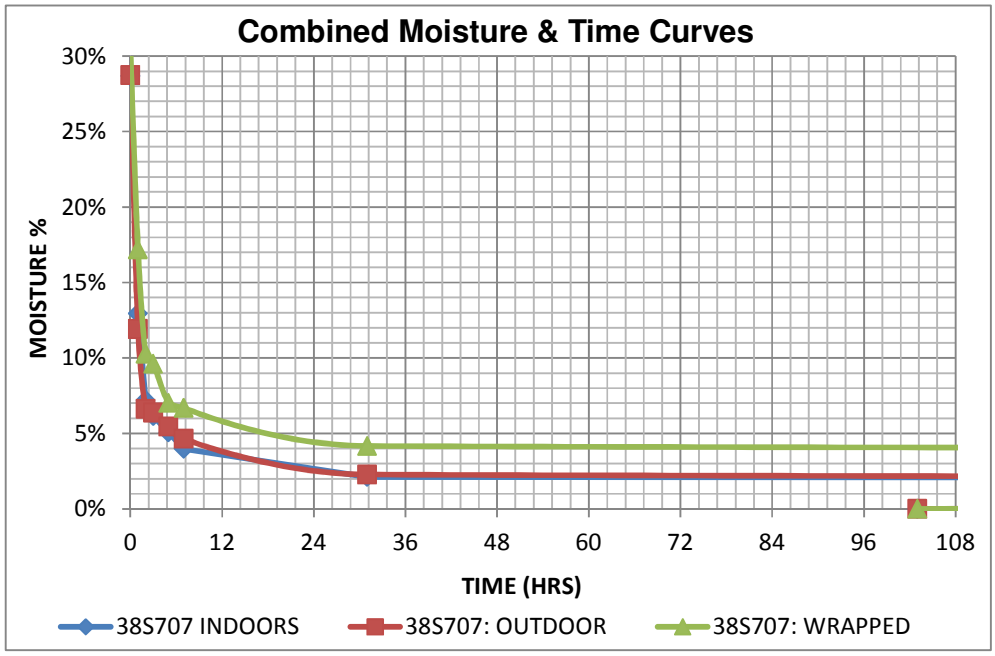


Figure 6.40: Evaluation of moisture loss with time in the corrugated sheets modified with 3% kaolin, as replacement of cement.

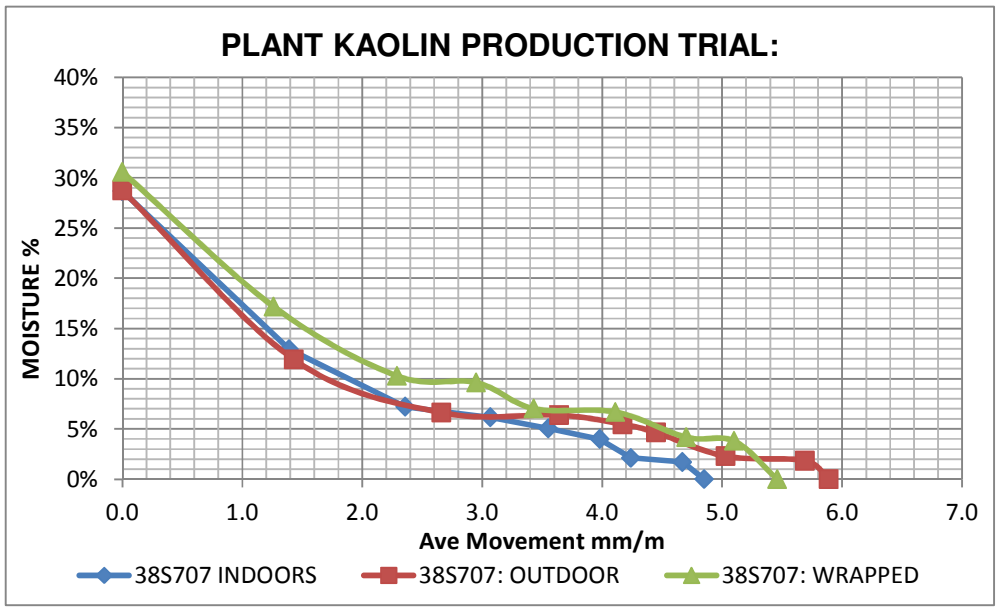


Figure 6.41: Movement determination in kaolin modified sheets with different curing conditions, tested at 22 days.

The wrapped sheets resulted in the highest movement as a consequence of the fast drying rate observed in Fig. 6.40. Drying the sheets from 16% to 6% moisture resulted in 2.02, 2.77 and 2.83 mm/m movement for sheets stored indoors, outdoors and wrapped indoors respectively. Reduction in moisture from the initial moisture content of the sheet to 5% moisture resulted in movement of 3.57, 4.33 and 4.51 mm/m for indoors, outdoors and wrapped indoors sheet respectively. Therefore, the sheets wrapped indoors resulted in edge cracking as shown in Figure 6.42.



Figure 6.42: A stack of 3% kaolin, replacing cement, modified corrugated sheets that were stored indoors shrink-wrapped in plastic.

The sheets that were cured indoors without wrapping did not show any edge or micro cracking, Fig. 6.43.

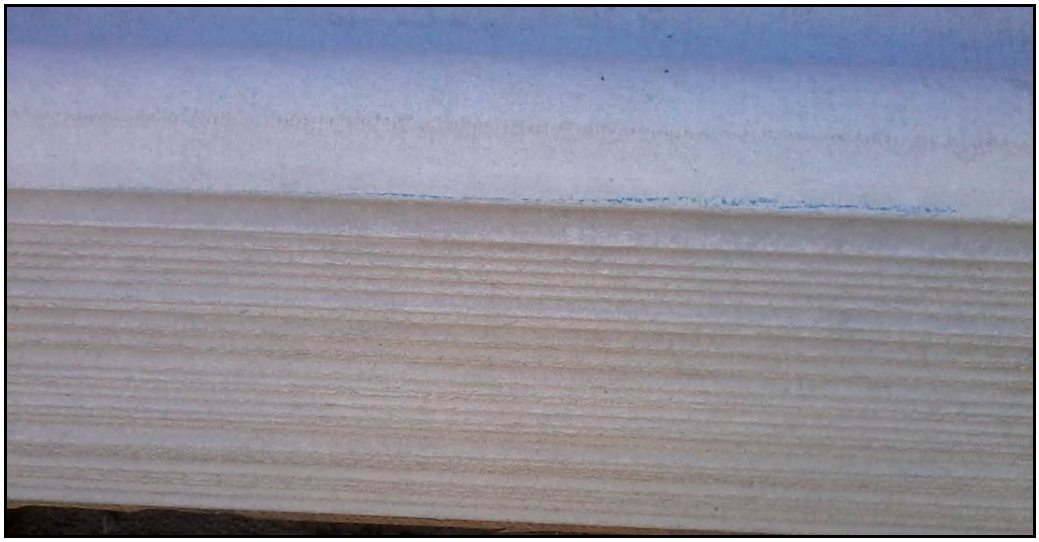


Figure 6.43: Corrugated sheets, 3% kaolin as replacement of cement, cured indoors without plastic wrapping. No cracks observed.

The sheets were subjected to wet-dry cycling for durability testing and the results are plotted in Fig. 6.44 below. The results showed the same pattern irrespective of curing conditions. Mohr et al. (2005a) described the mechanisms involved during the degradation of the fibrecement composites as consisting of three phases:

- Initial fibrecement or fibre interlayer debonding,
- Re-precipitation of secondary ettringite within void space created by debonding,
- Fibre embrittlement due to fibre cell wall mineralization.

Initially cellulose fibres swell and shrink without any hindrance but upon drying, diametrical fibre shrinkage generate a capillary pressure that cause the pore solution to be expelled through fibre ends and pits along the lumen. On subsequent drying of the sheets, re-precipitation of the hydration products occurs in the voids created by debonding. This re-precipitation of hydration products, such as ettringite, in these voids restrain fibre swelling upon rewetting as shown in the micrograph Fig. 6.45. Bentur and Akers (1989) discovered the embrittlement of pulp fibres due to formation of hydration

products within the fibre lumen. Also, Savastano and Agopyan (1999) validated the transportation of cement hydration products within the fibre lumen as well as around fibres due to wet-dry cycling. Thus, subsequent drying result in fibre shrinkage reduction and the driving force for expulsion of the pore solution is minimized. Hence, the pore solution remains within the fibre for a longer period.

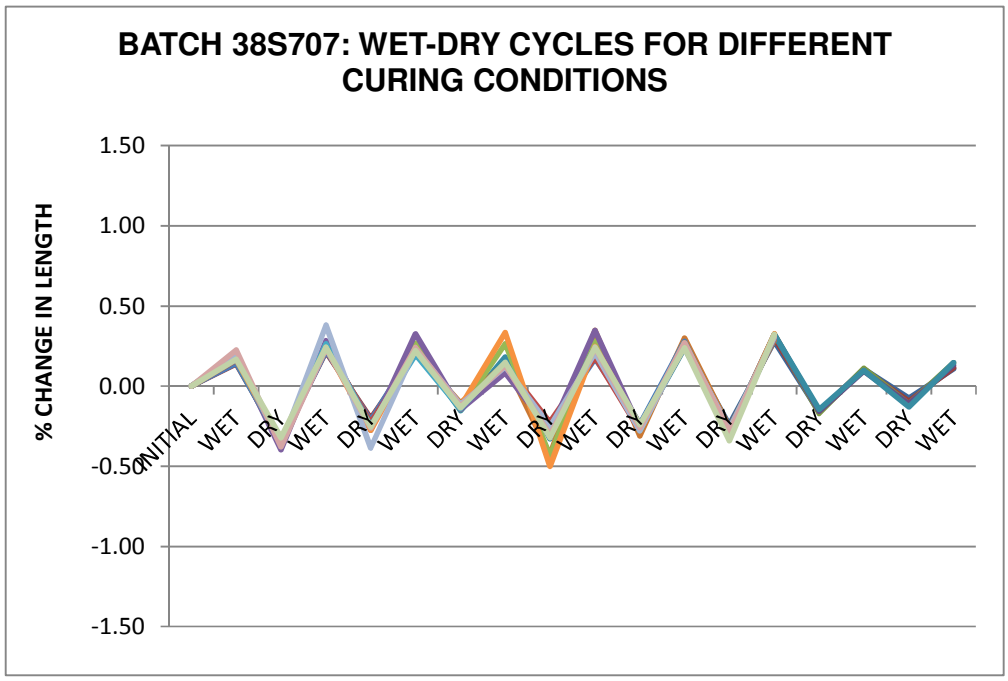


Figure 6.44: Change in length, as a result of wet-dry cycling, of kaolin modified sheets under different curing conditions.

The pore solution then migrate from the lumen to the matrix through the ends, fibre pits along the fibre and by diffusion through the cell wall resulting in deposition of hydration products, calcium hydroxide, within the fibre cell wall. This deposition decrease fibre ductility and lead to shorter fibre pull-out lengths in the composite.

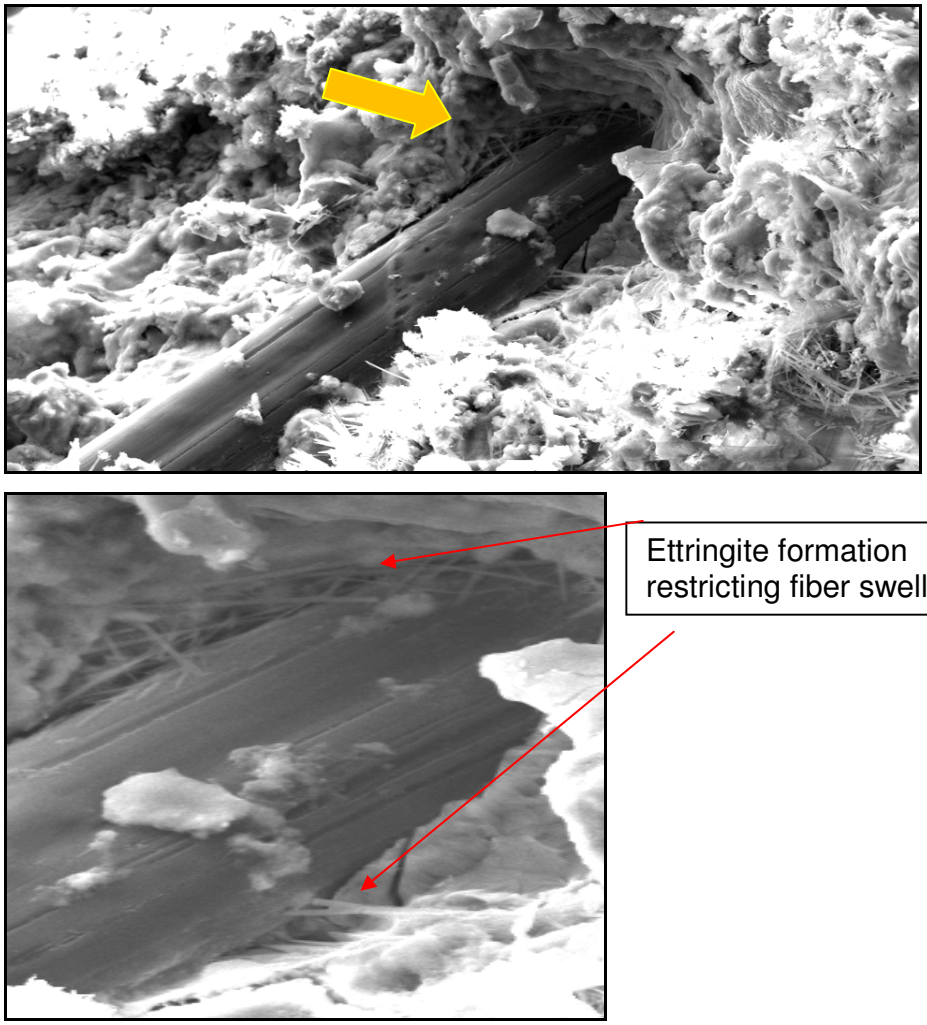


Figure 6.45: SEM micrograph showing needle-like ettringite formation which restricts fibre swelling, below insert of the area shown by the arrow.

Orientation of sheet stacks in relation to solar radiation

There were stacks exposed outdoors that did not crack and some had edge cracks. Also, crack formation depended on the location in the stock yard. The investigation was to find how and why the cracks occurred in certain location of the yard. A batch of corrugated sheets with 3% kaolin inclusion was produced in the Hatschek machine. Half of the batch was stacked outdoors with upturns facing severe solar radiation direction and the other half with the

downturns orientated in the same direction. Before exposure outdoors, half of the batch was shrink-wrapped with plastic after production and the other batch was not wrapped.

The density results are presented in Figure 6.46. Density development was observed over the curing period of 28 days for both curing conditions. The wrapped sheets showed an increase of 4% whereas the unwrapped sheet had a 3.4% increase over 28 days. The increment in density can be attributed to the filling of pores by the fine kaolin material hence refining the matrix structure.

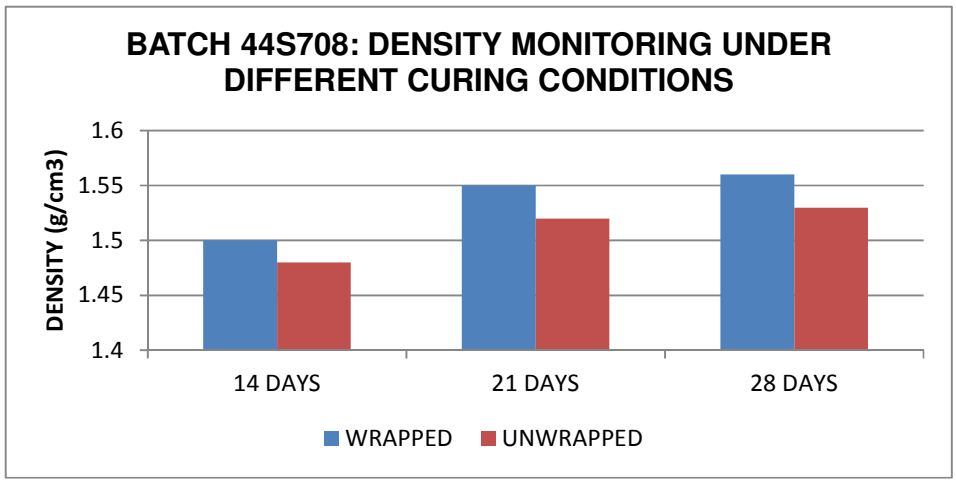


Figure 6.46: Development of density of kaolin modified sheets cured under different conditions, over 28 days.

The filling up of the voids between the larger cement particles contributed to a less porous composite. The water absorption value in Fig. 6.47 resulted in 18% and 10% reduction over 28 days for wrapped and unwrapped sheets respectively. The smallest reduction in water absorption for unwrapped sheets was due to the low moisture content of these sheets thus slower hydration reaction, which led to less formation of hydration products. With

less of calcium hydroxide in the matrix, the rate of the pozzolanic reaction was reduced hence less contribution to further refinement of the matrix.

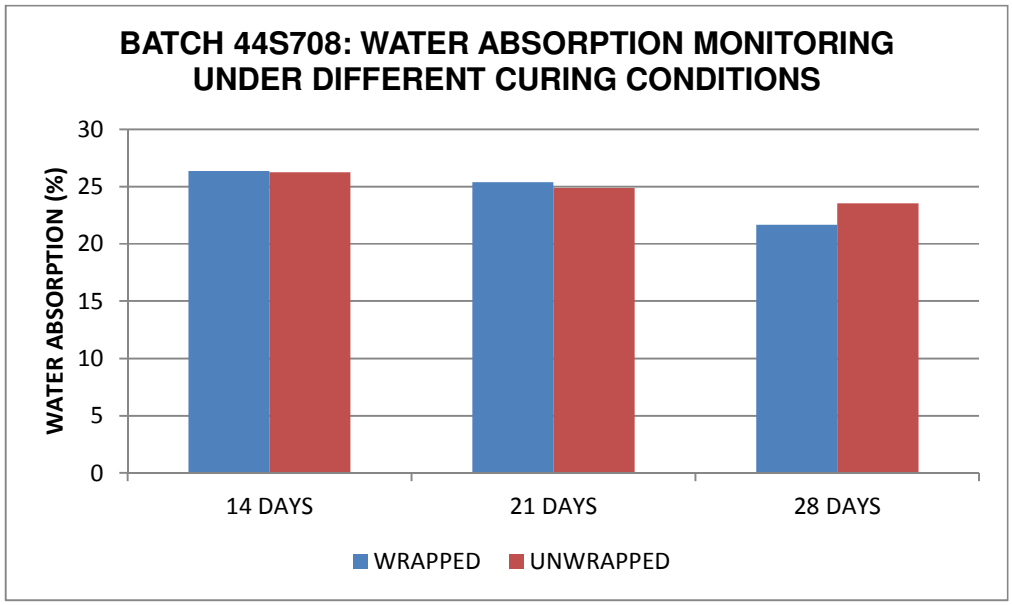


Figure 6.47: Reduction rate of water absorption for kaolin modified corrugated fibrecement sheets, incorporated with 3% kaolin as cement replacement, under different curing conditions.

The strength results in Fig. 6.48 indicated a 9% increase for wrapped sheets and 2% for unwrapped sheets over 28 days curing period. By unwrapping the sheets, the rate of moisture loss was increased which resulted in slower hydration. Therefore, less CSH was formed which led to a reduction in strength. Also, the reduction in calcium hydroxide resulted in less pozzolanic reaction products, secondary CSH, thus a reduction in strength.

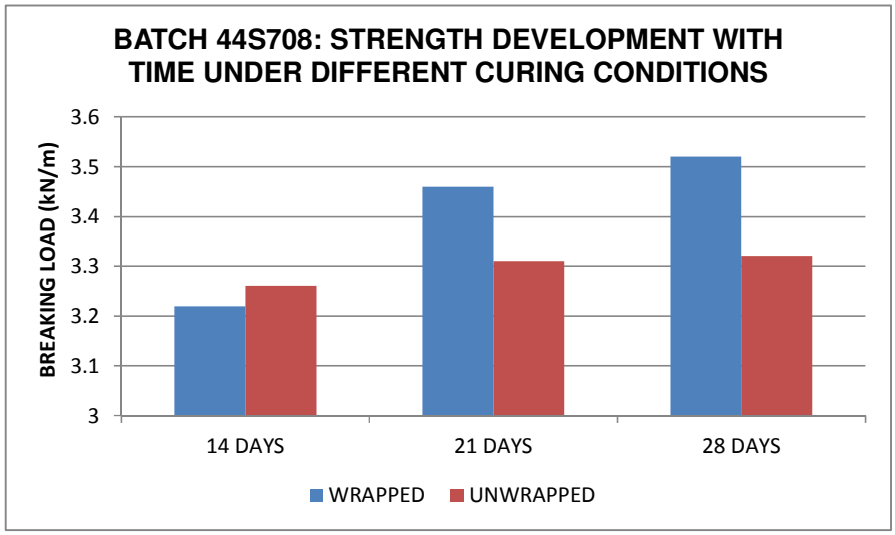


Figure 6.48: Development of strength in fibrecement corrugated sheets, with 3% inclusion as cement substitute, over 28 days curing under different conditions.

Quantitative analysis of mineralogical composition of corrugated sheets was done at 21 days and the results presented in Fig. 6.49. The unwrapped sheets exhibited high quantity of unreacted clinker, C_3S, confirming the slow rate of hydration reaction. This mineral is responsible for early strength in cement. The presence of high C_2S in sheets indicated the possibility of strength increases with aging as C_2S contributes to later strength in cement. With such high amount of unreacted clinker and the strength of the sheets above 3 kN/m, it implies that the strength was enhanced by the pozzolanic reaction which generated secondary CSH. The low portlandite, $Ca(OH)_2$, detected in the sheets confirmed its consumption by the silica in the kaolin. Calcite values were low hence the impact of carbonation can be eliminated.

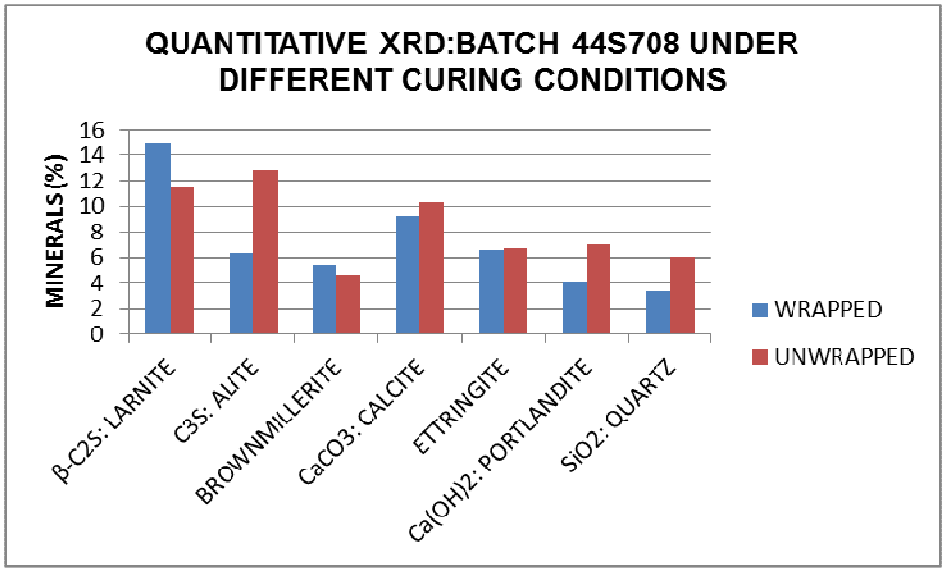


Figure 6.49: Quantitative XRD analysis for corrugated sheets incorporated with kaolin at 21 days curing under different conditions.

The sheets were then subjected to natural weathering exposure, after 14 days curing, outside with some stacks having the upturns in the direction of highest incidence of solar radiation and the others with downturns orientated in the same direction. Moisture-movement of these sheets was measured and the results are illustrated in Figs. 6.50 and 6.51. The results showed that the sheets with the upturns orientated in the direction of severe solar radiation were losing moisture at a higher rate than the sheets with downturns facing the same direction and the ones stored indoors.

The total movement experienced by the indoors (IND), upturn orientated in direction of solar radiation (UPT), downturn in the direction of solar radiation (DT) and average downturn sheets (AVDT) were 4.65, 5.81, 3.98, 4.59 mm/m respectively, Fig. 6.51. Reduction of moisture from 16% to 6% resulted in 21%, 8%, 38% and 17% movement for UPT, DT, IND and AVDT respectively.

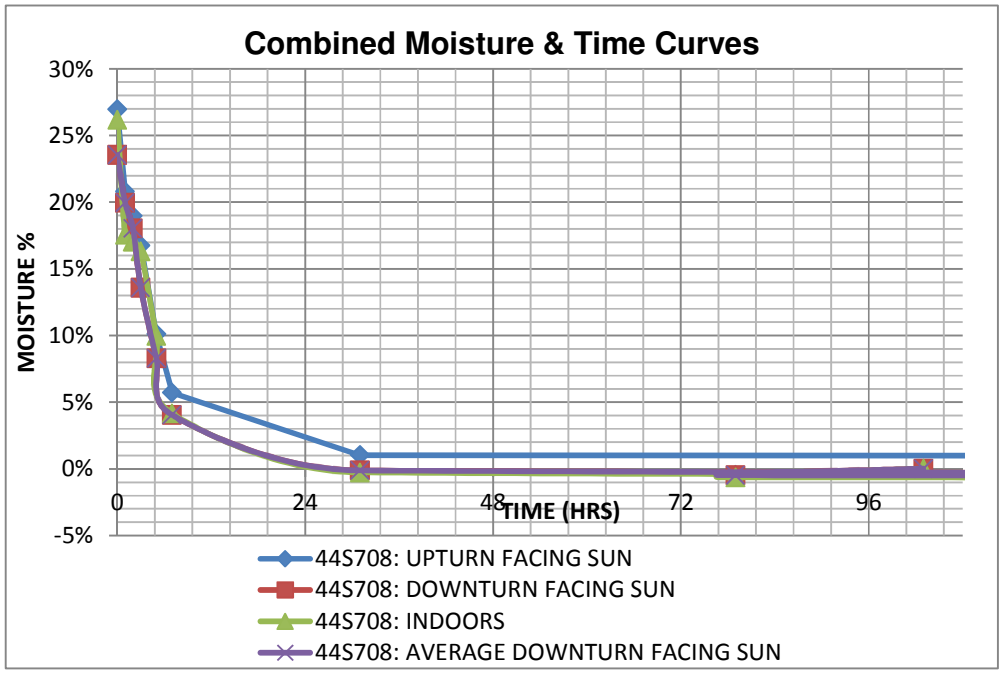


Figure 6.50: Evaluation of the rate of moisture loss in corrugated sheets under different curing conditions.

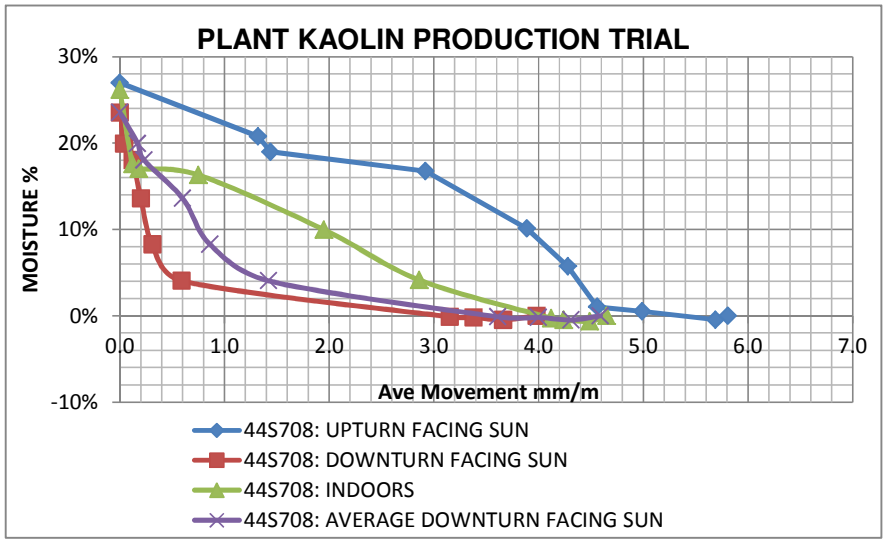


Figure 6.51: Moisture-movement curves of kaolin modified corrugated sheets, 3% replacing cement, cured under different conditions.

Moisture reduction from initial moisture, ~ 30%, to 5% resulted in movement of 74%, 13%, 59% and 28% for UPT, DT, IND and AVDT respectively. The sheets with upturns orientated in the direction of highest incidence of solar radiation exhibited the highest movement as predicted by the results in Fig. 6.50. The least movement was attained by the sheets with downturns in the direction of intense solar radiation. Random sampling of the sheets with downturns in the direction of solar radiation was done and average of the measurements was also plotted. The average results also showed less movement than the sheets stored indoors and the ones with upturns facing the sun. The sheets with upturns facing the sun developed big edge cracks, Fig. 6.52, whereas the sheets with downturns in the direction of highest incidence of solar radiation showed no sign of cracking, Fig. 6.53.

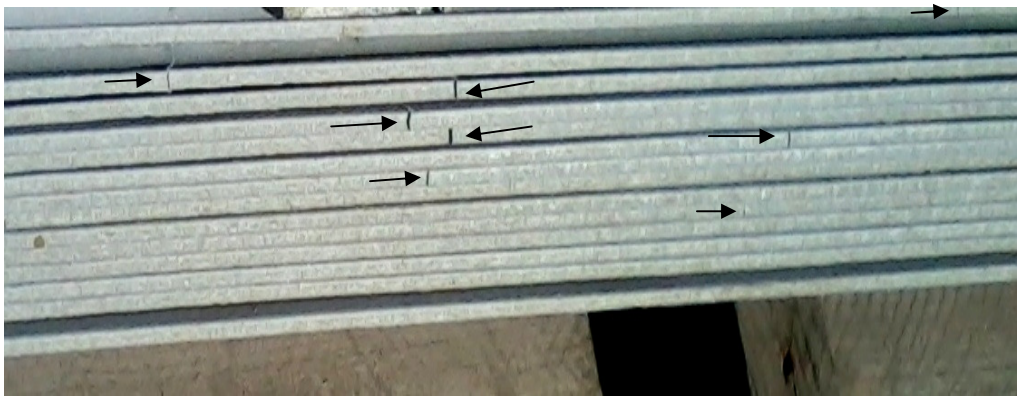


Figure 6.52: Corrugated fibrecement sheets, 3% kaolin replacing cement, with upturn orientated in the direction of highest incidence of solar radiation.

The cracks in the stack were not concentrated in a particular area but randomly distributed along the length of the sheet. The width of the cracks and propagation through the sheet were different in size. The formation of these cracks can be attributed to the higher rate of evaporation of moisture at these extreme temperatures thus increasing drying shrinkage as a stress-

induced edge crack. Also, the upturns exposed the composite fibre endings directly to the sunlight thus accelerated pore water evaporation. The edges dried faster than the center of the sheet in a stack thus resulting in higher moisture gradient and tensile stresses over the edge of the sheet.



Figure 6.53: Corrugated sheets, 3% kaolin replacing cement, with downturns orientated in the direction of highest incidence of solar radiation, no cracks observed.

The sheets stored indoors were exposed to natural weathering at different areas in the stock yard after 14 days curing. The stack that was kept close to the building, always in the shade of the building, did not crack whereas the stack that was placed at the center of the stockyard showed micro cracks after 28 days as seen in Fig. 6.54. Only a few sheets in the stack were cracked and the cracks were randomly distributed.

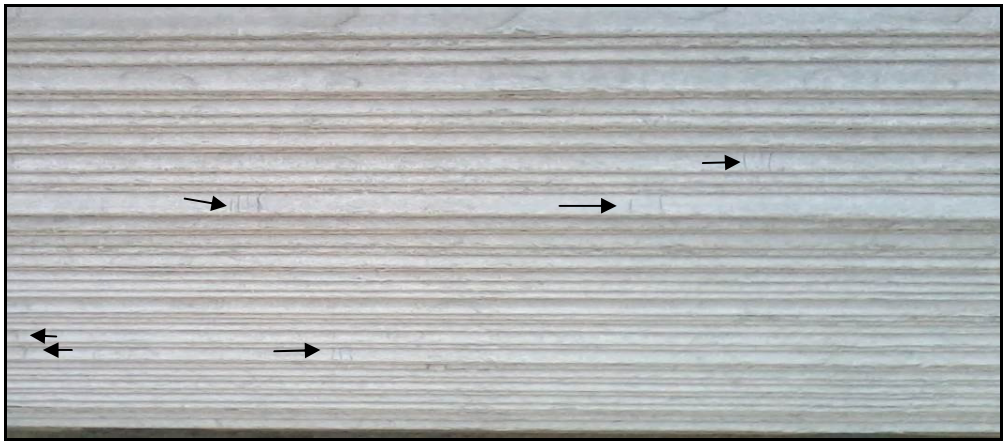


Figure 6.54: Corrugated sheets, 3% kaolin as substitute for cement, stored indoors wrapped then exposed outside without wrapping. Edge micro cracks observed.

The wet-dry cycling tests were conducted to determine the durability of these sheets and the results are illustrated in Fig. 6.55.

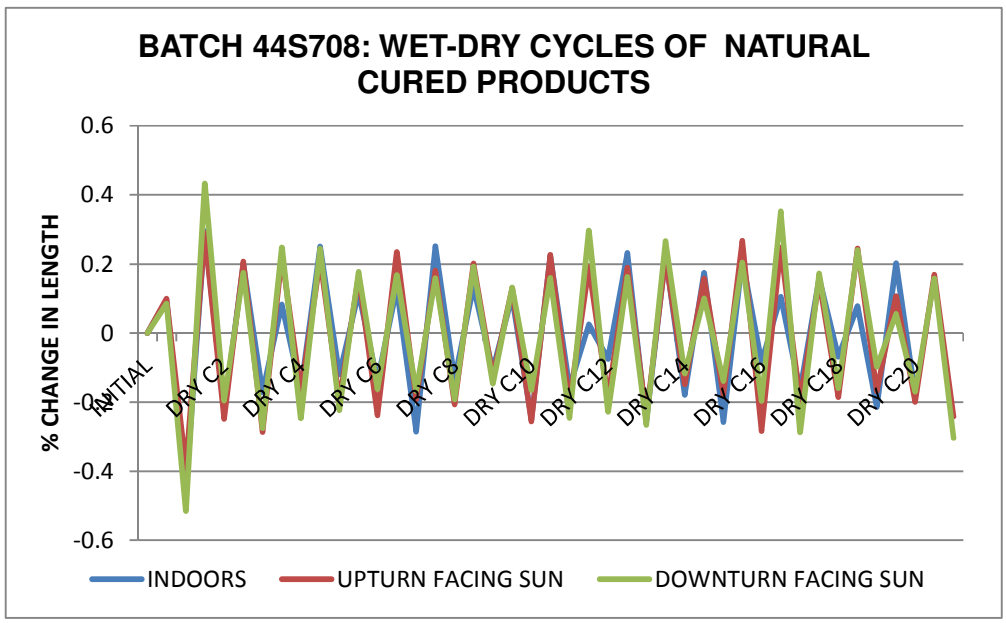


Figure 6.55: Durability test for kaolin modified corrugated sheets, cured under different conditions, subjected to 21 wet-dry cycles.

A huge initial shrinkage was observed for all curing conditions and it affected the fibre dimensional stability during subsequent wetting and drying. After initial drying and swelling the peaks decreased with subsequent wetting and drying. This can be attributed to the precipitation of the hydration products at the fibrecement interface. These hydration products can then restrain fibre swelling upon rewetting and reduce shrinkage during subsequent drying. Then the pore solution will diffuse from the lumen through the cell wall resulting in a deposition of hydration products within the fibre cell wall. Shorter fibre pull-out lengths in the composite result and complete fibre mineralization occurs beyond 10 wet/dry cycles (Mohr et al., 2005a).

The microstructure of the sheets was studied with the micrographs in Figures 6.56 – 6.59.

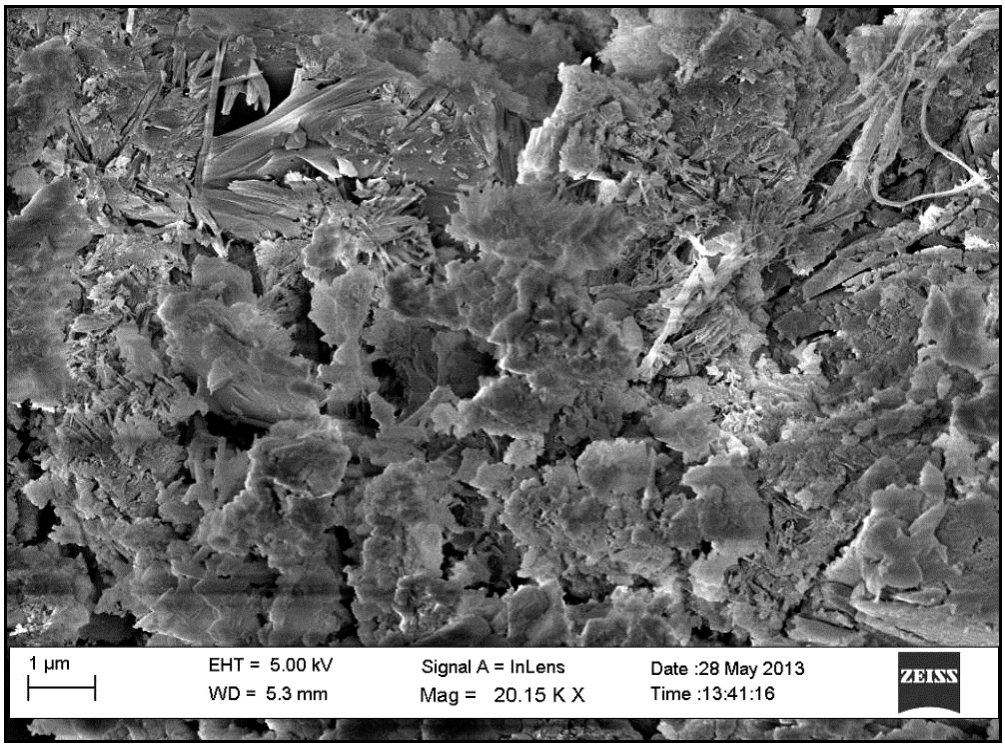


Figure 6.56: SEM micrograph of kaolin modified sheets stored indoors, showing hydration products

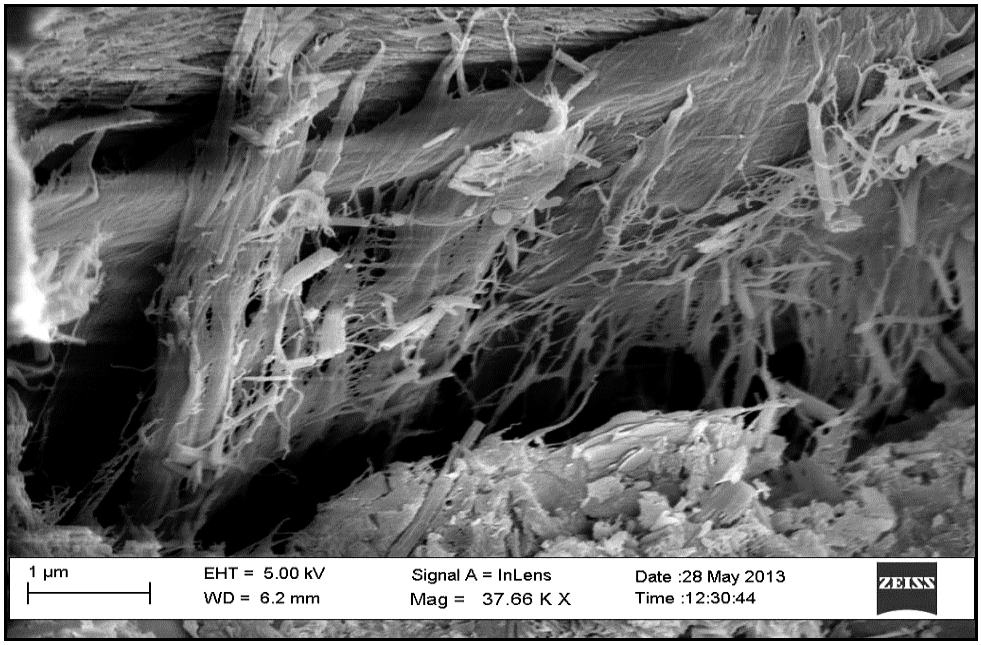


Figure 6.57: SEM micrograph of corrugated sheets indoors

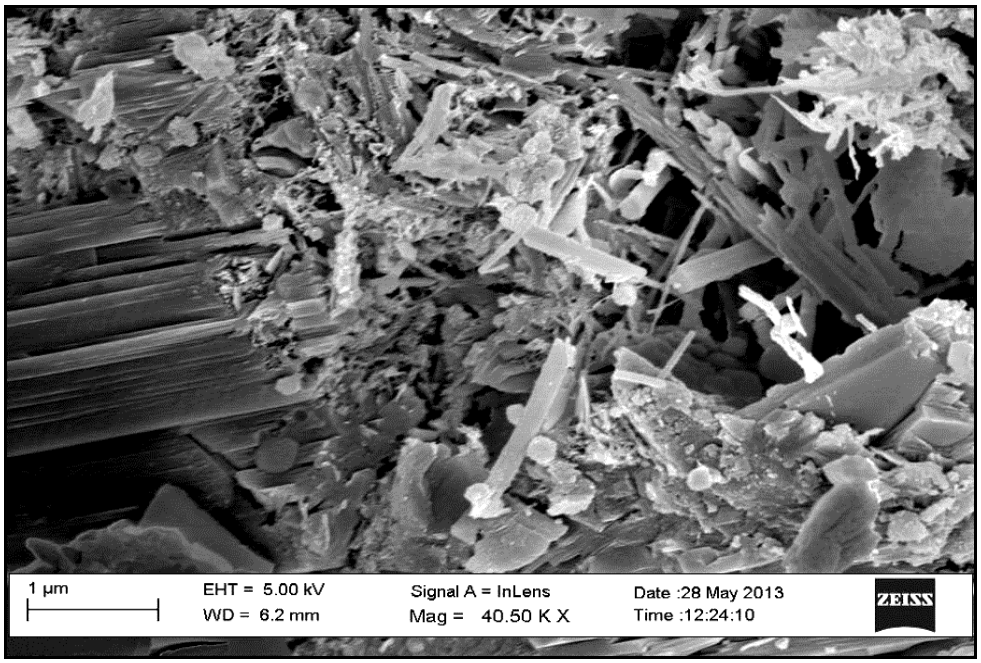


Figure 6.58: SEM micrograph showing ettringite crystal

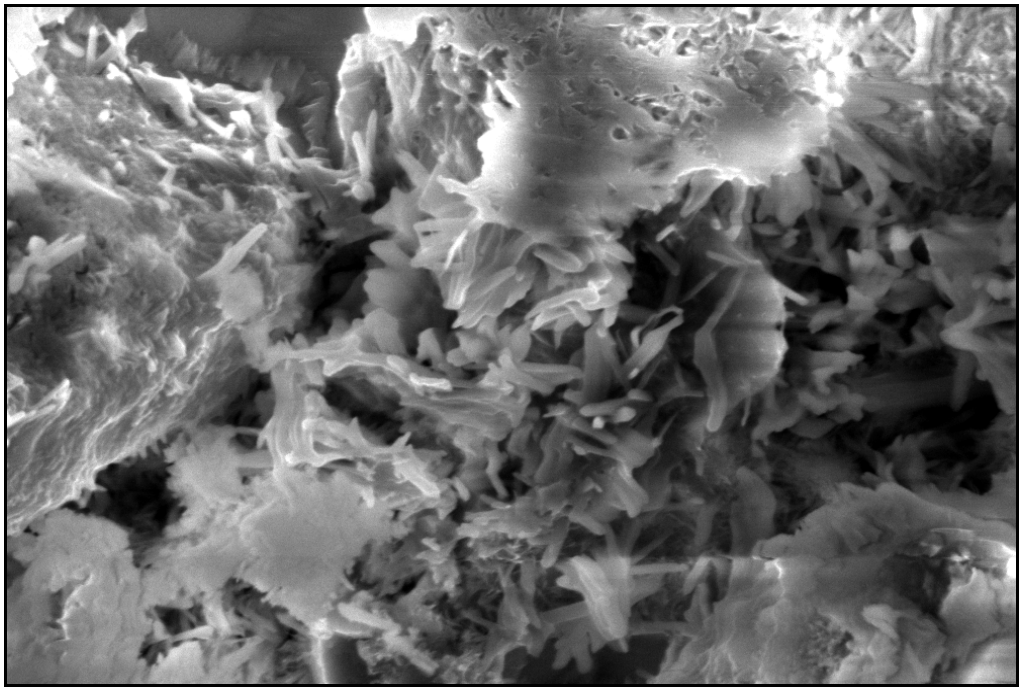


Figure 6.59: SEM micrograph of kaolin modified corrugated sheets illustrating presence of CSH and $CaCO_3$.

6.4 Summary

The effect of kaolin on the physical and mechanical properties of corrugated fibrecement sheets can be summarized as follows:

- Addition of kaolin to the mix, as cement replacement, resulted in refinement of the matrix due to the kaolin fine particles filling up the voids between the large cement particles. By filling up the pores the matrix became denser thus increasing the density of the sheets. The refinement of the matrix contributed to reduction in porosity hence the lower water absorption of sheets.
- Kaolin, as a pozzolan, reacted with the hydration product, $Ca(OH)_2$, generating secondary CSH thus enhancing the strength of fibrecement sheets.

- The kaolin sheets showed markedly lower permeability hence the diffusion of water was lower. This contributed to reduction in wet-dry shrinkage.
- The elimination of calcium hydroxide as a result of the pozzolanic reaction greatly enhanced durability and eliminated efflorescence.
- There was less micro cracking due to denser interfacial transition zone and refined pore structure.
- Selection of flocculants played a major role in the Hatschek process. Flocculants that result in formation of bigger flocks should be avoided due to reduction in production efficiencies and the impact on the mechanical properties of the composite.
- The rate of moisture loss in the sheets, not the moisture content, was found to be the important factor in elimination of cracks.
- With the correct formulation, curing conditions contributed to edge cracking.
- Better conditions were found to be areas were the rate of moisture loss was not rapid, i.e. shaded area or indoors for a longer period until the moisture in the sheet reached equilibrium with the surroundings.
- In hot areas, the stacks of sheets have to be stored with the downturns orientated in the direction of high incidence of solar radiation. This position resulted in no crack formation.

Therefore, the fibrecement edge cracking of corrugated sheets can be eliminated by refining the matrix structure, controlling the rate of moisture loss by choosing the adequate curing conditions, depending on the location and season.

Chapter 7: SUMMARY, CONCLUSIONS AND RECOMMENDATIONS

7.1 Summary and conclusions

The distinguishing characteristic of cellulose-based cement composite material is its ability to expand during rainy and shrink on sunny days as the water evaporates from the sheets. This movement results in drying shrinkage in corrugated fibrecement materials stacked in a pile of 40 sheets due to the edges drying faster than the central area of the sheet. Despite current knowledge on edge cracking occurring in corrugated fibrecement sheet and its mitigation techniques, the cracking problem continues indicating existence of drying shrinkage. Yet, the issue of edge cracking in stacks and how to mitigate it has not been fully resolved and gaps exist between research and application.

This thesis attempted to narrow some of these gaps through providing investigations related to volume changes in fibrecement materials at early stages of the curing process and techniques used to mitigate it. Moreover, new mix formulations for producing fibrecement materials with lower shrinkage and reduced probability for cracking, taking into consideration the environmental conditions. These mitigation techniques include surface modification of cellulose fibres, wollastonite microfibres as partial replacement for cement, addition of superplasticizer to the mix and kaolin inclusion as partial cement substitute.

At the beginning of this research, Chapter 1 provides a comprehensive literature review for the types of shrinkages in cementitious materials and the mitigation techniques researched thus far. The development of shrinkage can be particularly sensitive to exposure conditions in the field, including temperature variation, relative humidity and velocity of wind. Yet, existing research on drying shrinkage relied mostly on constant curing conditions.

Also, most of the research on mitigation strategies concentrated on molded cementitious materials not corrugated sheets. Thus, this thesis introduced a testing approach that captures the mechanism governing shrinkage of corrugated sheets and the role of mitigation techniques under simulated field-like conditions. The role of the mitigation strategy which had economic benefit was extended to natural exposure conditions.

Chapter 2 provided basic knowledge of the Hatschek process used for production of corrugated fibrecement sheets. The test methods to evaluate the mechanical properties and durability of composites were well documented. As the physical and mechanical properties of fibrecement composite materials changed, modification of the cement matrix and crystal structures developed. Thus, analytical methods to be used for phase identification and microstructural analysis were described. The physical and mechanical properties of all the raw materials used in this study were described in detail.

The core theme of this research was to achieve corrugated fibrecement sheets with the least movement and reduced risk for cracking, along with reducing its environmental and economic impact. Corrugated fibrecement sheets have a high environmental impact due to its high cement content, leading to high energy consumption and CO_2 emissions associated with cement production. In chapters 4 and 6 a concept for reducing drying shrinkage, at early age, was introduced. The concept consisted of partially replacing cement with other suitable more environmentally friendly materials. In chapter 4, the potential for using wollastonite microfibres as partial replacement for cement by weight and its capability to reduce shrinkage and improve cracking resistance was investigated. Chapter 6 explored utilization of natural kaolin as substitute for cement, by weight, and its effect on the movement or shrinkage of corrugated sheets and consequently on elimination of edge cracking.

Organosilanes, as cellulose surface treatment agents, were used in chapter 3 to transform the cellulose fibres from hydrophilic to hydrophobic state. Surface treated cellulose was added to the cement composite mix prepared in the Hatschek machine. Composites with pretreated cellulose fibres showed slight reduction in movement. This indicated that the treated fibres stabilized the dimension changes in the composite. The physical properties of the composites were enhanced by pretreatment of cellulose fibre prior to production. The insignificant change observed in wet-dry movement results of fibrecement composites indicated that slight reduction in drying shrinkage can be expected as well as minute resistance to cracking. The economic implications of using the organosilanes in fibrecement mix formulation were enormous hence this mitigation strategy was not feasible due to economic and performance reasons.

Commercially available natural wollastonite microfibres were used at 2%, 4%, 6% and 10% as partial substitution for cement, by weight. Research findings demonstrated that incorporating wollastonite microfibres to fibrecement mix promoted pore discontinuity which led to higher density, lower water absorption and wet-dry movement thus reduction in drying shrinkage. Incorporating wollastonite microfibres enhanced the flexural strength of fibrecement composites due to the improvement of the microfibre-matrix bond with age and modification in the microstructure of the transition zone in the vicinity of wollastonite. Wollastonite inclusion as partial replacement of cement reduced fracture energy of the composites thus resulting in strong but brittle materials. Brittleness in fibrecement composites results in cracking during installation.

Chapter 5 adopted a more fundamental approach based on reduction of water to the mix in an attempt to capture the effect of admixtures and superplasticizers on the drying shrinkage of fibrecement sheets. Addition of silicone resin admixture, 0.3%, to the fibrecement mix resulted in significant reduction in water absorption. This was due to the semi-permeable layer

formed on cement grains which acted as a diffusion barrier inhibiting transportation of water in and out of the composite resulting in reduction in permeability. Moreover, the silicone resin admixture slightly reduced the movement of fibrecement composites thus had no significant effect on drying shrinkage. Addition of 3% kaolin to the mix with silicone resin resulted in further reduction of wet-dry movement. On the other hand, superplasticizers were added at 10%, 15% and 20% of the total mix weight. As the plasticizer dosage increased in the mix, the water absorption of the composite decreased with time hence reduced volume change from drying to wetting. Also, the water released by superplasticizers was available for hydration processes hence the huge improvement in strength. As the curing process progressed, less water was available in the composites thus a substantial reduction in movement, with time, was observed. Consequently, the efficiency of superplasticizers in reducing drying shrinkage was improved. Admixtures and superplasticizers are expensive therefore it would not be of economic benefit in daily production.

The promising results contributed by the combination of silicone resin admixture and kaolin introduced in chapter 5 encouraged utilization of natural kaolin to optimize the gained benefit. In chapter 6, the effects of incorporating kaolin on the mechanical properties, durability and cracking were evaluated. Kaolin was added at 1%, 2%, 3% and 5% as partial weight replacement for cement. Inclusion of kaolin resulted in refinement of the cement matrix of the fibrecement composite thus reduction in porosity hence lower water absorption. The strength of the composites was enhanced by the pozzolanic reaction of kaolin. As the matrix became denser, permeability was improved contributing to a significant reduction in wet-dry movement. Therefore, the ingress and egress of moisture in the composite was inhibited resulting in a markedly reduced drying shrinkage. This observation was more evident in composites with 3% and 5% kaolin as replacement of cement.

Fundamental investigations described in this thesis proved that relying on constant curing conditions alone to evaluate the edge cracking behavior and efficiency of the mitigation techniques, ignoring exposure conditions, might yield misleading conclusions. In addition to current standard tests, standardization of moisture-movement tests, for prediction of cracking probability, should be taken into consideration. The second level of investigation covered the effect of kaolin inclusion, as partial cement substitute, in corrugated fibrecement sheets under various curing conditions. Results showed that shrink-wrapping the sheets with plastic was effective for reducing drying shrinkage, while the stack of sheets was indoors, but when exposed to outdoor environment with no wrapping, edge cracking developed in some of the sheets. On the other hand, un-wrapping the sheets at 14 days curing while indoors and conditioning the sheets at room temperature until the moisture content was below 10% before outdoor exposure, showed no appearance of edge cracks. It was discovered that exposure of a sheet stack to natural environmental conditions, directly after steam chamber and without wrapping, displayed no cracking for sheets stored in the shade whereas the stack of sheets that was directly exposed to the sun showed edge cracking, in all the sheets, along the length of the sheets.

No cracking was observed in a stack of sheets with ends facing down in the direction of high incidence of solar radiation whereas with ends facing upwards in the direction of high incidence of solar radiation resulted in wide edge cracks along the length of the sheet.

Edge cracking of corrugated fibrecement sheets, in a stack, is attributed to drying shrinkage and evaporation of water from the sheet surface. However, mechanisms and causes of cracking differ depending on the exposure conditions, mix formulation and the rate of moisture loss from the composite sheet.

For sheets exposed to drying, it was found that the drying shrinkage was due to the movement or loss of water. However, the rate of evaporation strongly

depended on the mix composition and was not always the governing factor for the cracking tendency. Depending on the characteristic of the composite, different mechanisms were found to be responsible. For composites with high moisture content, evaporation was the governing cause, whereas for sheets with low moisture content the exposure conditions proved to be the dominant cause. Kaolin presented the economic benefit as the material is less costly than cement and, the environmental benefit by replacing cement in the mix formulation. It can be concluded that kaolin was the only material that managed to eliminate edge cracking in stacked corrugated sheets, with adequate consideration of exposure curing conditions.

The best mitigation strategy for elimination of edge cracking in stacked corrugated fibrecement sheets can be briefly summarized in Table 7.1:

Table 7.1: Best mitigation technique

The optimum treatment for minimization of drying shrinkage in stacked corrugated fibrecement sheets was found to be the inclusion of 3% kaolin, as replacement of cement, in the standard mix formulation. These sheets had to be shrink-wrapped to accelerate the hydration process thus enhancing the effectiveness of kaolin hence reducing drying shrinkage.
Cracking of sheets also depended on the rate of moisture evaporation from the sheets. Therefore, this rate was significantly reduced by either storing the sheets in the shaded areas of the stockyard or orientating the down turns of the sheets in the direction of the high incidence of solar radiation.
The best mitigation technique for elimination of edge cracking in stacked corrugated fibrecement sheets was achieved by both modification of mix composition with 3% kaolin and the selection of adequate exposure conditions as highlighted above.

7.2 Recommendations for future research work

1. Edge cracking of corrugated sheets in a stack has been attributed to drying shrinkage and evaporation of water from the sheets. However, mechanisms and causes of edge cracking differ depending on exposure conditions, mix compositions, etc. It is recommended that the field tests, over years, be conducted to better quantify the actual sources of cracking and also quantify the benefits imparted by the kaolin mitigation technique.
2. This research demonstrated that there were corrugated sheets in a stack that did not crack. The appearance of the cracks did not occur at the same place and the width of the cracks was different. Therefore, more field work need to be done on understanding the curing mechanism of corrugated sheets in a stack.
3. It was illustrated that kaolin can be a very effective technique for reducing fibrecement composite shrinkage. However, to become a more versatile technique, further research must be done to: (i) investigate the effectiveness of kaolin with different mix compositions and materials; (ii) investigating long-term properties, over years, of these corrugated fibrecement sheets under natural weathering exposure.

APPENDIX A

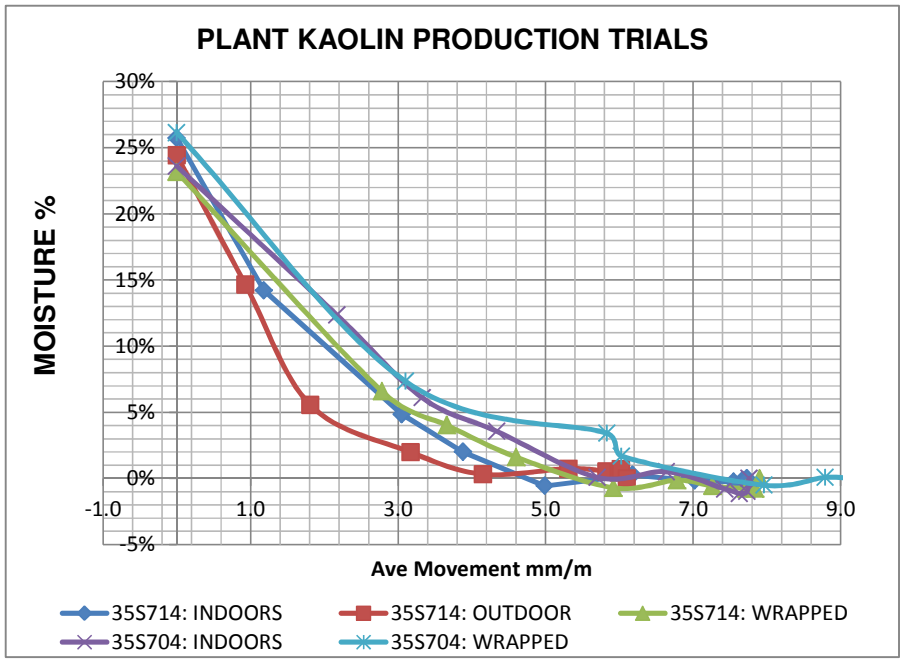


Figure A1: Production batch, 35S714, of fibrecement mix incorporated with 3% kaolin cured under different conditions. Moisture- movement curve indicated that the sheets cured outdoor had the least probability to crack.

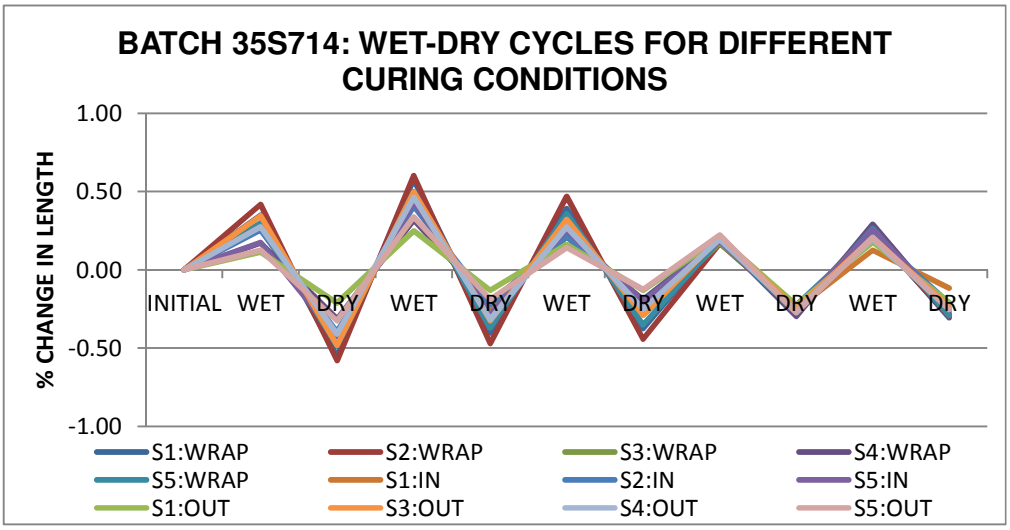


Figure A2: Wet-dry cycling curve for batch 35S714 for evaluation of durability of kaolin modified fibrecement sheets. Movement reduction noted after three cycles.

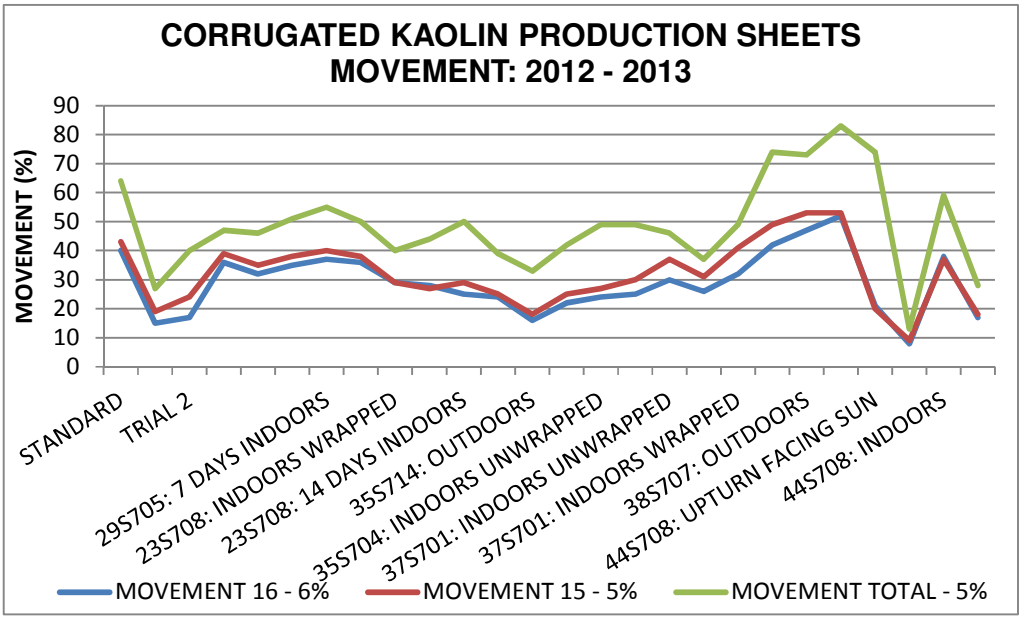


Figure A3: Movement measured in all the 3% kaolin incorporated fibrecement corrugated sheets produced between 2012 and 2013. The results demonstrated that this curve can be used for prediction of cracking

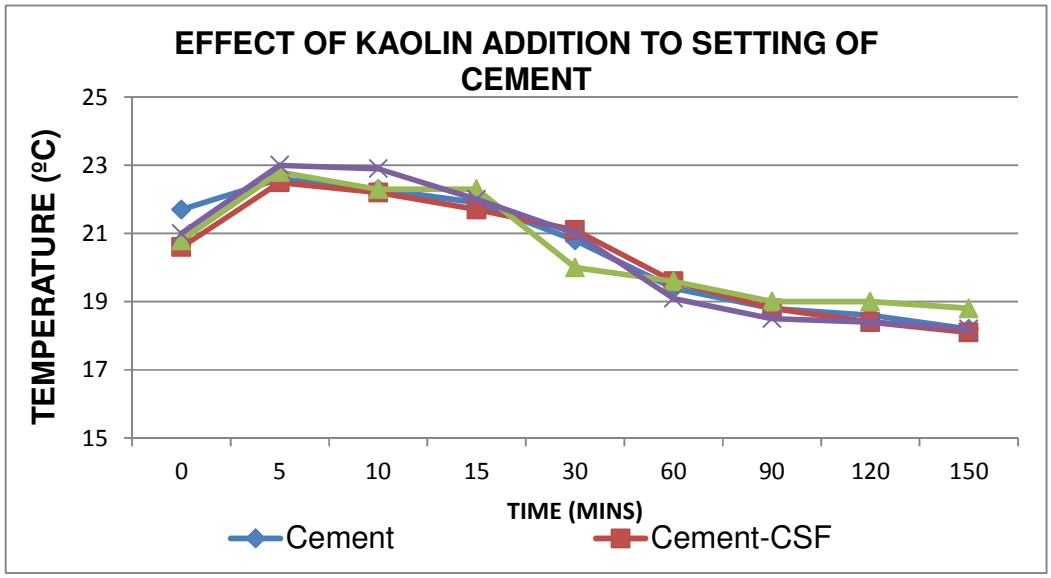


Figure A4: Effect of kaolin addition on cement setting, at levels between 1% and 5%. The observation showed no significant difference in setting of cement.

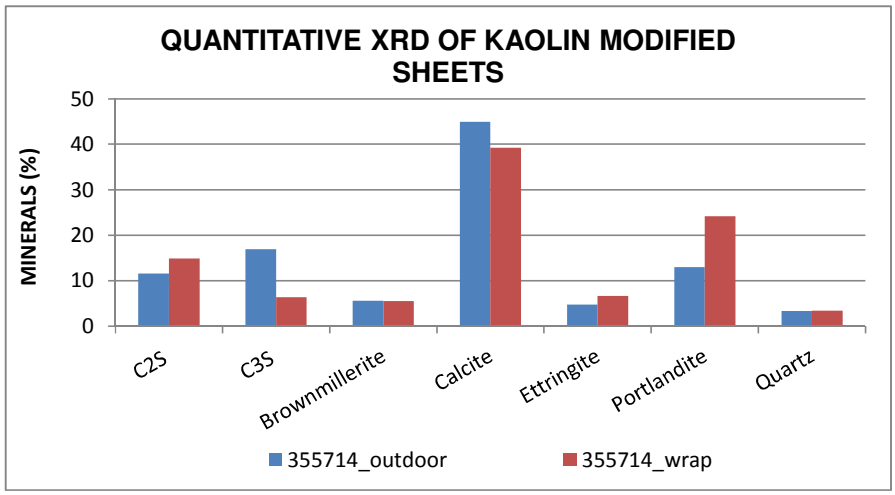


Figure A5: Minerals formed during the hydration process of kaolin modified sheets under different curing conditions.

APPENDIX B

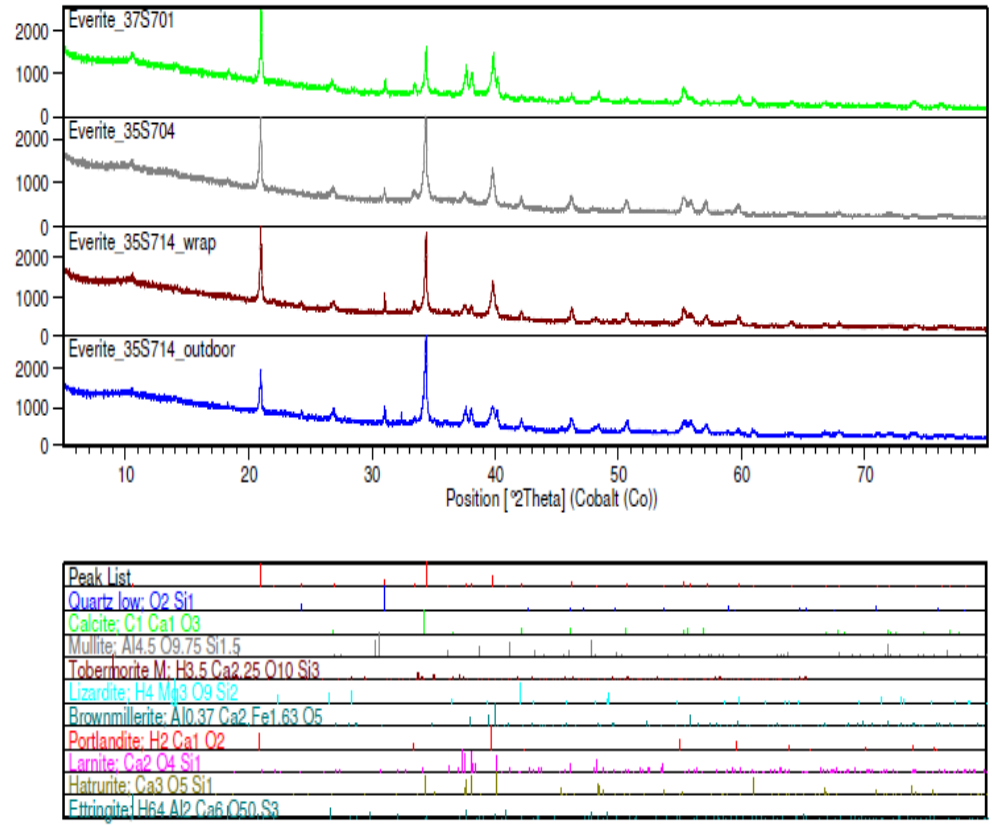


Figure B1: Quantitative XRD spectra ,for batches 37S701, 35S704 and 35S714, of fibrecement sheets incorporated with 3% kaolin, cured under different conditions – indoors unwrapped (green, black), indoors wrapped (brown) and outdoors (blue).

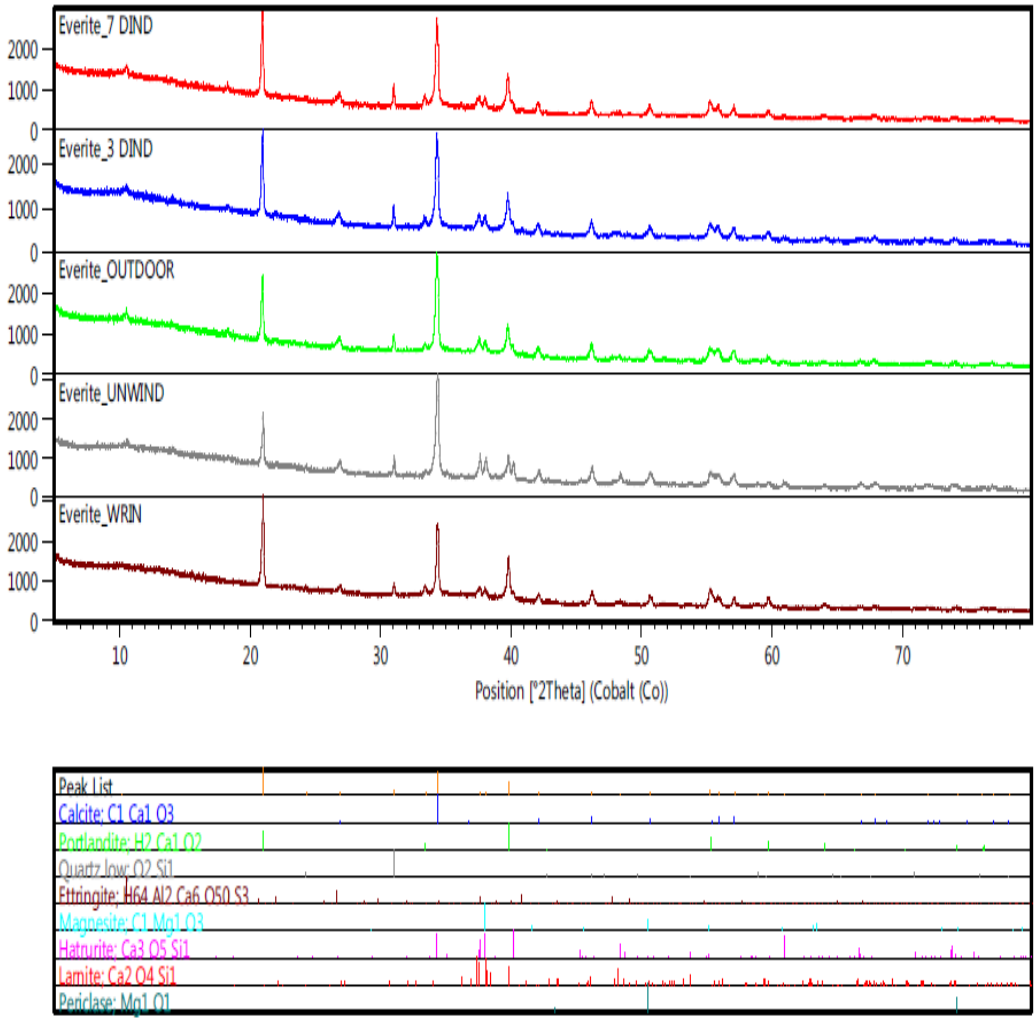


Figure B2: Quantitative XRD spectra for batch 29S705 of fibrecement corrugated sheets cured under various exposure conditions – 7d indoors (red), 3d indoors (blue), unwrapped indoors (black), wrapped indoors (brown) prior to outdoor exposure and outdoor exposure (green).

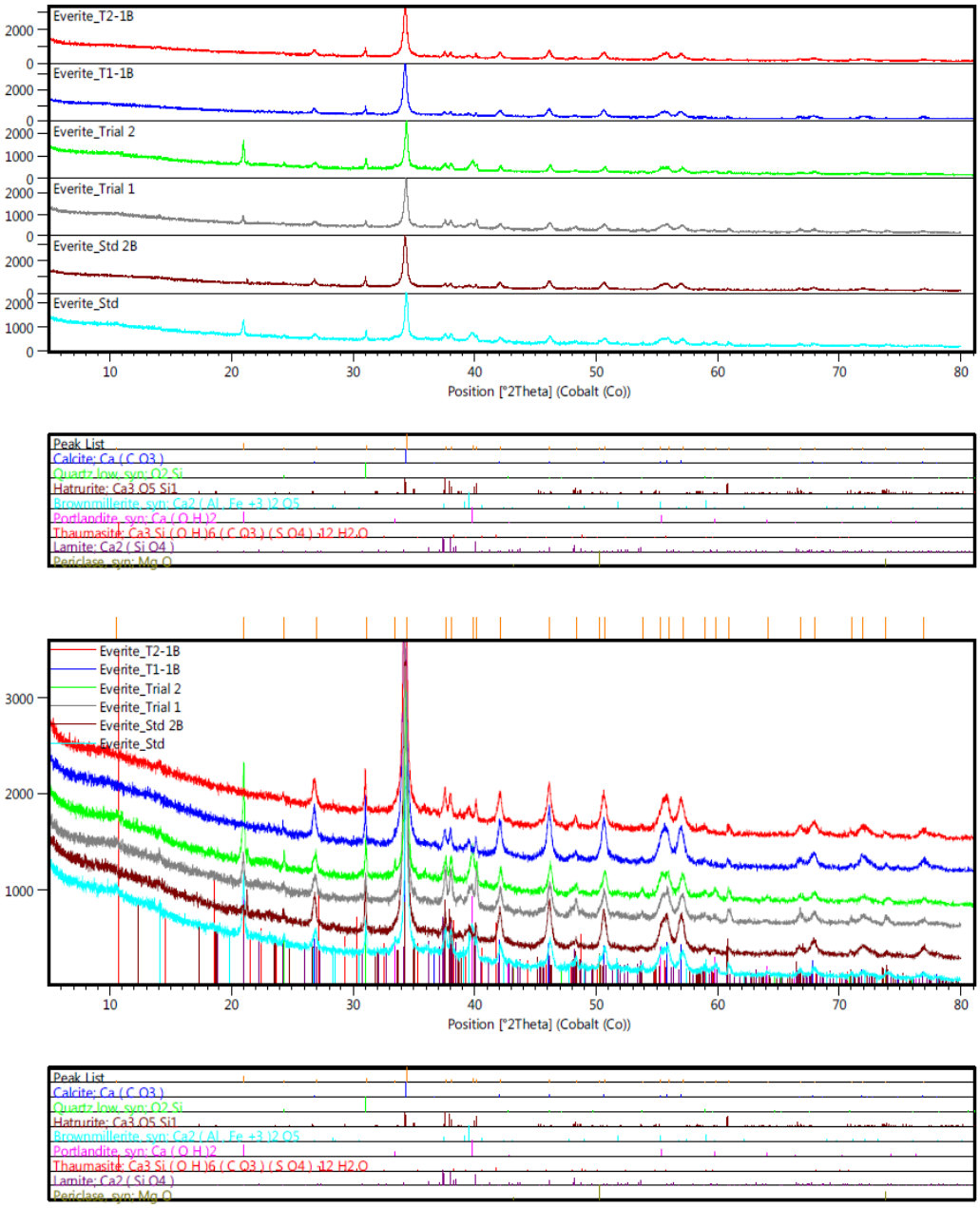
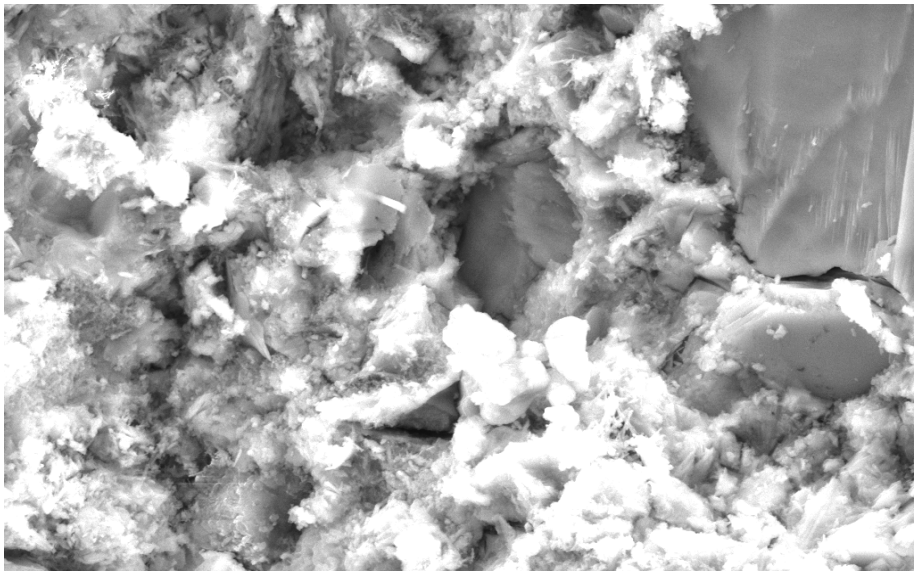


Figure B3: Quantitative XRD spectra of the first production trial of kaolin modified sheets, standard, trial 1 (3% kaolin), trial 2 (5% kaolin), all cured indoors for 14d thereafter outdoor exposure. The spectra with a B label, at the end, were the sheets subjected to accelerated carbonation.

APPENDIX C



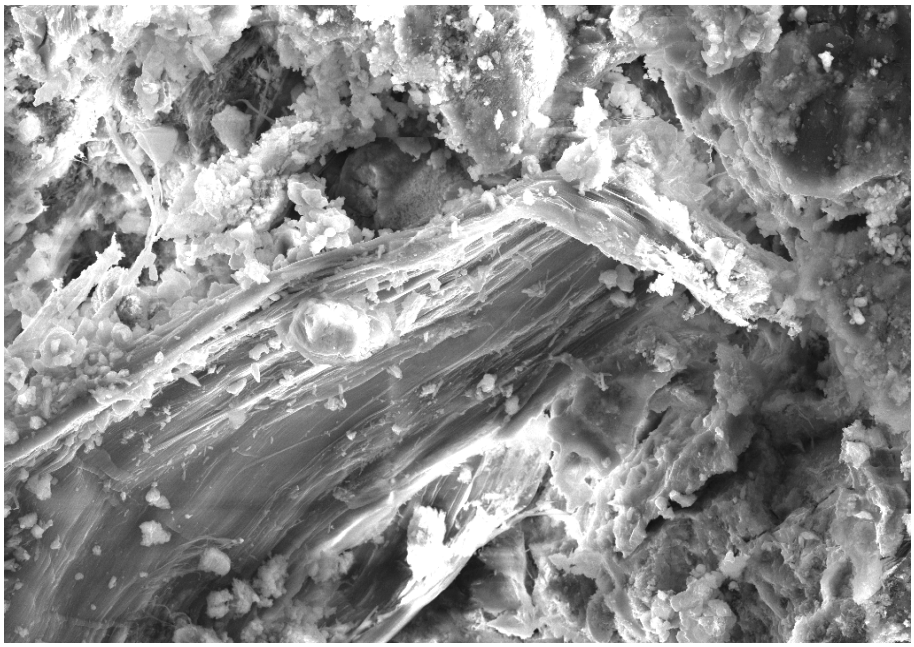
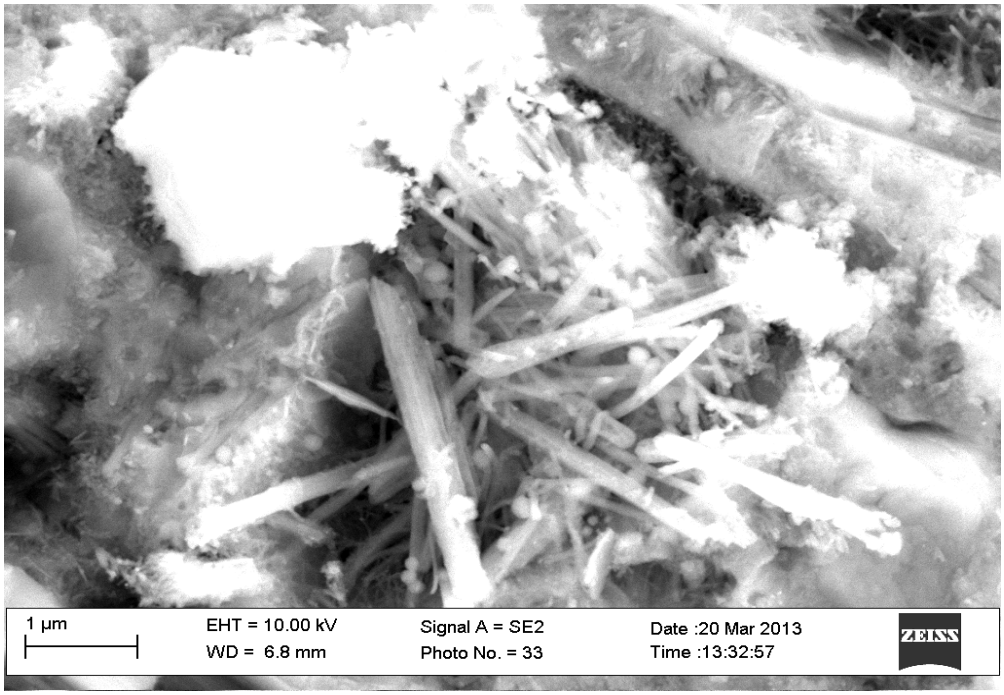


Figure C1: SEM micrographs for the kaolin modified corrugated fibrecement sheets, batch 37S701, stored indoors for 14 d prior to external exposure.



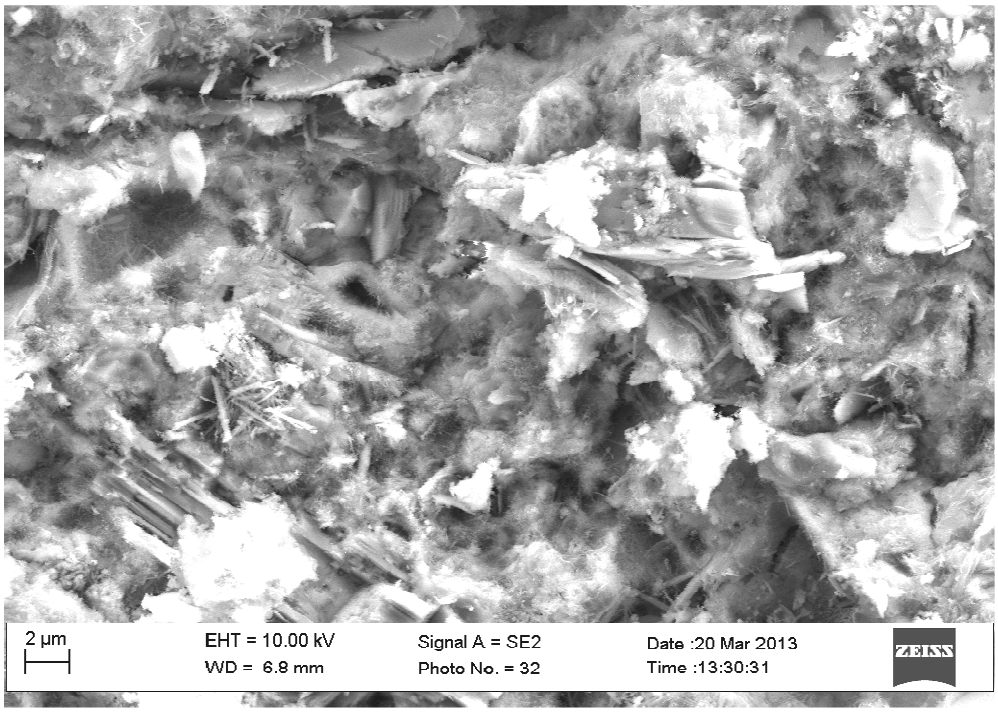
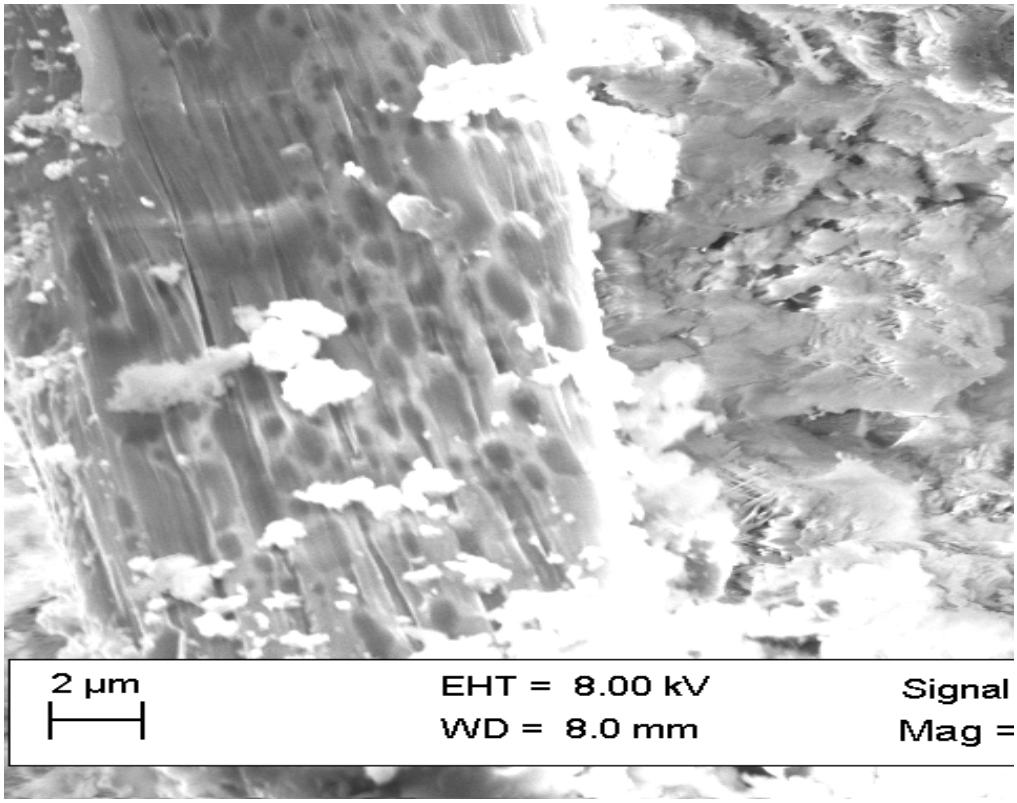


Figure C2: SEM micrographs for kaolin modified fibrecement sheets, production batch 35S704 stored indoors for 14 d before external exposure.



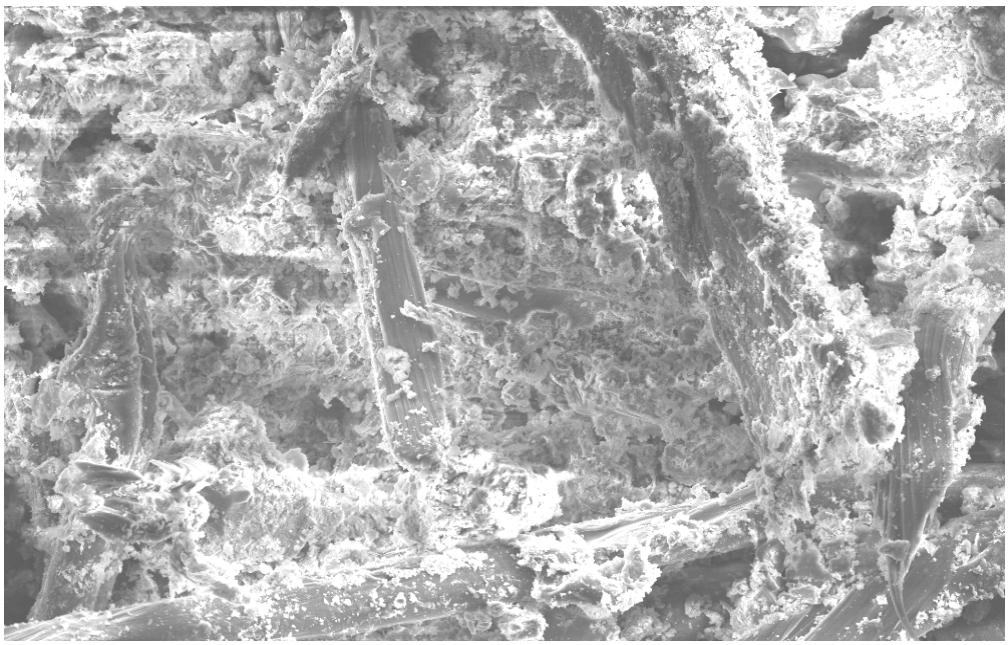


Figure C3: SEM micrographs of kaolin modified fibrecement sheets, batch 35S714 stored indoors unwrapped for 14 d prior to exposure outside.

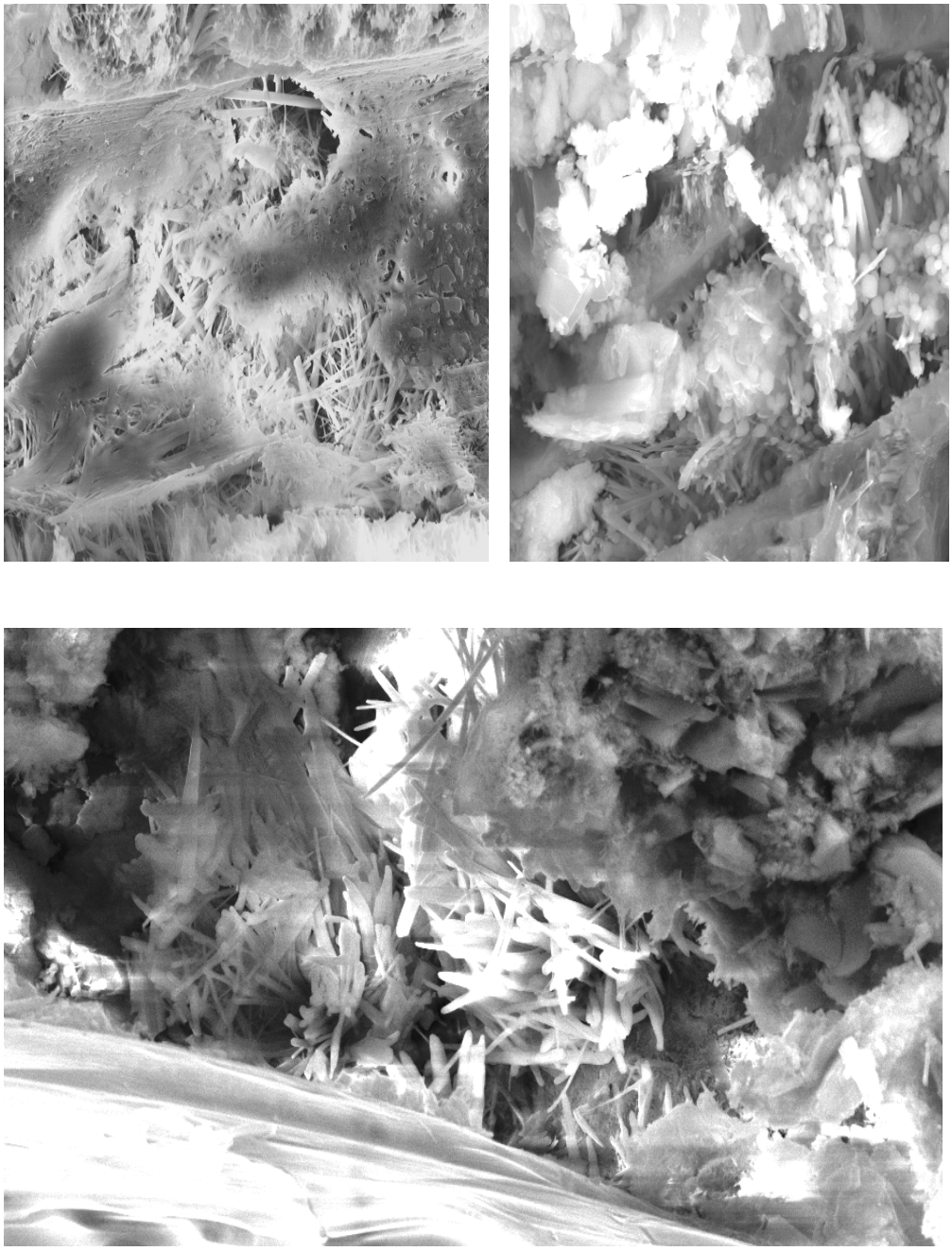


Figure C4: SEM micrographs of kaolin modified corrugated sheets, kept indoors wrapped, batch 35S714 for 14 d prior to exposure to natural environment.

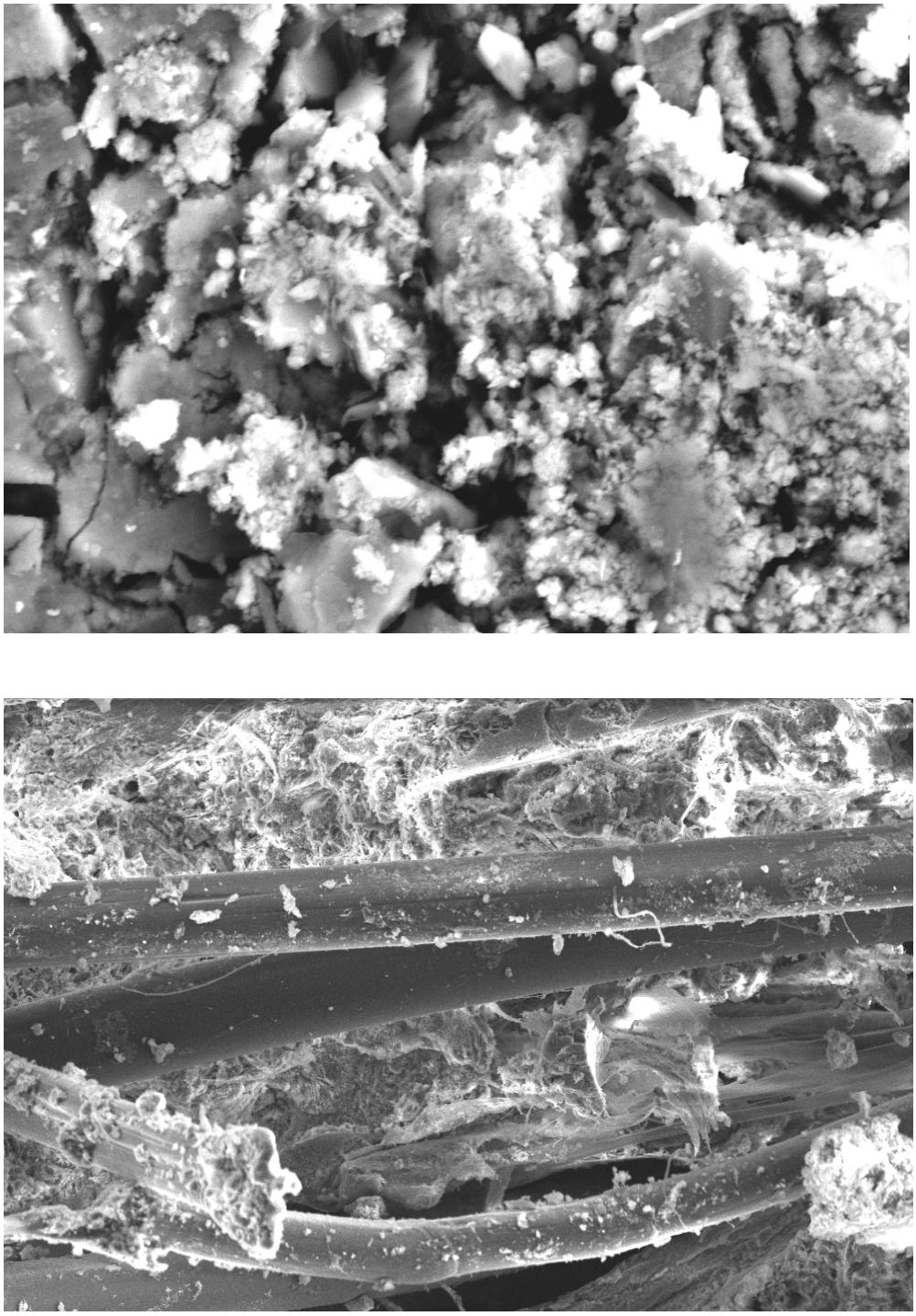


Figure C5: SEM micrographs of kaolin modified corrugated fibrecement sheets, batch 35S714 cured outdoors without wrapping.

REFERENCES

Abdelmouleh, M., Boufi, S., Salah, A., Belgacem, M.N. and Gandini A. (2002). Interaction of silane coupling agents with cellulose. *Langmuir*, vol. 18, pp. 3203 - 3208.

Alshamsi, A.M. (1997). Microsilica and ground granulated blast furnace slag effects on hydration temperature, *Cement and Concrete Research*, vol. 27, no. 12, pp. 1851 – 1859.

Akers, S.A.S and Studinka, J.B. (1989). Ageing behavior of cellulose fibrecement composites in natural weathering and accelerated tests, *International Journal of Cement Composites and Lightweight Concrete*, vol. 11, no. 2, pp. 93 - 97.

Akers, S.A.S. and Partl, M. (1990). Hygral and thermal expansion /shrinkage properties of asbestos-free fibrecement, *Cement and Concrete Composites*, vol. 12, pp. 19 - 27.

Akers, S.A.S. (2006). Cracking in fibrecement products, *Proceedings of the 10th International IBC Conference*, Sao Paulo, Brazil, pp. 59 - 67.

Almeida, A.E.F.S., Tonoli, G.H.D., Santos, S.F. and Savastano Jr., H. (2010). Effects of accelerated carbonation on kraft pulp fibre reinforced cement-based materials, *Proceedings of the 1st TMS-ABM International Materials Congress*, Rio de Janeiro, Brazil.

Antonovich, V. and Goberis, S. (2003). The effect of different admixtures on the properties of refractory concrete with Portland cement, *Materials Science*, vol. 9, pp. 379.

Arizumi, A. (1968). *Proceedings of the Fifth International Symposium of the Chemistry of Cement*, Tokyo, pp. 164 – 165.

Arliguie, G. and Grandet, J. (1991). The deterioration of building materials, *Proceedings of the International Symposium*, IUT, La Rochelle, pp. 245 - 253.

Azarov, G. M., Maiorova, E.V., Oborina, M.A. and Belgakov, A.V. (1995). Wollastonite raw materials and their applications (a review), *Glass and Ceramics*, vol. 52, no. 9, pp. 237 – 240.

Bae, G.Y., Min, B.G., Jeong, Y.G., Lee, S.C., Jang, J.H. and Koo, G.H. (2009). Super hydrophobicity of cotton fabrics treated with silica nanoparticles and water repellent agent, *Journal of Colloid Interface Science*, vol. 337, no. 1, pp. 170 – 175.

Bailey, S.W. (1980). Summary of recommendations of AIPEA nomenclature committee on clay minerals, *American Mineralogy*, vol. 65, pp. 1 – 7.

Balogh, A. (1996). New admixture combats concrete shrinkage, *Aberdeen's Concrete Construction*, vol. 41, no. 7, pp. 546 – 551.

Banthia, N. (1994). Carbon fibrecements: Structure, performance, applications and research needs, *ACI* SP- 142, in: J.I. Daniel, S.P. Shah (Eds.), Fibre reinforced concrete*, ACI Materials Journal*, Detroit, pp. 91 – 119.

Batic, O.R., Milanesi, C.A., Maiza, P.J. and Marfil, S.A. (2000). Secondary ettringite formation in concrete subjected to different curing conditions, *Cement and Concrete Research*, vol. 30, pp. 1407 - 1412.

Bear, F.E. *Chemistry of the soil*, 2nd ed., Reinhold Publishing, New York, 1965.

Belgacem, M.N., Bataille, P. and Sapieha, S. (1994). Effect of corona modification on the mechanical properties of polypropylene/cellulose composites, *Journal of Applied Polymer Science*, vol.53, pp. 397.

Bel-Hassen, R., Boufi, S., Brochier-Salon, M.C., Abdelmouleh, M. and Belgacem, M.N. (2008). Adsorption of silane onto cellulose fibres II. The effect of pH on silane hydrolysis, condensation and adsorption behavior. *Journal of Applied Polymer Science*, vol.108, pp.1958 – 1968.

Bellmann, F. (2004). On the formation of thaumasite, Part II, *Advances in Cement Research*, vol. 16, pp. 89 – 94.

Bentur, A. (2003). Early-age cracking in cementitious systems. *RILEM* Technical Committee181 – EAS: Early-age shrinkage induced stresses and cracking in cementitious systems, *RILEM*, Report 25, pp. 335.

Bentur, A. and Akers, S.A.S. (1989). The microstructure and ageing of cellulose fibre reinforced cement composites cured in a normal environment, *International Journal of Cement Composites and Lightweight Concrete*, vol. 11, no. 2, pp. 99 - 109.

Bentur, A. and Mindess, S. (1990). Fibre reinforced cementitious composites, *Elsevier Applied Science*, U.K., pp. 449.

Bentz, D.P., Geiker, M.R. and Hansen, K.K. (2001). Shrinkage reducing admixtures and early age desiccation in cement pastes and mortars, *Cement and Concrete Research*, vol.31, no. 7, pp. 1075 – 1085.

Bentz, D.P. and Jensen, O.M. (2004). Mitigation strategies for autogenous shrinkage cracking, *Cement and Concrete Composites*, vol. 26, no. 6, pp. 677 – 685.

Bentz, D.P. and Peltz, M.A. (2008). Reducing thermal and autogenous shrinkage contributions to early-age cracking, *ACI Materials Journal*, vol. 105, no. 4, pp. 414 – 420.

Berhane, Z. (1987). Durability of mortar roofing sheets reinforced with natural fibre, *Symposium on Building Materials for low income housing*, Bangkok: Thailand, pp. 321 – 327.

Berhane, Z. (1994). Performance of natural fibre reinforced mortar roofing tiles, *Materials and Structures*, vol. 27, pp. 347 – 352.

Bernard, J.H. and Rost, R. *Encyclopaedic knowledge of minerals* (in Czech), 1st ed., Academia, Prague, 1992.

Betterman, L.R., Ouyang, C. and Shar, S.P. (1995). Fibre-matrix interaction in micro fibre-reinforced mortar, *Journal of Advanced Cement Based Materials*, vol. 2, pp. 53 - 61.

Bezerra, E.M., Joaquim, A.P., Savastano Jr., H., John. V.M. and Agopyan, V. (2006). The effect of different mineral additions and synthetic fibre contents on properties of cement based composites, *Cement and Concrete Composites*, vol. 28, pp. 555 – 563.

Bish, D.L. (1993). Rietveld refinement of kaolinite structure at 1.5 K, *Clays and Clay Minerals*, vol. 41, pp. 738 – 744.

Bish, D.L. and Howard, S.A. (1988). Quantitative phase analysis using the Rietveld method, *Journal of Applied Crystallography*, vol. 21, pp.86 – 91.

Blanco, A., Fuente, E., Sanchez, L.M., Alonso, A., Tijero, J. and Negro, C. (2006). Optimal use of flocculants on the manufacture of fibrecement materials by the Hatschek process, *International Inorganic Bonded Fibre Composites Conference*, Brazil, pp. 145 – 155.

Botaro, V.R. and Gandini, A. *Cellulose*, vol. 5, 1998, pp.14.

Brindley, G.W. and Robinson, K. (1946). The structure of kaolinite, *Mining Magazine*, vol. 27, pp. 242.

Brochier-Salon, M.C., Bardet, M. and Belgacem, M.N. (2008). Solvolysis – hydrolysis of N-bearing alkoxysilanes: Reactions studied with 29SiMNR, *Silicon Chemistry*, vol.3, pp. 335-350.

Brooks, J.J., Megat Johari, M.A. and Mazloom, M. (2000). Effects of admixtures on the setting times of high strength concrete, *Cement and Concrete Composites*, vol. 22, no. 4, pp. 293 – 301.

Brooks, J.J. and Megat-Johari, M.A. (2001). Effect of metakaolin on creep and shrinkage of concrete, *Cement and Concrete Composites*, vol. 23, no. 6, pp. 495 – 502.

Buchmayer, K. (1999). Plant layout and startup of fibrecement manufacturing plants, in: Moslemi, A.A. (ed.), *Inorganic-bonded Wood and Fibre Composite Materials*, vol. 6, pp. 99 – 140.

Cabrera, J. and Frias, M. (2001). Mechanism of hydration of the metakaolin-lime-water system, *Cement and Concrete Research*, vol. 31, pp. 177 – 182.

Chan, Y.W. and Li, V.C. (1997). Age effect on the characteristics of fibre/cement interfacial properties, *Journal of Materials Science*, vol.32, no.19, pp. 5287 - 5292.

Chen, P.W. and Chung, D.D.L. (1993). Concrete reinforced with up to 0.2 vol % of short carbon fibres, *Composites*, vol. 24, no. 1, pp. 33 – 52.

Chen, P.W. and Chung, D.D.L. (1996). Low drying shrinkage concrete containing carbon fibres, *Composites*, vol. 27B, pp. 269 – 274.

Chen, P.W., Fu, X. and Chung, D.D.L. (1997). Microstructural and mechanical effects of latex, methyl cellulose and silica fume on carbon fibre reinforced cement, *ACI Materials Journal*, vol. 94, no. 2, pp. 146 – 155.

Chen, X.T., Zou, R.Z. and Chen, X.R. (1994). Kinetic-study of ettringite carbonation reaction, *Cement and Concrete Research*, vol. 27, no. 7, pp. 1383 – 1389.

Cheng-Yi, H. and Feldman, R.F. (1985). Hydration reactions in Portland cement-silica fume blends, *Cement and Concrete Research*, vol.15, pp. 585 - 595.

Clarke, A.R. *Microscopy techniques for materials science*, CRC Press, 2002.

Cohen, M.D. (1990). A look at silica fume and its actions in Portland cement concrete, *The Indian Concrete Journal*, vol. 64, no. 9, pp. 429 – 438.

Cole, W.F. and Kroone, B. (1960). Carbon dioxide in hydrated Portland cement, *JL56-56*, vol. 56, no. 6, pp. 1275 - 1296.

Cooke, T. Formation of films on Hatschek machines, Building Materials and Technology Pty Ltd, Australia.

Coutts, R.S.P. and Ridikas, V. (1982). Refined wood fibrecement products, *Appita*, vol. 35, no. 5, pp. 395 – 400.

D'Ambroisa, M.D. (2002). Early-age tensile creep and shrinkage of concrete with shrinkage reducing admixtures, *M.S. Thesis*, University of Illinois at Urbana-Campaign.

Diamond, S., White, J. and Dolch, W. (1964). Clay and Clays Minerals, *Proceedings of the 12th Conference*, Pergamon Press, New York, pp. 372 – 382.

Dias, C.M.R., Cincotto, M.A., Savastano Jr., H. and John, V.M. (2008). Long-term aging of fibrecement corrugated sheets – The effect of carbonation, leaching and acid rain, *Cement and Concrete Composites*, vol. 30, pp. 255 - 265.

Donchev, I., Ninov, J., Doykov, I., Petrova, N. and Dimova, L. (2010). On the formation of cement phases in the course of interaction of kaolinite with portlandite, *Journal of the University of Chemical Technology and Metallurgy*, vol. 45, no. 4, pp. 391 – 396.

Duda, R., Rejl, L. and Slivka, *D. Minerals* (in Czech), Aventinum, Prague, 1990.

Egerton, R.F. *Physical principles of electron microscopy: an introduction to TEM, SEM and AEM*, Springer, 2005.

El-Ashkar, N.H., Mohr, B.J., Nanko, H. and Kurtis, K.E. (2002). Durability of pulp fibrecement composites to wet/dry cycling, in: Anson, M., Ko, J.M., Lam, E.S.S. (Eds.), *Proceedings of the International Conference on Advances in Building Technology*, Elsevier, Oxford, pp. 233-237.

Esping, O. (2007). Early-age properties of self-compacting concrete – Effects of fine aggregate and limestone filler, *PhD Thesis*, Department of Civil and Environmental Engineering, Chalmers University of technology, Sweden.

Fabbri, A., Corvisier, J., Schubnel, A., Brunet, F., Goffe, B., Rimmele, G. and Barlet-Gouedard, V. (2009). Effects of carbonation on the hydro-mechanical properties of Portland cements, *Cement and Concrete Research*, vol. 39, pp.1156 - 1163.

Fan, M.Z., Bonfield, P.W., Dinwoodie, J.M. and Breese, M.C. (1999). Dimensional instability of cement-bonded particleboard: Mechanisms of deformation of CBPB, *Cement and Concrete Research*, vol. 29, pp. 923 – 932.

Fan, M.Z., Bonfield, P.W., Dinwoodie, J.M., Boxall, J. and Breese, M.C. (2004). Dimensional instability of cement-bonded particleboard: The effect of surface coating, *Cement and Concrete Research*, vol. 34, pp. 1189 – 1197.

Fiorelli, J., Dos Santos, S.F., Donizete, P., Cabral, M.R., De Freitas, Z.D. and Savastano Jr., H. (2012). Development of hybrid fibrecement corrugated sheets: a case study of edge cracks, *International Inorganic Bonded Fibre Composites Conference*, Canberra, Australia, pp. 181 - 187.

Flatt, R.J. and Houst, Y. (2001). A simplified view on chemical effects perturbing the action of superplasticizers, *Cement and Concrete Research*, vol. 31, no. 8, pp. 1169 – 1176.

Folliard, K.J. and Berke, N.S. (1997). Properties of High-performance concrete containing shrinkage reducing admixture, *Cement and Concrete Research*, vol. 27, no. 9, pp. 1357 – 1364.

Frias, M. and Cabrera, J. (1996). Pore size distribution of metakaolin paste, *Cement and Concrete Research*, vol. 26, pp. 1545 - 1553.

Frias, M.P. and Cabrera, J. (2002). The effect of temperature on the hydration rate and stability of the hydration phases of metakaolin-lime-water systems, *Cement and Concrete Research*, vol. 32, pp. 133 - 138.

Frost, R.L. (1998). Hydroxy deformation in kaolin, *Clays and Clay Minerals*, vol. 46, no. 3, pp. 280 – 289.

Fu, X. and Chung, D.D.L. (1998). Improving the bond strength of concrete to reinforcement by adding methyl cellulose to concrete, *ACI Materials Journal*, vol. 95, no. 5, pp. 601 – 608.

Gandini, A., Botaro, V., Zeno, E. and Bach, S. (2001). Activation of solid polymer surfaces with bifunctional reagents, *Polymer International*, vol. 50, pp.7.

Gaze, M.E. (1997). The effects of varying gypsum content on thaumasite formation in cement: lime: sand mortar at 5^0C, *Cement and Concrete Research*, vol. 27, no. 2, pp. 259 – 265.

Gleize, P.J.P., Cyr, M. and Escadeilas, G. (2007). Effects of metakaolin on autogenous shrinkage of cement pastes, *Cement and Concrete Composites*, vol. 29, no. 2, pp. 80 – 87.

Glisic, B. and Inaudi, D. (2006). Monitoring early and very early age deformation of concrete using fibre optic sensors, *Proceedings of the 2nd International Congress*, Naples, Italy, pp. 17 - 26.

Glover, S.M., Yan, Y.D., Jameson, G.J. and Biggs, S. (2001). Polymer molecular weight and mixing effects on flock compressibility and filterability, *6th World Congress of Chemical Engineering*, Melbourne, pp. 23 – 27.

Goldman, A. and Bentur, A. (1989). Bond effects in high strength silica fume concretes, *ACI Materials Journal*, vol. 86, no. 5, pp. 440 – 447.

Goldstein, J. *Scanning electron microscopy and X-ray microanalysis*, Kluwer Academic / Plenum Publishers, 2003.

Gollop, R.S. and Taylor, H.F.W. (2005). Microstructural and micro analytical studies of sulfate attack – I. Ordinary Portland cement paste, *Cement and Concrete Research*, vol. 35, pp. 2333 - 2339.

Gram, H.E. (1983). Durability of natural fibres in concrete, *Swedish Cement and Concrete Research Institute*, Research Forum, vol. 1, no. 83, pp. 225.

Grasley, Z.C. (2003). Internal relative humidity, drying stress gradients and hygrothermal dilation of concrete, *M.S. Thesis*, University of Illinois at Urbana-Champagne.

Gruber, K.A., Ramlochan, T, Boddy, A., Hooton, R.D. and Thomas, M.D.A. (2001). Increasing concrete durability with high reactivity metakaolin, *Cement and Concrete Composites*, vol. 23, pp. 479 – 484.

Gruner, J.W. (1932). The crystal structure of kaolinite, *Z. Krist*., vol. 83, pp. 75 – 88.

Hammer, T.A. and Fossa, K.T. (2006). Influence of entrained air voids on pore water pressure and volume change of concrete before and during setting, *Materials and Structures*, vol. 39, no. 9, pp. 801 – 808.

Haque, M.N. (1996). Strength development and drying shrinkage of high strength concretes, *Cement and Concrete Composites*, vol. 18, no. 5, pp. 333 – 342.

He, Z., Li, Z.J., Chen, M.Z. and Liang, W.Q. (2006). Properties of shrinkage-reducing admixture-modified pastes and mortar, *Materials and Structures*, vol. 39, no. 4, pp. 445 – 453.

Holt, E.E. (2001a). Early-age autogenous shrinkage of concrete, *PhD Thesis*, University of Washington, United States.

Holt, E.E. (2001b). Early-age autogenous shrinkage of concrete, Espoo 2001, Technical Research Centre of Finland, *VTT Publications*, vol. 446, pp. 184.

Holt, E.E. (2005). Contribution of mixture design to chemical and autogenous shrinkage of concrete at early-ages, *Cement and Concrete Research*, vol. 35, no. 3, pp. 464 – 472.

Holt, E. and Leivo, M. (2004). Cracking risks associated with early-age shrinkage, *Cement and Concrete Composites*, vol. 26, no. 5, pp. 521 – 530.

Hooton, R.D. and Thomas, M.D.A (2002). The use of lime in Portland cements: Effect of thaumasite form of sulphate attack, Portland Cement Association.

Huo, X.S. and Wong, L.U. (2006). Experimental study of early-age behavior of high performance concrete deck slabs under different curing methods, *Construction and Building Materials*, vol. 20, no. 10, pp. 1049 – 1056.

John, V.M., Agopyan, V. and Prado, T.A. (1998). Durability of cement composites and vegetable fibres for roofing, *Proceedings of 3rd Ibero-American Symposium on roofing for housing*, Sao Paulo, pp. 51 – 59.

John, V.M., Cincotto, M.A., Sjostrom, C., Agopyan, V. and Oliveira, C.T.A. (2005). Durability of slag mortar reinforced with coconut fibre, *Cement Concrete Composites*, vol. 27, pp. 565 - 574.

Johnson, R.M. and Melling, E.M. (1983). *US Patent*, no.4, 377, pp. 415.

Jones, F.R. *Interfacial phenomena in composite materials*, Butterworths: London, 1989.

Justice, J.M. and Kurtis, K.E. (2007). Influence of metakaolin surface area on properties of cement-based materials, *ASCE Journal of Materials in Civil Engineering*, vol. 19, no. 9, pp. 762 – 771.

Justice, J.M., Kennison, L.H., Mohr, B.J., Beckwith, S.L., McCormick, L.E., Wiggins, B., Zhang, Z.Z. and Kurtis, K.E. (2005). Comparison of two metakaolins and silica fume used as supplementary cementitious materials, *Seventh International Symposium on Utilization of High-Strength/High performance concrete*, Ed. Russell, H.G., Publication SP-228, American Concrete Institute, Farmington Hills, MI, vol. 1, pp. 213 – 236.

Kalbskopf, R., De Lhoneux, B., Van der Heyden, L. and Alderweireldt, L. (2002). Durability of fibrecement roofing products, *8th International Inorganic Bonded Fibre Composites Conference*, Sun Valley, Idaho.

Kamimura, K., Sereda, P.J. and Swenson, E.G. (1965). Changes in weight and dimensions in the drying and carbonation of Portland cement mortars, *Magazine of Concrete Research*, vol.17, no.50, pp.5 - 14.

Khan, A.A. (1995). Concrete properties and thermal stress analysis of members at early-ages, *PhD Thesis*, McGrill University, Canada.

Khatib, J.M. and Wild, S. (1998). Sulphate resistance of metakaolin mortar, *Cement and Concrete Research*, vol. 28, no. 1, pp. 83 – 92.

Khedar, S.F. and Abou-Zeid, M.N. (1994). Characteristics of silica fume concrete, *Journal of Materials in Civil Engineering*, vol. 6, no. 3, pp. 357 – 375.

Klein, C. and Hurlbut, C.S. *Manual of Mineralogy*, 21st ed., John Wiley and sons, Incl., New York, 1993, pp. 681.

Kinuthia, J.M., Wild, S., Sabir, B.B. and Bai, J. (2000). Self-compensating autogenous shrinkage in Portland cement-metakaolin-fly ash pastes, *Advances in Cement Research*, vol. 12, no.1, pp. 35 – 43.

Klemm, D., Phillip, B. and Heinze, T. Comprehensive Cellulose Chemistry: Fundamentals and Analytical methods, Wiley-VCH Verlag GmbH, Weinheim, vol. 1, pp. 9 – 31, 43 – 60 (1998).

Kokta, B., Maldas, D. and Beland, P. (1990a). The influence of coupling agents on mechanical properties of composites, *Journal of Vinyl Technology*, vol. 12, pp. 146.

Kokta, B., Maldas, D., Daneault, C. and Beland, P. (1990b). Composites of polyvinyl chloride-wood fibres, effect of silane as coupling agent, *Journal of Vinyl Technology*, vol. 12, no. 13, pp. 146 – 153.

Kronlof, A., Leivo, M. and Sipari, P. (1995). Experimental study on the basic phenomena of shrinkage and cracking of fresh mortar, *Cement and Concrete Research*, vol. 25, no. 8, pp. 1747 – 1754.

Lange, F., Mortel, H. and Rudert, V. (1997). Dense packing of cement pastes and resulting consequences on mortar properties, *Cement and Concrete Research*, vol.27, no.10, pp. 1481 - 1488.

Law, C.M. (2004). Effect of water reducing admixtures on the resistance of concrete to chloride ion penetration, *Final year thesis*, Department of Civil Engineering, National University of Singapore.

Lawler, J.S., Zampini, D. and Shah, S.P. (2005). Microfibre and macro fibre hybrid reinforced concrete, *Journal of Materials in Civil Engineering*, vol.17, no.5, pp. 595 - 604.

Lea, F.M. *The chemistry of cement and concrete*, 2nd Ed., Edward Arnold, London, 1970.

Lecomte, J-P. (2012). Use of silicone resin as Integral water repellent for mortar and fibre reinforced cement boards, *International Inorganic Bonded Fibre Composites Conference*, Canberra, Australia, pp. 199 - 210.

Lee, K., Lee, K.M. and Kim, B.K. (2003). Autogenous shrinkage of high performance concrete containing fly ash, *Magazine of Concrete Research*, vol. 55, no. 6, pp. 1268 – 1278.

Lee, Y., Yi, S.T., Kim, M.S. and Kim, J.K. (2006). Evaluation of basic creep model with respect to autogenous shrinkage, *Cement and Concrete Research*, vol. 36, no. 7, pp. 1268 – 1278.

Leung, C.K.Y. (1996). Design criteria for pseudo ductile fibre-reinforced composites, *Journal of Engineering Mechanics*, ASCE, vol. 122, no. 1, pp. 10 – 18.

Li, V.C. and Leung, C.K.Y. (1992). Tensile failure modes of random discontinuous fibre reinforced brittle matrix composites, *Journal of Engineering Mechanics*, ASCE, vol. 118, no. 11, pp. 246 – 264.

Li, V.C. and Wu, H.C. (1992a). Micromechanics based design for pseudo strain-hardening in cementitious composites, *Proceedings of 9th ASCE Conference on Engineering Mechanics*, L.D. Lutes and J.M. Niedzwecki, eds., Reston, Va., pp. 740 – 743.

Li, V.C. and Wu, H.C. (1992b). Conditions for pseudo strain hardening in fibre reinforced brittle matrix composites, *Applied Mechanics Review*, vol. 45, pp. 390 – 398.

Lim, S.N. and Wee, T.H. (2000). Autogenous shrinkage of ground-granulated blast-furnace slag concrete, *ACI Materials Journal*, vol. 97, no. 5, pp. 587 – 593.

Lin, S., Huang, R. and Weng, (2012). T. Effect of water soluble polymer and fibre on the early-age shrinkage cracking of cementitious composites, *Journal of Marine Science and Technology*, vol. 20, no. 3, pp. 295 – 303.

Low, N.M.P. and Beaudoin, J.J. (1993). Flexural strength and microstructure of cement binders reinforced with wollastonite microfibres, *Cement and Concrete Research*, vol.23, no.4, pp. 905 - 916.

Low, N.M.P. and Beaudoin, J.J. (1992). Mechanical properties of high performance cement binders reinforced with wollastonite microfibres, *Cement and Concrete Research*, vol.22, no.5, pp. 981 - 989.

Low, N.M.P. and Beaudoin, J.J. (1994b). Stability of Portland cement-based binders reinforced with wollastonite microfibres, *Cement and Concrete Research*, vol.24, no.5, pp. 874 - 884.

Low, N.M.P. and Beaudoin, J.J. (1994a). The flexural toughness and ductility of Portland cement-based binders reinforced with wollastonite microfibres, *Cement and Concrete Research*, vol.24, no.2, pp. 250 - 258.

Lura, P., Jensen, O.M. and Van Breugel, K. (2003). Autogenous shrinkage in high-performance cement paste: An evaluation of basic mechanisms, *Cement and Concrete Research*, vol. 33, no. 2, pp. 223 – 232.

Lura, P., Pease, B., Mazzotta, G., Rajabipour, F. and Weiss, J. (2007). Influence of shrinkage reducing admixtures on the development of plastic shrinkage cracks, *ACI Materials Journal*, vol. 104, no. 2, pp. 187 – 194.

Maholtra, V.M. *Superplasticizers in concrete*, Canada Center for Mineral and Energy Technology, Ottawa, Canada, 1978.

Malmros, G. and Thomas, J.D. (1977). Least squares structure refinement based on powder film intensity data, *Journal of Applied Crystallography*, vol. 10, pp. 107 – 111.

Mangat, P.S. and Azari, M.M. (1984). A theory for the free shrinkage of steel fibre reinforced cement matrices, *Journal of Materials Science*, vol.19, no.7, pp. 2183 - 2194.

Manns, W. and Wesche, K. (1969). Variation in strength of mortars made of different cements due to carbonation, *Proceedings of the international symposium on the chemistry of cement*, Part III, pp. 385 - 393.

Mathur, R., Misra, A.K. and Goel, P. (2007). Influence of wollastonite on mechanical properties of concrete, *Journal of Scientific and Industrial Research*, vol.66, no.12, pp.1029 - 1034.

McCormick, L. (2007). Metakaolin, Dr Kim Kurtis, *CEE 8813*, pp. 1 – 28.

McCullough, B.F. and Rasmussen, R.O. (1999). Fast track paving: concrete temperature control and traffic opening criteria for bonded concrete overlays, Federal Highway Administration, Washington D.C., *Report FHWA RD 98* – 167, pp. 191.

Mehta, P.K. (1987). Natural pozzolans: Supplementary cementing materials for concrete, CANMET-SP-86-8E, *Canadian Government Publishing Centre*, Supply and Services, Ottawa, Canada, K1A059.

Mehta, P.K. (1994). Volume change. Significance of tests and properties of concrete and concrete-making materials, STP 169C, *American Standards Testing Methods*, West Conshohocken, Pa., pp. 222.

Mihashi, H. and Leite, J.P. (2004). State-of-the-art report on control of cracking in early-age concrete, *Journal of Advanced Concrete Technology*, vol. 2, no. 2, pp. 141 – 154.

Mikail, R.S. and Youssef, A.M. (1974). Studies on fibre-reinforced Portland cement pastes. *Cement and Concrete Research*, no.4, pp.869 - 880.

Mindess, S. and Young, J.F. *Concrete*, Prentice-Hall Inc., Englewood Cliffs, N.J., pp. 488, 1981.

Mitchell, J.K. *Fundamentals of soil behavior*, 2nd Edition, John Wiley and Sons, NY, 1993.

Mohr, B.J, Nanko, H. and Kurtis, K.E. (2005a). Durability of kraft pulp fibrecement composites to wet-dry cycling, *Cement and Concrete Composites*, vol. 27, no. 5, pp. 435 - 448.

Mohr, B.J, Nanko, H. and Kurtis, K.E. (2005b). Durability of thermo mechanical fibrecement composites to wet-dry cycling, *Cement and Concrete Research*, vol. 35, no. 8, pp. 1646 - 1649.

Mohr, B.J., Biernacki, J.J. and Kurtis, K.E. (2006). Microstructural and chemical effects of wet/dry cycling on pulp fibrecement composites, *Cement and Concrete Research*, vol. 36, pp. 1240 - 1251.

Mohr, B.J., Biernacki, J.J. and Kurtis, K.E. (2007). Supplementary cementitious materials for mitigating degradation of kraft pulp fibrecement composites, *Cement and Concrete Research*, vol. 37, pp. 1531 - 1543.

Mollah, M.Y.A., Adams, W.J., Schennach, R. and Cocke, D.L. (2000). A review of cement-superplasticiser interactions and their models, *Advanced Cement Research*, vol. 12, no. 4, pp. 153 – 161.

Morton, W.E. and Hearle, J.W.S. *Physical properties of textile of textile fibres*, The Textile Institute Butterworths, Manchester, 1962, pp. 214 – 215.

Nasser, M.S. and James, A.E. (2006). The effect of polyacrylamide charge density and molecular weight on the flocculation and sedimentation behavior of kaolinite suspensions, *Separation Purification Technology*, vol. 52, pp. 241 – 252.

Neville, A.M. *Properties of concrete*, 4th Edition, Wiley, New York: John Wiley and sons, 1996, pp. 302 - 304.

Neville, A.M. *Properties of concrete*, 2005.

Ninov, J., Donchev, I. and Dimova, L. (2010). On the kinetics of pozzolanic reaction in the system kaolin-lime-water, *Journal of Thermal Analysis and Calorimetry*, vol. 101, pp. 107 – 112.

Nita, C., John, M., Dias, C.M.R., Savastano Jr., H. and Takeashi, M.S. (2004). Effect of metakaolin on the performance of PVA and cellulose fibres reinforced cement, Proceedings of the 9th *International Inorganic Bonded Fibre Composites Conference*, pp. 1 - 48.

Nmai, C.K., Tomita, R., Hondo, F. and Buffenbarger, J. (1998). Shrinkage reduction admixtures, *Concrete International*, vol. 20, no. 4, pp. 31 – 37.

Norman, M.P.L. (1993) Flexural strength and microstructure of cement binders reinforced with wollastonite microfibres, *Cement and Concrete Research*, vol. 23, pp. 905 - 916.

Ohama, Y. (1989). Carbon-cement composites, *Carbon*, vol. 27, no. 5, pp. 729 – 737.

Oluokun, F.A., Burdette, E.G. and Deatherage, J.H. (1990). Early-age concrete: strength prediction by maturity – another look, *ACI Materials Journal*, vol. 87, no. 6, pp. 565 – 572.

Pane, I. and Hansen, W. (2002). Early-age creep and stress relaxation of concrete containing blended cements, *Materials and Structures*, vol.35, no. 2, pp. 92 – 96.

Pane, I. and Hansen, W. (2005). Investigation of blended cement hydration by isothermal calorimetry and thermal analysis, *Cement and Concrete Research*, vol. 35, no. 6, pp. 1155 – 1164.

Paquet, O. (2010). Cellulose surface modification with organosilanes, *LPG2*, pp. 48 – 52.

Park, S.B. and Lee, B.I. (1993). Mechanical properties of carbon-fibre-reinforced polymer-impregnated cement composites, *Cement and Concrete Composites*, vol. 15, no. 3, pp. 153 – 163.

Persson, H. and Skarendahl, A. (1980). Sisal-fibre concrete for roofing sheets and other purposes, appropriate industrial technology for construction and building materials, New York: United Nations, *Monographs on Propriety Industrial Technical no. 12*.

Peter, M.A., Meier, S.A. and Bohm, M. (2008). Competition of several carbonation reactions in concrete: A parameter study, *Cement and Concrete Research*, vol. 38, pp. 1385 - 1393.

Philleo, R.E. Freezing and thawing resistance of high strength concrete, *NCHRP Synthesis of highway practice 129: TRB*, National Research Council, Washington, D.C., 1986.

Plueddemann, E.P. *Silane coupling agents*, Springer, 1990.

Poon, C.S., Kou, S.C. and Lam, L. (2006). Flexural strength, chloride diffusivity and pore structure of high performance metakaolin and silica fume concrete, *Construction and Building Material*, vol. 20, pp. 858 – 865.

Post J.E. and Bish, D.L. (1989). Rietveld refinement of crystal structures using powder X-ray diffraction data, *Mineralogical Society of America Reviews in Mineralogy*, vol. 20, pp. 277 – 308.

Powers, T.C. (1962). A hypothesis on carbonation shrinkage, *Journal of the Portland Cement Association Research & Development Laboratories*, pp. 40 - 50.

Rajabipour, F., Sant, G. and Weiss, J. (2008). Interaction between shrinkage reducing admixtures (SRA) and cement paste's pore solution, *Cement and Concrete Research*, vol. 38, no. 5, pp. 606 – 615.

Ramlochan, T., Thomas, M. and Gruber, K.A. (2000). The effect of metakaolin on alkali-silica reaction in concrete, *Cement and Concrete Research*, vol. 30, pp. 339 – 344.

Ransinchung, G.D. and Kumar, B. (2010). Investigation on paste and mortars of ordinary Portland cement admixed with wollastonite and micro silica, *Journal of Materials in Civil Engineering*, vol. 22, no. 4, pp. 305 – 313.

Rathod, J.D. and Patodi, S.C. (2010). Interface tailoring of polyester-type fibre in engineered cementitious composite matrix against pullout, *ACI Materials Journal*, vol. 107, no. 2, pp. 114 – 122.

Ray, D.T. and Hogg, R. (1987). Agglomerate breakage in polymer flocculated suspensions, *Journal of Colloid Interface Science*, vol. 116, pp. 256 – 268.

Reimer, L. *Scanning electron microscopy: physics of image formation and microanalysis*, Springer, 1998.

Rietveld, H.. (1969). A profile refinement method for nuclear and magnetic structures, *Journal of Applied Crystallography*, vol. 99, pp. 97 – 105.

RILEM Commission 42-CEA. (1981). Properties of set concrete at early-ages, *Materials and Structures*, vol. 14, no. 84, pp. 399 – 460.

Rojas, F.M. (2006). Study of hydrated phases present in a metakaolin-lime system cured at 60ºC and 60 months of reaction, *Cement and Concrete Research*, vol. 36, pp. 827 – 831.

Rojas, F.M. and Cabrera, J. (2002). The effect of temperature on the hydration rate and stability of the hydration phases of metakaolin-lime-water systems, *Cement and Concrete Research*, vol. 32, pp. 133 – 138.

Romauldi, J.P. and Batson, G.B. (1963). Mechanics of crack arrest in concrete, Journal of the Engineering Mechanics division, *Proceedings of the ASCE*, vol. 89, no. EM3, pp. 147 – 168.

Rowell, R.M. *Handbook of wood chemistry*, Wood Science, vol. 13, 1980, pp.102.

Sabir, B., Wild, S. and Bai, J. (2001). Metakaolin and calcined clays as pozzolans for concrete, *Cement and Concrete Research*, vol. 23, pp. 441 – 454.

SABS ISO 9933. South African Standard Specification for products in fibre-reinforced cement – Long corrugated or asymmetrical section sheets and fittings for roofing and cladding, 1995.

Sanjuan, M.A. and Toledo Filho, R.D. (1998). Effectiveness of crack control at early age on the corrosion of steel bars in low modulus sisal and coconut fibre-reinforced mortars, *Cement and Concrete Research*, vol. 28, no. 4, pp. 555 – 565.

Santos, S.F., Schmidt, R., Almeida, A.E.F.S., Tonoli, G.H.D. and Savastano Jr., H. (2012) Effects of supercritical carbonation curing on extruded vegetable fibrecement, *International Inorganic Bonded Fibre Composites Conference*, Canberra, Australia, pp. 131 - 138.

Savastano, H. and Agopyan, V. (1999). Transition zone studies of vegetable fibrecement paste composites, *Cement and Concrete Composites*, vol. 21, pp. 49 - 57.

Schindler, A.K. (2004). Effects of temperature on hydraton of cementitious materials, *ACI Materials Journal*, vol. 101, no. 1, pp. 72 – 81.

Schmidt, M. (1992). Cement with inter-ground additives: capabilities and environmental relief (I), *Zement Kalk Gips*, vol.45, no.7, pp. 64 - 69.

Scrivener, K.L., Fullmann, T., Gallucci, E., Walenta, G. and Bermejo, E. (2004). Quantitative study of Portland cement hydration by X-ray diffraction / Rietveld analysis and independent methods, *Cement and Concrete Research*, vol. 34, no. 9, pp. 1541 – 1547.

Shah, S.P., Weiss, W.J. and Yang, W. (1997). Shrinkage cracking in high performance concrete, *International Symposium on High Performance concrete*, New Orleans, Louisiana.

Shah, S.P., Weiss, W.J. and Yang, W. (1998). Shrinkage cracking – can it be prevented? *Concrete International*, vol. 20, no. 4, pp. 51 – 55.

Sharma, S.K., Ransinchung, G.D. and Kumar, P. (2013). Effect of wollastonite micro fibre addition in mortar and concrete mixes, *International Journal of Scientific and Engineering Research*, vol. 4, no. 5, pp. 91 – 94.

Silva, P.S. and Glasser, F.P. (1993). Phase relation in the system CaO-Al_2O_3-SiO_2-H_2O relevant to metakaolin-calcium hydroxide hydration, *Cement and Concrete Research*, vol. 23, pp. 627 – 639.

Slivka, V. (2002). *Mining and treatment of silicate* (in Czech), Silikatovy Svaz, Praha, pp. 443.

Smith, L.N. and Midha, P.S. (1997). A computer model for relating powder density to composition: employing simulations of dense random packings of monosized and bimodal spherical particles, *Journal of Materials Process Technology*, vol. 72, pp. 277 – 282.

Snelson, D., Wild, S. and O'Farrel, M. (2008). Heat of hydration of Portland cement-metakaolin-fly ash (PC-MK-PFA) blends, *Cement and Concrete Research*, vol. 38, no. 6, pp. 832 – 840.

Soroushian, P., Marikunte, S. and Won, J. (1995). Statistical evaluation of mechanical and physical properties of cellulose fibre reinforced cement composites, *ACI Materials Journal*, vol. 92, no. 2, pp. 172 – 180.

Soroushian, P., Marikunte, S. and Won, J. (1994) Wood fibre reinforced cement composites under wetting-drying and freezing-thawing cycles, *Journal of Materials Civil Engineering*, vol. 6, no. 4, pp. 595 - 611.

Soroushian, P., Won, J.P. and Hassan, M. (2012). Durability characteristics of CO_2-cured cellulose fibre reinforced cement composites, *Construction and Building Materials*, vol. 34, pp. 44 - 53.

Swapp, S. (2013). Scanning Electron Microscopy (SEM), *Geochemical Analytical Instruments and Techniques,* University of Wyoming.

Swenson, E.G. and Sereda, P.J. (1968). Mechanism of the carbonation shrinkage of lime and hydrated cement, *Journal of Applied Chemistry*, vol.18, pp. 111 - 117.

Taylor, H.F.W. *Cement chemistry*, 2nd Edition, Thomas Telford Publications, London, 1997.

Tazawa, E. (1999). Autogenous shrinkage of concrete, *Proceedings of the International workshop organized by the Japan Concrete Institute*, Taylor, New York.

Tazawa, E. and Miyazawa, S. (1995a). Experimental study on mechanism of autogenous shrinkage of concrete, *Cement and Concrete Research*, vol. 24, no. 8, pp. 1633 – 1638.

Tazawa, E. and Miyazawa, S. (1995b). Influence of cement and admixture on autogenous shrinkage of cement paste, *Cement and Concrete Research*, vol. 25, no. 2, pp. 281 – 287.

Termkhajornkit, P., Nawa, T., Nakai, M. and Saito, T. (2005). Effect of fly ash on autogenous shrinkage, *Cement and Concrete Research*, vol. 35, no. 3, pp. 473 – 482.

Thierry, A., Dangla, P., Villian, G. and Platret, G. A. (2005). A prediction model for concrete carbonation based on coupled CO_2-H_2O-ions transfers and chemical reactions, *10DBMC International Conference on durability of building materials and components*, Lyon, France.

Toledo Filho, R.D. (1997). Natural fibre reinforced mortar composites: Experimental characterization, *PhD Thesis*, Rio de Janeiro, pp. 472.

Toledo Filho, R.D., Ghavami, K., England, G.L. and Scrivener, K. (2003). Development of vegetable fibre-mortar composites of improved durability, *Cement and Concrete Composites*, vol. 25, pp. 185 - 196.

Toledo Filho, R.D., Scrivener, K., England, G.L. and Ghavami, K. (2000). Durability of alkali-sensitive sisal and coconut fibres in cement mortar composites, *Cement and Concrete Composites*, vol. 22, no. 6, pp. 127 - 143.

Tonoli, G.H.D., Rodrigues Filho, U.P., Savastano Jr., H., Bras, J., Belgacem, M.N. and Rocco Lahr, F.A. (2009). Cellulose modified fibres in cement based composites, *Composites*, vol. 40, pp. 2046 - 2053.

Topcu, I.B. and Elgun, V.B. (2004). Influence of concrete properties on bleeding and evaporation, *Cement and Concrete Research*, vol. 34, no. 2, pp. 275 – 281.

Trejo-O'Reilly, J.A., Cavaille, J.Y., Belgacem, M.N. and Gandini, A. (1998). Surface modification of cellulose fibres, *Journal of Adhesives*, vol. 67, pp.359.

Tu, X., Young, R.A. and Denes, F. *Cellulose*, vol.1, 1994, pp. 87.

Uchikawa, H., Hanehara, S. and Sawaki, D. (1997). The role of steric repulsive force in the dispersion of cement particles in fresh paste prepared with organic admixture, *Cement and Concrete Research*, vol. 27, no. 1, pp. 37 – 50.

Valdez-Gonzalez, A., Cervantes, J.M., Olayo, R. and Herrara-Franco, P.J. (1999). Chemical modification of henequen fibres with an organosilane coupling agent, *Composites*, Part B: Engineering, vol. 30, pp. 321.

Van Breugel, K. and De Vries, J. (1998). Mixture optimization of low water/cement ratio high strength concretes in view of autogenous shrinkage, *Proceedings of International Symposium on High Performance and Reactive Powder concrete*, Sherbrooke, Canada, pp. 365 – 382.

Vedalakshmi, R., Sundara Raj, A., Srinivasan, S. and Ganesh, B.K. (2003). Quantification of hydrated cement products of blended cements in low and medium strength concrete using TG and DTA technique, *Thermochim Acta*, vol. 407, pp. 49 – 60.

Vidovic, K., Ambrozik, M., Krnel, K., Kosmac, T. and Akers, S. (2010). The fracture strength of fibrecement corrugated sheets: a statistical approach using Weibull analysis, *International Inorganic Bonded Fibre Composites Conference*, pp. 116 – 128.

Walenta, G. and Fullmann, T. (2004). Advances in quantitative XRD analysis for clinker, cements and cementitious additions, *Advances in X-ray analysis*, vol. 47, pp. 287 – 296.

Weiss, J., Lura, P., Rajabipour, F. and Sant, G. (2008). Performance of shrinkage reducing admixtures at different humidities and at early ages, *ACI Materials Journal*, vol. 105, no. 5, pp. 478 – 486.

Weiss, W.J., Yang, W. and Shah, S.P. (1998). Shrinkage cracking of restrained concrete slabs, *Journal of Engineering Mechanics*, vol. 124, no. 7, pp. 765 – 774.

Wiegrink, K., Marikunte, S. and Shah, S.P. (1996). Shrinkage cracking of high strength concrete, *ACI Materials Journal*, vol. 93, no. 5, pp. 1 – 8.

Wild, S., Khatib, J.M. and Jones, H. (1996). Relative strength, pozzolanic activity and cement hydration in super-plasticized metakaolin concrete, *Cement and Concrete Research*, vol. 26, no. 10, pp. 1537 – 1544.

Winter, R.L., Akers, S.A.S., Jonker, J.A. and Mtsweni, N.B. (2012). Dual flocculation selection in fibrecement process, *International Inorganic Bonded Fibre Composites Conference*, Australia, pp. 255 – 263.

Xu, Y. and Chung, D.D.L. (1999a). Carbon fibre reinforced cement improved by using silane-treated carbon fibres, *Cement and Concrete Research*, vol. 29, pp. 773 - 776.

Xu, Y. and Chung, D.D.L. (1999b). Effect of carbon fibres on the vibration reduction ability of cement, *Cement and Concrete Research*, vol. 29, no. 7, pp. 1107 – 1110.

Xu, Y. and Chung, D.D.L. (1999c). Improving the workability and strength of silica fume concrete by using silane treated fume, *Cement and Concrete Research*, vol. 29, no. 3, pp. 451 – 453.

Xu, Y. and Chung, D.D.L. (1999d). Increasing the specific heat of cement paste by admixture surface treatments, *Cement and Concrete Research*, vol. 29, no. 7, pp. 1117 – 1121.

Xu, Y. and Chung, D.D.L. (2000). Reducing the drying shrinkage of cement paste by admixture surface treatments, *Cement and Concrete Research*, vol. 30, pp. 241 – 245.

Yamada, K., Takahashi, T., Hanehara, S. and Matsuhisa, M. (2000). Effects of the chemical structure on the properties of polycarboxylate-type superplasticizer, *Cement and Concrete Research*, vol. 30, no. 2, pp. 197 – 207.

Yamakawa, I., Kishtiani, K., Fukushi, I. and Kursha, K. (1990). Slump control and properties of concrete with a new superplasticizer, RILEM, *Symposium on "Admixture for concrete. Improvement of properties",* Editor: E. Vasquez, Chapman and Hall, London, pp. 94 - 105.

Yamane, C., Aoyagi, T., Ago, M., Sato, K., Okajima, K. and Takahashi, T. (2006). Structure of regenerated cellulose films from cellulose/aqeous NaOH solutions as a function of coagulation conditions, *Journal of Polymers*, vol. 38, pp. 819 -826.

Young, R.A. The Rietveld method, Oxford University Press, 1993.

Young, R.A., Mackie, D.B. and von Dreele, R.B. (1977). Application of the pattern fitting structure refinement method to X-ray powder diffractometer pattern, *Journal of Applied Crystallography*, vol. 10, pp. 262 – 269.

Yu, J.F., Wang, D.S., Ge, X.P., Yan, M.Q. and Yan, M. (2006). Flocculation of kaolin particles by two typical polyelectrolytes: a comparative study on the kinetics and flocculant structures, *Colloids Surface* A, vol. 290, pp. 288 – 294.

Zadoreki, P. and Flodin, P. (1985). *Journal of Applied Polymer Science*, vol. 30, pp.2419.

Zhang, J. and Li, V. (2001). Influence of fibres on drying shrinkage of fibre-reinforced cementitious composite, *Journal of Engineering Mechanics*, vol.127, no.1, pp.37 - 44.

Zhao, J. (1990). Mechanical properties of concrete at early-ages, *Master Thesis*, University of Ottawa, Canada.

Zhou, Y. and Franks, G.V. (2006). Flocculation mechanism induced by cationic polymers investigated by light scattering, *Langmuir*, vol. 22, pp. 6775 – 6786.

Zhu, Z., Li, T., Lu, J., Wang, D. and Yao, C. (2009). Characterization of kaolin flocs formed by polyacrylamide as flocculation aids, *International Journal of Mineral Processing*, vol. 91, pp. 94 – 99.

Zivica, V. and Bajza, A. (2001). Acidic attack of cement based materials – a review: Part 1. Principle of acidic attack, *Construction Building Materials*, vol.15, no. 8, pp. 331 - 340.

BIBLIOGRAPHY

Aldrige, L.P. (1982). Accuracy and precision of an X-ray diffraction method for analyzing Portland cements, *Cement and Concrete Research*, vol. 12, pp. 381 – 398.

Bensted, J. (2000). Mechanism of thaumasite sulphate attack in cements, mortars and concretes, *ZKG International*, vol. 53, pp. 704 – 709.

Bentur, A. (1994). Long-term performance of fibre reinforced cements and concretes, *Proceedings of Advances in Cement and Concrete*, ASCE, pp. 223 – 234.

Bezerra, E.M. and Savastano Jr., H. (2004). The influence of type and refinement of the cellulose pulp in the behavior of fibrecement with hybrid reinforcement – a regression analysis application, *17th ASCE Engineering Mechanics Conference*, University of Delaware, Newark, pp. 1 – 7.

Bjontegaard, O., Hammer, T.A. and Sellevold, E.J. (2004). On the measurement of free deformation of early-age cement paste and concrete, *Cement and Concrete Composites*, vol. 26, no. 5, pp. 427 – 435.

Bledzki, A.K. and Gassan, J. (1999). Composite reinforced with cellulose based fibres, *Progress in Polymer Science*, vol. 24, pp. 221 – 274.

Bolto, B. and Gregory, J. (2007). Organic polyelectrolytes in water treatment, *Journal of Water Research*, vol. 41, no. 11, pp. 2301 – 2324.

Cabrera, J.G. and Lynsdale, C.J. (1988). A new gas parameter for measuring the permeability of mortar and concrete, *Magazine Concrete Research*, vol. 40, pp. 177 – 182.

Castellano, M., Gandini, A., Fabbri, P. and Belgacem, M.N. (2004). Modification of cellulose fibres with organosilanes: under what conditions does coupling occur? *Journal of Colloidal Interface Science*, vol. 273, pp. 505 – 511.

De Lhoneux, B., Alderweireldt, L., Boersma, A., Bordin, R., Saenen, W., Van der Heyden, L. and Verleene, D. (2008). Selected issues of fibrecement sustainability: wood pulp refining energy and accelerated ageing of fibres and composites, *11th International Inorganic Bonded Fibre Composites Conference*, Madrid, Spain.

Duval, R. and Kadri, E.H. (1998). Influence of silica fume on the workability and the flexural strength of high performance concrete, *Cement and Concrete Research*, vol. 28, no. 4, pp. 533 – 574.

Grim, R.E. *Clay Mineralogy*, McGraw-Hill, New York, 1968.

Hooton, R.D. (1993). Influence of silica fume replacement of cement on physical properties and resistance to sulfate attack, freezing and thawing and alkali silica resistivity, *ACI Materials Journal*, vol. 90, no. 2, pp. 143 – 151.

Kuzel, H. and Pollmann, H.(1991). Hydration of C_3A in the presence of $Ca(OH)_2$, $CaSO_4 \cdot 2H_2O$ and $CaCO_3$, *Cement and Concrete Research*, vol. 21, pp. 885 – 895.

Lawler, J.S., Zampini, D. and Shah, S.P. (2003). Fracture processes of hybrid fibre reinforced mortar, *Materials and Structures*, vol. 36, no. 3, pp. 197 – 208.

Mac Vivar, R., Matuana, L.M. and Balatinecz, J.J. (1999). Ageing mechanisms in cellulose fibre reinforced cement composites, *Cement and Concrete Composites*, vol. 21, pp. 189 – 196.

McCormick, S.W., McCormick, C.L. and Butler, G.B. *American Chemical Society Series*, Washington, 1991.

Mehta, P.K. (1983). Mechanics of sulfate attack on Portland cement, concrete- another look, *Cement and Concrete Research*, vol. 13, no. 3, pp. 401 – 406.

Mehta, P. K. (1986). Cement replacement materials, *Concrete Technology and Design*, vol. 3, Ed. Swamy, R.N., Surrey University Press, pp. 134 – 169.

Mitchell, D.R.G., Hinczak, I. and Day, R.A. (1998). Interaction of silica fume with calcium hydroxide solutions and hydrated cement pastes, *Cement and Concrete Research*, vol. 28, no. 11, pp. 1571 – 1584.

Oliveira, C., da Silveira, N. and Rubio, J. (2010). Polymer structural and surface charge characterization on particles flocculation, *7th International Symposium on Natural Polymers and Composites.*

Quian, X. and Li, Z. (2001). The relationship between stress and strain for high performance concrete with metakaolin, *Cement and Concrete Research*, vol. 31, no. 11, pp. 1607 – 1611.

Savastano Jr., H. and Agopyan, V. (1992). Transition zone on hardened cement paste and vegetable fibre, In: *Swamy, R.N. ed. Fibre reinforced cement and concrete, RILEM*, London.

Scrivener, K.L. and Gartner, E.M. (1988). Microstructural gradients in cement paste around aggregate particles, *Materials Research Society Symposium Proceedings*, vol. 114, pp. 77 – 85.

Sellevold, E.J. and Nilsen, T. (1987). Condensed silica fume in concrete: a world view, *CANMET, Supplementary Cementing Materials for Concrete*, Ed. V.M. Maholtra, Canadian Government Publishing Centre, Ottawa, Canada, pp. 167 – 243.

Tonoli, G.H.D., Belgacem, M.N., Siqueira, G., Bras, J., Mendes, L.M., Lahr, F.A.R. and Savastano Jr., H. (2012). Processing changes of cement based composites reinforced with silane and isocyanate eucalyptus modified fibres, *Key Engineering Materials*, vol. 517, pp. 437 – 449.

Turcry. P. and Loukili, A. (2006). Evaluation of plastic shrinkage cracking of self-consolidating concrete, *ACI Materials Journal*, vol. 103, no. 4, pp. 272 – 279.

Vinson, K.D. and Daniel, J.I. (1990). Specialty cellulose fibres for cement reinforcement, *Proceedings of thin section fibre reinforced concrete and ferro cement, SP-124, ACI,* Detroit, pp. 1 – 18.

Wild, S., Sabir, B.B. and Khatib, J.M. (1995). Factors influencing strength development of concrete containing silica fume, Cement and Concrete Research, vol. 25, no. 7, pp. 1567 – 1580.

Yogendran, V., Langan, B.W. and Ward, M.A. (1991). Hydration of cement and silica fume paste, Cement and Concrete Research, vol. 21, no. 5, pp. 691 – 708.